William Zappa

Pilot-scale Experimental Work on the Production of Precipitated Calcium Carbonate (PCC) from Steel Slag for CO_2 Fixation

Thesis submitted in partial fulfilment of the
requirements for the degree of
Master of Science in Technology

Department of Energy Technology
School of Engineering, Aalto University

Espoo, 11th August 2014

Supervisor Professor Mika Järvinen
Advisor Arshe Said M.Sc. (Tech.)

AALTO UNIVERSITY
SCHOOL OF TECHNOLOGY
PO Box 12100, FI-00076 AALTO
http://www.aalto.fi

ABSTRACT OF THE MASTER'S THESIS

Author: William Zappa

Title: Pilot-Scale Experimental Work on the Production of Precipitated Calcium Carbonate (PCC) from Steel Slag for CO_2 Fixation

School: School of Engineering

Department: Energy Technology

Professorship: Energy Engineering and Environmental Protection | **Code**: ENE-47

Supervisor: Professor Mika Järvinen

Instructor(s): Arshe Said M.Sc. (Tech)

The production of steel is a very energy intensive process and the industry contributes a significant amount to global carbon dioxide (CO_2) emissions. Steel production also generates steel slag, a calcium-rich waste which has few useful applications and is partly landfilled. Producing precipitated calcium carbonate (PCC) from steelmaking slag (Slag2PCC) is a way to reduce CO_2 emissions while at the same time turning slag waste into a valuable product. In the Slag2PCC process, a solution of ammonium chloride (NH_4Cl) is used to extract calcium from steelmaking slag which is then bubbled with a CO_2-containing gas in a process called carbonation to form PCC. This thesis has focussed on how the process conditions during carbonation affect the carbonation process as well as the quality parameters of the PCC produced.

Carbonation tests were performed at laboratory scale (5L) and at a recently constructed pilot-scale Slag2PCC plant (200L). From the laboratory tests it was found that temperature, calcium concentration [Ca^{2+}], NH_4Cl solvent concentration [NH_4Cl], CO_2 flow and agitation speed have important effects on the carbonation process and the quality of the PCC produced. PCC particle size can be reduced by lower temperature, lower [Ca^{2+}], lower [NH_4Cl], lower CO_2 flow and higher agitation speed. It was also found that increasing [NH_4Cl] and CO_2 flow is likely to increase particle agglomeration. Temperature, [Ca^{2+}], [NH_4Cl], and calcium to carbonate ratio [Ca^{2+}]/[CO_3^{2-}] appear to be the most significant factors determining the crystal morphology. Work with the pilot plant showed that the equipment should be modified to improve mixing and solid suspension performance. While the production of rhombohedral calcite and aragonite polymorphs was successfully demonstrated, attempts to make scalenohedral PCC in the pilot plant based on conventional $Ca(OH)_2$ slurry carbonation conditions were not successful, believed to be due to the NH_4Cl, [Ca^{2+}], pH, or the difference in supersaturation conditions compared with conventional $Ca(OH)_2$ slurry carbonation.

The cost of PCC production from the Slag2PCC process was also estimated as 65 €/t based on the results of the pilot scale work. The CO_2 emissions of the Slag2PCC process were estimated as -0.229 tCO_2/tPCC, giving a CO_2 capture cost of 284 €/t. However, if the PCC can be produced at high quality and sold at market price (120 €/t), the process delivers a profit of 55 €/tPCC and CO_2 capture becomes profitable at 239 €/tCO_2.

Date: 11th August 2014 | Language: English | Number of pages: 126+16

Keywords: PCC, calcium carbonate, steel slag, carbon capture, mineral carbonation

Acknowledgements

This thesis would not have been possible without the help of many whose contributions I value greatly.

I want to acknowledge the very great contribution of Tuyen Nguyen from the Department of Forest Products Technology for her patience, discussions, and for performing all the SEM and z-potential analysis, as well as the PSD analysis and training me in the use of the equipment. Also to the head of the Bio-based Materials Technology group Thaddeus Maloney for allowing me to use his department's resources, his valuable discussions and feedback. Also from Forest Products Technology, my thanks go to Jonna Kuusisto for her information on PCC precipitation conditions and to Leena Nolvi for the surface area analysis.

From the Analytical Chemistry department I'd like to recognise the invaluable help of Kalle Salminen and Matti Pusa for their time, expert advice, friendly conversations and seemingly infinite patience with me performing the calcium analysis.

From Åbo Academy I'd like to thank Hannu-Petteri Mattila for his valuable discussions, feedback as well as experimental data.

From the department of Energy Technology thanks go to Seppo Poimuvirta and Vadim Desyantyk for their technical support in helping me set up the equipment for the laboratory-scale tests as well as the hard work that went into constructing the Slag2PCC pilot plant before I joined the project. I am also very grateful to Sanni Eloneva and Mika Järvinen for their discussions, and for giving me the opportunity to work on this thesis as a member of the Slag2PCC project team with the freedom to develop my own ideas and approach.

This work also made use of the Aalto University Nanomicroscopy Center (Aalto-NMC) premises.

Last but not least my sincerest thanks and gratitude go to Arshe Said for his support, help in performing all the pilot-scale tests, his valuable discussions, and without whom this thesis would not have been possible.

Finally, I would like to thank the SELECT board and KICInnoEnergy for giving me the opportunity and financial means to study as part of the program, an experience that has been rewarding, challenging and humbling.

Contents

Figures

Tables

Abbreviations

ACC	Amorphous calcium carbonate
ANOVA	Analysis of variance
CCS	Carbon capture and sequestration
CGM	Crystal growth modifier
CM	Coated mechanical paper
CO_2CR	CO_2 to calcium ratio (moles of CO_2 added per mole of calcium per minute)
CR	Carbonation reactor
CWF	Coated woodfree printing and writing paper
DoF	Degrees of freedom
EC	European Commission
EDTA	Ethylenediaminetetraacetic acid
ER	Extraction reactor
GCC	Ground calcium carbonate
GLR	Gas to liquid ratio
GLM	General linear model
HX	Heat exchanger
IAP	Ion activity product
M	mol/L
Mtpy	Million (10^6) tonnes per year
PCC	Precipitated calcium carbonate
PSD	Particle size distribution
SEM	Scanning electron microscope
SLR	Slag to liquid ratio
SMI	Specialty Minerals Inc.
SSA	Specific surface area
ST	Solvent tank
UM	Uncoated mechanical paper
US	Ultrasound
UWF	Uncoated woodfree printing and writing paper
[…]	Concentration of …

Symbols

a	activity (mol/L); interfacial area (m^2/m^3)
Agg_{d90}	difference in particle size before and after ultrasound based on d_{90} (%)
B	crystal birth rate function
c	concentration (g/L, mol/L, M)
Δc	absolute supersaturation (g/L, mol/L)
d_{50}	50% passing size (µm)
d_{90}	90% passing size (µm)
D	diffusivity (m^2/s); crystal death rate function
G	crystal growth rate function
H	Henry's law constant ($atm.kg^{-1}.mol^{-1}$)
ΔH_r	heat of reaction (kJ/mol)
k	reaction rate constant ($mol.L^{-1}.s^{-1}$, s^{-1}…); mass transfer coefficient (m/s)
K	equilibrium constant, solubility product (-)
L	size fraction (µm)
I	ionic charge strength ($kmol/m^3$)
m	mass (g,kg); molality (mol/kg H_2O)
M	molarity (mol/L); molecular weight (g/mol)
n	population density (-)
N'	molar flux, specific transport rate ($mol.s^{-1}.m^{-2}$)
p	partial pressure (atm)
s	supersaturation ratio (-)
S	fundamental supersaturation (-)
$\hat{v}$	ideal gas molar volume (L/mol)
V	volume (L)
x	mass fraction (-); mole fraction (-)
z	ion charge (-)

Greek Letters

α	level of statistical significance (-)
γ	activity coefficient (-)
η	conversion, efficiency (%,-)
μ	chemical potential (J/mol)
σ	relative supersaturation (-)
υ	moles of ions per mole of salt (-)

Subscripts

car	carbonation
ext	extraction
a	based on activity
c	based on concentration
g	gas-side
l	liquid-side

Superscripts

US	with ultrasound
0	initial
i	at the interface
∞	in the bulk phase
$*$	at equilibrium
$+$	cation
$-$	anion

1 Introduction

More than 1.4 billion tonnes of steel are manufactured globally every year. The production of steel is a very energy intensive process based predominantly on fossil fuels, thus the iron and steel industry is a significant source of anthropogenic carbon dioxide (CO_2) accounting for around 6.7% of global emissions [1]. In the coming decades there will be continuing growth in the volume of steel produced, thus the CO_2 emissions from the iron and steel industry as a whole will increase unless efforts are made to reduce them. In Finland, more than 3.5 million tonnes of steel are produced each year, giving rise to around 3 million tonnes of CO_2 emissions annually [2, 3]. In addition to CO_2 emissions, the production of steel also generates a significant amount of solid waste by-product known as slag. Producing precipitated calcium carbonate (PCC) from steelmaking slag has been proposed as a potential method of reducing the CO_2 emissions from the steel industry by locking-up CO_2 in a stable mineral form, whilst at the same time turning steel slag waste into a valuable product [4, 5].

In the Slag2PCC process, a solution of ammonium chloride (NH_4Cl) is used to extract calcium from steelmaking slag. The resulting Ca-rich solution is bubbled with CO_2 gas which reacts to form PCC. This PCC could replace limestone used in the production of steel reducing virgin material consumption and associated CO_2 emissions or, if the PCC can be produced at sufficiently high quality, it could be sold at a higher price as a commodity chemical to several other industries. In addition to the steel industry, the €2.5 billion pulp and paper industry has a significant presence in Finland and is a major consumer of PCC [6]. The presence of both these industries in close proximity in Finland therefore presents an excellent opportunity to develop mutually beneficial synergies between the two, at a time when both are being confronted with environmental and economic challenges.

Whilst earlier work on the Slag2PCC process has focussed on the extraction of calcium from steel slag, the focus of this thesis is on the precipitation of PCC via carbonation of the Ca-rich solution resulting from the extraction step. To commercialise the Slag2PCC process a greater understanding is needed of the carbonation process, how precipitation factors affect the quality of the PCC, whether PCC can be produced of sufficiently high quality, and how the process can be improved in the future. This is achieved through a thorough survey of the literature, collation of relevant physical and chemical data, equilibrium modelling, laboratory-scale experiments, as well as experimentation on the Slag2PCC pilot plant recently built in the Department of Energy Technology at Aalto University.

The Slag2PCC project is part of the Carbon Capture and Storage Program (CCSP) research program coordinated by CLEEN Ltd. with funding from TEKES – the Finnish Funding Agency for Technology and Innovation. The CCSP consortium consists of 17 industrial partners and 9 research partners including Aalto University and Åbo Academy.

1.1 Scope of Work

This work focuses on the carbonation side of PCC production from steelmaking slags using pilot-scale equipment in order to identify any challenges of scale-up from laboratory-scale work and to identify whether PCC can be produced at sufficiently high quality to be used as a filler or coating in the pulp and paper industry. After a review of the background literature on steelmaking slag and PCC, the Slag2PCC process will be outlined as well as the results of recent research on this topic. This discussion will set the stage for the present round of laboratory and pilot-scale experimental work focussed on how carbonation process factors affect the quality of the PCC produced. Based on the pilot plant data, the production cost of PCC from the Slag2PCC process will be estimated as well as the cost of CO_2 capture. To keep the endpoint of commercialisation of the Slag2PCC process clearly in perspective, the business potential of the production of PCC from steel slag will also be discussed.

1.2 Main Research Questions

The purpose of this thesis is to try to answer the following main research questions.

From a *technical* perspective,

- How do carbonation process variables affect the quality of the PCC produced?
- How does the NH_4Cl solvent affect precipitation of PCC?
- Can commercial quality PCC be produced from steel slag?
- What challenges and difficulties are encountered during scale-up of the Slag2PCC process?
- What is the CO_2 impact of the Slag2PCC process?
- What improvements can be made to the pilot plant?
- How can the Slag2PCC process be improved?

From a *business* perspective,

- How large is the market for PCC?
- What is the cost of PCC produced from the Slag2PCC process?
- Is the Slag2PCC process cost competitive with other forms of CO_2 capture?

2 Steelmaking Slag

In the manufacture of steel approximately 1.8 tonnes of CO_2 are emitted for every tonne of steel produced thus the iron and steel industry is a significant source of CO_2, accounting for around 6.7% of global emissions [1]. In addition to the direct and indirect emissions of CO_2, the production of steel also generates 400 Mtpy of solid waste by-product known as slag, 50 Mtpy of which comes from Europe [7]. Figure 2.1 below presents a basic schematic of an integrated steelmaking process.

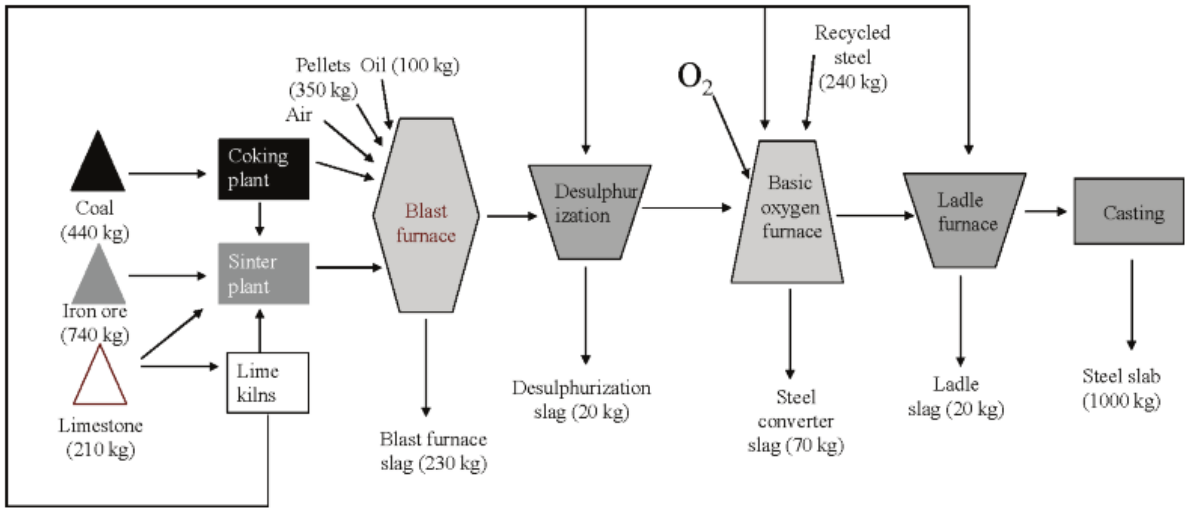

Figure 2.1 - Simplified diagram of a typical integrated steel manufacturing process indicating major material flows [8]

There are several different types of slag produced at different stages of the steelmaking process in varying quantities which depend on the chemistry, raw materials and other factors particular to the production method used. Figure 2.2 below shows the typical amount of steel slag by-products yielded per tonne of steel produced via the integrated process above utilising a blast furnace (BF) and basic oxygen furnace (BOF), and from an electric arc furnace (EAF). On average the production of one tonne of steel results in 200 kg (EAF) to 400 kg (BF/BOF) of by-products. The different slag by-products are generally named for the furnace from where they originate e.g. BF slag, BOF slag, EAF slag. Together, BOF slag and EAF slag are commonly referred to as steel slag or steel converter slag.

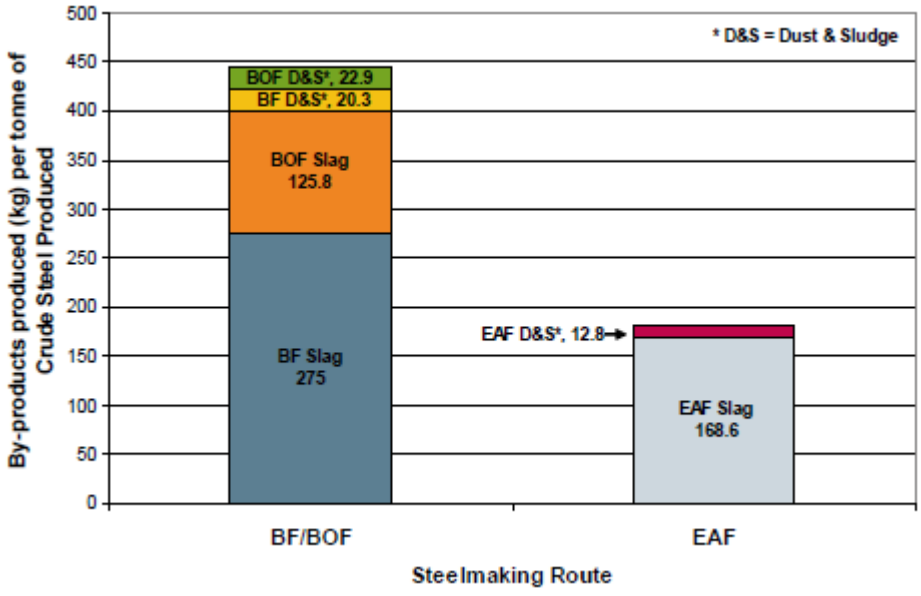

Figure 2.2 - Steelmaking by-products by steelmaking route [9]

The composition of these slags vary, as shown in Table 2.1 below.

Table 2.1 - Typical iron and steel slag compositions (%) [10]

	BF slag	BOF slag	EAF slag		Ordinary cement (for comparison)
			Oxidizing	*Reducing*	
CaO	41.7	45.8	22.8	55.1	64.2
SiO_2	33.8	11.0	12.1	18.8	22.0
Fe (total)	0.4	17.4	29.5	0.3	3.0
MgO	7.4	6.5	4.8	7.3	1.5
Al_2O_3	13.4	1.9	6.8	16.5	5.5
S	0.8	0.06	0.2	0.4	2.0
P_2O_5	<0.1	1.7	0.3	0.1	-
MnO	0.3	5.3	7.9	1.0	-

BF slag is a non-metallic by-product consisting essentially of amorphous silicates and alumino-silicates of calcium and other base metals that is developed in a molten condition simultaneously with iron in a blast furnace [11, 12]. In a BF, iron oxide is reduced to metallic iron by addition of carbon (normally as coal). Limestone is usually added to react with and remove impurities in the ore, forming BF slag. The molten iron product collects in the bottom of the furnace and the BF slag floats on top of it as a liquid phase. The compounds listed in Table 2.1 are a simplification of the actual composition of the slags. In BOF slag for example, crystalline phases of srebrodolskite ($Ca_2Fe_2O_5$), CaO, iron, calcium silicate (Ca_2SiO_4) and calcium iron oxide ($Ca_2Fe_{15.6}O_{25}$) are all present [13].

Figure 2.3 below shows how blast furnace and steel slags (including BOF slag and EAF slag) are currently utilised in Europe.

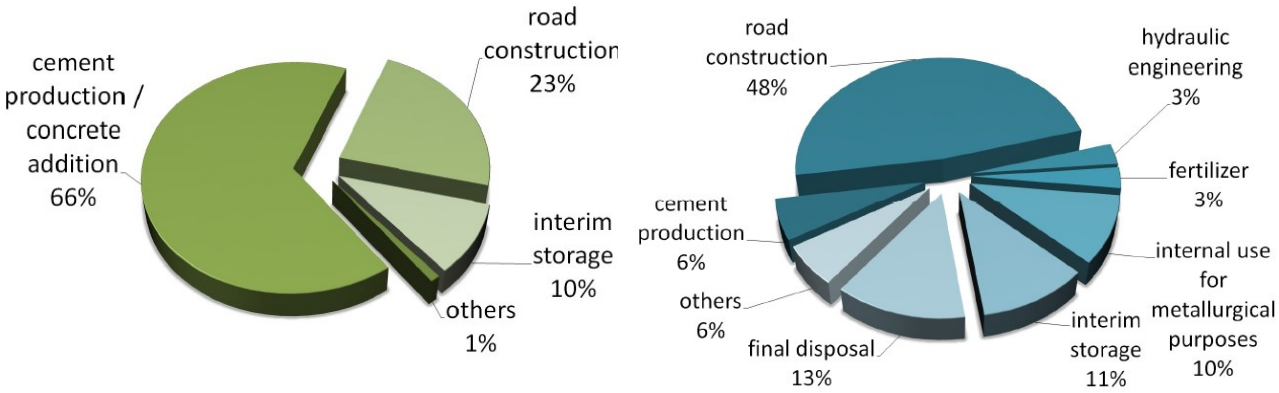

Blast furnace (BF) slag (25.6Mt) **Steel slag (22.3Mt)**

Figure 2.3 - Use of blast furnace and steel slag in Europe (2010) [7]

Well-established markets for BF slag have already been developed and it is mainly used as a raw material for cement manufacturing. In some countries, up to 80% of the cement contains granulated BF slag. Using slag prevents it going to landfill as waste, saves energy, natural resources, and significantly reduces CO_2 emissions in cement production. Replacing Portland cement with slag cement in concrete can save up to 59% of the embodied CO_2 emissions and 42% of the embodied energy required to manufacture concrete and its constituent materials. However, steel slag is less suitable to use for cement production and the higher occurrence of free lime (CaO) in steel slag restricts its use as a construction material [8]. As a result a large amount of this material is stockpiled or landfilled for final disposal, representing both a significant economic and environmental cost. In light of this, new utilization options are sought for the cheap and readily available BOF slag. One promising option is the production of PCC from steel slag.

3 Precipitated Calcium Carbonate (PCC)

Calcium carbonate ($CaCO_3$) is a very common mineral and exists as the three anhydrous polymorphs of calcite, aragonite and vaterite [14]. Calcite is the most thermodynamically stable phase at room temperature under normal atmospheric conditions and given enough time, vaterite and aragonite will transform into calcite [15]. Of these three crystal forms only aragonite and calcite have been reported to have major commercial applications and are produced on an industrial scale [16, 17]. Vaterite belongs to the hexagonal crystal system and most commonly presents as spherulitic or disclike crystals [18]. Calcite belongs to the hexagonal-rhombohedral system, in which it has been observed to occur in more than 300 forms including, rhombohedral (cubic), truncated prismatic, scalenohedral (rosette shaped), spheroidal and chain-like agglomerates [18, 19]. Aragonite belongs to the orthorhombic system and usually presents as a needle-like structure. Figure 3.1 on the next page shows just a few examples of the wide variety of crystal morphologies that can be produced. Aside from the anhydrous polymorphs mentioned, hydrated (water-containing) pseudopolymorphs are also known to exist. An amorphous form of $CaCO_3$ (ACC) with varying composition usually presents as an intermediate phase before transforming to one of the other crystalline phases. Monohydrocalcite ($CaCO_3.H_2O$) and a hexahydrate form ($CaCO_3.6H_2O$), also known as the mineral ikaite, are two other hydrated forms [20].

$CaCO_3$ is a very versatile mineral that is used in many industries. The most common source of $CaCO_3$ is limestone, a hard sedimentary rock composed primarily of $CaCO_3$ and magnesium carbonate ($MgCO_3$) with varying levels of impurities. It is found in mineral deposits all over the world, although only a few can be economically mined and an even smaller number contain $CaCO_3$ deposits of sufficiently high quality to be used in industries other than the construction industry. Only if the purity, whiteness, and homogeneity are acceptable is commercial extraction for high quality applications considered worthwhile [21]. After quarrying, further treatment is required to produce natural $CaCO_3$ of the highest quality, known generically as ground calcium carbonate (GCC) [22].

When very high quality $CaCO_3$ is produced synthetically in an industrial precipitation process then the product is known as precipitated calcium carbonate (PCC). The quality of industrially-produced PCC generally surpasses that of even the highest quality natural GCC as the process can be tailored and controlled to produce a wide variety of PCC products with very high purity and different crystal properties. For this reason PCC can be sold at a higher price, as shown in Table 3.1 below which gives prices for typical GCC and PCC products in the US and UK. Although the prices vary with location and quality, the price of PCC in the UK was above 400 €/t in 2012, approximately 60% more than a similar GCC product in the US.

Table 3.1 - Typical prices of Kaolin, GCC and PCC [23]

Product	Country	Price (2012)	
		USD/t	*€/t**
GCC, coated, fine grade, ex-works	UK	103	80
GCC, uncoated chalk, ex-works	UK	75	58
GCC, coarse 22-50µm, FOB	USA	26	20
GCC, medium 10-22µm, FOB	USA	105	82
GCC, 3µm, untreated, FOB	USA	185	144
GCC, 0.7-1.1µm, stearate coated, FOB	USA	400	311
GCC, 0.7-1.1µm, uncoated, FOB	USA	290	226
PCC, coated, ex-works	UK	550	428
PCC, uncoated, ex-works	UK	550	428
PCC, fine 0.4-1.0µm, surface treated, ex-works	USA	375	282

* *average 2012 exchange rate 0.778 €/USD*

Despite these high merchant prices, prices available to large consumers can be much lower, particularly from satellite plants and prices in the range of 100-120 €/t are to be expected [24] [25]

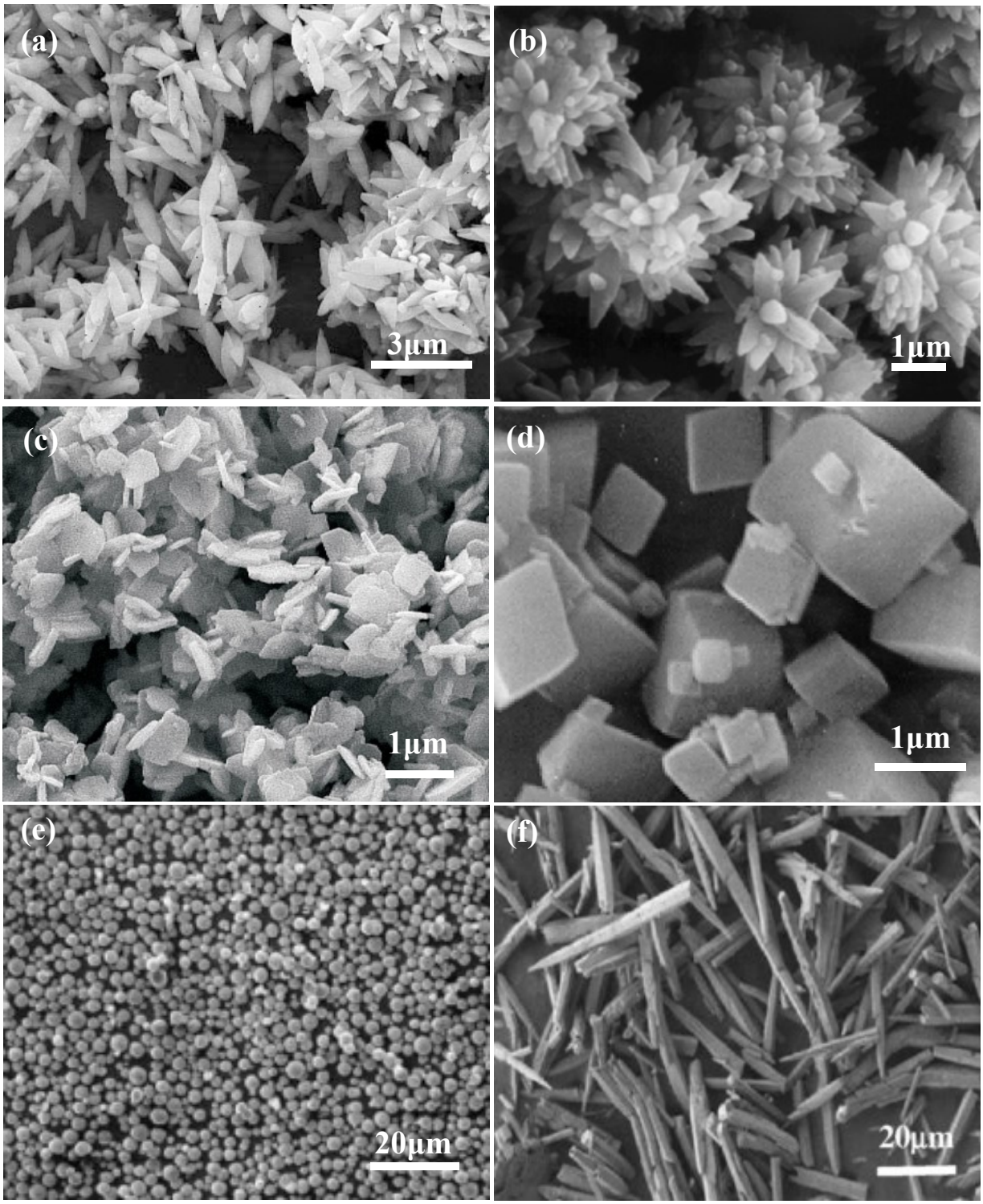

Figure 3.1 – SEM micrographs of different $CaCO_3$ morphologies
(a) calcite - scalenohedral [26]
(b) calcite - clustered scalenohedral [27]
(c) calcite – platelike [26]
(d) calcite – rhombohedral [28]
(e) vaterite - spherical [29]
(f) aragonite – needles [29]

3.1 Existing PCC Production Technologies

PCC is produced in a number of ways, the most significant of which on an industrial scale are [4],

- Carbonation, also known as the 'milk of lime' process
- the Lime-Soda process, and
- the Solvay process.

It is only in the carbonation process that PCC is produced as the primary product. In the Solvay and Lime-soda processes PCC is produced as a secondary product or by-product. Figure 3.2 below depicts a simplified schematic of the three processes showing the main inputs, outputs and materials used in common between the three. It is important to note that every method, directly or indirectly, uses raw limestone as the source of calcium. These three main conventional PCC production methods will be briefly outlined in the following sections.

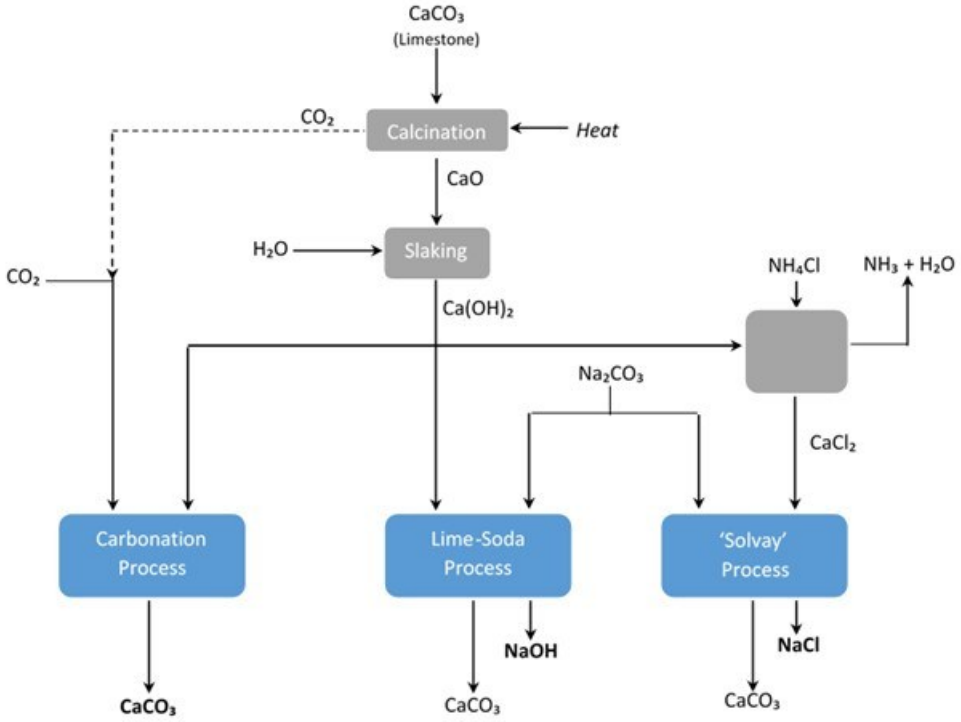

Figure 3.2 - Main commercial PCC production methods (based on [24] and [37])

3.1.1 Carbonation

Carbonation is the most common PCC production method currently used and is generally considered the most simple and cost-efficient of the available technologies [4, 30]. In this process, limestone (mainly $CaCO_3$) is calcined in a lime kiln at a temperature between 900-1000°C. The high temperature causes thermal decomposition of the limestone and release of CO_2 gas to yield lime (CaO). This calcined lime product, also known as quicklime, is then slaked with water to produce calcium hydroxide ($Ca(OH)_2$) or slaked lime. The resulting 'milk of lime' slurry is then bubbled with a CO_2-containing gas, for which purified lime kiln exhaust gas is often used. The CO_2 reacts with the solid $Ca(OH)_2$ in solution causing $CaCO_3$ to precipitate and the resulting suspension of PCC is screened at about 50µm and either used directly as an aqueous suspension containing 20 to 70% solids, or de-watered using rotary vacuum filters, pressure filters or centrifuges [16, 31]. The resulting moist cake can then be dried in rotary, spray or flash driers. Some grades of PCC are surface coated with an additive to improve handling characteristics and dispersability in, for example, plastics. These additives, which include fatty

acids, resins and wetting agents help to reduce the surface energy of the $CaCO_3$ and improve dispersion in organic materials.

The calcination, slaking and carbonation processes are depicted by the reaction scheme below [4].

$$CaCO_{3(s)} \xrightarrow{Heat} CaO_{(s)} + CO_{2(g)} \qquad \Delta H^{1000°C} = 163\ kJ/mol \tag{3.1}$$

$$CaO_{(s)} + H_2O_{(l)} \rightarrow Ca(OH)_{2(s)} \qquad \Delta H^{20°C} = -65\ kJ/mol \tag{3.2}$$

$$Ca(OH)_{2(s)} + CO_{2(g)} \leftrightarrows CaCO_{3(s)} + H_2O_{(l)} \qquad \Delta H^{20°C} = -113\ kJ/mol \tag{3.3}$$

Depending on the process conditions and limestone quality, carbonation can be used to produce very high quality PCC (>99%) with very low levels of impurities. A disadvantage of carbonation is that the CO_2 utilisation typically approaches only about 60%, and the unreacted CO_2 is difficult and expensive to recover [32].

Ever since the shift from acid to alkaline papermaking in the early 1980s, an increasing number of pulp and paper manufacturers have been constructing so-called 'satellite' PCC plants at or nearby their paper mills in order to produce their own PCC on-site via the carbonation process thereby saving on transport costs and other overheads [33]. These plants require a supply of limestone while the CO_2 is typically supplied from a steam-generating plant in the mill or from the mill recovery system [23]. In many cases the satellite plant is owned and operated by another company with expertise in PCC production; this business model largely spearheaded by Specialty Minerals Inc. (SMI) in the United States. Although this model can greatly reduce transport costs, it often obliges the paper mill operator to commit to purchasing a certain minimum amount of PCC in a long term contract, whether they need the PCC or not [34]. For on-site PCC production via the carbonation process three cost variables are important: CO_2 availability, PCC production volume (with 20,000 tpy as a typical minimum) and the cost of lime, with the latter being the most significant [35].

Aside from standard carbonation, a modified process termed 'inverse carbonation' has also been developed which involves first carbonating an aqueous solution with CO_2 down to a low pH, then mixing this solution with the milk of lime to precipitate PCC [36].

3.1.2 Lime-soda Process

PCC is also produced by the lime-soda process, in which milk of lime is reacted with sodium carbonate (Na_2CO_3) to form PCC and sodium hydroxide (NaOH) solution. The overall process is represented in the equation below [37],

$$Ca(OH)_2 + Na_2CO_3 \leftrightarrows CaCO_3 + 2NaOH \tag{3.4}$$

This method is usually used by commercial alkali manufacturers to make a relatively course PCC as a by-product of sodium hydroxide recovery [4, 34].

3.1.3 Solvay Process

PCC can also be produced by reacting calcium chloride ($CaCl_2$) with sodium carbonate (Na_2CO_3) to form $CaCO_3$ and sodium chloride (NaCl), represented by the equation below.

$$Na_2CO_3 + CaCl_2 \leftrightarrows CaCO_3 + 2NaCl \tag{3.5}$$

This is reportedly the simplest of the three methods but it requires a low-cost source of $CaCl_2$ to be financially viable [37]. As a result PCC plants using this method have historically been located near plants using the Solvay process to produce Na_2CO_3 from limestone and brine, with $CaCl_2$ produced as a by-product. It is for this reason (and probably the fact that Eq. (3.5) is actually the reverse of the overall Solvay process) that this PCC production method is commonly known as the Solvay method of PCC production, but it is also referred to as the calcium chloride-sodium carbonate double salt decomposition process [24].

As a result of differences between the three outlined processes the quality of PCC produced by each varies. This is shown in Table 3.2 below which gives typical impurity levels for PCC produced by the three methods. Solvay-produced PCC contains chlorine, which is not present in the other processes, but it contains less $MgCO_3$, Al_2O_3 and Fe_2O_3 than PCC produced via the carbonation or lime-soda method, most probably because in the Solvay method the calcium is used indirectly (as $CaCl_2$) and the impurities present in the original limestone are removed earlier in the process.

Table 3.2 - Typical chemical composition of PCC by production process (%) [37]

	Carbonation	Lime-soda	Solvay
$CaCO_3$	98.36	98.43	98.62
$CaSO_4$	0.08	0.78	0.63
$MgCO_3$	0.7	0.37	0.21
Al_2O_3	0.09	0.07	0.01
Fe_2O_3	0.07	0.06	0.01
SiO_2	0.1	0.04	0.02
NaCl	-	-	0.1
%H_2O loss	0.6	0.25	0.3
pH (sat. sol)	9.4	10.3	8.5

3.2 Applications of PCC

As mentioned previously PCC is used as a raw material in a wide variety of industries, as shown in Table 3.3 which also gives an indicative share of the sectoral consumption of total PCC in Europe based on data for 2002. It is clear that the pulp and paper industry is the largest consumer of PCC in Europe and given the strong presence of the industry in Finland it would be a convenient target market for the Slag2PCC product, thus the use and requirements of PCC by this industry are looked at in more detail.

Table 3.3 – Applications of PCC in Europe

Industry	Application	% Total EU PCC consumption [38]
Pulp & Paper	Used as a filler and coating to improve paper physical properties and reduce the cost of papermaking	87
Paints and coatings	Used in the manufacture of emulsion paint and powder coatings as an anti-setting agent, opacifying agent and anti-rust agent.	5
Adhesives and sealants	Nano-sized PCC is a primary rheological additive in some high-performance sealants and adhesives to reinforce, strengthen and impart thixotropic properties, reducing sagging [39]	5
Plastics	Used as a filler and to improve impact strength, stiffness and dimensional stability, mainly for rigid PVC and unsaturated polyesters. In plastic applications the PCC surface is usually coated with surface agents to improve its hydrophobicity and dispersability in polymer matrices [40] [41]	2
Cosmetics and personal care	Used in the manufacture of powders for its free flowing properties and fluffiness. PCC is an important ingredient in toothpaste, foundations, various creams and gloves [42]	<1
Pharmaceuticals	Used in antibiotic fermentation processes for pH control and flocculation. High purity, high surface area PCC is also used in calcium supplement tablets [43]	<1
Others		<1

3.2.1 Use of PCC in the Pulp & Paper Industry

PCC is used in the pulp and paper industry as both a filler and a coating material in the production of paper. Finely-divided white mineral fillers such as PCC are added to paper to improve the optical and physical properties of the sheet. The particles fill in the spaces and crevices between the cellulose fibre, producing a denser, softer, brighter, smoother and more opaque sheet. Another reason for adding fillers is that the fibre raw material is often the main cost factor in paper production, thus maximising the proportion of fillers, which are often less costly than pulp, can reduce raw fibre consumption and hence the cost of papermaking [30, 44]. The maximum proportion of filler in the sheet is limited by the resulting reduction in strength, bulk and sizing quality. Typical levels of mineral fillers used in European paper are shown in Figure 3.3, as well as the industry best practice. It can be seen that uncoated papers contain approximately 20% filler and can be as high as 35%.

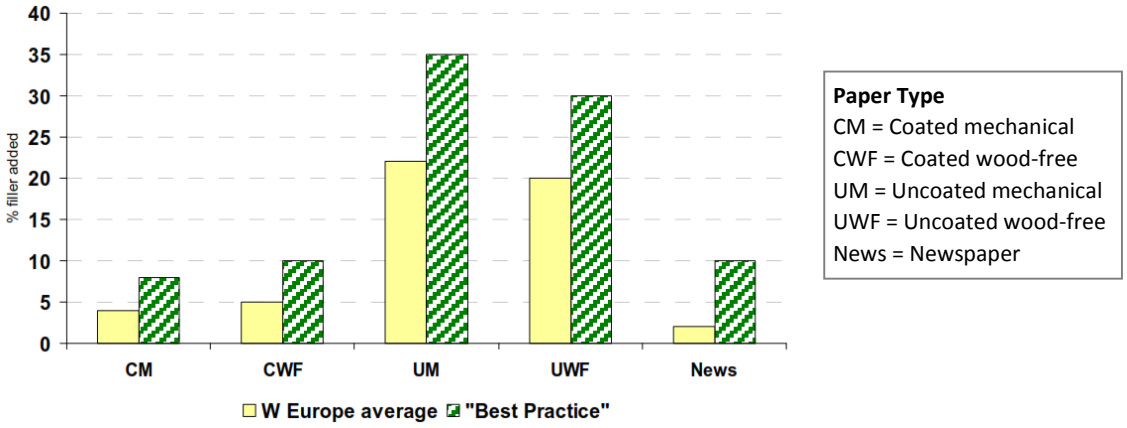

Figure 3.3 - Typical levels of freshly added mineral fillers in European paper [47]

PCC can only be used in natural or alkaline papermaking systems because it is soluble at low pH levels, although some special acid-resistant grades are available [44, 45]. One of the main functions of fillers and coating pigments such as PCC is to boost light scattering in the paper matrix. Filler pigments such as PCC affect light scattering in paper matrices through two separate mechanisms: Increasing the surface area of the paper matrix, and preventing bonding between fibres [46]. Light scattering occurs both in the fibrous base paper and in the coating layer matrices. This scattering depends on the PSD, SSA, flocculation and refractive index of the particles. The resulting pore size distribution of the surrounding media is also important [46]. In coating applications, the smaller the particle size the glossier the coating will be [16]. Due to the narrow PSD of PCC and small particle sizes achievable, PCC is usually selected for paper requiring a porous and bright coating.

As a coating, PCC offers many benefits including [16]:

- High brightness
- High light scattering (opacity)
- High bulking effect
- Good fibre coverage
- Adjustable ink properties (good printability), and
- Low blistering tendency.

The combination of different physical properties of the PCC determine how well it performs as a coating. For example, improved printability occurs when the proper particle size, size distribution and shape can be selected to achieve the desired particle packing and pore size distribution within the coating layer. If the pores in the coating layer are too large then printing ink penetrates too deeply into the paper and ink demand is high. If the pores are too small then the capillary effect pulls solvent into the coating layer before the ink film can level and printed gloss decreases [16]. Some paper mills have found that PCC alone does not fulfil the filler requirements and some GCC must be used along with the PCC. In general, the production and delivery of PCC for coating applications requires a higher level of knowledge and know-how than PCC made for filling applications, which constitutes a barrier to switching from the production of filler PCC to the production of coating PCC, particularly for satellite plants [48].

Table 3.4 shows the typical properties of major pigments used in the paper industry. As can be seen the quality of PCC surpasses that of the other minerals used in terms of brightness, particle size and surface area, however this improved quality comes with a higher price as was shown in Table 3.1 which gives prices for typical Kaolin, GCC and PCC products in the US and UK. Although the prices vary with location and quality (with UK prices somewhat higher than those in the US), the price of PCC in the UK is above 400 €/t, approximately 60% more than a similar GCC product in the US.

Table 3.4 - Typical properties of major pigments used in the paper industry [16]

Parameter	Kaolin	Talc	GCC	PCC
ISO brightness (%)	86	85	93	95
b-value (%)	3.5	3.0	1.0	0.8
90% < (µm)	3.0	6.0	2.0	0.8-2.0
Average particle size (µm)	0.7	2	0.8	0.4-2.0
Specific surface area (m^2/g)	6	5	11	4-11
Slurry solids (%)	67-72	67-70	74-78	71-75
Refractive index	1.55-1.57	1.55-1.60	1.49-1.66	1.49-1.67
Density (g/cm^3)	2.65	2.71	2.71	2.71-2.83

3.3 Quality Requirements for PCC in the Pulp & Paper Industry

As has been shown there are many different uses for PCC and the properties required from the PCC vary in each application. For pharmaceutical-grade PCC for example, a high purity product is required, whereas brightness and particle size distribution may be less of a concern. Thus, each application or industry has different requirements for PCC quality. Even within the same industry there can be a need for multiple PCC products with different quality requirements.

In the pulp and paper industry, the main properties of PCC which determine the product quality are: purity, refractive index, crystal shape (or morphology), specific surface area (SSA), particle size distribution (PSD), specific gravity, brightness or whiteness, and surface charge [49]. Many of these parameters are interrelated (i.e. small particles have high SSA) and precise control over precipitation conditions is important for ensuring high quality PCC because, it is not just the average values of these parameters which are important, but their distribution. The following sections outline these factors and their importance for papermaking.

Table 3.5 presents the results of a survey of quality parameters for several commercially available PCC grades produced by some of largest manufacturers of PCC in the Nordic countries: MTI, Omya and Schaefer Kalk.

3.3.1 Purity

Purity is a critical PCC parameter in the pulp and paper industry because the purity of the PCC largely determines its brightness. Impurities such as manganese and iron can lead to discolouring even in low concentrations and sulphur compounds should also be avoided as these can interfere in the papermaking process [4, 16]. Commercial PCC pigments typically contain at least 97% but more commonly 99% $CaCO_3$, with the remainder being $MgCO_3$ as well as other mineral impurities [16]. This level of purity is much higher than that normally available with GCC.

3.3.2 Morphology

Commercial PCC products are usually available in one of four main forms [31].

- a scalenohedral form of calcite, which is the main form required by most customers. For a given median particle size it has a high surface area (e.g. 10 – 15m^2/g for a median particle size of 1-3 µm);
- a prismatic form of calcite, primarily used as a coating material but is also used a paper filler;
- a rhombohedral form of calcite, also used as a coating and filler material; and
- an aragonite form consisting of fine needles, used in specialised applications requiring very high surface area.

These basic crystal shapes are shown in Figure 3.4 below and should be recognisable from the SEM micrographs in Figure 3.1.

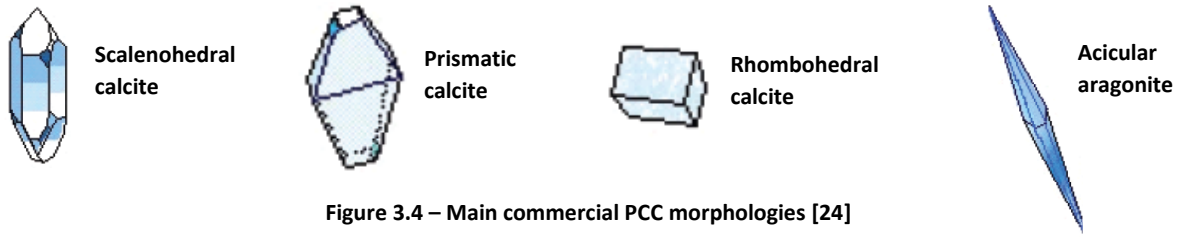

Figure 3.4 – Main commercial PCC morphologies [24]

Only the calcite and aragonite forms of PCC are known to have industrial applications. In the production of PCC vaterite (usually spherical) can also form, but this is unstable and has no known commercial applications. ACC can also form as an intermediate during precipitation but this also has no known industrial applications. The morphological transitions between ACC, vaterite, calcite and are governed by the thermodynamics of the system which depend on a number of factors including temperature, concentrations, pH and reaction time [50]. Because of its thermodynamic stability under standard conditions and its ability to appear in different rhombohedral (cubic), prismatic (barrel-shaped) and scalenohedral (triangular) morphologies, calcite is the most important polymorph in industrial papermaking applications [51] . The rhombohedral and prismatic forms are useful in paper coating applications. In filled papers, large prismatic morphologies are favoured for improving drainage on the paper machine and providing a bulky finished product [52]. Scalenohedral calcite can present as a collection of discrete particles or a cluster of individual crystals arranged in a rosette or star pattern. The latter morphology is commonly used in paper filling because this unique shape scatters light efficiently, significantly enhancing paper opacity [52]. Large scalenohedral particles which are not truly solid but contain a significant void volume, result in a relatively low effective particle density and increases paper sheet bulk [53]. Needle-like aragonite is used in paper coatings to produce high gloss finishes and is better at covering substrates at lower coating thicknesses.

3.3.3 Brightness

In most cases the role of pigment-coated paper is to serve as a medium for conveying printed information, thus the quality of the surface is the most important property of the paper. Aside from the mechanical requirements of being smooth, continuous, ink receptive and durable, the surface should also be bright and preferably white so that the printed text and images are easy and pleasing to read. For paper, absolute brightness is defined as the reflectance of blue light (peaking at wavelength 457 nm) in terms of a perfectly reflecting and diffusing surface. Whiteness differs from brightness in that it encompasses all reflected light in the visible spectrum (400-700 nm) [37]. Brightness is related to whiteness in that a very white sheet can only be made from components which

have a high brightness, such as PCC. The maximum brightness of the final paper depends on the maximum brightness of the component pulp, filler and coating materials, thus the brightness of the PCC, irrespective of whether it's used as a coating or filler, is a critical quality parameter.

3.3.4 Particle Size Distribution (PSD)

The requirements for PSD vary depending on the particular application of PCC, but the most important features are the top size (largest particle), the slope of the PSD curve, and the mean particle size often reported as the 50% passing size (d_{50}) equivalent to the mass mean diameter [37]. When used as a paper filler, the PSD is purposely made very narrow with most particles <2 µm. This is because a narrow PSD results in a more porous sheet, whereas a wide PSD will result in a denser sheet with fewer pores as in a wider distribution, smaller particles can fill the pores created by larger particles [16]. If the paper is too porous then chemical consumption during the papermaking process will increase, however if it is not porous enough it may not hold inks well. Proper particle size of PCC fillers and pigments is also essential for achieving optimum light scattering and should be considered along with the PSD, density and other aggregate properties. For optimum scattering, the most effective particle size is about half the wavelength of the incident light and the particles should have as narrow a distribution as possible around this size [54]. In coating applications, the absence of course, rather than the presence of fine PCC particles is a more important factor in determining the gloss of the coating and PCC particles or agglomerates larger than about 5µm rapidly lower the gloss [37].

The PSD also has an influence on the papermaking process [30] [55]. Large, non-uniform particles in fillers increase the abrasiveness of the paper, leading to wire abrasion and metal loss in the paper machine. The abrasion potential of fillers is influenced by the particle structure, the particle fineness, and the particle hardness. Relatively coarse plate-shaped pigments tend to be less abrasive than non-platy ones of similar size. Increasing the filler fineness decreases the abrasion potential in the wire section of paper machine (where the pulp suspension is formed into an endless web by dewatering) significantly.

Although a narrow PSD and high purity are two common objectives in any precipitation process, the very small particle size required for PCC is somewhat unusual. In many industrial crystallization processes the objective is to produce a coarse product because fine particles are more difficult to separate from solution (in filtration or gravity separation for example), have poorer flow properties, and cause dust problems during transport and handling. In the case of PCC however, it is often produced as a slurry rather than as a powder thus avoiding the need for costly separation and product drying [38].

3.3.5 Specific Surface Area (SSA)

The PSD and morphology of the crystals affects the SSA of PCC [35]. For a given mass of particles, finer particles will have a higher SSA and this is usually evident in the specifications of most PCC grades. Particle size and surface area influence a number of aspects of papermaking, including brightness and the function of retention chemicals. For example, finer filler particles consume more retention aids and sizing agents [35] .

3.3.6 Slurry Concentration

Coating PCC is usually delivered in slurries containing over 70% dry material as opposed to 18-20% for fillers. Coating PCC therefore requires an additional dewatering stage and as a consequence, the cost of producing coating PCC is generally significantly higher than filling PCC or GCC [48].

3.3.7 Surface Charge

The surface charge of PCC is important in papermaking, as well as other applications, because it affects its miscibility with the pulp, which influences both the papermaking process and the mechanical properties of the final paper. The surface of PCC can develop either a positive or negative charge depending on the solution conditions during precipitation and the adsorption of excess ions on the PCC surface. If there is an excess of calcium (Ca^{2+}) cations present during precipitation the PCC surface will become positively charged, but it will become negatively charged if there is an excess of carbonate (CO_3^{2-}) and/or some other spectator anion [35]. Stoichiometric amounts of Ca^{2+} and CO_3^{2-} give a zero surface charge. In most on-site PCC plants however it is more common for PCC to exhibit a slight positive surface charge, typically in the range +10 to +25 mV or higher [52]. This surface charge is known as the zeta-potential (ζ-potential), and a positive PCC ζ-potential is particularly useful in paper filling applications as cellulose pulp fibre in water carries a slight negative charge. Due to the resulting electrostatic attraction between the negatively-charged fibre and positively-charged PCC, the use of PCC can allow the papermaker to reduce the amount of chemicals needed to cause mineral fillers to be retained in the paper making process. This is an advantage of PCC over clay, talc and GCC as these materials typically carry a negative surface charge if they have not been coated [35]. By contrast, dried PCC can be similar to most GCC products and can have a negative charge, depending on whether dispersants have been used [56].

To highlight the importance of PCC surface charge in other applications, in the plastics industry the dispersion of PCC filler particles in the polymer matrix is of great importance, especially when using PCC of high specific surface area with a tendency to agglomerate. However, the incompatibility of PCC hydrophilic surface with the hydrophobic polymers is a problem and the calcite surface is often modified by a variety of surfactants, such as fatty acids or one of their salts [19].

Table 3.5 – Quality parameters for several commercially available PCC products used in the pulp and paper industry

PCC Product	Supplier	Application/Properties	Grade	Morphology	Purity (%$CaCO_3$)	Brightness (dry)	pH (slurry)	Median size d_{50} (µm)	Nominal SSA (m^2/g)
Albacar[1238]	SMI*	Filler: Increases paper whiteness, brightness, and opacity. HO grade best for optical properties, LO best for strength and calliper.	HO	Calcite, clustered scalenohedral	n/a	>94.5	7.5-9.5	1.3	12
			5970		98	98	n/a	1.9	7
			LO		n/a	>94.5	7.5-9.5	2.2	6
Albafil[1248]	SMI	Filler: Improved paper runnability, porosity control, enhanced scattering with minimal strength loss. S grade best for porosity control, XL for strength and sizing.	S	Calcite, prismatic	97	97	n/a	0.7	10
			M		97	97	n/a	0.9	8
			L		n/a	n/a	n/a	1.4	6
			XL		n/a	n/a	n/a	2.0	4
Megafil[1258]	SMI	Filler: Provides stiffness, strength, opacity and bulk. Grade 1000 is best for optical properties and porosity, 3000 best for strength and calliper.	1000	Calcite, prismatic	n/a	n/a	n/a	1.1	7
			2000		n/a	n/a	n/a	1.5	6
			3000		n/a	n/a	n/a	2.2	4
Albaglos[1268]	SMI	Coating: Paper and paperboard surface coating where high brightness and gloss (S) or matte is desired (XL)	S	Calcite, prismatic	n/a	n/a	n/a	0.6	9
			L		n/a	n/a	n/a	1.5	5
			XL		n/a	n/a	n/a	2.2	4
Opacarb[1278]	SMI	Coating: Gives high brightness and opacity increases not attainable with other PCC grades.A40 gives the highest gloss, A60 best fibre coverage.	A 40	Aragonite	n/a	n/a	n/a	0.4	12
			A 50		n/a	n/a	n/a	0.5	10
			A 60		n/a	n/a	n/a	0.6	9
Syncarb[9]	Omya	Filler: Pure white, anionically dispersed PCC for high brightness, opacity and bulk in papermaking	F0474-MJ 52%	Calcite, scalenohedral	99	95	9.3	1.8	5.5
Precarb[10]	Schaefer Kalk	No grade-specific uses given but Precarb is used in the pulp and paper, plastics, and pharmaceuticals industries	100	Calcite, scalenohedral	99	99 (DN 53163) 97 (R_{457})	n/a	1	9
			140	Calcite, scalenohedral	99	93 (R_{457})	n/a	1.3	9
			150	Calcite, scalenohedral	99	98 (DN 53163) 96 (R_{457})	n/a	3	5
			400	Calcite, scalenohedral + aragonite (35%)	99	99 (DN 53163) 97 (R_{457})	n/a	0.8	8
			724	Calcite, rhombohedral	99	98 (DN 53163) 96 (R_{457})	n/a	0.5	40
			800	Calcite, platelike	96	99 (DN 53163) 97 (R_{457})	n/a	1.1	17

n/a: not available

*Specialty Minerals Inc. (SMI) is a wholly owned subsidiary of Minerals Technologies Inc. (MTI)

[1] [49]; [2] [57]; [3] [27]; [4] [58]; [5] [59]; [6] [60]; [7] [61]; [8] [62];[9] [63];[10] [26]

3.4 Target PCC Quality

Given the wide variety of PCC applications and quality requirements, it should be decided *a priori* the intended market for the PCC and thus the PCC quality to be targeted in the experimental work. Even in the same market, e.g. the pulp and paper industry, many different types of PCC products are used. At this stage no price information is available on the different grades of commercial PCC products, but a reasonable assumption to make is that those products with a higher price would probably be more difficult to manufacture and/or cost more to produce (higher temperature, need for additional reagents etc.). Given that the demand of different types of PCC may fluctuate depending on market price, an ideal outcome of this series of experimental work would be a 'recipe' for how to produce PCC of varying parameters (SSA, PSD, morphology) as a function of the precipitation conditions. In this way, the PCC production process and equipment could be designed and commercialised in such a way as to maximise flexibility of the type of PCC that could be produced. While it would be interesting from an academic point of view to be able to produce PCC of any morphology, size and PSD, it should be kept in mind that the focus of the Slag2PCC process at this stage is on the production of PCC for the pulp and paper industry. The selection and range of parameters investigated in this experimental work will therefore be narrowed down as far as possible so as to concentrate on the production of PCC which could be used in the pulp and paper industry, based on the information available in the literature.

In the absence of detailed technical information from commercial pulp and paper plants about the quality requirements of PCC, the assumption is made that if PCC can be produced with the same quality as the commercially available grades outlined in Table 3.5 then this should be of sufficient quality for pulp and paper plants.

It is evidently clear from the data gathered in Table 3.5 that there are several minimum requirements for any grade of PCC to be used in the pulp and paper industry:

i) Narrow particle size distribution
ii) Very high purity (mostly $x_{CaCO_3} \geq 99\%$, though some grades $\geq 97\%$)
iii) Very small particle size ($d_{50} \leq 3$ µm)
iv) Scalenohedral calcite, rhombohedral calcite or aragonite morphology

Until these requirements are met then it is unlikely that the PCC from the Slag2PCC process could be used as a filler or coating.

4 PCC Production from Steelmaking Slag (Slag2PCC)

Mineral CO_2 sequestration by the carbonation of alkaline Ca/Mg silicate minerals has received considerable interest since the early 1990s as a means of locking-up anthropogenic CO_2 emissions on a large scale and helping to mitigate global warming [64, 65, 66]. In principle, mineral carbonation mimics the natural weathering process by which calcium- and magnesium-containing minerals are converted to calcium and magnesium carbonates by atmospheric CO_2; albeit at a greatly accelerated rate [65]. This process is represented by the equation below.

$$(Ca, Mg)SiO_{3(s)} + CO_{2(g)} \rightarrow (Ca, Mg)CO_{3(s)} + SiO_{2(s)} \quad (4.1)$$

Although natural magnesium silicate deposits of serpentine ($Mg_3Si_2O_5(OH)_4$) and olivine ($(Mg,Fe)_2SiO_4$) are quite abundant with significant potential for CO_2 storage, the potential of natural calcium silicates (e.g. basalt, wollastonite ($CaSiO_3$)) is much lower as they tend to contain less calcium or are less abundant [24]. Aside from these natural sources of alkaline silicate materials, a number of industrial wastes and by-products including steelmaking slag, combustion ash residues from power plants and incinerators, as well as waste cement are an attractive option for carbonation as they are readily available, generally unwanted (hence low-cost) and often located close to a source of CO_2 [24, 65, 67].

Carbonation processes can be classified as either direct or indirect [24, 67]. Direct carbonation is the simplest approach to mineral carbonation and the principal approach is that a suitable solid feedstock is carbonated in a single process step [67]. For an aqueous process this means that both the extraction of metals from the feedstock and the subsequent reaction with CO_2 to form carbonates takes place in the same reactor. If the carbonation is divided into several steps it is classified as indirect carbonation. In this case the reactive component (usually magnesium or calcium) is first extracted from the feedstock in one vessel and subsequently carbonated in a second vessel. While more complex, indirect carbonation can produce a very high purity carbonate product if the extracting solvent is selective as fewer impurities from the original material are present in the solution where precipitation takes place.

In Finland, where both the iron and steel and pulp and paper industries have a strong presence, the production of PCC by indirect carbonation of steelmaking slag has been proposed as a potential method of simultaneously reducing the CO_2 emissions from the steel industry and turning a waste stream into a valuable product [4, 5]. In the Slag2PCC process, a solvent (typically a solution of NH_4Cl) is used to extract calcium from steelmaking slag. The resulting Ca-rich solution is bubbled with CO_2 gas which reacts to form PCC. This PCC can replace limestone used in the production of steel thus reducing virgin material consumption and associated CO_2 emissions or, if the PCC can be produced at sufficiently high quality, it could be sold at a higher price to the pulp and paper industry. PCC in paper and paperboard constitutes long-term storage for the captured CO_2 except in cases where the paper or sludge from recycled paper is combusted [3]. Another potential benefit of this process is that the removal of free CaO from steel converter slag may stabilise and render it suitable for use as a construction material [8].

The extraction step in which calcium in the steel slag is dissolved can be described by the following reactions [50],

$$CaO_{(s)} + 2NH_4Cl_{(aq)} + H_2O_{(l)} \leftrightarrows CaCl_{2(aq)} + 2NH_4OH_{(aq)} \quad (4.2)$$

$$CaO_{(s)} + H_2O_{(l)} \leftrightarrows Ca^{2+} + 2OH^-_{(aq)} \quad (4.3)$$

$$2CaO_{(s)} \cdot SiO_{2(s)} + 2NH_4Cl_{(aq)} + H_2O_{(l)} \leftrightarrows CaCl_{2(aq)} + CaO_{(s)} \cdot SiO_{2(s)} + 2NH_4OH_{(aq)} \quad (4.4)$$

The net carbonation and precipitation reactions are then given as [50],

$$2NH_4OH_{(aq)} + CO_{2(g)} \leftrightarrows (NH_4)_2CO_{3(aq)} + H_2O_{(l)} \quad (4.5)$$

$$(NH_4)_2CO_{3(aq)} + CaCl_{2(aq)} \leftrightarrows CaCO_{3(s)} + 2NH_4Cl_{(aq)} \quad (4.6)$$

Based on the stoichiometry of the foregoing reactions, it can be seen that the ammonium salt consumed in the extraction step is regenerated in the carbonation step, allowing it to be reused continuously. A simplified schematic of the Slag2PCC process is shown in Figure 4.1. Not shown in this figure are the PCC washing, spent slag washing and filtration steps.

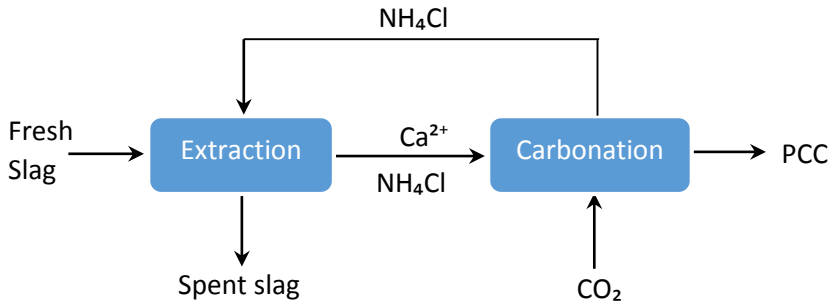

Figure 4.1 - Simplified process scheme of the Slag2PCC process [50]

The price of granulated EAF slag, BOF slag and BF slag was approximately 8 €/t in 2010 [68]. The price of quicklime is around 85 €/t (US price 116 USD/t in 2012). Assuming steel slag is 32% Ca by mass (45% CaO) and quicklime is 71% Ca, the effective raw calcium costs from slag and quicklime are approximately 25 €/t Ca, and 119 €/t Ca respectively. If only 50% of the calcium in slag can be extracted the cost becomes 50 €/t Ca, increasing to 83 €/t Ca if only 30% is extracted. Thus the use of steelmaking slags as a source of calcium for PCC production is financially attractive despite its lower calcium content, although the economics are highly dependent on the amount of calcium which can be extracted.

Aside from the issue of calcium extraction from slag which has been extensively studied [4, 5, 8, 24], previous work on the development of the Slag2PCC process has highlighted that there are several major aspects of the process which must be addressed for it to be viable, namely

- PCC Quality
- Solvent loss
- CO_2 capture efficiency
- After-treatment processes

The quality of the PCC produced by the Slag2PCC process is of utmost importance to the commercial viability of the technology. If the PCC is of poor quality then it cannot be sold at a high price to the pulp and paper industry, or alternatively, a pulp and paper plant would not be able to realise significant cost savings by fully substituting Slag2PCC product for their existing PCC product due to the reduction in quality.

Based on the stoichiometry of reactions (4.2)-(4.6) the ammonium salt consumed in the extraction step is regenerated in the carbonation step which should allow it to be reused in a continuous process, however this would only be the case in an ideal system. In practice solvent may be lost from the system in several ways [50]:

- It will be present in the PCC filter cake after filtration as moisture
- It may become incorporated in the PCC crystal structure during crystal growth and be removed along with the PCC product
- It may be present in the crystal pores or adsorbed on the surface of the PCC crystals which is then removed with the PCC product
- It may precipitate on the solid slag residue during the extraction step
- It may react with an impurity forming an insoluble salt which is removed with the PCC
- It may be stripped from the solution by the carbonating gas as ammonia (NH_3) vapour

Solvent losses represent increased process costs as additional makeup solvent would be required and the work of Eloneva et al. [24] showed that the consumption of solvent is a key factor in determining the overall economics of the Slag2PCC process. Thus loss of solvent should be avoided as much as possible. Mannisto [69] estimated the NH_3 losses to be less than 1% during carbonation depending on the flow rate of carbonating gas.

Mattila et al. [70] have shown that while the Slag2PCC process does in principle offer significant environmental benefits, if intensive after-treatment processes are required for purifying the PCC from the Slag2PCC then the benefits are eroded and it can pollute more than conventional PCC production technologies. In particular, if high concentrations of NH_4Cl solvent are used then washing of the solids is necessary for recovering the salt from the steel slag residue after extraction and from the produced PCC; the former for environmental reasons and the latter for product quality reasons. Recovery of the water and solvent in this way could constitute the most energy-consuming step of the Slag2PCC process if this is accomplished with evaporation. Mattila [71] has proposed using very low concentrations of NH_4Cl (0.01M) to reduce the need for washing, however this would have an adverse effect on calcium extraction efficiency and necessitate a multi-stage extraction process.

5 Extraction of Calcium from Steel Slag

Before being used in the production of PCC, the calcium must be extracted from the steel slag as effectively as possible. Although steel slag can contain up to 50% CaO it also contains many other elements which, if also dissolved, may re-precipitate with the PCC and reduce the final PCC product purity. Furthermore, the effective calcium cost from slag increases with decreasing extraction efficiency as shown in section 3.4, thus it is important that the extraction process is both selective for calcium and efficient in terms of the amount of solvent required. As the focus of this work is not on the extraction aspect of the process the theoretical aspects of extraction will not be given a full treatment. Instead this section presents the main results of the extraction experiments performed as part of the Slag2PCC project and in particular those aspects which have consequences for the precipitation experiments and the Slag2PCC process as a whole.

5.1 Solvent Selection

A number of studies on the selective extraction of calcium from steel slag have been undertaken. Eloneva [24] attempted to produce PCC using calcium selectively extracted from steelmaking slag with acetic acid; this solvent being highlighted as promising by Kakizawa et al. [72]. It was found that although the calcium was dissolved selectively, the amount of alkali required to increase the pH high enough for PCC precipitation would be uneconomically high. A number of other solvents were tried at various concentrations with a wide range of calcium extraction efficiencies reported as shown in Figure 5.1. Calcium extraction efficiency (η_{ext}) is defined by the equation below, where $c_{Ca^{2+}}$is the calcium concentration in solution after extraction (g/L), V is the volume of solvent used (L), m_{slag} is the mass of slag used (g) and x_{Ca} the mass fraction of calcium in the slag.

$$\eta_{ext} = \frac{c_{Ca^{2+}} V}{m_{slag} x_{Ca}} \tag{5.1}$$

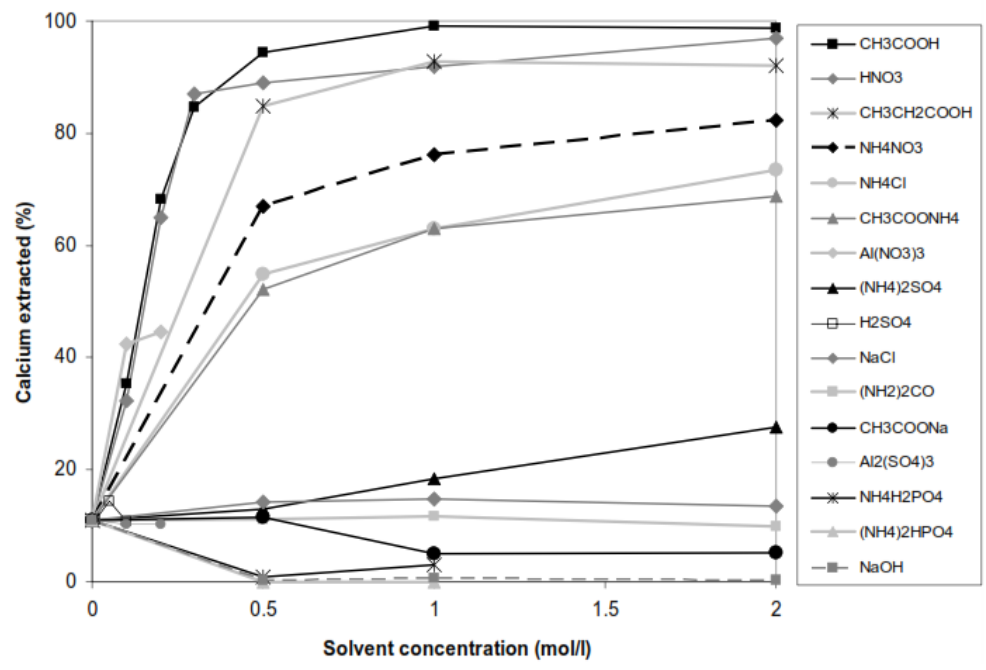

Figure 5.1 - Dissolution of calcium from steel converter slag (1 g) in various concentrations of different solvents (50 ml) at room temperature [24]

Of the other solvents studied only NH_4Cl, ammonium acetate (CH_3COONH_4) and ammonium nitrate (NH_4NO_3) were found to be as selective for calcium as acetic acid, although their extraction efficiency was poorer. Both NH_4Cl and NH_4NO_3 are salts of a weak base and a strong acid, giving aqueous solutions that are acidic. CH_3COONH_4 is a salt of a weak acid and weak base and its aqueous solution should be effectively neutral, however it was found to dissolve calcium from the slag almost as efficiently as NH_4NO_3 and NH_4Cl, indicating that solution acidity was not the only factor at play in the dissolution of calcium from steel converter slag with these salts [24]. Of the three salts, NH_4Cl has been selected as the most promising to use in the Slag2PCC process due to its lower cost [73].

5.2 Effect of Extraction Conditions on Calcium Extraction Efficiency

The extraction of calcium from steel converter slag using these three ammonium salts was further studied by Said et al. [5]. They investigated the effect of slag particle size, solvent concentration, slag/solvent ratio and extraction time on calcium extraction efficiency. The results of this work are summarised here.

5.2.1 Effect of Particle Size

As could be expected from mass transfer principles, Said et al. [5] found that the smaller the slag particle size the higher calcium extraction efficiency, as shown in Figure 5.2. With smaller particle size the solid-liquid interfacial area is larger, extraction rate is higher and more calcium is available for dissolution. For each solvent, most of the available calcium (80-90%) was extracted after about 20 minutes. Continuing the extraction for an additional 40 minutes led to only a marginal increase in extraction efficiency.

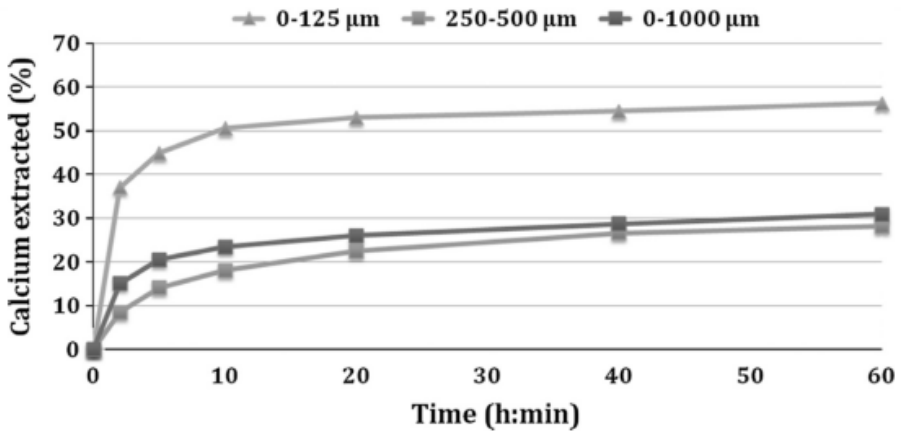

Figure 5.2 - Effect of slag grain size and extraction time on calcium extraction efficiency (1M NH_4Cl, 20 g slag/L) [5]

5.2.2 Effect of Solvent Concentration

The effect of solvent solution strength on calcium extraction efficiency was less pronounced than the effect of slag particle size. As can be seen in Figure 5.3 a doubling of the solvent strength from 1 to 2 M only increased extraction efficiency by between 5 and 10 percentage points, thus a strength between 0.5-1 M seems most optimum.

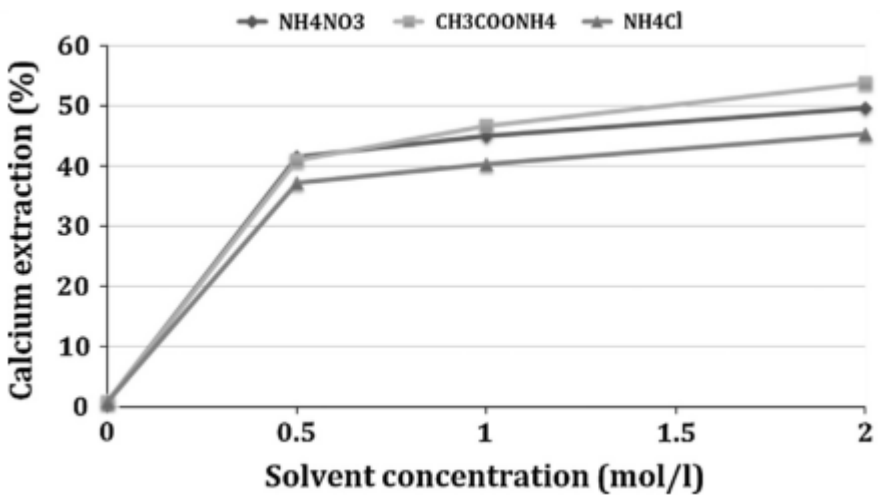

Figure 5.3 – Effect of solvent strength on calcium extraction efficiency from steel slag (1h extraction, 20 g slag/L) [5]

5.2.3 Effect of Solid to Liquid Ratio (SLR)

The ratio of solid slag to liquid solvent (SLR) (g/L), defined in equation (5.2) below, also had a strong influence on calcium extraction as can be seen in Figure 5.4,

$$SLR = m_{slag}/V \tag{5.2}$$

Calcium extraction was highest at low solids concentrations and reduced with increasing solids. Operating at low levels of solids would increase the size and cost of the extraction equipment, and given rate of extraction efficiency deterioration appears to display a minimum between 20 and 50 g/L this could prove to be an attractive operating range. Figure 5.4 shows that extraction efficiency deteriorated very strongly in particular for NH_4Cl at high SLR, but as these were only single-run tests, it may be erroneous and should be verified.

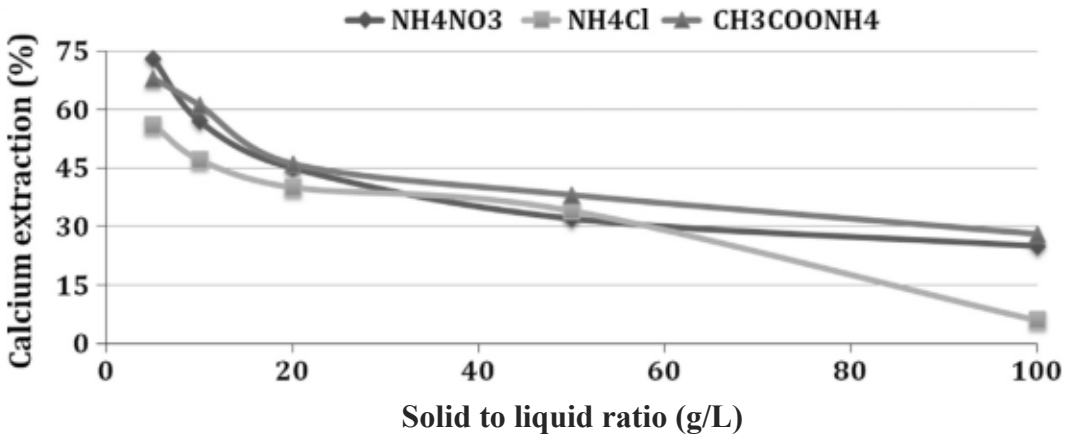

Figure 5.4 - Effect of solid to liquid ratio (SLR) on calcium extraction efficiency (1M NH_4Cl, slag 74-125µm) [5]

5.2.4 Effect of Temperature

Temperature did not appear to have a significant effect on calcium extraction efficiency in the study by Eloneva et al. [8] using acetic acid as solvent. Mattila et al. [50] also found that temperature had minimal effect on extraction kinetics with NH_4Cl and NH_4NO_3 solvents.

6 Precipitation of PCC

The second step in the Slag2PCC process is the reactive crystallisation or precipitation of $CaCO_3$ as PCC via carbonation of the Ca-rich solution from the extraction stage. Despite its widespread use and familiarity the process of carbonation and PCC precipitation is complex and still not completely understood. This complexity arises because PCC can precipitate in multiple crystalline forms (calcite, aragonite, and vaterite) and many of the variables during precipitation such as solution pH, composition, temperature, and ionic strength are interrelated and can interact with each other [74]. Further complicating matters is the fact that carbonation is a multiphase (solid, liquid and gas) process, which means that gas-liquid mass transfer must also be taken into consideration, in addition to chemical reaction kinetics, crystal growth (liquid-solid mass transfer) and diffusion within solution.

The process of nucleation and growth of solid particles from a supersaturated solution is commonly referred to as crystallization or precipitation. The processes of nucleation and crystal growth require supersaturation, but there are several ways to induce supersaturation in a solution. Although the terms crystallization and precipitation are often used interchangeably when referring to the production of solids from solution in this general sense, they actually have quite traditional specific definitions. When external means such as temperature, evaporation or pressure are used to reduce the solubility of an unreactive solute in a solution to produce a solid this is known as *crystallization* [75]. When another component is added to the solution which reacts with the solute and produces a sparingly soluble or insoluble species (as is the case of adding CO_2 to a solution containing Ca^{2+} to form PCC) this is known as reactive crystallization, or more commonly *precipitation*. Whichever means is used to achieve supersaturation, the system attempts to achieve thermodynamic equilibrium through nucleation and the growth of nuclei.

This section begins with some background crystallisation theory and data for the NH_4Cl-CO_2-Ca-H_2O system which are necessary to provide a basis for the subsequent discussion and experimental work in Chapter 7. After this the chemical reactions and equilibria relevant for carbonation are discussed, followed by a review of the literature on the factors affecting PCC production in order to inform the design of the experimental work.

6.1 Crystallization Theory and Phenomena

As a basis for the experimental work and subsequent discussion it is appropriate to cover some fundamental crystallization concepts. However, crystallisation is a complex topic and a full treatment is not possible. Only those aspects which are relevant to the present work and will be considered here.

6.1.1 Solubility

The solubility of a solute in a solvent can be expressed in a number of ways such as mol/L or g/L. In the case of a sparingly soluble salt in water however, it is often expressed in terms of the concentration solubility product, K_c, which for any salt is determined by the product of the solvated ion concentrations raised to their respective stoichiometric coefficients in a saturated solution. In the case of a salt dissolving into x cations and y anions with charges z^+ and z^-,

$$M_xA_y \leftrightharpoons xM^{z+} + yA^{z-} \tag{6.1}$$

$$K_c = (c_+)^x(c_-)^y \tag{6.2}$$

where $c_+$and c_- are the concentrations of the cation and anion respectively. This is possible because at very low ionic concentrations the solution approaches an ideal solution, in which the interactions between solute and solvent molecules are identical to those between the solute molecules and the solvent molecules themselves [76]. From tabulated values of K_c one can determine the concentration of salt ions in equilibrium with the crystal, i.e. its solubility for a given temperature and pressure. However, the simple concentration solubility product while useful, is limited only to very dilute solutions, i.e. very sparingly soluble salts (<10^{-3} M). Thus it would be acceptable for determining the solubility of $CaCO_3$ in pure water (K_c= $3.36 \cdot 10^{-9}$ [77]), however, as will be shown the NH_4Cl solvent considerably increases the solubility of $CaCO_3$.

In concentrated solutions (>10^{-3} M) and solutions in which multiple different ions exist, the equilibrium solute concentration can no longer be determined from the simple solubility product K_c because there can be strong interactions between the ions and the solution cannot be considered ideal. In this case it is more accurate to use the activity solubility product, K_a, defined as [76]

$$K_a = (a_+)^x (a_-)^y \tag{6.3}$$

where the activities of cation and anion, a_+ and a_-, are defined as the product of their concentrations in solution and an activity coefficient, γ, introduced to account for non-ideal solution behaviour [76].

$$a = c\gamma \tag{6.4}$$

Non-ideal solution behaviour results from electrostatic interactions between charged ions and molecules in solution which have the effect of reducing the effective concentration of these species when they react. A species with an activity coefficient of 0.5 means that the effective concentration of the species is only 50% of the actual molar/molal concentration which can have a significant impact on its reaction rate. Using equation (6.4), equation (6.3) can be rewritten as,

$$K_a = (c_+\gamma_+)^x (c_-\gamma_-)^y \tag{6.5}$$

where γ_+ and γ_- are the activity coefficients for the cation and anion respectively. In the case of ideal solutions or heavily diluted electrolytes (infinite dilution), γ is unity. Rearranging the equations allows K_a to be related to K_c with the following expression,

$$K_a = K_c(\gamma_\pm)^\upsilon \tag{6.6}$$

where $\gamma_\pm$ is the mean ionic activity coefficient and υ ($= \upsilon_+ + \upsilon_- = x + y$) is the total number of moles of ions in 1 mole of solute i.e. the number of ions in a formula unit of the salt (e.g. $CaCO_3$ = $Ca^+ + CO_3^{2-}$ thus υ = 2).

6.1.1.1 Solubility of $CaCO_3$ in the CO_2-NH_4Cl-H_2O System

The effect of the NH_4Cl solvent on the solubility of $CaCO_3$ is demonstrated in Figure 6.1 and Figure 6.2 which show the solubility of $CaCO_3$ in pure water and in water containing varying concentrations of NH_4Cl respectively [78]. At 25°C the solubility of $CaCO_3$ in pure water is 0.056 g/L. Adding only 0.125 M NH_4Cl the solubility increases to 0.285 g/L, a 5-fold increase. At an NH_4Cl concentration of 1 M which was identified as a likely target solvent concentration in the Slag2PCC process, the solubility of $CaCO_3$ at 25°C is 0.678 g/L, a 12-fold increase.

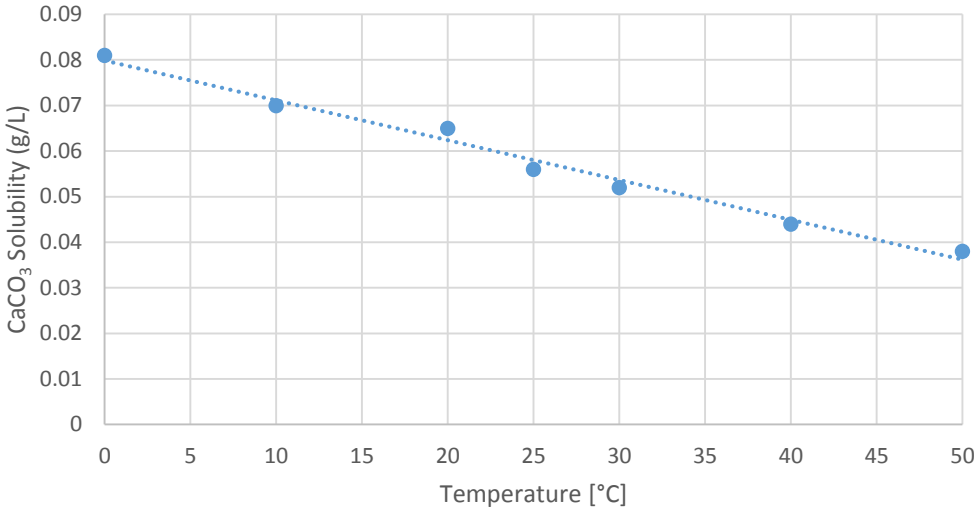

Figure 6.1 - Solubility of $CaCO_3$ (calcite) in water [78]

$CaCO_3$ is a somewhat unusual solid in that its solubility in pure water decreases with temperature rather than increases, as is the case with most salts. However, the data in Figure 6.2 shows that with the addition of NH_4Cl solvent this behaviour changes and it becomes more soluble at higher temperatures.

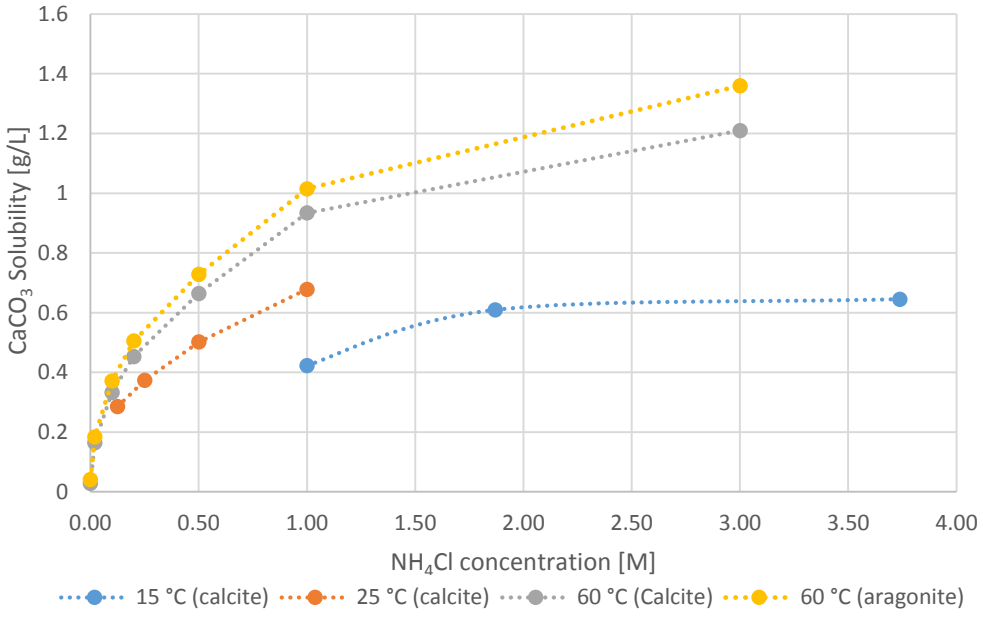

Figure 6.2 - Effect of NH_4Cl solvent strength and solution temperature on the aqueous solubility of $CaCO_3$ [78]

6.1.1.2 Solubility of CO_2 in the CO_2-NH_4Cl-H_2O System

Another feature of the $CaCO_3$-NH_4Cl-H_2O system to consider is the solubility of CO_2 in solution, as well as the effect of CO_2 partial pressure on the solubility of $CaCO_3$. Increasing the partial pressure of CO_2 in the gas phase in contact with water or an aqueous will increase the solubility of CO_2 in the solution by Henry's law, however at low pressures (1-2 atm) the effect of pressure on the solubility of CO_2 in water is negligible. For the CO_2-NH_4Cl-H_2O system, Findlay and Shen [79] found that the solubility of CO_2 in aqueous NH_4Cl was lower than in pure water and decreased further with increasing solution

concentration. They also found that at low pressures (1-2 atm) the solubility of CO_2 in NH_4Cl solution was independent of pressure as is the case with pure water. Rumpf et al. [80] produced data on the solubility of CO_2 in NH_4Cl solutions at pressures of up to 90 bar and temperatures from 40 to 60 °C, showing that at these high pressures the solubility of CO_2 does increase. Although it would be beneficial for the Slag2PCC process to increase the solubility of CO_2 gas in the solution, this would require energy intensive gas compression if flue gas was used. Thus, focusing on carbonation at or close to atmospheric pressure seems more reasonable, in which case the CO_2 partial pressure will be determined by the mole fraction of CO_2 in the carbonating gas.

Figure 6.3 below shows solubility data for CO_2 in aqueous solutions of NH_4Cl taken from the literature as a function of both temperature and NH_4Cl concentration. These data however only apply strictly to physical solubility i.e. $CO_{2(aq)}$ in solutions of pure NH_4Cl. In the Slag2PCC process the Ca-rich solution will also contain OH^- and other ions which can react with CO_2 and affect the amount which can be taken into solution. The figure shows that CO_2 solubility decreases with both increasing salt concentration and increasing temperature.

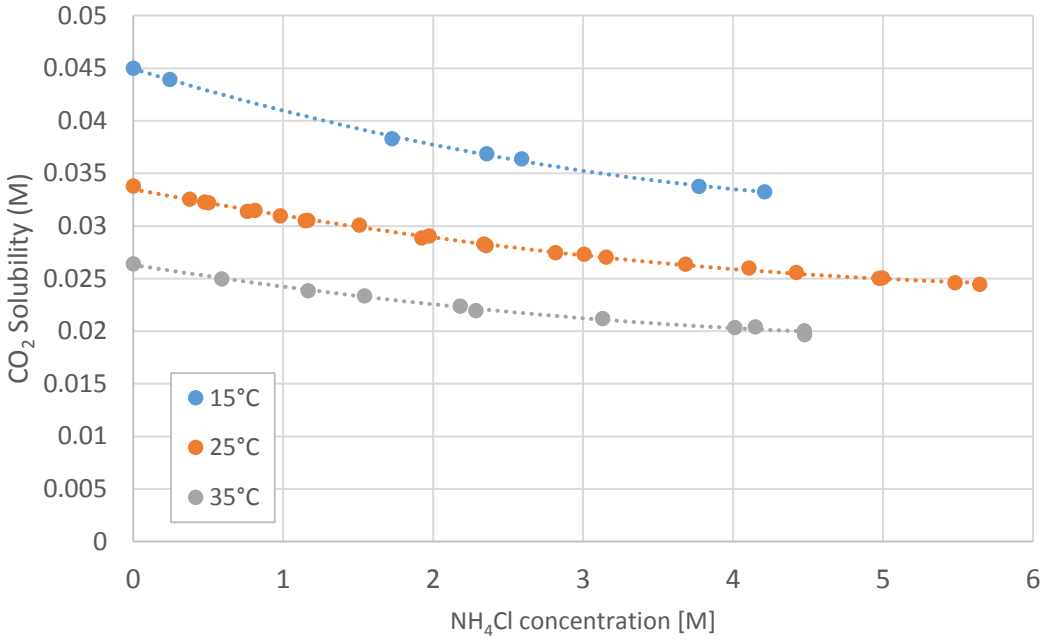

Figure 6.3 - Solubility of CO_2 in aqueous solutions of NH_4Cl [81]

6.1.2 Supersaturation

The driving force for precipitation is commonly thought of as the difference between the concentration of a solute c, and the equilibrium value c^*. This deviation can be expressed in several different ways in the literature where it is found as an absolute supersaturation Δc, a supersaturation ratio s, or as a relative supersaturation σ [82].

$$\Delta c = c - c^* \tag{6.7}$$

$$s = {}^{c}/_{c^*} \tag{6.8}$$

$$\sigma = {}^{\Delta c}/_{c^*} \tag{6.9}$$

These relations are usually sufficient for precipitation from solutions of low-concentration which can be approximated as ideal or nearly ideal, however for more complex systems a more detailed treatment of supersaturation is usually necessary.

The fundamental thermodynamic driving force for crystallization is the difference between the chemical potential μ, of the given substance in the transferring and transferred states, e.g. in solution (state 1) and in the crystal (state 2) [76]. This may be written, for the simple case of an unsolvated solute crystallizing from a binary solution, as

$$\Delta\mu = (\mu_2 - \mu_1) \tag{6.10}$$

The chemical potential is defined in terms of the standard potential, μ_0, and the activity

$$\mu = \mu_0 + RT\ln(a) \tag{6.11}$$

where R is the universal gas constant, T is the absolute temperature, a is the activity of the solute as before. Combining the two equations allows the driving force for crystallization to be expressed as

$$\frac{\Delta\mu}{RT} = \ln\left(\frac{a}{a^*}\right) = \ln(S) \tag{6.12}$$

where a^* is the activity of a saturated solution and S is the fundamental supersaturation,

$$S = e^{\Delta\mu/RT} \tag{6.13}$$

For solutions of electrolytes it is more appropriate to use the mean ionic activity, $a_\pm$, defined in the previous section.

$$a = a_\pm^\upsilon \tag{6.14}$$

Supersaturations in aqueous solutions of sparing soluble electrolytes (such as $CaCO_3$) are best expressed in terms of the solubility product,

$$S = \left(\frac{IAP}{K_a}\right)^{1/\upsilon} \tag{6.15}$$

where IAP is the ion activity product of the ions in solution (e.g. $a_+ \cdot a_-$), and K_a is the activity solubility product of the salt as defined earlier (i.e. the value of IAP at equilibrium). In the case of $CaCO_3$ the above equation written out in full is given by [82],

$$S = \sqrt{\left(\frac{a_{Ca^{2+}} \cdot a_{CO_3^{2-}}}{K_a}\right)} = \sqrt{\left(\frac{\gamma_\pm^2 \cdot c_{Ca^{2+}} \cdot c_{CO_3^{2-}}}{\gamma_\pm^{*2} \cdot c^*_{Ca^{2+}} \cdot c^*_{CO_3^{2-}}}\right)} \tag{6.16}$$

Thus, the driving force for precipitation of $CaCO_3$ depends on the ratio between the actual and equilibrium ion concentrations (i.e. the solubilities), as well as the activity coefficients. Activity coefficients can be estimated by several methods in the literature, most of which rely on data about the interaction between ions and molecules in solution. The ionic strength of the solution I also has a strong effect on the activity coefficient and is calculated from the sum of the concentration c_i, and charge z_i, of every ion in solution as shown in equation (6.18).

$$I = \frac{1}{2}\sum c_i z_i^2 \tag{6.17}$$

According to Zemaitis et al. [83] the most important interactions in the system CO_2-NH_3-H_2O are considered to be between NH_4^+-OH^-, $NH_{3(aq)}$- $NH_{3(aq)}$, $NH_{3(aq)}$-OH^-, H^+-HCO_3^-,H^+-CO_3^{2-}, $CO_{2(aq)}$-H^+, $CO_{2(aq)}$-HCO_3^-, $CO_{2(aq)}$-CO_3^{2-}, $CO_{2(aq)}$-$CO_{2(aq)}$, $NH_2CO_2^-$-$NH_{3(aq)}$, $NH_2CO_2^-$-H^+, and $NH_2CO_2^-$-NH_4^+. In addition to these ions and interactions, the presence of Ca^{2+} and Cl^- should also be taken into account. More detailed information on data for these interactions and activity coefficient calculations specifically for the Slag2PCC process are given in Appendix C.

6.1.3 Nucleation

Nucleation is the process by which solid particles are formed in a liquid solution. As nucleation leads to an increase in the total number of particles i.e. the population, it is also known as a crystal birth process. The rate of nucleation plays an important role in controlling the final PSD and is therefore a critical factor to understand and ideally, to control [75].

Nucleation processes are generally classified as either primary or secondary [76]. If nucleation occurs without the prior presence of solution-own crystals (solute crystals formed out of the solution), this is known as primary nucleation. Primary nucleation can also be either homogenous, in which the solid nuclei form spontaneously from a homogeneous liquid phase, or it can be heterogeneous, which is when nucleation is induced by the presence of a foreign solid particle. If solution-own crystals are involved then this is known as secondary nucleation [84]. These different nucleation process are shown in Figure 6.4.

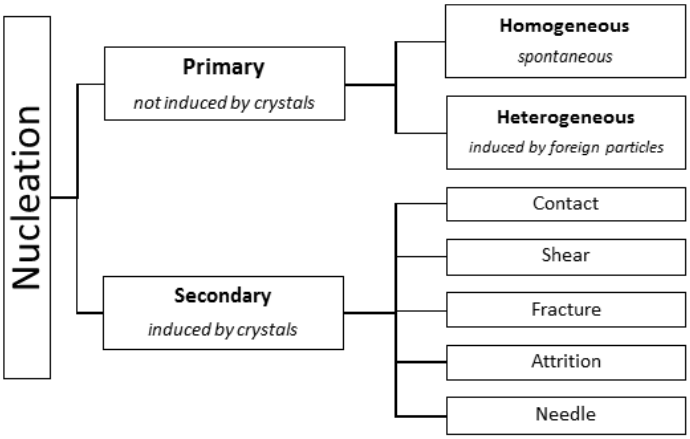

Figure 6.4 - Mechanisms of nucleation [84, 76]

6.1.4 Crystal Growth

The well-known 'Ostwald's step rule' for precipitating systems posits that it is not necessarily the most thermodynamically stable phase which appears first; rather the system transforms into one which most closely resembles itself whose formation is accompanied by the smallest loss of free energy [85] [76]. Subsequent phase transformations then occur stepwise until the most stable phase appears. Although this does not hold for all systems, in the precipitation of $CaCO_3$ a sequence of phase transformations is believed to occur in accordance with the rule of Ostwald. The first step is the formation of an amorphous $CaCO_3$ (ACC) phase, which then transforms to a crystalline vaterite phase. This in turn transforms to either aragonite or calcite depending on the precipitation conditions. Aggregation processes also occur and several transformation pathways to the most stable phase are possible as shown Figure 6.5. Not shown in this figure is the aragonite polymorph.

There are two possible pathways by which crystal phase transformations which can occur: (i) a solid-state transition or (ii) a solution-mediated transformation or dissolution-recrystallization transformation. In the first pathway the transformation is due to internal rearrangements of the crystal lattice, whereas in the second the transformation takes place through the dissolution of the less stable phase and subsequent nucleation and growth of the more stable phase. The solution-mediated transformation is the primary mechanism in the precipitation of PCC as the energies for the solid-state transformations of the metastable polymorphs into calcite are relatively high [85].

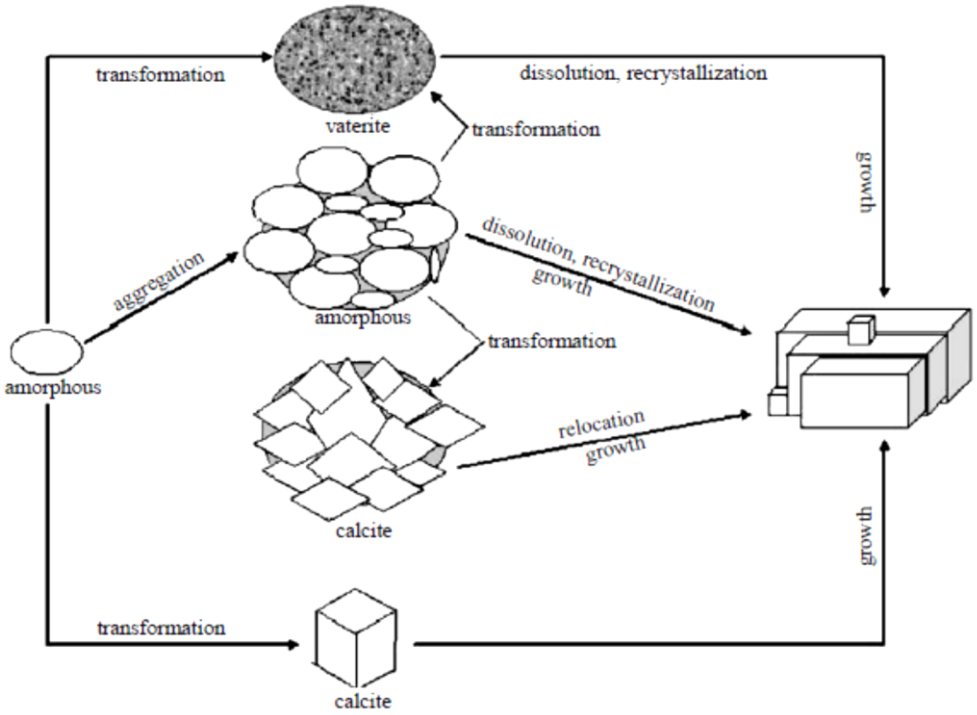

Figure 6.5 - Morphological transformations in precipitation of $CaCO_3$ [15]

6.1.5 Crystal Shape

Crystal shape, or morphology, can be either thermodynamically or kinetically controlled [75]. Thermodynamic control is only significant at low supersaturation, in which case growth proceeds in such a way that the total free energy of a crystal – the sum of the free energies of its volume, surfaces, edges and corners – is minimised [76] . At high supersaturation ratios however, morphology is generally determined by the rate of the slowest growing crystal face. For calcite crystals, the dominant rhombohedral face {104} contains equimolar amounts of Ca^{2+} and CO_3^{2-} ions (and is hence non-polar), thus to positively influence the growth of the {104} face an equivalent coverage with Ca^{2+} and CO_3^{2-} ions is required [86] [87]. Growth of the face is described to go through the formation of the uncharged soluble complex $CaCO_3^0$ at the crystal/solution interface [88]. Given that the langmurian adsorption coefficient for CO_3^{2-} is higher than that for Ca^{2+} ($K_{CO_3^{2-}}$= 3x10^7 cm^3/mol, $K_{Ca^{2+}}$=10^6 cm^3/mol [89]), excess Ca^{2+} in the solution is usually necessary to have similar relative adsorptions of Ca^{2+} and CO_3^{2-} to favour the formation of $CaCO_3^0$. As a consequence, under stoichiometric $[Ca^{2+}]/[CO_3^{2-}]$ conditions it is possible to produce rhombohedral shapes, but under nonstoichiometric conditions with Ca^{2+} in excess, the morphology of the precipitated calcite is normally the scalenohedral one [87]. When the relative growth rate of the {104} face is high enough that it is no longer the slowest growing face, the scalenohedral form is obtained. De Leeuw & Parker [90] and Sekkal & Zaoui [91] give a more thorough account of the compositional and structural differences between the surfaces of calcite, vaterite and aragonite as well as their associated hydration and attachment energies.

6.1.6 Agglomeration

Another factor adding to the complexity of $CaCO_3$ precipitation is crystal agglomeration. Agglomeration is the mechanism by which smaller particles join together and create larger particles. If agglomerates that form during PCC production are not broken down then the effective particle size increases which can result in substandard optical properties, particularly in coating applications [37]. The different polymorphs of PCC display different agglomeration tendencies, with calcite shown to agglomerate much more strongly than vaterite [92]. As will be discussed in 6.5.8, higher CO_2 concentrations in the carbonating gas have also been reported to lead to high levels of agglomeration. While natural $CaCO_3$ produces an essentially agglomerate-free dispersion in water, PCC is more difficult to disperse and is reported to require both high-solids and high-shear mixing for thorough wetting and breaking down of aggregates [37]. Domingo et al. [87] report that in commercial manufacture of PCC where the scalenohedral form is usually obtained, agglomeration cannot typically be avoided without the use of additives. Dispersion agents can be used to modify the surface charges of solid particles in solution in order to reduce the electrostatic attractive forces between them and inhibit the formation of agglomerates [93, 94].

6.2 Chemical Reactions and Relevant Equilibria

To properly study, understand and eventually model the Slag2PCC carbonation process it is necessary to know which chemical species can form and to have an appreciation of the potential reactions and relevant chemical equilibria in the system. Based on information gathered from the literature the following chemical reactions and equilibria are all relevant for the CO_2-NH_3-Cl-Ca-H_2O system.

Vapour-liquid equilibria			
$CO_{2(g)} \rightleftarrows CO_{2(aq)}$			(6.18)
$NH_{3(g)} \rightleftarrows NH_{3(aq)}$			(6.19)
$H_2O_{(g)} \rightleftarrows H_2O_{(l)}$			(6.20)
Liquid phase equilibria	$\log_{10}(K^{25})$	ΔH_r^{25} (kJ/mol)	
$CO_{2(aq)} + OH^-_{(aq)} \rightleftarrows HCO^-_{3(aq)}$	7.642	-46.1	(6.21)
$HCO^-_{3(aq)} + OH^-_{(aq)} \rightleftarrows CO^{2-}_{3(aq)} + H_2O_{(l)}$	3.664	-41.1	(6.22)
$CO_{2(aq)} + H_2O_{(aq)} \rightleftarrows H_2CO_{3(aq)}$	0.009	-0.1	(6.23)
$H^+_{(aq)} + HCO^-_{3(aq)} \rightleftarrows H_2CO_{3(aq)}$	6.366	-9.8	(6.24)
$H^+_{(aq)} + CO^{2-}_{3(aq)} \rightleftarrows HCO^-_{3(aq)}$	10.335	-14.7	(6.25)
$Ca^{2+}_{(aq)} + HCO^-_{3(aq)} \rightleftarrows CaHCO^+_{3(aq)}$	1.054	+1.5	(6.26)
$Ca^{2+}_{(aq)} + CO^{2-}_{3(aq)} \rightleftarrows CaCO^0_{3(aq)}$	10.662	-26.0	(6.27)
$Ca^{2+}_{(aq)} + OH^-_{(aq)} \rightleftarrows CaOH^+_{(aq)}$	1.180	+21.7	(6.28)
$Ca^{2+}_{(aq)} + Cl^-_{(aq)} \rightleftarrows CaCl^+_{(aq)}$	0.148	+4.7	(6.29)
$NH_4^+{}_{(aq)} + HCO^-_{3(aq)} \rightleftarrows NH_4HCO_{3(aq)}$	0.468	-29.1	(6.30)
$NH_4^+{}_{(aq)} + Cl^-_{(aq)} \rightleftarrows NH_4Cl_{(aq)}$	-1.317	-14.2	(6.31)
$NH_{3(aq)} + H^+_{(aq)} \rightleftarrows NH_4^+{}_{(aq)}$	9.458	-53.0	(6.32)
$NH_{3(aq)} + CO_{2(aq)} \rightleftarrows NH_2COOH_{(aq)}$	7.3	-	(6.33)
$NH_2COO^-_{(aq)} + H^+_{(aq)} \rightleftarrows NH_2COOH_{(aq)}$	6.82	-	(6.34)
$NH_{3(aq)} + HCO^-_{3(aq)} \rightleftarrows NH_2CO^-_{2(aq)} + H_2O_{(aq)}$	0.484	-	(6.35)
$H^+_{(aq)} + OH^-_{(aq)} \rightleftarrows H_2O_{(aq)}$	13.998	-55.8	(6.36)
Solid-liquid equilibria			
$Ca^{2+}_{(aq)} + CO^{2-}_{3(aq)} \rightleftarrows CaCO_{3(s),vat}$	7.769	+15.8	(6.37)
$Ca^{2+}_{(aq)} + CO^{2-}_{3(aq)} \rightleftarrows CaCO_{3(s),arg}$	8.237	+11.2	(6.38)
$Ca^{2+}_{(aq)} + CO^{2-}_{3(aq)} \rightleftarrows CaCO_{3(s),cal}$	8.307	+11.7	(6.39)

The thermodynamic equilibrium constant as well as the heat of reaction at 25°C for most of the reactions have been listed alongside. These have been calculated using HSC Chemistry 5 [95] based on reaction thermodynamic data. The effect of temperature on the equilibrium constants has also been determined with the equilibrium constants correlated with temperature using standard regression techniques. These correlations have been provided in Appendix B as well as reaction rates for some of the most important reactions which would be useful in future dynamic modelling.

Equations (6.18) and (6.19) represent the equilibrium between the CO_2 and NH_3 present in the gas and liquid phase. Liquid water will also be in equilibrium with a certain amount of water vapour (6.20).

Equations (6.21)-(6.36) describe the aqueous molecular and ionic equilibria which exist between the carbonate species (6.21)-(6.25), calcium complexes (6.26)-(6.29), ammoniacal and carbamic species (6.30)-(6.35), as well as the water association/dissociation equilibrium (6.36). Equations (6.37)-(6.39) describe the precipitation of vaterite, aragonite and calcite respectively.

Although the equilibrium constants for some of the formation reactions are very small and these components are unlikely to form in any significant quantity (e.g. $NH_4Cl_{(aq)}$, $CaCl^+$), they have still been listed for completeness as they are commonly encountered in the literature and should at least be considered in equilibrium calculations. For example, De Visscher and Vanderdeelen [96] suggest that the metal carbonate species $CaCO_3^0$ and $CaHCO_3^+$ are required to correctly describe $CaCO_3$ solubility data. Neutral ion species also recommended by Harvie et al. [97]. Carbamic species have been included as Mani et al. [98] have shown that carbamate can form in solutions of $CO_{2(aq)}$ and $NH_{3(aq)}$ and Matilla et al. [50] suggested this may explain anomalous pH behaviour during carbonation.

6.3 Mechanism and Kinetics of PCC Precipitation

The mechanism by which $CaCO_3$ is formed during carbonation of calcium-containing alkaline solution is reportedly well known [99] [100]. It involves several steps as summarised below.

1) Absorption of CO_2 gas into solution

$$CO_{2(g)} \leftrightarrows CO_{2(aq)} \tag{6.18}$$

2) Reaction of aqueous CO_2 with hydroxide ions to form bicarbonate

$$CO_{2(aq)} + OH^-_{(aq)} \leftrightarrows HCO^-_{3(aq)} \tag{6.21}$$

3) Subsequent reaction of bicarbonate with further hydroxide to form carbonate

$$HCO^-_{3(aq)} + OH^-_{(aq)} \leftrightarrows H_2O_{(l)} + CO^{2-}_{3(aq)} \tag{6.22}$$

4) Reaction between carbonate and dissolved calcium to precipitate $CaCO_3$

$$CO^{2-}_{3(aq)} + Ca^{2+}_{(aq)} \leftrightarrows CaCO_{3(s)} \tag{6.39}$$

Ionic reactions such as steps 2, 3 and 4 are usually very fast. Step 1 occurs at the gas-liquid interface and step 2, which is a relatively fast reaction, can occur at the interface or in the bulk solution according to the two-film theory of mass transfer (see Figure 6.6) [100]. Thus according to Han et al. [15] the controlling step in carbonation reactions is usually the absorption of CO_2 (Step 1) into solution. This is widely supported by the literature [28, 101, 102]. The rate of transport of CO_2 through the gas film is governed by the following equation [100],

$$N'_{CO_2} a = k_G a (p^{\infty}_{CO_2} - p^{i}_{CO_2}) \tag{6.40}$$

where N'_{CO_2} is the molar flux of CO_2 (mol.s^{-1}.m^{-2}), a is the gas-liquid interfacial area (m^2/m^3), k_g is the gas-side mass transfer coefficient (mol.s^{-1}.m^{-3}.atm^{-1}), $p^{\infty}_{CO_2}$ is the CO_2 partial pressure in the bulk gas and $p^{i}_{CO_2}$ at the interface (atm).

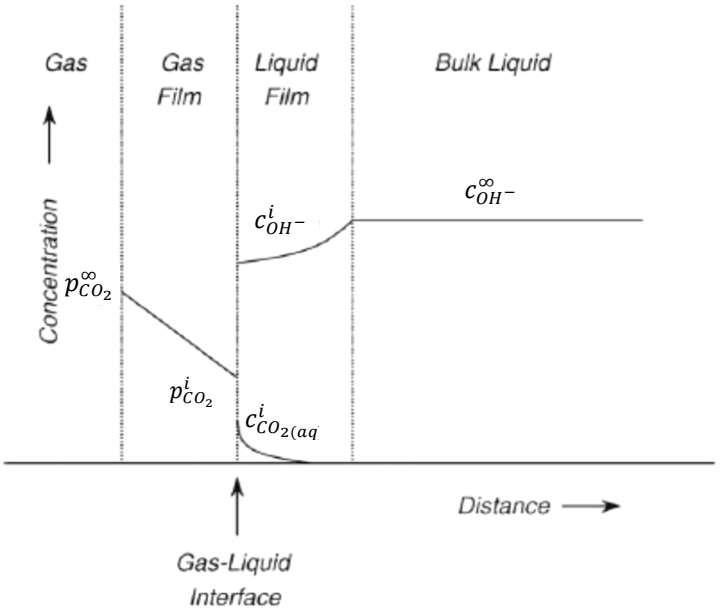

Figure 6.6 – Typical concentration profiles in gas-liquid absorption of CO_2 into an alkaline solution [100]

Once the CO_2 dissolves at the interface, it will react with OH^- at the interface. However, if OH^- becomes depleted at the gas liquid interface due to steps 2 and 3 then the rate of absorption of CO_2 can be significantly reduced. If agitation is sufficiently vigorous and the concentration gradient through the liquid film is sufficiently small, the interface OH^- concentration approaches the bulk solution concentration and in this case the rate of CO_2 uptake by reaction with OH^- (mol/s) is given by Gómez-Díaz et al. [99] as

$$N_{CO_2} = c^*_{CO_2} a \sqrt{c^{\infty}_{OH^-} D_{CO_2} k} \tag{6.41}$$

where $c^*_{CO_2}$ and D_{CO_2} are the solubility (equilibrium concentration) and diffusivity of CO_2 in the aqueous phase, k is the rate constant for the reaction between CO_2 and OH^- to form HCO_3^- (equation (6.21)) and $c^{\infty}_{OH^-}$ is the bulk concentration of OH^- in the aqueous phase. For this approach to be valid the following conditions must be satisfied,

$$\frac{\sqrt{c^{\infty}_{OH^-} D_{CO_2} k}}{k_L} \gg 1 \tag{6.42}$$

$$\frac{\sqrt{c^{\infty}_{OH^-} D_{CO_2} k}}{k_L} \ll \frac{c^{\infty}_{OH^-}}{c^*_{CO_2} z} \sqrt{\frac{D_{OH^-}}{D_{CO_2}}} \tag{6.43}$$

If the first condition is not satisfied this implies part of the reaction between CO_2 and OH^- is carried out at the interface and the other part in the bulk liquid. In this case, Gómez-Díaz et al. [99] give the rate of CO_2 uptake as,

$$N_{CO_2} = c^*_{CO_2} a \sqrt{c^{\infty}_{OH^-} D_A k + k_L^2} \tag{6.44}$$

where k_L is the liquid side mass transfer coefficient.

Looking at equations (6.21) and (6.23) there is actually competition between the reactions of CO_2 with H_2O and with OH^- to form carbonic acid or bicarbonate. The second order rate constant of the reaction of CO_2 with OH^- is ~10^7 times faster than that with H_2O (see Appendix B). As a result at high pH, the hydroxide path is faster, whereas at low pH the water path is faster, with a crossover pH of 8.5 [103].

The reaction between CO_3^{2-} and Ca^{2+} is usually very fast and according to Juvekar and Sharma [100] steps 3 and 4 are essentially instantaneous. Reddy & Nancollas [14] posited that after a brief initial surge due to surface and bulk nucleation, the growth of calcite from a supersaturated solution is a second-order surface-controlled reaction. In a subsequent work they determined the activation energy for calcite crystal growth as approximately 46.1 kJ/mol [104]. Many authors have investigated the kinetics of $CaCO_3$ precipitation according to various models. Inskeep & Bloom [105] for example provide a comparison of different calcite growth models with experimental data. One such model is that of Davies & Jones [106] based on the adsorption layer model which assumes there is a monolayer of hydrated ions covering crystals in aqueous solutions and that hydration or dehydration of lattice ions at surface sites precedes dissolution or precipitation. Applied to calcite the rate equation is,

$$R = sk_{DJ}\gamma_2^2\left(\sqrt{c_{Ca^{2+}}c_{CO_3^{2-}}} - \sqrt{K_{cal}}\gamma_2^{-1}\right)^2 \tag{6.45}$$

where s is the crystal surface area, k_{DJ} is an absorption layer rate constant, γ_2 is the divalent ion activity coefficient and K_{cal} the solubility product of calcite. However, Inskeep & Bloom found that mechanistic models, such as that of Plummer et al. [107], which described elementary reactions at the crystal surface were more successful at predicting calcite precipitation rates. More complicated microscopic models based on kink creation, propagation and collision (CPC) theory for calcite crystal growth in the presence of impurities have also been developed, such as that of Nielson et al. [108]. Many models have a common $(c - c^*)^2$ dependence, highlighting the importance of deviation from equilibrium i.e. supersaturation, as a significant driver for precipitation.

These chemical rate laws are only useful in determining the rate of growth of crystal mass. However, in the production of PCC it is not just the amount or rate of crystal produced which is important. The PSD is also a critical parameter for quality which should be considered and modelled if possible. For this reason the system can be described using not only chemical and mass transfer kinetics, but also a population balance which relates the size L of the particles and their population density, n. The general form of the population balance equation is expressed as [109]:

$$\frac{\partial n}{\partial t} + \frac{\partial (Gn)}{\partial L} + D(L) - B(L) + n\frac{\partial (\ln V)}{\partial t} + \sum_k \frac{n_k \dot{V}_k}{V} = 0 \tag{6.46}$$

The population density n is the number of particles in the size range ΔL per unit volume V of slurry. Equation (6.46) includes terms for the crystal growth rate G, death rate D, and birth (nucleation) rate B in each size fraction. Garside et al. [109] give a full account on how these terms can be determined from either dynamic or continuous crystal growth experiments. Table 6.1 on the following page presents $CaCO_3$ nucleation rate B^0 and linear growth rate G data gathered from the literature which could be used as a starting point and compared with growth rate data to be determined later from the Slag2PCC process.

Table 6.1 – Reported $CaCO_3$ nucleation and linear growth rates from the literature

Reference	Method and System	σ	Seed size (μm)	Agitation rate (rpm)	T(°C)	Nucleation Rate – B^0 (number/m³.s)	Linear Crystal Growth Rate - G (m/s)
Nancollas & Reddy [110]	free-drift, liquid-liquid (Na_2CO_3 + $NaHCO_3$+$CaCl_2$)	0.25-1.1	10	385	25 30	- -	$4.52 \times 10^{-11}\ \sigma^{2.19}$ $5.83 \times 10^{-11}\ \sigma^{2.19}$
Giannimaras & Koutsoukos [110]	pH-stat, liquid-liquid ($NaHCO_3$ + $Ca(NO_3)_2$)	0.42-1.93	1	n.r.	25 30	- -	$1.02 \times 10^{-11}\ \sigma^{2.41}$ $1.32 \times 10^{-11}\ \sigma^{2.41}$
Christoffersen & Christoffersen [110]	pH-stat, liquid-liquid (K_2CO_3 + $KHCO_3$ + $Ca(NO_3)_2$)	0.6-3.3	3	n.r.	37 30	- -	$3.00 \times 10^{-11}\ \sigma^{2.00}$ $2.46 \times 10^{-11}\ \sigma^{2.00}$
Tai et al. [110]	pH-stat, liquid-liquid (Na_2CO_3 + $CaCl_2$)	0.27-2.86 0.37-2.86 0.59-2.86	2 5 8	800	30	- - -	$1.89 \times 10^{-11}\ \sigma^{2.28}$ $3.63 \times 10^{-11}\ \sigma^{2.07}$ $4.18 \times 10^{-11}\ \sigma^{2.19}$
Kotaki & Tsuge [111]*	free-drift, carbonation ($Ca(OH)_2$ + CO_2(10%)	n.r.	unseeded 0.49 0.88 0.92	357	20	$1.1 \times 10^{10} – 3.8 \times 10^{11}$ $3.0 \times 10^{9} – 1.6 \times 10^{10}$ $1.1 \times 10^{10} – 7.1 \times 10^{10}$ $1.7 \times 10^{9} – 7.7 \times 10^{9}$	$6.9 \times 10^{-11} – 1.3 \times 10^{-9}$ $1.1 \times 10^{-10} – 1.2 \times 10^{-9}$ $1.2 \times 10^{-10} – 7.9 \times 10^{-10}$ $1.8 \times 10^{-10} – 9.3 \times 10^{-10}$

*Growth rates were determined as a power function of reaction time, not supersaturation

6.4 Equilibrium Calculations

In preparation for the experimental work and to develop an understanding of the dominant equilibria at play during carbonation, the software Hydra and Medusa [112] were used to perform preliminary equilibrium calculations on the CO_2-NH_3-Cl-Ca-H_2O system representative of the carbonation stage of the Slag2PCC process. These calculations were done considering only the components available in the software databank: Ca^{2+}, $NH_{3(g)}$, NH_4^+, Cl^-, H_2CO_3, $CaCO_{3(s)cal}$, HCO_3^-,CO_3^{2-},$CO_{2(g)}$, $CaCl^+$, $CaHCO_3^+$, H^+ and OH^-. The carbamic and neutral associated ion species ($NH_4Cl_{(aq)}$, $CaCO_3^0{}_{(aq)}$ etc.) could not be included as they were not available. Calculations were performed for 25°C with specified inputs of 0.1 M $[Ca^{2+}]_{TOT}$, 0.1 M $[CO_3^{2-}]_{TOT}$, 1 M $[NH_4^+]_{TOT}$, and 1 M $[Cl^-]_{TOT}$ to represent carbonation in a 1 M NH_4Cl Ca-rich solution after the stoichiometric amount of CO_2 for 100% conversion of $CaCO_3$ has been added. Ideal solution behaviour was assumed and activity coefficients were left at the program default of 1. This equilibrium analysis ignores precipitation/dissolution kinetics which will not be the case in practice, even though ionic reactions are typically very fast and concentrations are usually close to equilibrium. The calculations also only consider the solid and liquid phases, gaseous species are not included. Figure 6.7 and Figure 6.8 show the speciation of Ca^{2+} and CO_3^{2-} with varying pH.

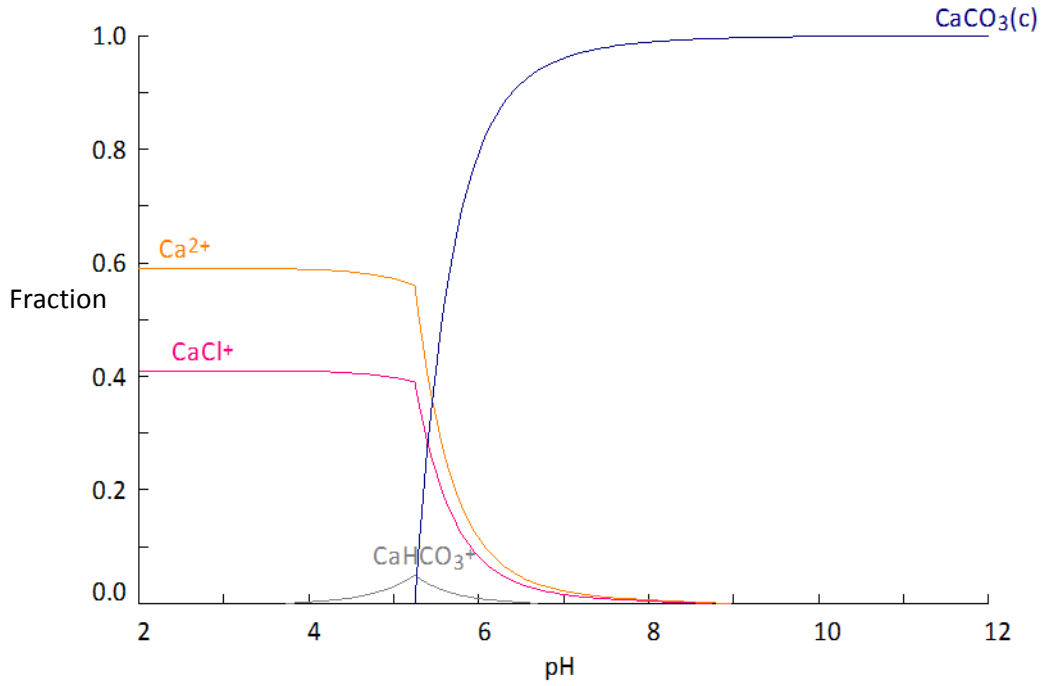

Figure 6.7 – Equilibrium calcium speciation in the CO_2-NH_3-Cl-Ca-H_2O system as a function of pH $[Ca^{2+}]_{TOT}$ = 0.1 M, $[CO_3^{2-}]_{TOT}$ = 0.1 M, $[NH_4^+]_{TOT}$ = 1 M, $[Cl^-]_{TOT}$ = 1 M, T = 25°C

The figure above shows that that dissolved calcium is present as both free Ca^{2+} and associated with chloride as $CaCl^+$. Figure 6.7 also shows that above a pH of 8 essentially all CO_2 is present as PCC but below a pH of 5.2 solid PCC is not stable and will completely dissolve. At a pH of 6 approximately 80% of the calcium is present as solid PCC. This increases to 90% at pH 6.35 and 95% at 6.78. Thus, allowing the carbonation to stop in a pH region above about 6.4 should result in acceptable (>90%) conversion of the dissolved Ca^{2+} to PCC. However, the slope of the curve is very sharp in the pH region 5.2-6, so this should be avoided.

Figure 6.8 shows that some of the CO_2 added is always present as HCO_3^-, with the $CaHCO_3^-$ complex only formed below a pH of about 6.5. Once pH enters the acidic region H_2CO_3 starts to form and below pH becomes the dominant carbonate species.

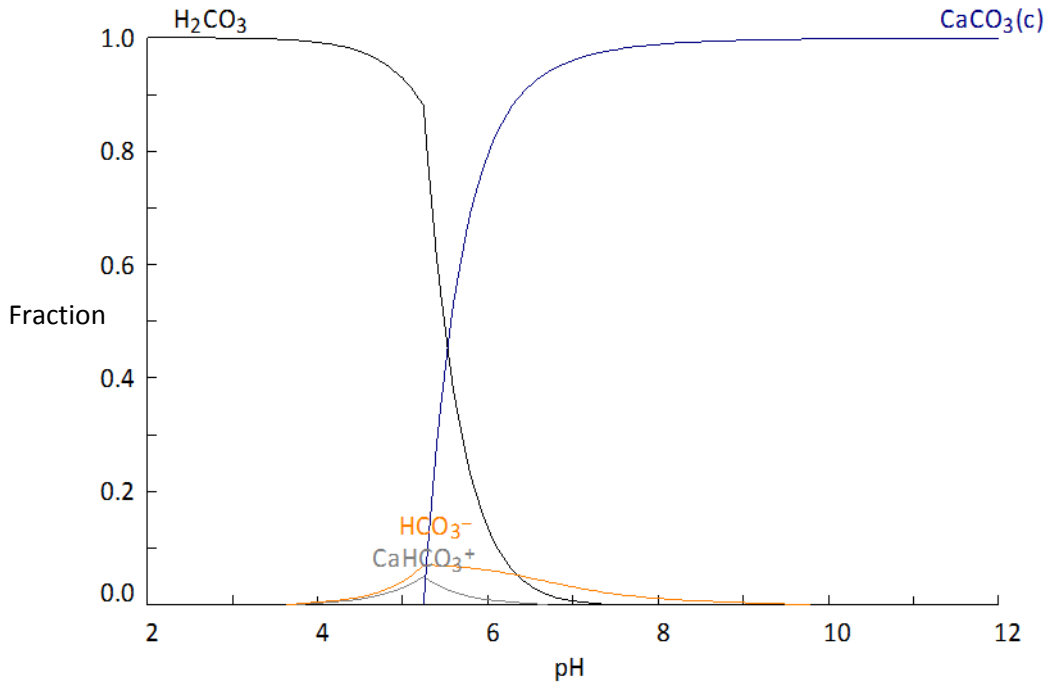

Figure 6.8 - Equilibrium carbonate speciation in the CO_2-NH_3-Cl-Ca-H_2O system as a function of pH
$[Ca^{2+}]_{TOT}$ = 0.1 M, $[CO_3^{2-}]_{TOT}$ = 0.1 M, $[NH_4^+]_{TOT}$ = 1 M, $[Cl^-]_{TOT}$ = 1 M, T = 25°C

It should be remembered that these figures show only the species fractions when stoichiometric amounts of Ca^{2+} and CO_3^{2-} are added at equilibrium. If carbonation is stopped before the stoichiometric amount of CO_2 has been added, the results are quite different as shown in Figure 6.9 calculated with CO_3^{2-} at 50% the stoichiometric requirement. This figure shows that when calcium is in excess, it can form complexes with NH_3 under conditions of alkaline pH. These complexes may affect carbonation if their dissociation kinetics are slow and they hinder the reaction with CO_3^{2-}.

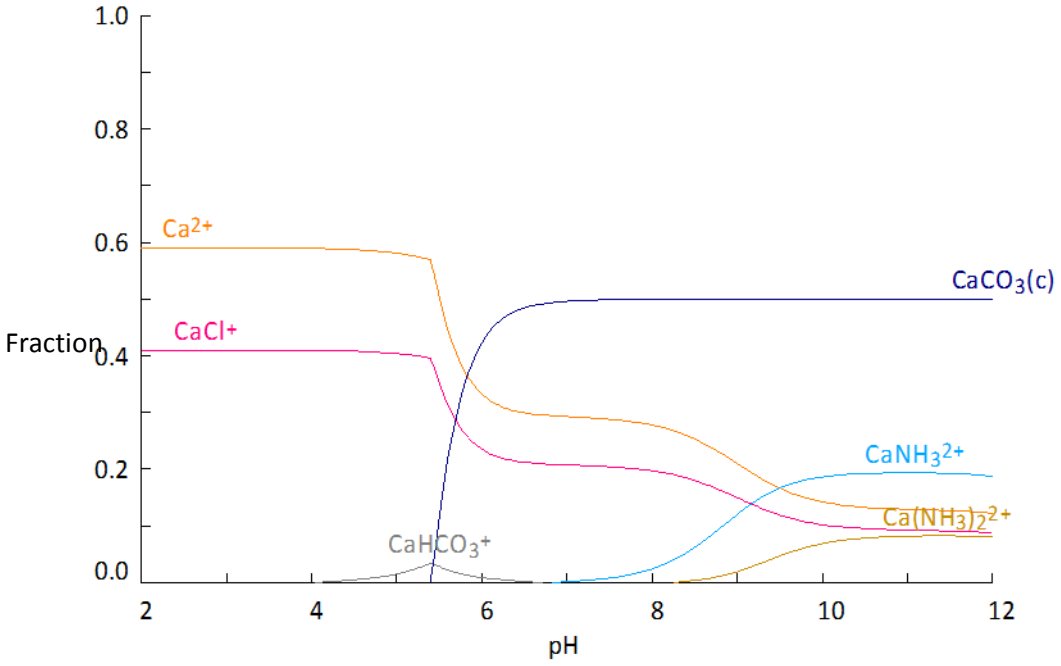

Figure 6.9 - Equilibrium calcium speciation in the CO_2-NH_3-Cl-Ca-H_2O system as a function of pH
$[Ca^{2+}]_{TOT}$ = 0.1 M, $[CO_3^{2-}]_{TOT}$ = 0.05 M, $[NH_4^+]_{TOT}$ = 1 M, $[Cl^-]_{TOT}$ = 1 M, T = 25°C

Figure 6.10 shows the speciation of NH_3 with pH under stoichiometric Ca^{2+} and CO_3^{2-} conditions. It can be seen that NH_4^+ is not stable under alkaline conditions and the formation of $NH_{3(aq)}$ becomes favoured.

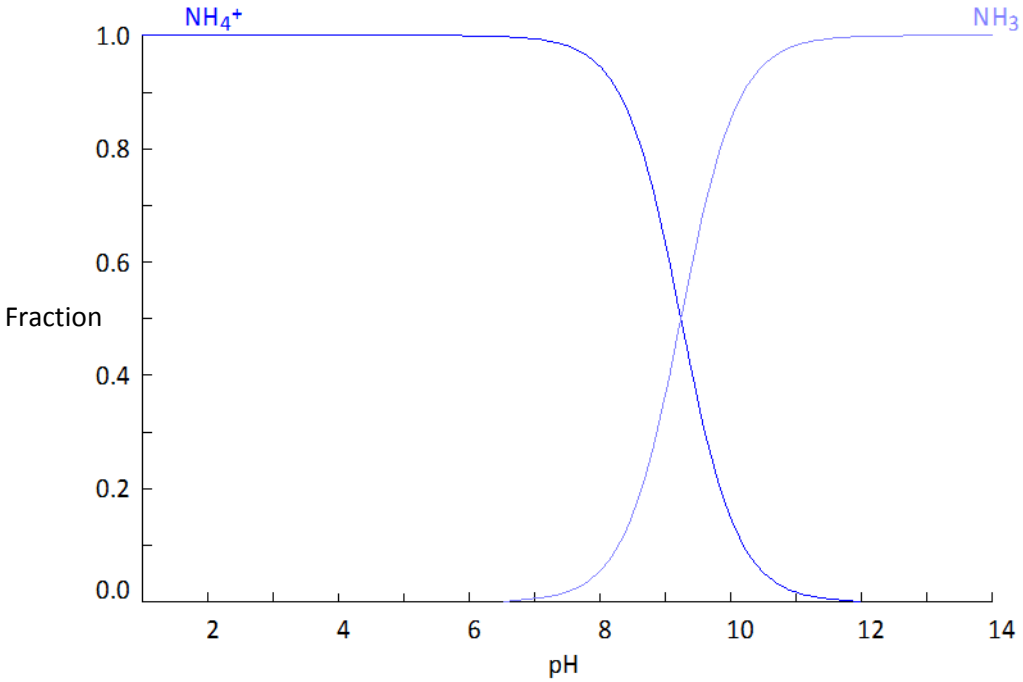

Figure 6.10 - Equilibrium ammonium speciation in the CO_2-NH_3-Cl-Ca-H_2O system as a function of pH $[Ca^{2+}]_{TOT}$ = 0.1 M, $[CO_3^{2-}]_{TOT}$ = 0.1 M, $[NH_4^+]_{TOT}$ = 1 M, $[Cl^-]_{TOT}$ = 1 M, T = 25°C

Some of this gas will remain in aqueous solution but some will also be present in the gas phase, with the equilibrium determined by Henry's law below which states the solubility of a solute in a liquid phase is directly proportional to the partial pressure of the solute in the gas phase [83].

$$p_i = y_i P = H_i x_i \tag{6.47}$$

where p_i is the partial pressure of solute i in the gas phase, y_i is the mole fraction of the solvent in the gas phase, P is the total pressure , x_i is the liquid mole fraction of species i, and H_i the Henry's law constant. This has consequences for extraction because as calcium dissolves from slag, the pH of the solvent solution will increase due to the formation of OH^- via reactions (4.2)-(4.4). As pH increases the equilibrium proportion of $NH_{3(aq)}$ will increase as shown in Figure 6.10 which, in accordance with Henry's law, will release ammonia from solution to increase the partial pressure of $NH_{3(g)}$ to maintain equilibrium. Thus, this is the mechanism of solvent loss from the extraction process. During carbonation the opposite occurs and pH will decrease due to the consumption of OH^-. This will reduce the equilibrium proportion of $NH_{3(aq)}$ in solution and reduce the partial pressure of $NH_{3(g)}$ as NH_4^+ becomes the dominant species. While this should reduce solvent losses in theory, they may be higher from carbonation than extraction due to the carbonating gas which will strip out $NH_{3(g)}$.

The preceding calculations were all performed assuming unity activity coefficients and ideal solution behaviour. To investigate the impact of non-ideal solution behaviour, the Medusa software was used to estimate activity coefficients of the components. For a solution with $[Ca^{2+}]_{TOT}$ = 0.1 M, $[CO_3^{2-}]_{TOT}$ = 0.1 M, $[NH^{4+}]_{TOT}$ = 1 M, $[Cl^-]_{TOT}$ = 1 M, the ionic strength was estimated at 1.2 M using equation (6.17). Medusa estimates activity coefficients using the method of Helgeson et al. [113] which, while only recommended for ionic strengths up to about 0.4 M at 25°C, is more accurate than that of Debye-Hückel (though not as good as that of Pitzer) given in Appendix C.

Figure 6.11 shows the calcium speciation as a function of pH including activity coefficient estimation. While the chart is similar to Figure 6.7 in most respects there are some notable differences. Firstly, less calcium is associated with chloride as the $CaCl^+$ complex. Secondly, the whole plot seems to have been shifted to the right. Now at a pH of 6, only 50% of the calcium is present as solid PCC. This increases to 90% at pH 7.0 and 95% at 7.6. Thus, one effect of increasing ionic strength and including activities seems to be to reduce the pH stability window of $CaCO_3$ causing it to dissolve at a higher pH. Whilst only a preliminary finding, this should be confirmed with more accurate activity coefficient estimation. If the pH stability window indeed does shift, this shows that accurate activity coefficient estimation will be vital for effectively understanding and modelling the Slag2PCC process.

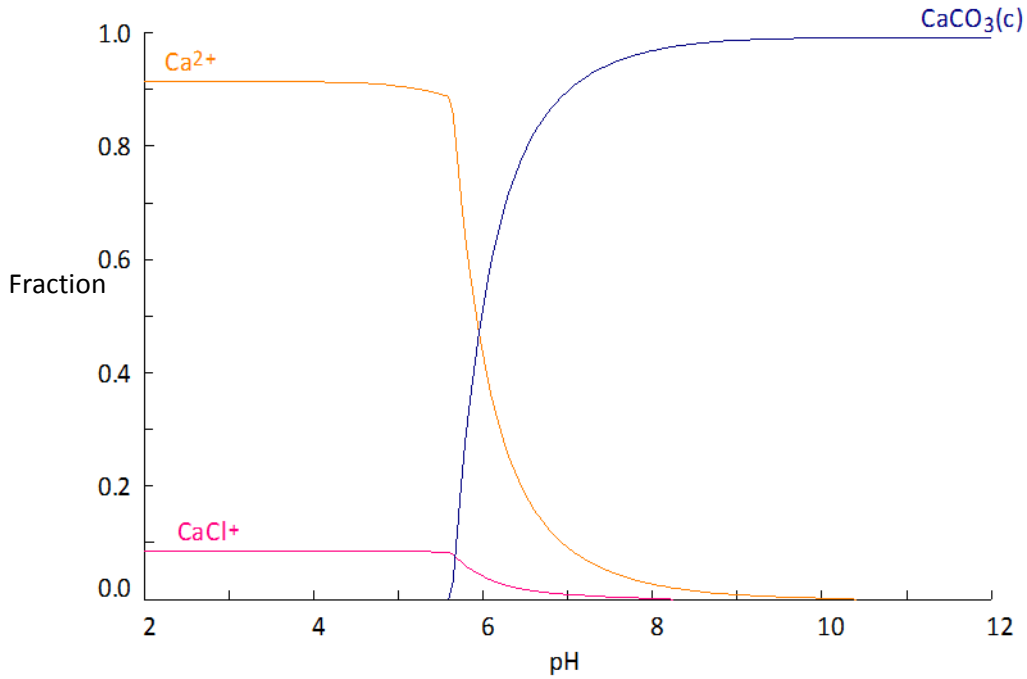

Figure 6.11 - Equilibrium calcium speciation in the CO_2-NH_3-Cl-Ca-H_2O system as a function of pH including activities $[Ca^{2+}]_{TOT}$ = 0.1 M, $[CO_3^{2-}]_{TOT}$ = 0.1 M, $[NH_4^+]_{TOT}$ = 1 M, $[Cl^-]_{TOT}$ = 1 M, T = 25°C, I = 1.2 M, T = 25°C

While Medusa provides useful equilibrium calculations with constant total component concentrations, it does not have the ability to perform calculations with increasing concentrations of a component. Thus HSC Chemistry 5 [95] was used to perform equilibrium calculations with CO_2 continuously added to the system, simulating the effect of the carbonation process. The same input component concentrations were used as with Medusa (1 M NH_4Cl, 0.1 M Ca^{2+}). The version of HSC Chemistry used was not able to estimate activity coefficients and so these were left equal to one.

Figure 6.12 shows the calculated calcium (red), ammonia (purple) and carbonate (blue) species speciation as well as pH during carbonation as a function of CO_2 added. The components NH_4Cl, NH_4HCO_3, NH_4Cl, $CaOH^+$ were included in the calculations but their concentrations were so low that they are negligible. Carbamate species were not in the HSC chemistry database and thus were also not included. The calculations show that over the course of carbonation the pH drops from a value of 9 to about 6.75 after twice the stoichiometric requirement of CO_2 has been added. The solution shows significant buffering capacity around a pH of 6.5 corresponding to the pK_a of H_2CO_3. Maximum conversion of Ca^{2+} to $CaCO_3$ (96.2%) occurs just after the pH equivalence point of 7.67. Approximately 30% of the dissolved ammonia in solution is bound with chloride as NH_4Cl with the rest present as free NH_4^+ or dissolved gaseous NH_3. The HSC Chemistry calculations also support the Medusa calculations that some of the dissolved calcium is associate with chloride as the complex $CaCl^+$.

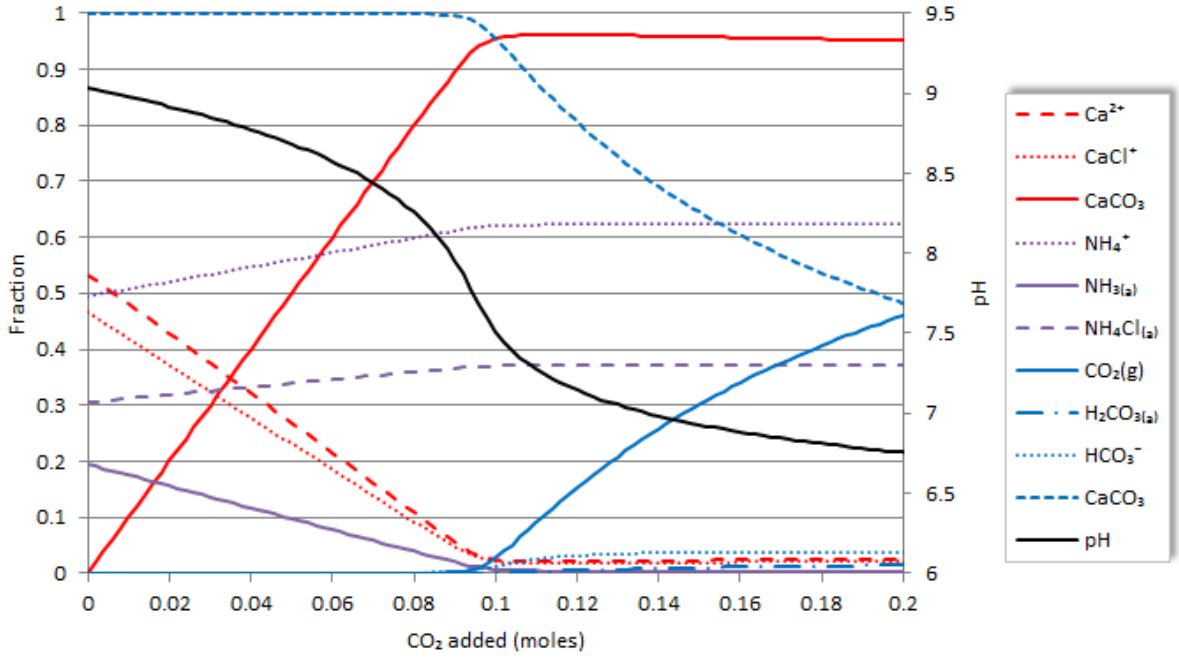

Figure 6.12 – Calculated equilibrium pH, Ca^{2+}, NH_4^+ and CO_3^{2-} speciation as a function of CO_2 added during carbonation [Ca^{2+}] = 0.1 M , [NH_4Cl] = 1 M

6.5 Factors Affecting the Precipitation of PCC

Based on general precipitation theory as well as an extensive review of the literature on $CaCO_3$ precipitation a large number of factors have been deemed significant in determining PCC quality and the efficiency of the precipitation process. The aim of this section is to present a brief review and analysis of the impacts these factors have on the process of $CaCO_3$ precipitation, as identified from the literature. There are several instances in which the literature is not in agreement on the impact on a particular factor and these are highlighted. There is also considerable evidence in the literature that many of these factors interact with each other in the precipitation process and these have been highlighted where they were noted.

The majority of research on PCC production available in the literature has focussed on liquid-liquid-solid reactive processes rather than gas-liquid-solid carbonation due to the simplicity of operation and easier control of process variables [114]. Minimal data could be found on PCC precipitation via carbonation of a Ca-rich solution containing NH_4Cl solvent other than that published by others involved with the Slag2PCC project at Åbo Academy or Aalto University. In light of this, information was gathered from many different $CaCO_3$ precipitation processes as although the conditions may not be identical, the fundamental mechanisms governing the precipitation of $CaCO_3$ should be similar and the data may still yield useful information. In any case the experimental conditions and context from which the data was taken are also included.

In addition to the causal relationships between precipitation conditions PCC quality, it is also important to keep in mind that precipitation is only one stage in the overall Slag2PCC process and while certain conditions may be advantageous for precipitation, they may be disadvantageous for extraction. Thus where necessary, implications of varying these parameters within the context of the entire Slag2PCC process on a commercial scale are given, bearing in mind the objective of the Slag2PCC work of capturing CO_2 from industrial flue gases.

6.5.1 Temperature

Temperature has been the subject of many studies and is reported to affect many aspects of PCC production including morphology, carbonation rate and conversion efficiency. Mattila et al. [50] observed that although the carbonation kinetics are not appreciably affected at higher temperatures, gas absorption into the liquid is less effective and CO_2 solubility is lower, and instead of reacting to precipitate $CaCO_3$ a large amount of CO_2 escapes the solution in gaseous form. This finding is supported by Kodama et al. [115] who studied both the extraction and precipitation steps of producing PCC from steel slag. They found that the absorption of CO_2 was highest at lower solution temperatures and reduced with increasing temperature. They proposed a maximum practical precipitation reaction temperature of 80°C, while noting that the conversion for the extraction reaction was better at higher temperatures. This is somewhat at odds with Feng et al. [116] who found that limewater carbonation at higher temperatures (80°C) occurred quicker than at lower temperatures (ambient), and that at higher temperatures the initial solution pH is lower. In the same study Kodama et al. found that temperature had a strong effect on the PCC morphology. They found that cubic calcite was formed at lower temperatures (40-60°C). At higher temperatures, the fraction of calcite decreased and some needle-shaped aragonite was generated at 90°C. Sun et al. [117] also studied the production of PCC from steelmaking slag with NH_4Cl solvent and found that temperature influenced the PCC morphology with scalenohedral particles being produced at 20°C becoming more rhombohedral as the temperature increased to 80°C. Under their reported optimum extraction conditions (solid/liquid ratio 100 g/L, 2M NH_4Cl, 2 hour extraction, 60°C, pure CO_2, 400rpm agitation, particle diameter 38µm<d<250µm) and carbonation conditions (10 bar CO_2 pressure, initial pH 9 (adjusted with NH_4OH), $[Ca^{2+}]$ ~0.37 M, 60°C, 1 hour carbonation, 400 rpm agitation), they produced crystalline aggregates of approximately 1µm width and 2.5µm length. However, they only used 100 mL of solution. Their findings regarding morphology are contrary to that of Hubbe [56] who notes that lower temperatures during precipitation tend to produce rhombohedral (cubic) particles, whereas higher temperatures produce scalenohedral particles.

Chen et al. [29] studied the effect of precipitation temperature on PCC morphology using double injection of the $CaCl_2$ and NH_4HCO_3 solutions at a molar ratio of 1:1. They found that lamellar vaterite particles, a mixture of vaterite, aragonite and calcite, and pure aragonite whiskers were formed at temperatures of 30-40 °C, 50-70 °C and 80 °C respectively. Hu and Deng [118] studied the precipitation of PCC from solutions of $CaCl_2$ and $MgCO_3$ and also found that higher temperatures are favourable for aragonite formation, but they found an optimum temperature for aragonite formation of 60°C, above which calcite began to form again. Chen et al. also performed thermodynamic calculations showing that the value of $[CO_3^{2-}]/[Ca^{2+}]$ decreased with increasing temperature, suggesting this as a driving factor in the transition from vaterite to aragonite at higher temperatures. The amount of calcite produced during their experiments was surprisingly low compared to other values reported in the literature and the amount of vaterite was quite high. However their experimental runs only ran for 45 minutes and the pH was low varying only between 7.5 and 7 which could explain this. Vaterite, being thermodynamically unstable will eventually decompose to calcite, suggesting that longer reaction times may have resulted in a higher proportion of calcite.

Temperature can also affect product purity through its impact on the diffusivity of components in solution. Lower solution temperatures reduce the diffusion coefficient of ions in solution. If the rate of crystal growth exceeds the rate at which ions can diffuse away from the crystal, they can become trapped within the crystal structure.

6.5.2 pH

Tai & Chen [119] studied the polymorphism of PCC precipitated from solutions of $CaCl_2$ and Na_2CO_3 in a constant composition, constant pH environment. They found that solution pH and temperature were the most important factors in determining PCC morphology, with high-purity calcite, aragonite and vaterite obtained at pH>12, pH≈11 and pH<10 respectively when precipitation was conducted at room temperature (24°C). At lower temperatures (7°C), only vaterite and calcite were formed with nearly pure calcite produced at pH>11. At high temperature (58°C) a similar trend was seen but aragonite was produced instead of vaterite. Chen et al. [74] subsequently investigated the effects of pH, calcium ion concentration, bicarbonate to carbonate ion ratio and gas-liquid mixing mode on the morphology and growth rate of PCC in a gas-liquid-solid reactive crystalliser. They again found that pH was the most important factor that influences the formation of polymorphs of PCC, followed by the calcium ion concentration. When the pH was lower than 7.8, the amount of PCC produced was small and below a pH of 8.0 nearly pure vaterite was formed. The maximum yield of calcites occurred at a pH of around 8.6. However Hostomsky & Jones [120], in their work on the precipitation of $CaCO_3$ from $Ca(NO_3)_2$ and Na_2CO_3, found that vaterite formed only at pH ≥ 9.5 (initially as agglomerates of spherical particles, becoming agglomerates of thick hexagonal platelets after 20 minutes), with calcite only forming at pH ≤ 8.5 as rhombic agglomerates. Chen et al. [74] found a small amount of aragonite was only produced at high pH and calcium ion concentration, perhaps because all their experiments were conducted at 30°C which is below the typically reported limit of aragonite stability of about 50°C [4]. Hu & Deng [118] also found that high pH is beneficial to the formation of aragonite.

Feng et al. [116] observed that the solution pH value during carbonation appeared to correlate well with particle size, with a higher pH value indicating a smaller average particle size. Their results also suggested that the absolute pH value would be a better indicator of particle size than the rate of change of pH, i.e. the carbonation rate. In addition they found that precipitation takes place immediately at high pH, while induction time increases with decreasing solution pH – pointing to a strong dependence of PCC nucleation rate on solution pH. Jung et al. [28] also report that higher pH leads to small particle size during carbonation.

According to Han et al. [15] a pH of 7.5 is low enough to start triggering the dissolution of $CaCO_3$ after a carbonation reaction has completed. However, the high concentration of HCO_3^- ions usually present at the end of the reaction tends to inhibit the dissolution of the produced PCC when the equilibrium below is considered:

$$CaCO_{3(s)} + 2H^+_{(aq)} + CO^{2-}_{3(aq)} \leftrightarrows Ca^{2+}_{(aq)} + 2HCO^-_{3(aq)} \tag{6.48}$$

In the pH range of 6-7 will be HCO_3^- while CO_3^{2-} ions will be dominant at high pH. Most carbonation reactions are taken as far to completion as possible to maximise CO_2 capture and calcium utilisation which would result in a final pH of 6-8. This will mean the dominant ion is HCO_3^-. After the PCC product is removed this solution will ideally be reused in the extraction stage, however when the extracted Ca^{2+} comes in contact with residual HCO_3^- (which would not be present in fresh solvent solution) it can cause precipitation of PCC in the extraction reactor according to the following equation:

$$Ca^{2+}_{(aq)} + HCO^-_{3(aq)} \leftrightarrows CaCO_{3(s)} + H^+_{(aq)} \tag{6.49}$$

This would reduce the efficiency of the overall process as calcium would be lost from the system as PCC with the spent slag. Thus, in a semi-batch or continuous process a method of dealing with the residual bicarbonate ions is required. In the Slag2PCC process, there is an allowance in the design for

some Ca-rich solution to be kept aside from the main carbonation to be mixed with the carbonated solution in order to precipitate any remaining carbonates.

Higher pH levels also increase the solubility of CO_2 in the liquid as well as the rate of absorption. This is because the higher concentration of OH^- ions leads to a more rapid reaction with CO_2 at the gas-liquid interface, leading in turn to an increase in the amount of HCO_3^- and CO_3^{2-} ions available via equations (6.21) and (6.22). This shows that the effect of pH during carbonation is not straightforward due to the complex equilibria involved.

6.5.3 Reactant Concentration and Supersaturation

Agnihotri et al. [121] and Wei et al. [122] found in their limewater carbonation studies that a higher initial concentration of $Ca(OH)_2$ resulted in smaller PCC particles. At lower concentrations larger particles and wider PSDs were produced. Jung et al. [28] based on their carbonation studies using $Ca(OH)_2$ and CO_2 found that $CaCO_3$ particle growth and size can be inhibited by the presence of excess ionic species in solution, in cases where agitation is sufficient and mass transport is not a limiting factor. They found that when carbonation proceeded at stoichiometric conditions and the concentration of excess ions should be at a minimum, they achieved a maximum mean particle size. When the reaction occurred under either conditions of excess CO_2 (limiting Ca^{2+}) or excess Ca^{2+} (limiting CO_2) the mean particle size became smaller and quite remarkably so, from which they concluded that crystal growth was being slowed by the adsorption of excess charged ionic reactants on the surface of the crystals, thereby blocking growth sites and inhibiting the surface integration step in crystal growth. They also observed that at stoichiometric conditions (or approximately stoichiometric) cube-like calcite was obtained however as the concentration of $Ca(OH)_2$ increased from 0.005 M up to 0.1 M the morphology became more spindle-like and elongated (though still calcite). These results are in agreement with Jung et al. [123] and with the theory presented in 6.1.5. The work of Hu and Deng [118] on the synthesis of aragonite mentioned earlier also found that reducing Ca^{2+} concentration increased the fraction of aragonite produced at 70°C (60% at 1M Ca^{2+}, 93% at 0.1M Ca^{2+}, 100% at 0.025M Ca^{2+}), but that the aragonite aspect ratio reduced at the same time. Domingo et al. [87] and López-Periago et al. [124] report that the base conditions required to obtain rhombohedral calcite are low concentrations of CO_2 and Ca^{2+} ions, but that these low concentrations are not acceptable at an industrial scale. More generally they report that in limewater carbonation, low $Ca(OH)_2$ concentrations favour rhombohedral calcite, whereas high $Ca(OH)_2$ concentrations favour scalenohedral calcite. This implies that higher Ca^{2+} ion concentration and/or higher pH favours the formation of scalenohedral calcite. Higher concentrations of reactant are also reported to increase the propensity for agglomeration, leading to larger particles and a bimodal particle distribution [120].

Supersaturation is the driving force for any precipitation process and was defined earlier by equation (6.16). In liquid-liquid precipitation of PCC it is possible to fix the concentrations of Ca^{2+} and CO_3^{2-} and temperature so that initial supersaturation is known. However, in gas-liquid carbonation the only concentration which can be easily fixed is that of Ca^{2+} because the CO_3^{2-} supply to the reaction is determined by mass transfer from the gas to liquid phases. A high level of supersaturation favours crystal nucleation rather than crystal growth, leading to a very large number of very small particles. However, in batch precipitation supersaturation will quickly reduce as Ca^{2+} is consumed and crystal growth and agglomeration become the dominant mechanisms.

6.5.4 Conductivity

Several studies on the precipitation of PCC have monitored solution conductivity during the reaction and several have used it as an independent variable [51]. An advantage of measuring conductivity is

that it can provide a fast and easy way to estimate the ionic content in solution. However, conductivity is only an indicative measurement of the total number of free ions in solution (Ca^{2+}, CO_3^{2-},Cl^-,NH_4^+, etc.) and it not a selective measurement for Ca^{2+} or CO_3^{2-}. It has been used in lime water carbonation experiments as an indicator of supersaturation (effectively calcium concentration) [51], and also as an indicator of when carbonation should cease because when conductivity is at a minimum, this indicates the lowest free [Ca^{2+}], maximum PCC, with subsequent carbonation only causing PCC to dissolve again, increasing [Ca^{2+}] and hence conductivity. However, in the Slag2PCC process the solvent ions (NH_4^+ and Cl^-) will also increase conductivity. In fact, the concentration of solvent ions will likely be much higher than the concentration of dissolved calcium and carbonate species if a solvent strength of 0.1-1M is used which may make it more difficult to detect changes in the concentrations of these species using this method.

6.5.5 Agitation

According to Jones et al. [125] the mean crystal size of PCC in limewater carbonation increases with solution stirring rate due to a reduction in mass transfer resistance, as predicted by the film theory of gas-liquid mass transfer with chemical reaction. They found experimentally that in batch precipitation, small discrete calcite crystals (<1µm) are formed initially in the vicinity of the gas-liquid interface followed by subsequent primary crystal growth reaching around 6µm in the bulk. Reddy & Nancollas [14] found in their work on calcite precipitation from supersatured solutions that the crystal growth rate constant was independent of the stirring rate of the solution. Agitation can also affect particle size via agglomeration and attrition process. While moderate agitation can increase agglomeration rate by increasing the collision frequency between particles, high levels of agitation and reduce particle size due to shear and particle breakage [120].

6.5.6 Residence Time

Residence time is a critical parameter for any precipitation process. In the case of batch precipitation it is the length of time that the precipitation reaction is allowed to proceed. In a continuous process, which usually includes some recycling of undersize crystal as seed, the residence time is not a single number but instead a distribution as the particles are not all in the reactor system for the same length of time.

Jones et al. [125] studied the precipitation of $CaCO_3$ by introducing CO_2 into the headspace above an agitated limewater solution. They found that small discrete calcite crystals (<1µm) were formed initially in the vicinity of the gas-liquid interface during the early stage of batch precipitation, followed by subsequent primary crystal growth reaching around 6µm in the bulk solution. In batch precipitation however it is important to remember that unless it is held constant (e.g. by the addition of alkali), the pH of the solution will decrease over time due to the consumption of CO_3^{2-} ions via equation (6.25).

Franke & Mersmann [82] investigated the influence of operational conditions on the precipitation of $CaCO_3$ using the system of $CaNO_3$ and Na_2CO_3. During their experiments only vaterite and aragonite were formed, and they found that reactant concentration and residence time dictated which morphology was predominant. Low reactant concentrations, long residence times and low agitation led to the formation of aragonite, whereas high reactant concentrations and short residence times favoured vaterite. They explained these findings as consistent with solubility data on calcite, aragonite and vaterite available in the literature [126]. The solubility product of vaterite being higher than that of aragonite, vaterite is unstable compared to aragonite at lower concentrations and thus for lower levels of supersaturation formation of aragonite should be expected. It is not clear why they did not produce calcite.

Hu & Deng [118] observed that if calcite exists in a PCC suspension aging will result in the transformation of any aragonite into calcite, as expected from their respective stabilities. Sarkar & Mahapatra [85] studied the synthesis of all three main crystal forms and the transformations between them. They found that vaterite transforms to aragonite in distilled water in about 1.5 hours under reflux or in about 30 days under equilibration at 25 °C; that vaterite transforms to calcite in mother liquor in about 3 hours under reflux or in about 30 days under equilibration at 25°C, and that aragonite does not convert to calcite under any of these conditions.

Aside from providing the time required for the precursor precipitates (e.g. ACC and vaterite) to transform into the stable crystal morphology, longer residence time also gives the PCC crystals more time to grow and hence increases crystal size.

6.5.7 Bubble Size

Bang et al. [127] studied the SSA and particle size of PCC by using CO_2 microbubbles (typically smaller than 50µm) produced using a microbubble generator. Microbubbles, due to their higher surface tension, have an advantage over normal bubbles because they can be retained in solution for much longer due to the weaker buoyancy forces, also providing a much greater gas-liquid interfacial area and faster precipitation rate. They found that both microbubbles and a standard bubble generator produced PCC with primary particle size approximately 100-500 nm, but the secondary particle size produced with microbubbles (2µm) was much smaller than that produced with standard bubbles (8µm). They also found that the particle SSA was inversely proportional to the size of the primary particles, which agglomerate to form the secondary particles. Feng et al. [116] and Xian et al. [102] also found that particle size decreases with decreasing bubble size.

6.5.8 CO_2 Concentration

The concentration of CO_2 in the carbonating gas is an important parameter because the use of pure CO_2 as the carbonating gas would require the separation and purification of CO_2 from flue gases or some other source – a potentially complex and expensive step. If flue gas (<20% CO_2) can be used directly for carbonation, the process can be simpler and less costly. In a study by Eloneva et al. [8] on the production of PCC from steelmaking slag using acetic acid as a solvent, the concentration of CO_2 in the carbonating gas did not appear to affect the amount of PCC formed, suggesting that flue gasses could be used as a source of CO_2 for carbonation without the need for expensive and energy intensive separation and purification of CO_2 from flue gases. However, lower CO_2 concentrations (10% vol) increased pH stabilisation time indicating a slower precipitation rate. This drawback could be offset by increasing the gas flow, or increasing the solution temperature. Vucak et al. [128] found that a high degree of PCC agglomeration occurred when pure CO_2 was used in carbonation, with the primary crystals becoming bound together by a mass of amorphous solid. They also found that increasing CO_2 concentration in the gas phase tended to decrease slightly the primary particle size. Feng et al. [116] on the other hand found that particle size decreased with decreasing CO_2 concentration, but they were in agreement that agglomeration was significant when pure CO_2 was used and not significant when a lower CO_2 concentration (25% CO_2) was used. When agglomerates were formed with pure CO_2, treatment with ultrasound for 6 minutes was sufficient to break the agglomerates. Han et al. [15] found in their experiments on the carbonation of $CaCl_2$ solutions that increasing either the flow rate or CO_2 concentration in the carbonating gas tended to favour the formation of spherical vaterite, which they attributed to the slowing down of the transformation of vaterite to calcite. Gómez-Díaz et al. [99] report that calcite aggregation phenomena can be due to high local supersaturation reached in the liquid film near the gas/liquid interface. They posit that CO_2 accumulates at the liquid film creating a high concentration compared to the bulk. Due to the fast liquid-phase reaction the solid phase is

produced quickly and the probability of collision of the individual crystals is very high, leading to aggregation of the calcite crystals. A higher CO_2 concentration in the gas phase will increase the solubility in the liquid, thus if this mechanism is correct, higher CO_2 concentration and CO_2 flow are likely to increase agglomeration.

6.5.9 Seeding

Under supersaturation conditions, calcite crystal growth rate has been found to be a linear function of the weight of seed crystal used to initiate growth [14]. If the solvent solution is to be continuously recycled in either a batch or continuous process then it is likely that small particles remaining in solution from the previous carbonation will act as seed crystals and nucleation sites for the subsequent carbonation if they are not dissolved first.

6.5.10 Calcium to Carbonate Ratio $[Ca^{2+}]/[CO_3^{2-}]$

The ratio between Ca^{2+} and CO_3^{2-} ions has been commented on by several authors as an operational factor in PCC production but this has mainly been in liquid-liquid precipitation of $CaCO_3$. In gas-liquid carbonation such as the Slag2PCC process, the initial concentration of Ca^{2+} is determined by the level of calcium extraction. The initial concentration of CO_3^{2-} is essential zero in solution and is only formed after the flow of CO_2 begins, thus tight controlling the concentration ratio $[Ca^{2+}]/[CO_3^{2-}]$ is difficult in carbonation. However, it is known to be a major parameter effecting PCC morphology and reaction rate.

Garciá-Carmona et al. [88] proposed a method of producing a variety of calcite morphologies using limewater carbonation based on adjustment of the electrical conductivity of the system at fixed values of 1, 3, 5 and 7 mS/cm (by addition of $Ca(OH)_2$) within the temperature range of 20-30°C. They suggest that at higher conductivities and temperatures above 25°C predominantly scalenohedral crystals are formed due to the higher $[Ca^{2+}]/[CO_3^{2-}]$ ratio, which is itself a consequence of the higher dissolved $Ca(OH)_2$ concentration. They found that when the ratio $[Ca]_{tot}/[CO_3]_{tot}$ was 1.02 or 1.03 the morphology was rhombohedral; when $[Ca]_{tot}/[CO_3]_{tot}$ was 1.06 the morphology was rhombo-scalenohedral and when $[Ca]_{tot}/[CO_3]_{tot}$ was 1.11 the morphology was scalenohedral. This was supported by the work of Ukrainczyk et al. [51] who used conductivity to infer that the ratio $[Ca]_{tot}/[CO_3]_{tot}$ determines the transition between predominantly scalenohedral to rhombohedral calcite morphology, with higher $[Ca]_{tot}/[CO_3]_{tot}$ favouring scalenohedral. Chen & Xiang [29] studied the liquid-liquid reactive crystallization of $CaCO_3$ using NH_4HCO_3 and $CaCl_2$ found that a system with low $[Ca^{2+}]/[CO_3^{2-}]$ ratio may be favourable for the formation of lamellar vaterite, while a system with high $[Ca^{2+}]/[CO_3^{2-}]$ ratio at 80°C was favourable for the formation of aragonite whiskers. Gómez-Morales et al. [129] observed a decrease in the nucleation rate (increase in the induction time) and an increase in the growth rate when an excess of Ca^{2+} is present in the bulk solution (higher $[Ca]_{tot}/[CO_3]_{tot}$ ratios). They also note that the ζ-potential of calcite become positive at high concentrations of Ca^{2+}, and under these conditions the surface of calcite acts as a sink for HCO^{3-} and CO^{2-} ions, potentially increasing the growth rate.

6.5.11 Solvent Concentration

In test work by Matilla et al. [50] the concentration of the ammonium salt was not observed to directly affect the kinetics of the carbon reaction. However, at high solvent concentration and high original slag to liquid ratio, the pH of the solution behaved unusually. Instead of a gradual decline in pH as is typically seen during carbonation, a sudden drop of 2 pH units was observed 20-30 mins after the reaction was started, after which it essentially remained constant. This behaviour was put down to the generation

of carbamate ($NH_2CO_2^-$) ions from the reaction of NH_3 with bicarbonate, which will be the dominant species in solutions with a high NH_3:NH_4^+ ratio.

$$NH_{3(aq)} + HCO_{3(aq)}^- \leftrightarrows NH_2CO_{2(aq)}^- + H_2O_{(l)} \quad (6.50)$$

Apart from lime, steel converter slag contains a large amount of SiO_2, MgO and Fe_2O_3. At higher solvent concentrations it is likely that more of these compounds will dissolve and may co-precipitate with PCC or become trapped in the crystal lattice during carbonation, reducing product purity. Also, previous experiments with using NH_4Cl solvent in the SlagPCC process identified that the produced PCC contained a notable amount of chlorine (0.23-0.44%), probably as some solvent is also likely to adsorb on the surface of the PCC or precipitate as $CaCl_2$ [69]. This will also reduce the purity of the final product and furthermore the potential impact of chlorine on the papermaking process is not known. Jung et al. [123] studied the effect of monovalent salt ions (NH_4^+, NO_3^- Cl^-, Na^+ etc.) on PCC precipitation with limewater and H_2CO_3 solution (formed by bubbling CO_2 through water). When CO_3^{2-} was in excess they found that presence of monovalent salts, and particularly NH_4Cl (0.25M) caused such a reduction in particle size (~100nm) that they could not determine the morphology. Under stoichiometric and excess Ca^{2+} however it appears that the presence of salts can have the opposite effect and cause a massive increase in particle size (up to 100µm), as was observed with 0.25M $NaNO_3$. NH_4Cl was not tested under the same conditions of excess Ca^{2+} (as would be the case in Slag2PCC carbonation) so the potential effect of NH_4Cl in this case is not certain. Jung et al. also found that increasing salt concentrations promoted crystal agglomeration, with the mean size of the agglomerates increasing proportionately with the solution ionic strength. It is believed that this is due to the charged surfaces of the PCC crystals becoming effectively neutralised or shielded by the salt ions. This reduces the width of the electric double layer surrounding the crystals and reduces the electrostatics repulsive forces between crystals, leading to more successful particle collisions [123, 130]

6.5.12 Effect of Additives and Impurities

Many studies have investigated the effect of additives and impurities on the growth of PCC crystals. Additive chemicals, commonly known as crystal growth modifiers (CGMs) are frequently added to precipitation solutions in order to achieve certain product characteristics that may be difficult or even impossible to achieve in pure-component systems. As CGMs are typically expensive they should usually be minimised, unless their use is justified or required from an economic or product quality point of view. Impurities in the solution can also impact and potentially suppress crystal growth, thus it is useful to identify which poisons can interfere with PCC production and should be avoided. A survey of the literature has found that the following additives and impurities have been found to affect one or more aspects of PCC precipitation:

- **Sodium stearate ($C_{18}H_{35}NaO_2$)**
  Ukrainczyk et al. [19] studied the influence of sodium stearate on the production of PCC via the semicontinuous carbonation of slaked lime. They found that under the conditions of their experiment calcite was the only morphological form produced. They also concluded that addition of sodium stearate could increase the SSA of the PCC formed, with a value of 51 m^2/g achieved at a stearate concentration of 17 mM.

- **Terpineol ($C_{10}H_{18}O$)**
  Xiang et al. [102] showed that terpineol can accelerate the absorption of CO_2 into solution as it reduces the surface tension of bubble, preventing bubble aggregation and improving the stability of small bubbles. In their limewater carbonation experiments the addition of 0.1-1 vol% terpineol reduced the diameter of PCC particles from 150 to 90-120 nm. Addition of

more terpineol caused larger particles to be produced, suggesting an optimum level of terpineol exists, beyond which the terpineol starts to limit CO_2 diffusion. Feng et al. [116] found an interaction between temperature and terpineol concentration, with higher temperatures (80°C) enhancing the effect of terpineol (or vice versa) and forming even smaller particles. However, the effect of temperature was not sensitive to the amount of terpineol added in the range of 0.1-1 vol%.

- **Dispersion agents**
  By far the most commonly used dispersing agents in papermaking applications to prevent agglomeration and aggregation are the alkali metal and ammonium salts of polyacrylic acid (PAA) [93]. Skuse et al. [94] have patented a mixture of a salt of poly(acrylic) acid (normally ammonium or sodium) and either i) a soluble salt of an acrylic acid-acrylamide copolymer, or ii) a soluble hexameta-, pyro- or poly-phosphate salt as a dispersion agent for PCC to be used in the food industry. Varma et al. [131] showed that dispersion agents such as citric acid, sodium metaphosphate and PAA could generate $CaCO_3$ nanocrystals. Citrate ions in particular were also shown to inhibit the precipitation of aragonite while specifically promoting the formation of calcite. Cheng et al. [132] found that monodispersed cubic calcite composite particles could be produced optimally with PAA concentration between 1–2 g/L, $CaCO_3$ between 4–16 mM, pH 10 and temperatures between 60–80°C. However, the PCC was not pure and contained approximately 1.4% PAA.

- **Zinc chloride ($ZnCl_2$)**
  Xiang et al. [133] noticed that there was an obvious decrease in PCC particle size when 1% $ZnCl_2$ solution was added during limewater carbonation. Spherical PCC was formed with mean diameter of 0.2µm.

- **EDTA**
  Xiang et al. [133] found that adding ethylenediaminetetraacetic acid (EDTA) between 0.25-1% increased the rate of limewater carbonation, reduced reaction time from 80 to 40 minutes and produced smaller particles, which they deduced as being a result of the faster carbonation rate. This is not supported by the work of Feng et al. [116] who found that adding EDTA slightly increased average particle size during carbonation.

- **Magnesium and other di- and trivalent metal ions**
  The presence of Mg^{2+} ions is widely known to increase the fraction of aragonite in PCC and in sufficient quantity can prevent the formation of calcite completely [118, 134]. It also inhibits the transformation of vaterite and aragonite into calcite. Other ions such as Ni^{2+}, Co^{2+}, Fe^{3+}, Zn^{2+} and Cu^{2+} also encourage aragonite formation and in general any impurity ions with a small ionic radius and higher hydration energy than that of Ca^{2+} favour aragonite formation. On the other hand Mn^{2+}, Cd^{2+}, Ca^{2+}, Pb^{2+} and Ba^{2+} ions have been shown to favour calcite formation [134]. Strontium also favours the formation of aragonite and strontium salts are used in the synthesis of aragonite [135].

- **Neutral salts and monovalent ion impurities**
  Neutral salts such as NaCl have been found to promote the transformation of calcite to aragonite [62]. Na^+ and K^+ have been shown to modify the PCC crystals from regular rhombohedral and spindle shapes to more irregular forms as their small ionic radii (0.098 and 0.133 nm respectively) mean they can be incorporated into the $CaCO_3$ crystal lattice. According to Jung et al. [123] NH_4^+ ion on the other hand is larger (0.148 nm) and less easily incorporated

into the crystal lattice. Instead, NH_4^+ is believed to interfere with the adsorption of Ca^{2+} onto the growing crystal surface and can change the morphology from a spindle shape to rhombohedral when Ca^{2+} is in excess, but generally only at high concentrations (>0.05M) [123].

- **Precipitation inhibitors**
  Even at the 0.6ppm level, metaphosphates have been shown to retard or completely inhibit $CaCO_3$ precipitation due to surface adsorption. The effect is even stronger in the presence of ammonium salts [62]. Polyphosphate compounds have also been used as effective dispersants for PCC to prevent agglomeration [37]. Polyphosphate reacts with PCC at a rate that accelerates sharply with temperature.

- **Carbohydrates & Amines**
  Wenk et al. [136] and Deutsch et al. [137] mention that processes for producing scalenohedral PCC by carbonation of $Ca(OH)_2$ typically rely on the use of additives such as monosaccharides (e.g. fructose, glucose), disaccharides (e.g. sucrose), polysaccharides (e.g. starch) at a level of 0.1-0.5 wt%, or amines such as triethanolamine, mannitol, N-ethyl diethanolamine added during the slaking of quicklime or prior to carbonation.

6.5.13 Effect of Pressure

Domingo et al. [87] investigated the precipitation of PCC using supercritical and high pressure CO_2 and found that it offers a potential way of increasing calcium conversion and reaction rate. Higher pressures will increase the solubility of CO_2 in solution can be useful in the formation of cubic calcite (which requires stoichiometric $[Ca^{2+}]/[CO_3^{2-}]$) in solutions with high $[Ca^{2+}]$ and where the scalenohedral form is normally obtained.

7 Experimental Work

Given the lack of data on the reactive crystallisation of $CaCO_3$ by carbonation of Ca-rich aqueous solutions of NH_4Cl, as well as delays with the pilot plant equipment to be discussed later, it was decided to divide the experimental park of this work into two stages. The first stage would be to investigate and confirm the effect of various carbonation parameters on the carbonation process and the quality of the PCC produced using batch carbonation experiments in a laboratory-scale 5L glass reactor. The second stage would essentially be a scale-up exercise, taking the learnings from the laboratory and applying them in the pilot plant with the aim of producing high quality PCC from steel slag.

7.1 Laboratory-Scale Experimental Work

Although PCC precipitation has been studied extensively for decades, the majority of data available in the literature is based on liquid-liquid crystallization experiments rather than gas-liquid carbonation. Furthermore, of the data on gas-liquid carbonation which have been found, most tests have focussed on varying only one or two factors. This allows the effect of individual variables to be investigated, but not the interactions between them. Furthermore, the findings of the literature review have shown that the literature is not always in agreement on the effect of different factors on the precipitation process, and that literature studies are not necessarily comparable due to different experimental conditions. In the pilot Slag2PCC plant, it would be valuable to know *a priori* which easily manipulable process variables or factors could be used to control the PCC quality and precipitation process. For this reason, it was decided to perform a set of factorial experiments investigating these factors on a smaller laboratory scale (5L reactor) which could be done more quickly and cheaply than using the pilot plant (200L reactor). The findings of these tests could then be used directly or as a basic for further work using the pilot plant equipment. Thus the focus of these tests would not be to try to produce the best quality PCC, to determine the range of possible crystals that can be produced, the carbonation kinetics or to investigate the fundamental mechanisms involved in PCC precipitation, but instead to identify how each factor affects carbonation and which easily manipulable process variables available could be used to control the PCC quality in the pilot plant.

7.1.1 Factorial Experiment Design and Methodology

As highlighted in the literature review there are many possible precipitation variables which could be considered including temperature, initial Ca^{2+} concentration, initial pH, NH_4Cl solvent concentration, carbonating gas flow, CO_2 concentration, bubble size, agitation speed and reaction time. The number of runs required for a factorial experiment double for every additional factor that is considered thus it would be impractical to include every possible factor. Also given the size of the pilot equipment (200L), it would be very time consuming and expensive (in terms of reagents) to perform such a large number of experiments of this sort using the pilot equipment. However, to reduce the number of experimental runs required, a fractional factorial experiment can be performed which reduces the number of runs required at the cost of some confounding between factors and interactions. Confounding is when the effect of one factor cannot be distinguished from the effect of another factor. After considering all possible factors, factor levels and experiment designs, an un-replicated resolution V 2-level 16-run half-fraction factorial design was selected based on only five factors: Initial temperature (A), Ca^{2+} concentration [Ca^{2+}] (B), NH_4Cl concentration [NH_4Cl] (C), CO_2 flow rate (D), and agitation speed (E). The rationale for this choice of factors is discussed in the following section. Using the design generator E = ABCD, this design requires only 16 experimental runs, whist avoiding confounding between main effects and second order interactions. The full alias and confounding structure for the experiment is:

A + BCDE, B + ACDE, C + ABDE, D + ABCE, E + ABCD, AB + CDE, AC + BDE, AD + BCE, AE + BCD, BC + ADE, BD + ACE, BE + ACD, CD + ABE, CE + ABD, DE + ABC. This means, for example, that the effect of A (temperature) cannot be distinguished from the 4-way interaction BCDE. The advantage of this design structure is that no main effects (A,B,C,D,E) or 2-way interactions (AB,BC,DE etc…) are aliased with each other and their individual contributions can be determined. Third order and higher interactions are quite rare, thus this design permits a significant amount of information to be gathered from a relatively small number of experiments. One drawback of an un-replicated fractional factorial design such as this however is that it is saturated, meaning that the total degrees of freedom (DoF) in the experiment (total runs – 1) is equal to the number of main effects and interactions considered (i.e. 16-1 = 5 (main factors) + 10 (2-way interactions). This has consequences for the analysis of the results which will be discussed later.

7.1.2 Factor Levels and Experimental Runs

The low and high levels used for each factor in the experiment are shown in Table 7.1 below.

Table 7.1 - Factor levels for the laboratory scale experiment

Factor		Units	Low Level	High Level
A	Initial temperature	°C	15	25
B	Initial Ca^{2+} concentration	M	0.040	0.048
C	NH_4Cl solvent concentration	M	0.1	0.5
D	CO_2 flow rate	L/min	0.4	1.2
E	Agitation speed	rpm	300	555

These factors and levels were chosen for the following reasons:

- Carbonation temperature had been suggested as an important parameter both from the literature review and from discussions with the pulp and paper department at Aalto University. Lower temperatures in particular are of interest as previous work undertaken at Aalto University and Åbo Academy has focussed mainly on temperatures at 20°C and above [5] [138]. Temperature is also easily controlled with the laboratory equipment, as well as in the pilot plant with the use of a heat exchanger. Initially the low level was set at 5°C, but when carbonation was attempted at this low temperature no PCC was produced after one hour of carbonation even though pH had reached acidic conditions, thus the low level was increased to 15°C. This phenomena will be discussed later. The high temperature level was set at 25°C as the intention was to produce calcite not aragonite, thus higher temperatures were avoided.

- The concentration of calcium and NH_4Cl solvent are important factors because together they represent the level of calcium extraction efficiency from the slag i.e. higher [NH_4Cl] should in general yield higher [Ca^{2+}] due to the improved extraction efficiency. Furthermore, the presence of NH_4Cl solvent in calcium carbonation is something quite unique to the Slag2PCC process and as far as can be ascertained the impact of the solvent on the precipitation of PCC has not been studied. By including both [Ca^{2+}] and [NH_4Cl] as factors their individual effects as well as any interactions can be studied. The levels of [Ca^{2+}] and [NH_4Cl] were originally selected such that the carbonation reactions were expected to take between 30 min and 1 hr. In order to vary the levels of NH_4Cl and Ca^{2+} independently while using the same source of slag for each experiment for consistency, the Ca-rich solution for all experiments was based on a single batch extraction run from the pilot plant equipment. The intention had been to perform the extraction with a low [NH_4Cl] (0.1 M), stop the extraction after 5 minutes when approximately 50% of the calcium had been extracted, withdraw 50% of the solution, recycle the slag then take extraction to completion with the remaining slag and solution. This would result in two

Ca-rich stock solutions with the same [NH_4Cl] but different [Ca^{2+}] (low and high) as required for the factorial experiment. The high [NH_4Cl] runs would be performed by dissolving additional solid NH_4Cl into the solution. However, when the extraction was performed it proved to be more difficult and time consuming to recycle slag into the reactor than expected, thus extraction in the first stage was higher than intended and it was decided to add additional slag in the second step to ensure that the two solutions had sufficiently different [Ca^{2+}] values.

- Agitation rate is a factor that is manipulated easily at both laboratory scale and in the plant and scale-up is reasonably straightforward. The levels were picked such that the lowest speed (300 rpm) was enough to completely mix the reactor without causing shear and breakup of the CO_2 bubbles. The faster speed (555 rpm) was picked so that the gas bubbles, introduced at the eye of the impeller, were broken up and dispersed into many much smaller bubbles.

- Carbonating gas flow is another parameter which can be manipulated easily in the pilot plant and can be scaled from the laboratory to the pilot plant by using the gas to liquid ratio (GLR), which is the ratio between the flow rate of carbonating gas into the reactor and the volume of liquid in the reactor. GLR has units of L CO_2/(L liquid.min). Pure CO_2 was used for all tests. Although CO_2 bubble size and CO_2 concentration were also potential factors, the necessary equipment was not available in the laboratory to test these parameters adequately.

- A consequence of this approach is that the pH was not directly controlled in the experiment. In reality, using pH as a process lever would require fixing the extent of extraction or carbonation, or adding chemicals which would be costly. Thus pH was only monitored.

The following table shows the factor-level combinations used for each of the 16 experimental runs.

Table 7.2 - Run matrix for the laboratory-scale factorial experiment

Run	Initial T (°C)	[Ca^{2+}] (M)	[NH_4Cl] (M)	CO_2 flow (L/min)	Agitation speed (rpm)
1	15	0.040	0.1	0.4	555
2	25	0.040	0.1	0.4	300
3	15	0.040	0.5	0.4	300
4	25	0.040	0.5	0.4	555
5	15	0.040	0.1	1.2	300
6	25	0.040	0.1	1.2	555
7	15	0.040	0.5	1.2	555
8	25	0.040	0.5	1.2	300
9	15	0.048	0.5	0.4	555
10	25	0.048	0.5	0.4	300
11	15	0.048	0.1	1.2	555
12	25	0.048	0.1	1.2	300
13	15	0.048	0.1	0.4	300
14	25	0.048	0.1	0.4	555
15	15	0.048	0.5	1.2	300
16	25	0.048	0.5	1.2	555

7.1.3 Calcium Solution Preparation

The calcium stock solution for the factorial experiment was prepared using the pilot plant equipment located in the laboratory of the Energy Technology department at Aalto University. 135L of 0.1M NH_4Cl solvent solution was made by mixing 121.5L of tap water with 13.5L of 1M of pre-prepared NH_4Cl solution. The pH of the resulting solution was 7.3. To this solvent solution was added 6.75 kg of steel converter slag (over a period of 5 minutes) which had been sieved to <250µm. Extraction of calcium was then performed with agitation (170 rpm) at room temperature (23°C). After 10 minutes the pH of the solution had reached 9.8, agitation was stopped, and approximately half of this 'low-Ca' solution was withdrawn, filtered to remove slag and pumped into a separate storage tank. The slag from the filters was then recycled back into the extraction reactor. This process took approximately 20 minutes due to the difficulty of recycling the slag. Agitation was then turned on and extraction continued for another hour. However, even after one hour no further increase in pH was observed and it was thought that the delays in adding, filtering and recycling the slag meant that maximum extraction had been achieved. So, a further 1kg of sieved slag was added and extraction continued for 30 mins. The resulting 'high-Ca' solution was then filtered and stored in a separate tank. To determine the amount of calcium dissolved in the low-Ca and high-Ca solutions, samples of both were taken to the Aalto University School of Chemistry and titrated with 0.1M EDTA under alkaline conditions (pH 12) using Patton Reeder indicator (HHSNNA). The analysis yielded results of 0.040 and 0.048 mol Ca^{2+}/L for the low- and high-Ca solutions respectively. Whilst not as accurate as other methods such as Inductively Coupled Plasma Atomic Emission Spectrometry (ICP-AES), this complexometric titration method is straightforward, quick, inexpensive, and was considered to provide sufficiently accurate results (+/- 5%) for the purposes of the factorial. Details of the calcium analysis are given in Appendix A.

7.1.4 Equipment Setup

Figure 7.1 and Figure 7.2 depict the equipment setup used for the laboratory experiments.

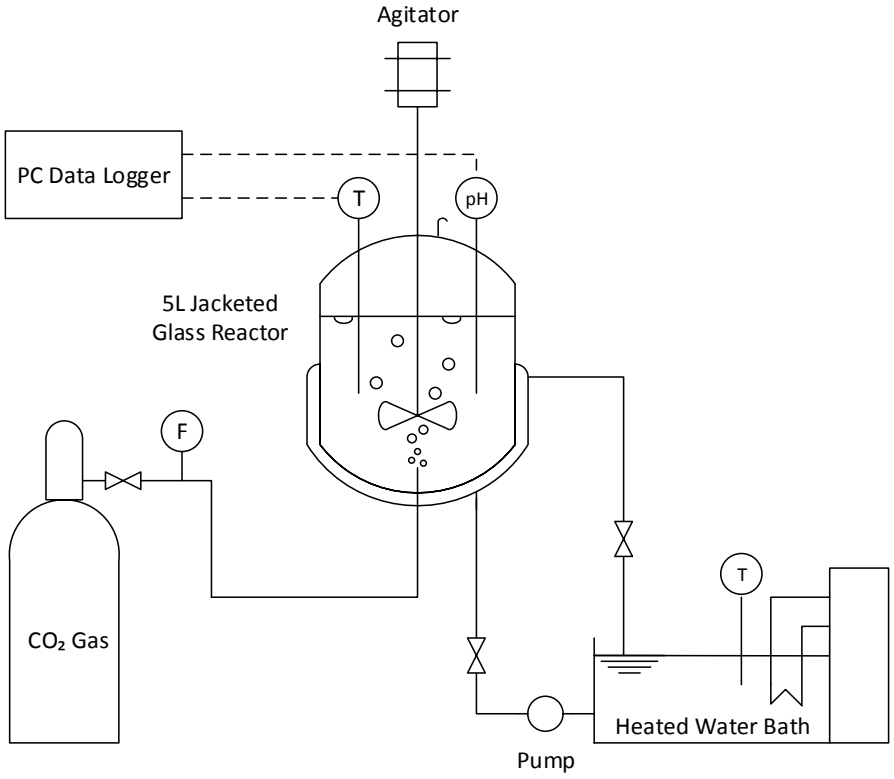

Figure 7.1 - Laboratory experiment equipment setup

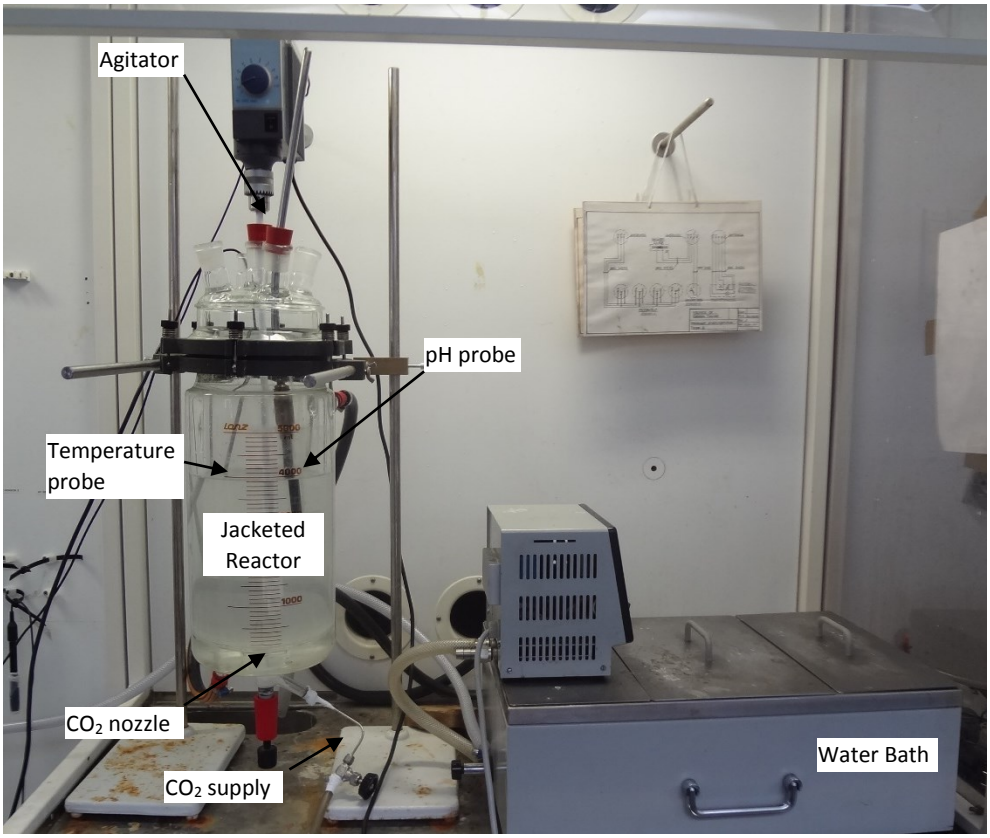

Figure 7.2 - Photo showing the equipment configuration for the laboratory scale test work

7.1.5 Experimental Procedure

For each test run 4L of calcium solution was used. The agitation speed and CO_2 flow were set manually at the start of each experiment. The initial solution temperature was controlled with the water bath thermostat. Chilled water was used for the low temperature runs. Once the flow of CO_2 was started and carbonation begun, the water bath was turned off, the reactor jacket isolated, and the solution temperature allowed to increase over the course of the experiment due to the exothermic carbonation reaction (although some heat would be lost to the water still in the jacket). The flow of CO_2 was set using a rotameter and sparged at the base of the reactor through a single 0.5 mm diameter tube positioned directly below the agitator. The temperature and pH of the solution was recorded and logged at five second intervals during carbonation. To estimate the induction time of the carbonation reaction, the time taken for the agitator to completely disappear from view (i.e. the time for the initially transparent solution to go completely opaque) was also recorded.

For the high [NH_4Cl] runs, 85.6g of anhydrous NH_4Cl were dissolved in each calcium solution before each run to bring the concentration up to 0.5 M. When this was first done, it was noticed that the solution temperature and pH dropped by approximately 1°C and 1 pH point respectively. The temperature drops as the dissolution of NH_4Cl is an endothermic reaction. The pH drops because NH_4^+ is a Brønstead-Lowry acid and can donate an H^+ ion to form a neutral NH_3 molecule via equation (6.32). As this drop in pH would not be comparable with the other runs and would effectively introduce pH as another factor in the experiment that would be inherently confounded with [NH_4Cl], it was decided to add 50% NaOH solution dropwise to return the solution pH to the level it was before the addition of NH_4Cl, typically requiring between 40 and 50mL. Whilst not ideal from an experimental consistency point of view due to the introduction of Na^{2+} ions, this was deemed the best way to assess the effect of additional ionic strength on PCC precipitation while keeping initial pH essentially constant across

the experiments. Solubility data showed that the sodium should remain in solution, but the risk was accepted that the Na^{2+} introduced may affect the results for the high [NH_4Cl] runs.

After each test the reactor was scrubbed to remove $CaCO_3$ scale and if necessary rinsed with dilute hydrochloric acid (HCl) to aid with scale removal which at times proved difficult. All equipment was washed first with water and then twice with distilled water after each test. In line with previous work conducted at Aalto, carbonation was stopped and carbonation time recorded once the pH of the solution had stabilised, typically in the range of 6.5-7.1. After carbonation was complete, the solution was withdrawn and filtered through GE Healthcare Whatman Grade 3 Qualitative Filter paper to collect the PCC. In most cases this was sufficient, but in several runs some of the particles were so fine that they passed through the filter medium. In these cases, the solution was split into cylindrical flasks, left for one hour to settle and the resulting solids decanted and collected. Whether filtered or decanted, the solid PCC was washed twice with distilled water before being put into airtight sample jars. The mass of PCC produced in each run was not measured, but instead a sample of the filtered solution was also taken and analysed for [Ca^{2+}] by EDTA complexometric titration to determine the calcium conversion. The solid PCC samples were taken to the department of Forest Products Technology for PSD analysis using a Malvern Mastersizer 2000. Given the potential for agglomeration, PSD measurements were taken under three conditions: i) the raw solid sample ii) the sample after being treated with ultrasound (US) (strength 500) for 2 minutes, and iii) with ultrasound turned off and left for 2 minutes. Scanning Electron Microscope (SEM) imaging was used to qualitatively determine the PCC morphology.

The response variables considered in the factorial experiment were the particle 50% and 90% passing size (the size 50% and 90% of particles are smaller than) before ultrasound (d_{50}, d_{90}) and after ultrasound (d_{50}^{US}, d_{90}^{US}) (µm), the induction time t_{ind} (min), carbonation time t_{carb} (min), maximum temperature rise (ΔT_{max}), calcium conversion η_{Ca} (%) and CO_2 conversion η_{CO_2} (%). Induction time was measured in addition to the total carbonation time as this is closely linked to the particle nucleation rate. The calcium conversion, sometimes referred to in the literature as carbonation efficiency, represents the molar conversion of Ca^{2+} to $CaCO_3$. Because the mass of precipitate was not weighed, calcium conversion was estimated instead from the calcium concentration results using the equation below.

$$\eta_{Ca} = 1 - \frac{c^0_{Ca^{2+}}}{c_{Ca^{2+}}} \tag{7.1}$$

where $c^0_{Ca^{2+}}$ is the initial concentration of Ca^{2+} in the Ca-rich solution before carbonation (M) and $c_{Ca^{2+}}$ is the concentration of calcium remaining in solution after carbonation (M).

Analogous to the calcium conversion, a CO_2 conversion, η_{CO_2}, can be defined as the fraction of CO_2 fed which reacts to form $CaCO_3$. Again as the mass of crystal was not weighed, CO_2 conversion could only be roughly estimated based on calculated calcium conversion, the CO_2 flow Q_{CO_2} (L/min), and the carbonation time using the equation below.

$$\eta_{CO_2} = \frac{\eta_{Ca} c^0_{Ca^{2+}} V}{Q_{CO_2} t_{car}} \tag{7.2}$$

It should be mentioned that the calcium and CO_2 conversion defined here, when expressed as percentages, would be more accurately termed conversion *efficiencies* as conversion is normally expressed as a fraction between zero and one. In this work however the terms conversion and conversion efficiency are used interchangeably.

In addition, the PSD results for were used to calculate a Agg_{d90} value, defined as the difference between the d_{90} result analysed before (d_{90}) and after (d_{90}^{US}) the application of ultrasound, expressed as a percentage of the d_{90} after u. This was calculated using the formula below.

$$Agg_{d90} = \left(\frac{d_{90}}{d_{90}^{US}} - 1\right) \tag{7.3}$$

In other words, an Agg_{d90} of 30% indicates that the d_{90} before the application of ultrasound was 30% larger than after the application of US. While not a recognised or standard measure, it was thought to be a potentially useful way of comparing agglomeration between runs and gaining additional information about the effect of precipitation variables on the tendency of the PCC to agglomerate.

7.1.6 Results for Main Effects

Table 7.3 shows the response variables results for each run of the factorial experiment, as well as the initial and final pH of the solution. From simple inspection of the data it is not easy to determine the significance of each factor given the variety of factor level combinations used. To interpret the data, the software Minitab® 16 [139] was used to perform statistical analysis of the factorial results.

Table 7.3 - Run results for the factorial experiment

Run	pH		t_{ind} (min)	t_{car} (min)	Before US		After US		Agg_{d90} (%)	ΔT_{max} (°C)	η_{Ca} (%)	η_{CO_2} (%)
	Initial	Final			d_{50} (µm)	d_{90} (µm)	d_{50}^{US} (µm)	d_{90}^{US} (µm)				
1	9.8	6.4	7.2	17.8	30	58	23	42	40	0.9	83	45
2	9.6	6.5	5.9	24.4	46	88	37	64	38	0.8	71	28
3	9.8	6.9	17.8	68.4	51	94	41	72	30	3.3	99	14
4	9.6	6.9	7.2	72.3	54	102	43	79	29	1.8	99	13
5	9.8	6.4	6.3	14.5	23	42	18	30	40	0.1	70	16
6	9.6	6.3	2.5	9.2	46	100	38	69	45	0.8	71	25
7	9.8	6.8	8.4	21.6	49	93	39	72	29	2.5	99	15
8	9.7	6.9	10.1	56.9	55	105	45	78	35	2.2	99	6
9	9.9	6.9	16.8	68.2	44	87	35	69	27	4.0	99	17
10	9.8	7.1	10.3	63.7	60	115	51	90	27	2.1	99	18
11	9.9	6.4	3.3	7.5	33	62	25	45	40	0.8	66	34
12	9.7	6.6	3.2	13.3	88	170	69	122	39	0.6	75	22
13	10.1	6.8	6.6	19.6	50	95	36	65	47	0.9	69	41
14	9.7	6.5	3.6	15.8	56	104	41	69	52	0.9	76	55
15	10.0	7.1	14.0	46.7	65	131	51	85	54	3.2	99	8
16	9.8	7.0	5.7	24.9	69	136	55	94	45	3.0	99	15

Main effects plots for each of the response variables are shown in Figure 7.3 - Figure 7.11. The data points in a main effects plot are the means of the response variable from each experimental run at the low and high levels of each factor, with a reference line drawn at the overall mean of the response data. The design of the factorial is such that for every factor level combination, there is an equal number of runs at the high and low level of every other factor. Thus when comparing the average values of a response variable between the high and low runs of a given factor, one would expect to see a difference between the means if the factor has an impact. This is easily seen on a main effects plot as a large gradient (positive or negative) connecting the low and high level averages. The stronger the effect, the steeper the gradient. If the factor has no impact, then the difference between means should be zero and the gradient between results should be small and approach the horizontal.

However, experimental error and random factors may cause a variable to appear like it has an impact while it may only be coincidental.

To identify whether a factor has a truly significant effect, analysis of variance (ANOVA) methodology was performed on the factorial results. ANOVA is essentially an extension of the t-test for means, which tests the null hypothesis that the means of two populations are equal for the case where the population variances are assumed to be equal [140]. In a two level factorial for example, it tests that the means of all runs at the low and high levels of a factor are equal which, if the factor has no effect, should be true. ANOVA works by comparing the variance between group means versus the variance within groups as a method of determining whether they are all part of one larger population or separate populations with different characteristics. The main result of an ANOVA test is a p-value ranging from 0 to 1 which indicates the appropriateness of rejecting the null hypothesis. Normally the accepted level of significance, α, is determined beforehand and fixed. Commonly used values for α are 0.10 and 0.05, representing 90% and 95% confidence respectively that the null hypothesis should be rejected. A value of 0.1 has been selected in this work, thus if the p-value calculated for a factor is < 0.1 the difference between means for the two factor levels is deemed statistically significant and one can say with 90% certainty that the factor has an impact. The ANOVA method can also be used to fit the experimental data according to a model for the i^{th} response variable containing terms for the main effects (A,B etc.) and each interaction term (AB,AC etc.) by calculating model coefficients (ζ_i^0, ζ_i^A , , ζ_i^A etc.) and an error term (ϵ_i). When only main effects are included and interaction terms are excluded, this is known as a general linear model (GLM).

$$Y_i = \zeta_i^0 + \zeta_i^A A + \zeta_i^B B + \zeta_i^C C + \zeta_i^{AB} AB + \zeta_i^{AC} AC + \zeta_i^{BC} BC + \zeta_i^{ABC} ABC + \cdots + \epsilon_i \qquad (7.4)$$

One drawback of an un-replicated fractional factorial design such as this however is that it is saturated, meaning that the total degrees of freedom (DoF) in the experiment (total runs – 1) is equal to the number of main effects and interactions considered (i.e. 16-1 = 5 (main factors) + 10 (2-way interactions). As a result, there are no DoF remaining to calculate the error term and p-values cannot be calculated when all main factors and interactions are included in the model. However, p-values for the main factors can be calculated by excluding 2-way interactions from the model and using these runs to determine an error term based only on main factors i.e. using a GLM. This was done and Table 7.4 below shows the ANOVA results for the calculated p-values considering only the main effects with statistically significant p-values bolded. Also shown is a calculated R^2 value based on the GLM showing the amount of variation in the observed response values that is explained by a linear combination of the considered factors. A high R^2 value suggests a good model fit and that the most important factors are included in the model. Detailed results from the ANOVA calculations are given in Appendix D.

Table 7.4 – Calculated main effect p-values by ANOVA using a GLM for the laboratory-scale factorial

	t_{ind}	t_{car}	Before US		After US		Agg_{d90}	ΔT_{max}	η_{Ca}	η_{CO_2}
			d_{50}	d_{90}	d_{50}^{US}	d_{90}^{US}				
Initial Temperature	**0.010**	0.709	**0.015**	**0.008**	**0.015**	**0.013**	0.870	0.125	0.687	0.804
[Ca^{2+}]	0.832	0.559	**0.031**	**0.037**	**0.033**	**0.058**	0.212	0.139	0.561	**0.088**
[NH_4Cl]	**0.001**	**0.000**	0.127	**0.049**	0.130	**0.053**	**0.074**	**0.000**	**0.000**	**0.000**
CO_2 flow	**0.053**	**0.004**	0.425	0.348	0.293	0.476	0.273	0.479	0.277	**0.004**
Agitation speed	0.231	0.128	0.208	0.162	0.298	0.292	0.942	0.519	0.524	**0.023**
R^2 (%)	*80%*	*87%*	*67%*	*71%*	*67%*	*67%*	*42%*	*87%*	*95%*	*86%*

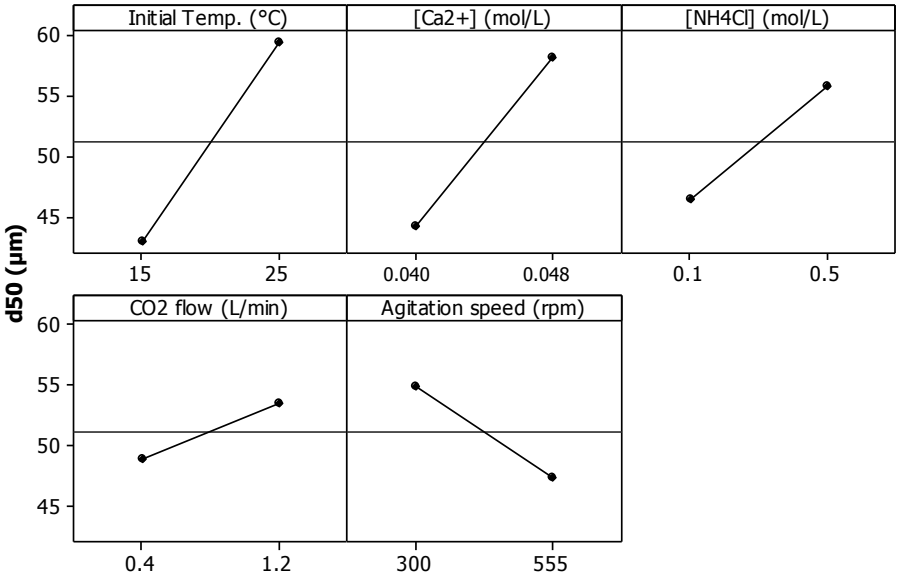

Figure 7.3 - Main effects plot for d_{50} (no US)

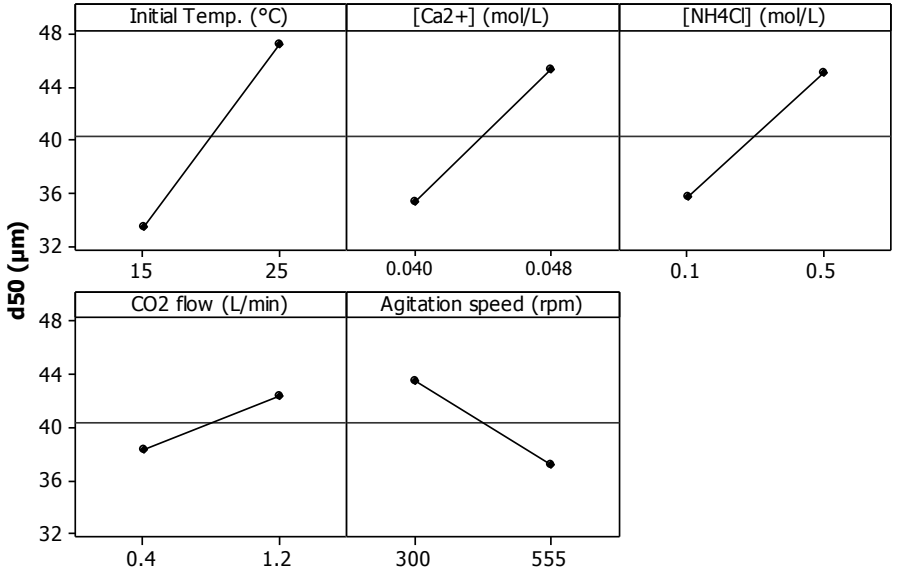

Figure 7.4 - Main effects plot for d_{50} (with US)

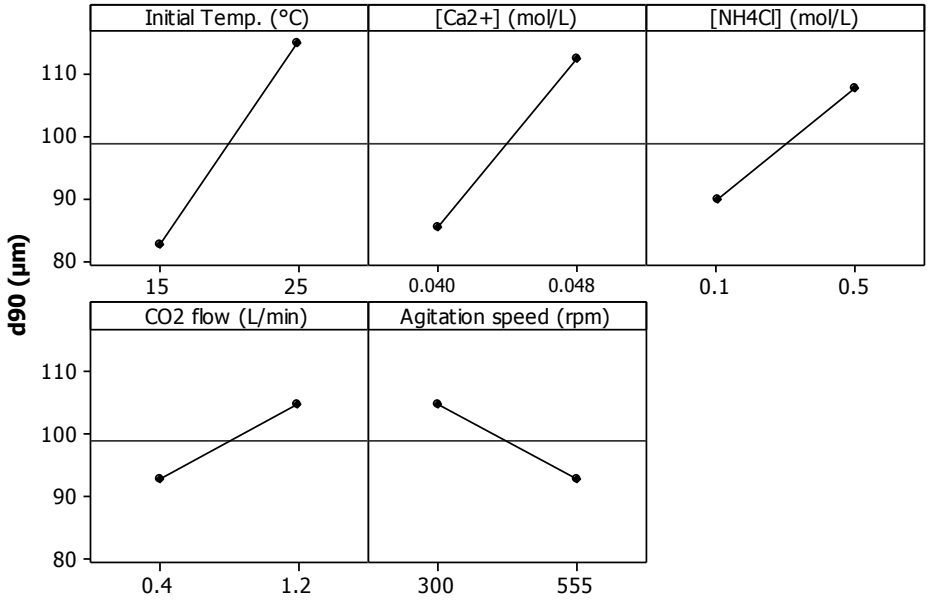

Figure 7.5 - Main effects plot for d_{90} (no US)

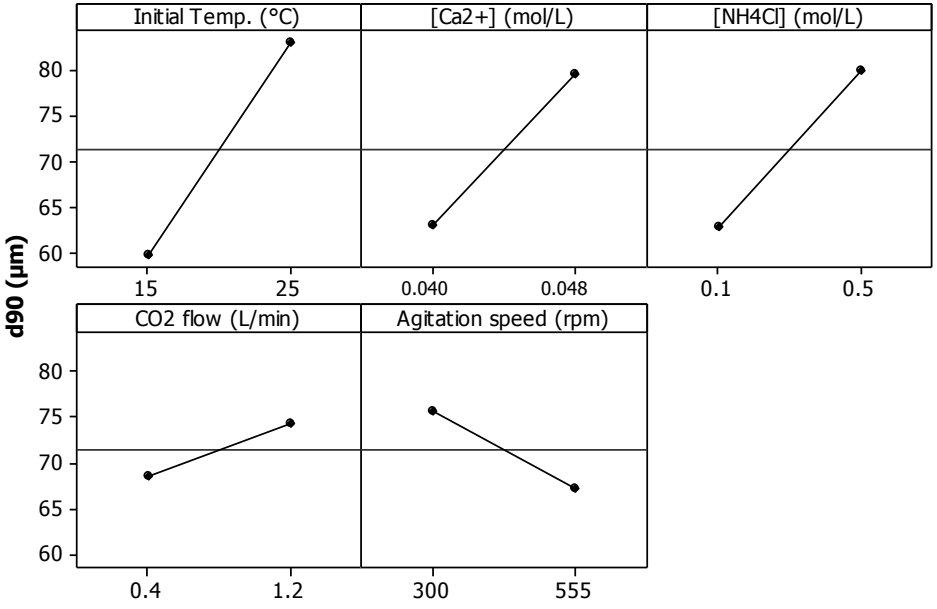

Figure 7.6 - Main effects plot for d_{90} (with US)

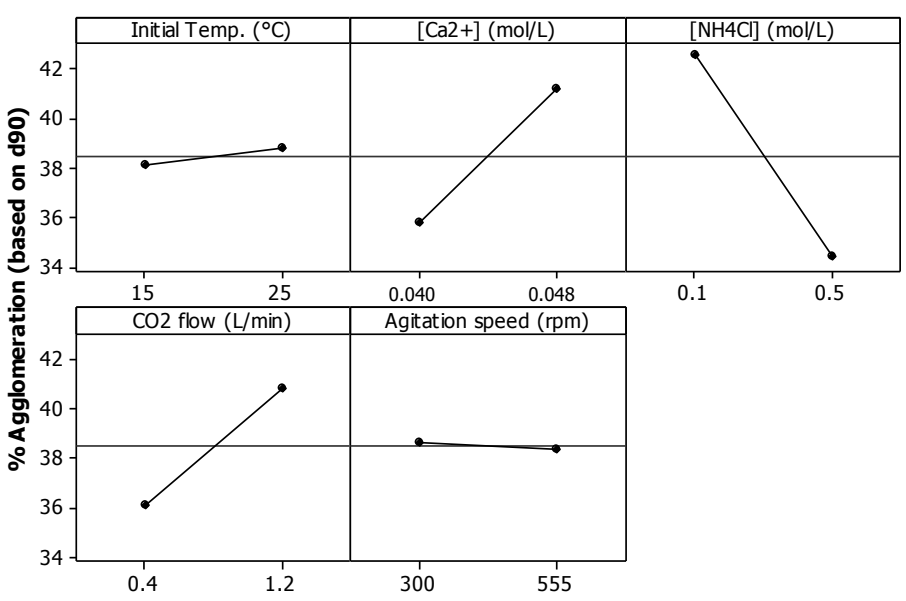

Figure 7.7 - Main effects plot for Agg_{d90}

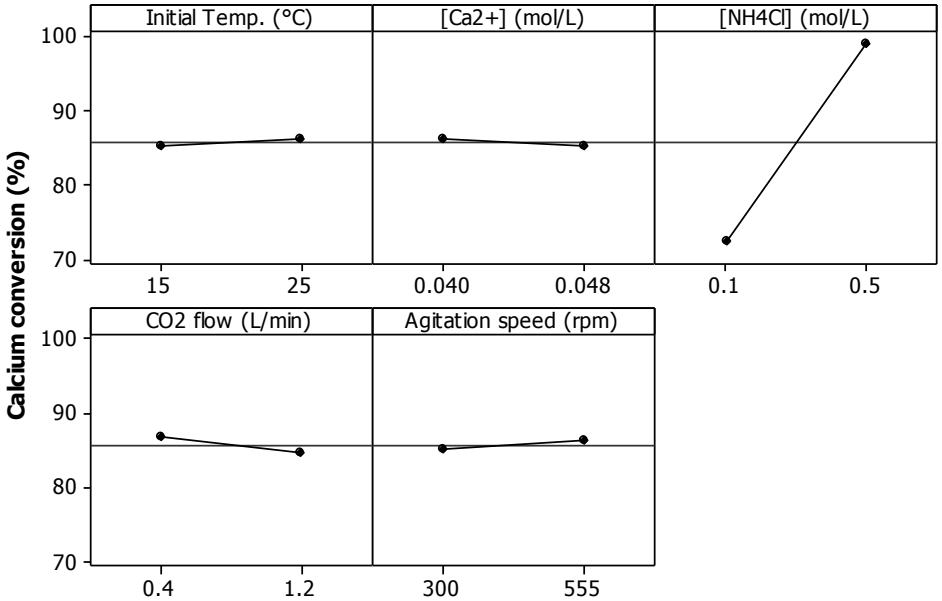

Figure 7.8 - Main effects plot for calcium conversion

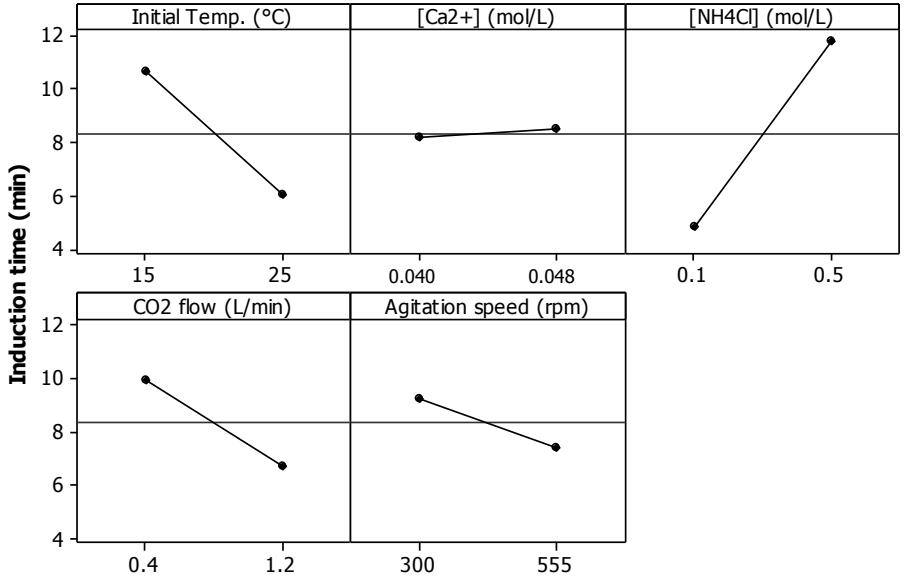

Figure 7.9 - Main effects plot for induction time

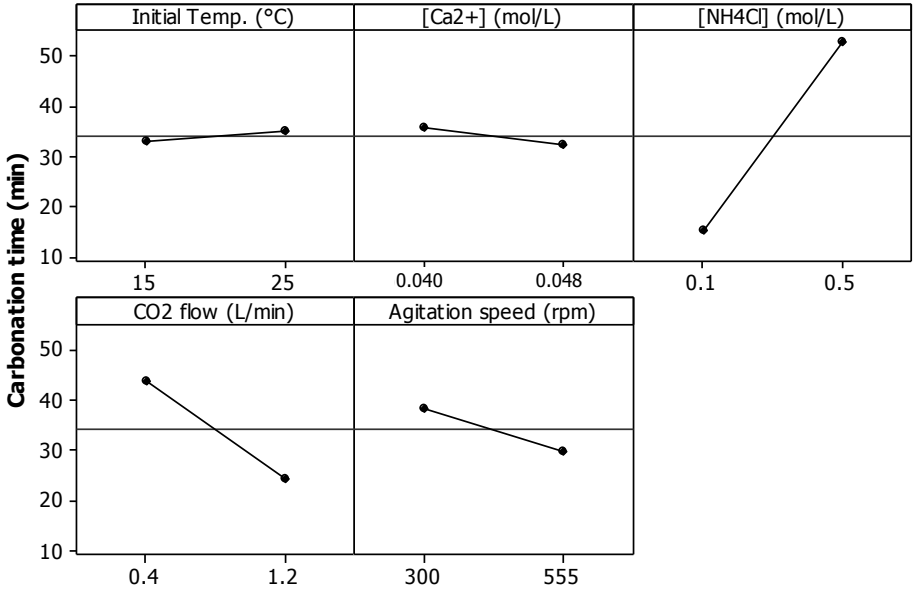

Figure 7.10 - Main effects plot for carbonation time

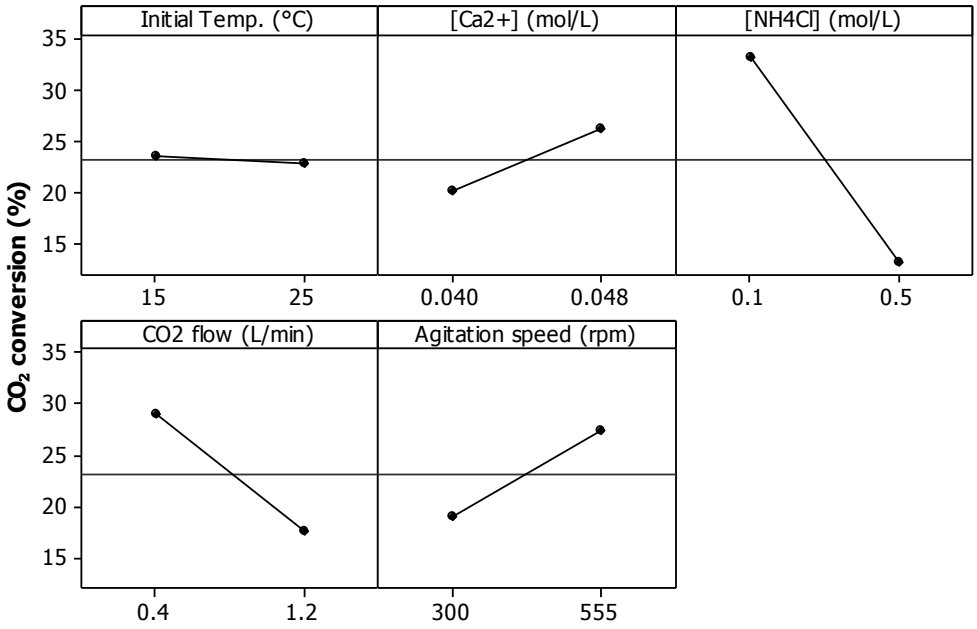

Figure 7.11 - Main effects plot for CO_2 conversion

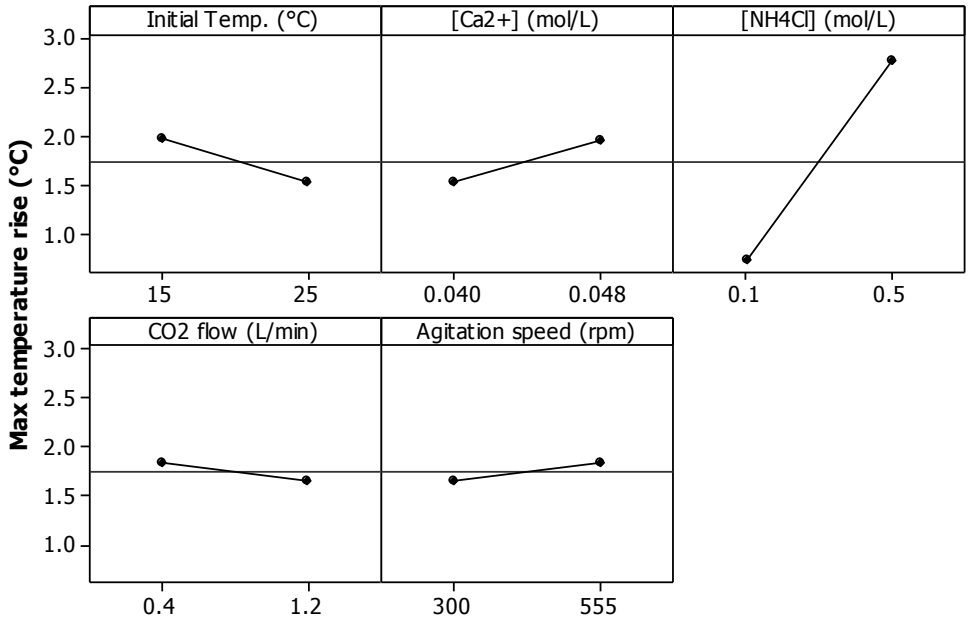

Figure 7.12 - Main effects plot for maximum temperature rise

Table 7.4 as well as the main effect plots should be taken as complimentary as given the limited number of experiment runs, the very strong impact of NH_4Cl, and potential for experimental error, a factor with p-value >0.1 does not indicate that it has no effect; merely that based on the analysis it is statistically less likely. Agitation speed, for example, probably has an effect on induction, carbonation time and particle size, even though the p-values are slightly above the cut-off point.

7.1.6.1 PSD and Agglomeration

From the d_{50} and d_{90} results before and after ultrasound (Figure 7.3-Figure 7.6), it seems that all the factors considered may have an effect on PCC particle size though only temperature, $[Ca^{2+}]$ and $[NH_4Cl]$ are shown as statistically significant. The strongest effect is from initial temperature which shows a strong positive correlation with d_{50} and d_{90}, i.e. higher temperatures give coarser particles. The $[Ca^{2+}]$, $[NH_4Cl]$ and CO_2 flow also appear to be positively correlated with particle size, although the effect of the latter is much weaker. Agitation speed displays a negative correlation with particle size with higher agitation resulting in smaller particles, contrary to the findings of Jones et al. [97]. The positive correlation between temperature and particle size is in agreement with the literature. This is most likely due to the impact on the linear crystal growth rate as shown in Table 6.1, with a 5°C drop in temperature reducing crystal growth rate by approximately 30%. The positive correlation with $[Ca^{2+}]$ however was not seen in the literature, with most data available suggesting that if anything higher concentration should produce the opposite effect and reduce particle size. It is also interesting that the effect of $[Ca^{2+}]$ appears strong despite the small difference between the high and low concentration levels. The effect of $[NH_4Cl]$ on particle size seems most likely due to the significant increase in carbonation time for the high $[NH_4Cl]$ runs (discussed later) which would give the particles more time to grow and agglomerate. This would imply that the $[NH_4Cl]$ may also have an effect on the precipitation kinetics. However, the literature review also found that high ionic strength itself can cause significant agglomeration due to surface charge shielding, thus it may be a combination of the two. The R^2 value for all the PSD metrics from the ANOVA calculation were quite low (~70%) showing that a considerable part of the variability in PSD was due to factors not considered in the experiment.

Figure 7.13 shows the full PSD results for each factorial run after the application of ultrasound. All runs resulted in the production of particles too coarse to be used directly as PCC for filler applications. The distributions could be considered bimodal in most cases with the major peak between 10 and 100µm, with a much smaller peak below 10µm. The presence of particles with size >1000µm is most likely due to foreign material in the sample or clumps of particles not well dispersed during sample preparation.

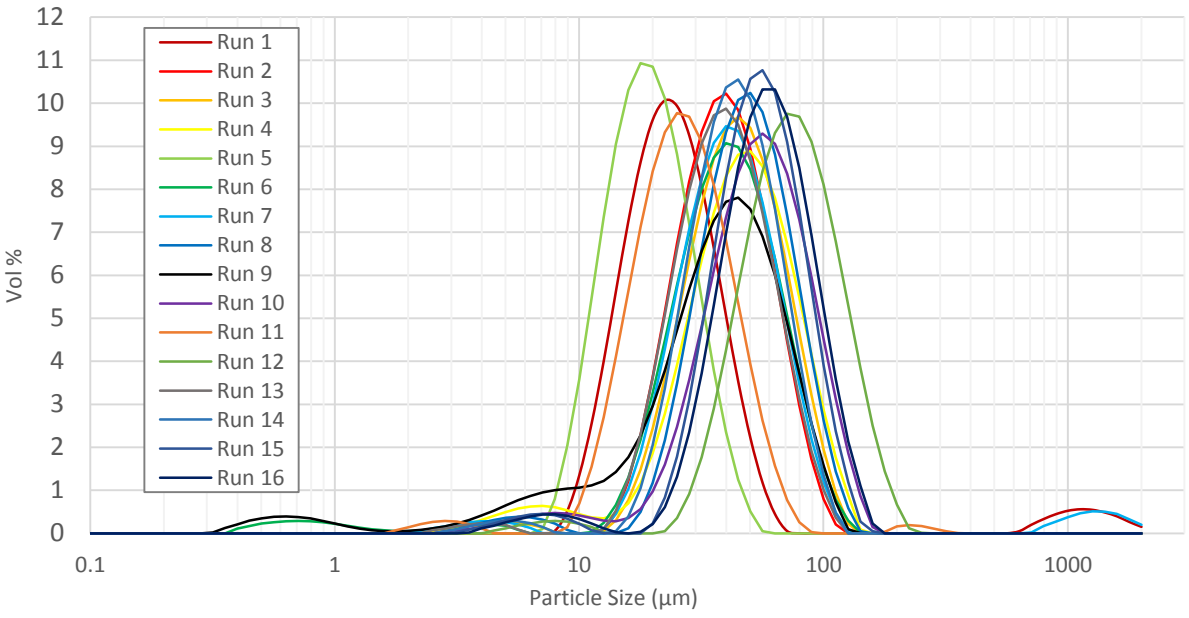

Figure 7.13 - Full PSD results for each factorial run (after ultrasound)

The effect of ultrasound on the PSD result analysis is exemplified in Figure 7.14. Ultrasound was able to break the large agglomerates and bring the distribution closer to the primary particle size.

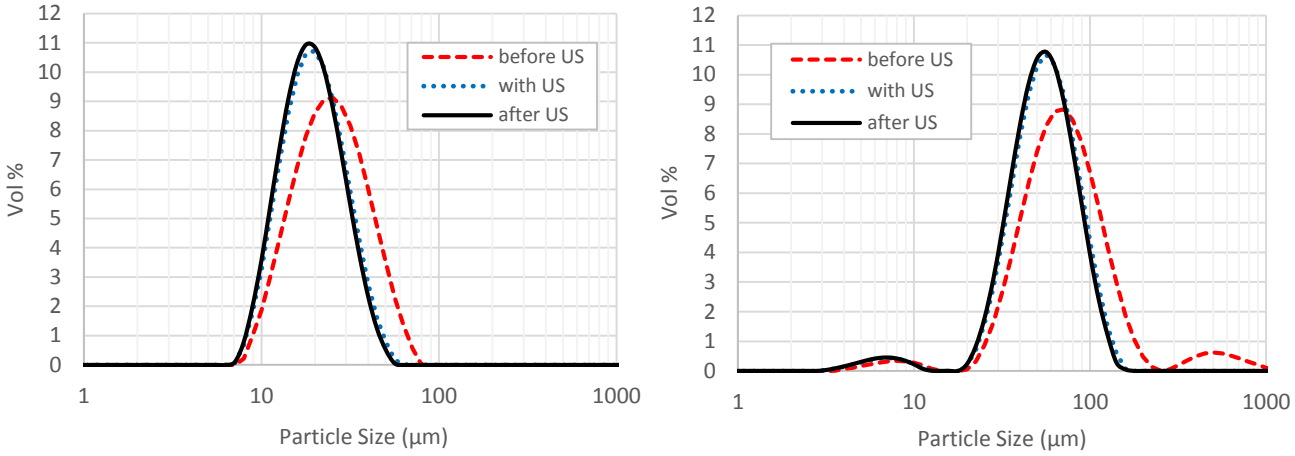

Figure 7.14 – PSD results for Run 5 (left) and Run 15 (right) before and after two minutes of ultrasound

Longer application of ultrasound may have broken down the agglomerates even further, but this was not investigated.

Based on the calculated values of Agg_{d90}, Figure 7.7 would seem to suggest that of the factors studied [Ca^{2+}], [NH_4Cl] and CO_2 flow may have an impact on the tendency of the PCC to agglomerate. The only factor deemed statistically significant was [NH_4Cl] with higher concentrations giving lower Agg_{d90}. Higher CO_2 flow and [Ca^{2+}] may also increase agglomeration. However, the R^2 value for Agg_{d90} was very low showing that the considered factors explained only 50% of the variation in this parameter and other unconsidered variables were playing a role.

Agglomeration may have occurred while the carbonation reaction was taking place, or in the delay between when the sample was taken and analysed, typically 7-14 days. Without knowing how the PCC aggregates in the sample jar after sampling, no conclusion can be drawn at this stage. Interestingly, agitation did not appear to have any effect on agglomeration, contrary to what was expected from the literature review. The strongest effect on agglomeration was from [NH_4Cl] which displayed a strong negative correlation. This finding is contrary to the literature which suggested that higher solution ionic strength shielded the PCC surfaces from each other, reducing the width of the EDL leading to more successful collisions and agglomeration. One potential explanation for this finding may be that the strong negative correlation with [NH_4Cl] was because the agglomerates formed in the high [NH_4Cl] runs were more strongly held together, thus the ultrasound treatment may not have been sufficient to break the agglomerates and the reported Agg_{d90} would be lower. Thus it should be kept in mind that Agg_{d90} is a very crude metric for agglomeration. It is also uncertain whether the two minutes of ultrasound was sufficient to break all the agglomerates, or whether the primary crystals may also have been broken during this process. Discussions with Prof. Maloney however suggest that the level of ultrasound used should have been sufficient to break normal levels of PCC agglomeration, adding weight to the theory that the NH_4Cl may increase the strength of the PCC agglomerates. The positive correlation with [NH_4Cl] and particle size, as well as the SEM micrographs also suggest it increases agglomeration.

A correlation between agglomeration and CO_2 flow would be supported by the literature that a build-up of CO_2 in the liquid film can quickly react to form crystals which have a higher frequency of collision success in the film and agglomerate quickly.

7.1.6.2 Induction Time

From the calculated p-values in the ranges studied, initial temperature, CO_2 flow and [NH_4Cl] have a statistically significant effect on induction time. Figure 7.9 suggests that agitation speed may also effect induction time, even though the calculated p-value was above the tolerance. While temperature, CO_2 flow and agitation are negatively correlated with induction time (i.e. higher temperature, agitation and CO_2 flow reduce induction time), [NH_4Cl] exhibits a strong positive correlation.

The negative correlations may be explained in terms of the kinetics of the overall process and remembering that induction time is also an indication of nucleation rate. Higher agitation and CO_2 flow will increase the rate of CO_2 mass transfer from the gas to the liquid phase by equation (6.18), setting the whole precipitation process off much quicker as at the start of carbonation Ca^{2+} is in surplus while CO_3^{2-} is the limiting reagent. Higher temperature will increase the rate of reactions (6.21) - (6.39), thus at lower temperatures the rate at which $CO_{2(aq)}$ is converted to $HCO_3^-{}_{(aq)}$, $CO_3^{2-}{}_{(aq)}$ and finally $CaCO_3$ will be slower, meaning it will take more time before the PCC becomes visible. The reason for the strong positive correlation between [NH_4Cl] and induction time is not entirely clear. It may be that the higher ionic content of the solution slows the absorption of CO_2 into solution, thereby bottlenecking the entire precipitation process, or it may slow the diffusion of reactive species through the liquid film. Higher spectator ionic content may also reduce the activity of the reacting ions in solution, reducing their effective concentrations and thus their rates of reaction. Adsorption of ionic species on the crystal surface may also block and slow crystal growth.

Induction time was easy to measure in the low [NH_4Cl] runs as the transition from transparent solution to opaque took only 3-5 seconds, but for the high [NH_4Cl] runs the change was gradual and took been 2-3 minutes making it difficult to determine exactly when the agitator disappeared. Thus in these tests, the solution began turning opaque quite some time before the reported induction time.

7.1.6.3 Carbonation Time and pH

The results for total carbonation time were essentially the same as for induction time, except that only [NH_4Cl] and CO_2 flow reported statistically significant effects, not temperature. Another difference is that the p-value for the effect of agitation on carbonation time was quite close to being statistically significant and when performing the test runs those with stronger agitation took place noticeably faster. The runs with high [NH_4Cl] had significantly longer carbonation time, probably for the same kinetic reasons described above for induction time.

The literature was not in agreement on the effect of temperature, with one source reporting temperature has no effect and another reporting a positive correlation with carbonation rate. This seemed surprising given the fact that temperature had such a strong impact on induction time. As the total carbonation time also includes the induction time the two response variables are not completely independent, and so another variable ‘growth time’ was defined as the length time from the end of the induction period to the end of the carbonation. It was found that temperature shows a slight positive effect on growth time whereas the effect on induction time is negative, thus these two effects partially cancel out when only the overall carbonation time is considered. This contrary effect of temperature on growth time was not statistically significant however, and so no firm conclusion can be drawn on the effect of temperature on the growth time at this stage.

Two different types of pH behaviour were seen during the factorial tests. Some runs exhibited a single equivalence point (Runs 1-2, 4-5, 12, 14) and the other exhibited two (Runs 3, 6-9, 10-11, 13, 15-16). Figure 7.15 and Figure 7.16 on the following page show typical profiles for the recorded pH during the

carbonation runs, with runs 1 and 7 given here as examples of a single and double equivalence point run respectively. The temperature profiles for the same runs are given in Figure 7.17 and Figure 7.18. The dashed region of the pH trends indicates the induction period when the agitator was still visible. The red dots show the calculated rate of change in pH.

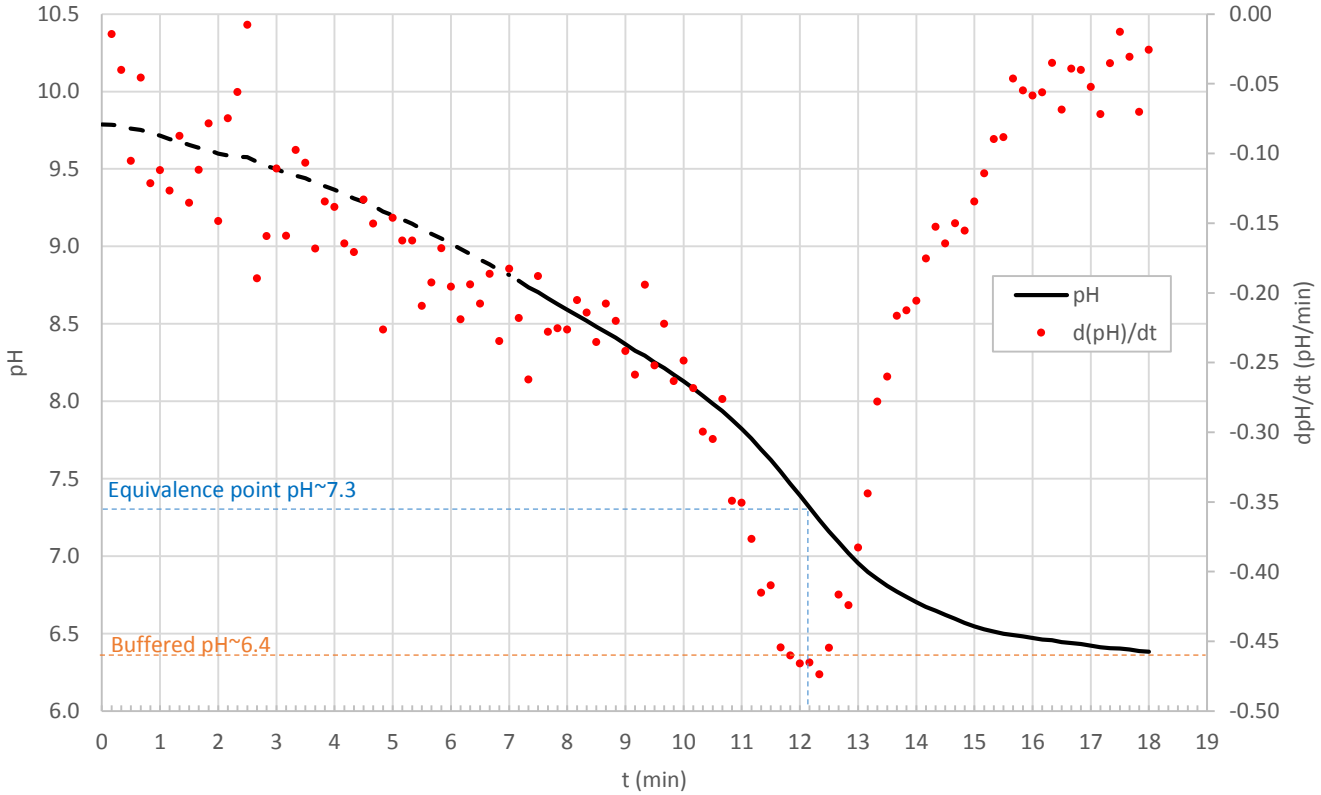

Figure 7.15 - Recorded pH and calculated rate of pH change for a typical single equivalence point run (Run 1)

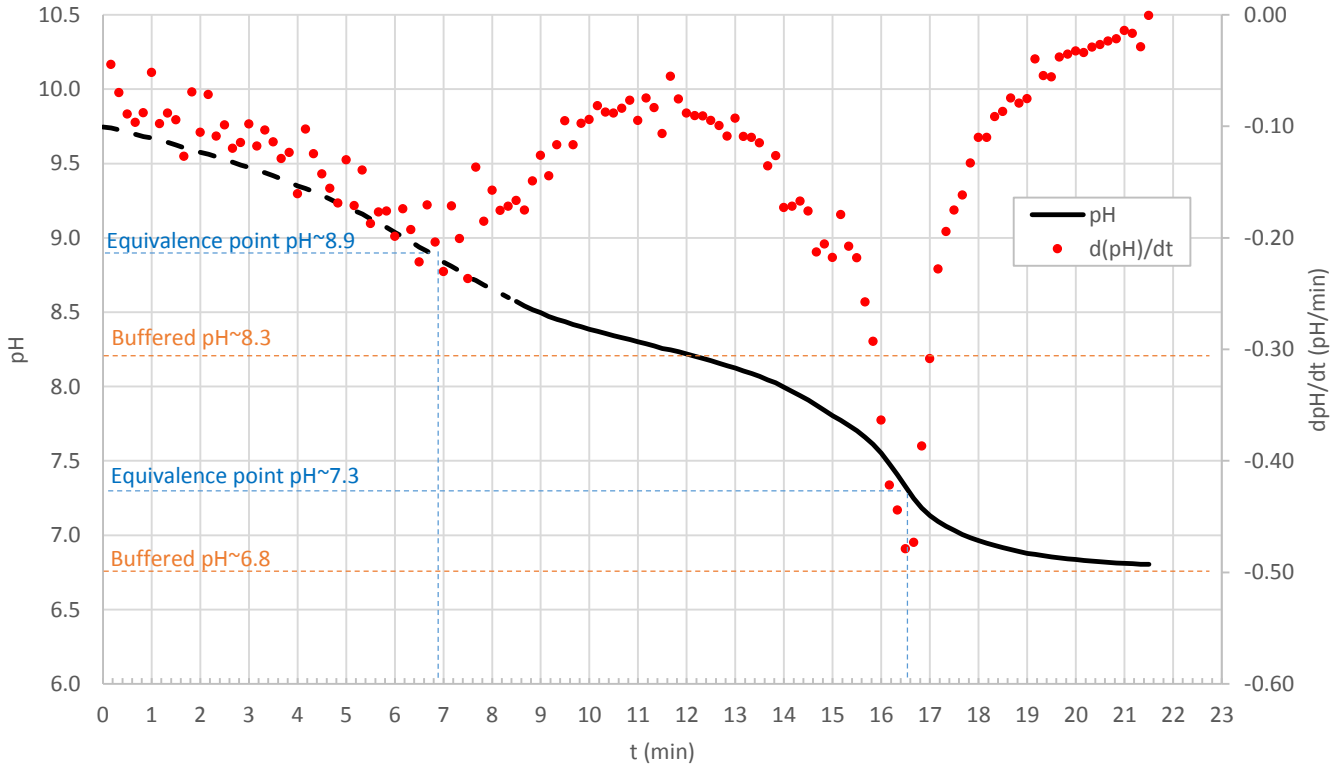

Figure 7.16 - Recorded pH and calculated rate of pH change for a typical double equivalence point run (Run 7)

Throughout the course of the carbonation, the pH falls as OH^- ions are consumed by reaction with CO_2 to form HCO_3^-, CO_3^{2-} and H_2CO_3, thus the final solution pH is very closely linked to carbonation time.

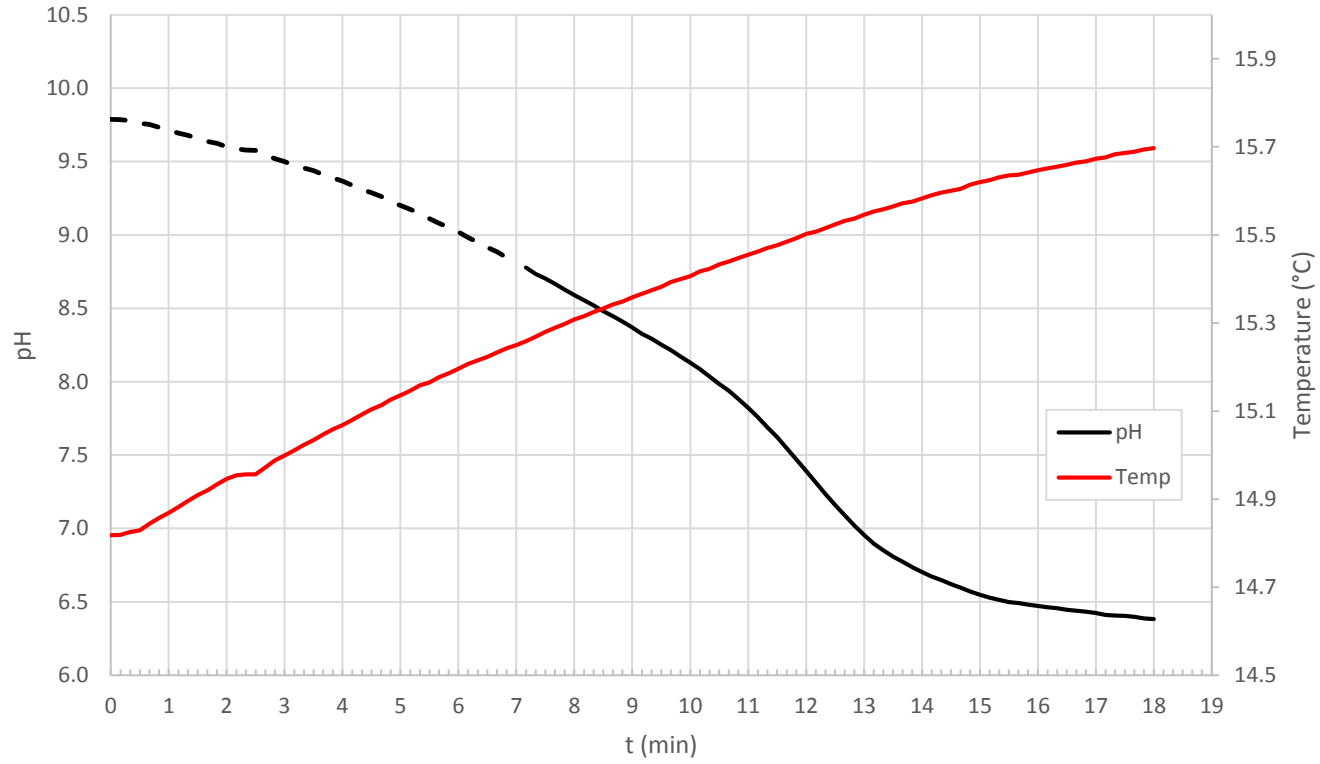

Figure 7.17 - Recorded temperature profile for a typical single equivalence point run (Run 1)

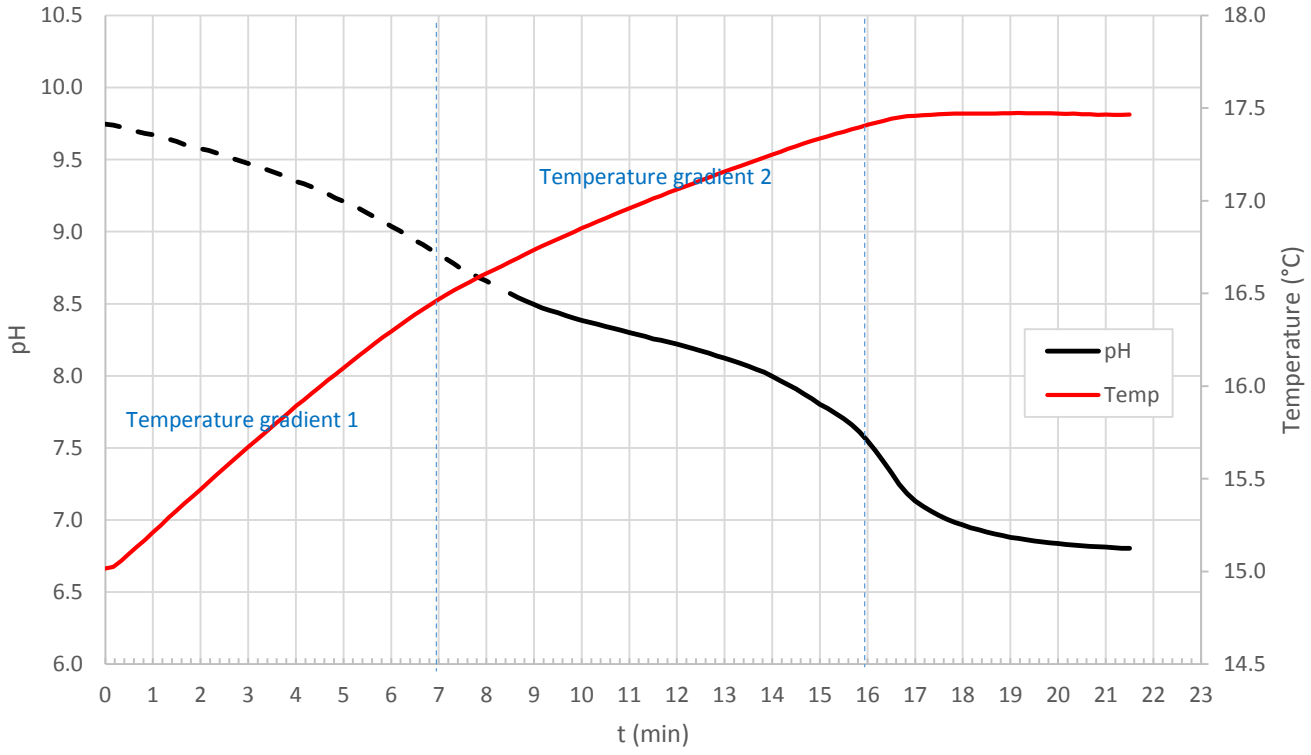

Figure 7.18 - Recorded temperature profile for a typical dual equivalence point run (Run 7)

In some ways, the carbonation process can be considered analogous to a titration of OH^- with H_2CO_3. In a standard titration of OH^- by H_2CO_3 at 25°C, an equivalence point is seen at pH 8.34 which is the midpoint between the pK_a values for the dissociation of HCO_3^{2-} (10.4) and H_2CO_3 (6.4) given by the reverse of equations (6.24) and (6.25) and in the pH range of 6.4-10.4, HCO_3^- will be the dominant ion in solution. However, the presence of NH_4Cl and Ca^{2+} in solution affect the pH behaviour in Slag2PCC carbonation. Figure 7.15 and Figure 7.16 show that an equivalence point always occurred at a pH of around 7.3, shown by the maximum in pH differential. Whilst not identical, this matches quite well with the calculated equivalence point of 7.67 from HSC Chemistry in Figure 6.12. Thus this equivalence point is believed to correspond to the midpoint of the HCO_3^- and H_2CO_3 dissociations, shifted slightly from the standard midpoint of 8.4 due the presence of NH_4Cl which would affect the activity coefficients in solution. Simulating a standard H_2CO_3/OH^- titration in Medusa with activity coefficient estimation and ionic strength at 1M does shift the equivalence point down to a pH of 7.9 which seems to support this idea. The single equivalence point runs exhibited strong buffering capacity as pH approached 6.4. The ability of a buffer system to flatten out changes in pH is strongest when the value of the solution pH is near the pK_a of the acid in the buffer system. With pH 6.4 corresponding to the pK_a of reaction (6.24) and the conversion of HCO_3^- to H_2CO_3, this adds further weight to the theory.

The dual equivalence point runs, in addition to one equivalence point at pH 7.3, showed an additional equivalence point at a pH of approximately 8.9. This behaviour was also seen by Matilla et al. [50] in their work when high concentrations of NH_4Cl were used during carbonation. They suggested that at high $NH_{3(aq)}/NH_4^+{}_{(aq)}$ ratios, the dominant species in solution will not be HCO_3^- but $NH_2CO_2^-$ due to reaction (6.35), and that the reason for slower carbonation kinetics in high [NH_4Cl] solutions was the lower availability of CO_3^{2-} due to a portion of the available HCO_3^- reacting to form $NH_2CO_2^-$. Figure 7.18 shows that the temperature during the dual equivalence point runs appeared to have two distinct gradients on either side of the first equivalence point, unlike the smoother temperature increase seen in Figure 7.17. If the formation of carbamate were exothermic, this may explain the greater degree of heat generation in this region of higher pH when $NH_{3(aq)}$ will be the dominant species over NH_4^+. However, heat of formation or reaction data for NH_2COO^- could not be found to confirm this. Six out of the eight factorial runs performed with high [NH_4Cl] exhibited two equivalence points which seems to support this, but so did three of the low [NH_4Cl] runs, possibly suggesting some dynamic species effect. The presence of NH_4Cl constitutes another Lewis acid-based pair (NH_4^+/NH_3) in the system and can be expected to affect pH during carbonation. In particular, the solution will also exhibit buffering capacity around a pH of 9.5 due to the equilibrium between $NH_{3(aq)}$ and NH_4^+ and around 8 due to the precipitation of $CaCO_3$ which further complicates the interpretation of the first equivalence point. There did not appear to be any strong connection between the induction time and the second equivalence point in those runs where it occurred.

During the experiment runs it was noticed that in some runs, the carbonating solution would begin to become more transparent towards the end of the experiment, suggesting that some of the particles were starting to redissolve. The transition point was difficult to identify by eye and so to better capture when this occurred several carbonation runs were recorded using a digital camera and the times matched with the logged pH data. In those runs where the solution did start to become transparent, this occurred when the pH dropped below a pH of about 8. This seems to confirm that the PCC was redissolving due to the formation of carbonic acid and lower pH.

7.1.6.4 Calcium Conversion

The only factor which showed a statistically significant effect on calcium conversion was [NH_4Cl]. The high [NH_4Cl] runs produced noticeably more solid product during the experiments and the calculated calcium conversion using the complexometric method was over 99% for each of the high [NH_4Cl] runs while for the low runs the efficiency was in the range of 65-75%. There are several potential reasons for this:

- Precipitation of a sodium salt (e.g. Na_2CO_3, $NaHCO_3$ etc.)
- Interference of NH_3 with complexometric analysis
- Higher final solution pH
- Slowed dissolution kinetics

Firstly, there is the risk that some of the sodium introduced with the NaOH in the high [NH_4Cl] runs may also have precipitated as either Na_2CO_3, $NaHCO_3$ or NaCl which would explain the higher amount of solids, however the maximum amount of these salts which could be produced from the sodium added was verified before the tests to be below their reported solubilities, so this should not have occurred to any great extent. The amount of solids produced in these runs was also approximately consistent with what would be expected at close to 100% conversion of calcium. If significant amounts of sodium in addition to calcium had precipitated then this should have been clear from the amount of solids produced.

Secondly, calcium is known to form stable complexes with NH_3 in solution, which means that the presence of NH_3 can affect the reported concentration of calcium via complexation with EDTA as fewer Ca^{2+} ions are free to complex with EDTA. At 0.1M NH_3 approximately 94% of the calcium is present as Ca^{2+}, but at 0.5M NH_3 this reduces to 74%. This was known before the tests and accounted for in the analysis based on Ca-NH_3 reported speciation as described in Appendix A, but it is possible that the complex mixture of components including Cl^- from the solvent and other dissolved metals from the slag also affected the analysis.

Thirdly, the final pH of the runs performed at high [NH_4Cl] were on average about 0.5 pH points higher than the low [NH_4Cl] tests. This was not deliberate, but simply a feature of when the second equivalence point was reached and the buffering capacity of the solution. As demonstrated in the equilibrium calculations earlier the stability of $CaCO_3$ is very sensitive to pH in the range of 5-7, thus taking into account the fast rate of pH change in this region and possible pH measurement errors, it's plausible that this small difference in pH could have a large impact on the equilibrium stability of $CaCO_3$ and hence the final amount of PCC produced. The high [NH_4Cl] runs also did not show signs of becoming significantly more transparent once pH fell below 8.

A fourth possibility is that the additional ionic content slowed down the dissolution kinetics as well as the precipitation kinetics in the high [NH_4Cl] runs, thus even though the pH reached similarly low levels as in the other runs, the dissolution rate may have been sufficiently slow that a higher proportion of PCC particles survived.

7.1.6.5 CO_2 Conversion

All factors apart from initial temperature exhibited a statistically significant effect on CO_2 conversion. The [NH_4Cl] had the strongest effect, with higher concentration giving a lower conversion. This may be due to the diminishing solubility of CO_2 in higher concentrations of NH_4Cl but from Figure 6.2, in the region of 0.1-0.5 M NH_4Cl, the solubility difference is small and in reality the effect is more likely to be due to the longer carbonation times seen with the high [NH_4Cl] runs. The measurement of CO_2 gas flow

by rotameter is not particularly accurate and any error in gas flow (due to difficulties reading the value or wrongly calibrated temperature and pressure) will be accumulated with increasing carbonation time. Increasing CO_2 flow reduced CO_2 conversion efficiency which was unsurprising as from observing the gas bubbles leaving the solution the flow rate of CO_2 into the reactor was higher than the rate at which it could be taken up into solution in every test, thus a large amount of excess CO_2 simply did not react. Increasing agitation rate improved CO_2 conversion efficiency most likely due to the improved gas-liquid mass transfer. In the range of 15-25°C temperature did not seem to have any effect on CO_2 conversion. Although one might expect this to effect CO_2 efficiency due to the higher solubility of CO_2 at lower temperature, once the solution becomes saturated with CO_2, excess CO_2 would still leave the solution. The impact of temperature on mass transfer in this range thus may also be small.

7.1.6.6 Maximum Temperature Rise

Only [NH_4Cl] yielded a statistically significant correlation with maximum temperature rise with higher concentration giving a greater temperature rise during carbonation. Temperature rise is closely linked with calcium conversion because by combining the two exothermic reactions (6.21) and (6.22) to form bicarbonate and carbonate as well as the endothermic calcite formation reaction (6.29), the overall heat of reaction is calculated as -75.4 kJ/mol $CaCO_3$ produced. As the high [NH_4Cl] runs also reported high calcium conversion these runs would be expected to have a larger temperature rise. However, as discussed in 7.1.6.4, sodium salts may also have precipitated which would have an impact on temperature rise. Aside from the precipitation of sodium salts, another possible reason for the larger temperature rise in the high [NH_4Cl] runs is the formation of carbamate.

As the temperature was not actively controlled during the experiment and the system was not thermally isolated, the temperature measurements should be treated with some scepticism. For example, if the solution was being cooled in preparation for a 15°C test using 4°C water in the jacket, this chilled liquid would absorb heat from the carbonation reaction even though the jacket was isolated, thus the carbonation temperature rise would be understated.

7.1.7 Morphology

SEM micrographs were taken from samples of each of the 16 factorial runs. All runs yielded clustered agglomerates of rhombohedral calcite of various sizes. No scalenohedral calcite or aragonite was observed. Some spherical vaterite and potentially ACC was observed in runs 1, 2, 3, 4, 6 and 12. Figure 7.19 on the following page presents a selection of the SEM micrographs highlighting the main phenomena:

(a) Large 10-30 µm agglomerates of rhombohedral calcite with primary particle size 2-8 µm
(b) Chain-like structures of very small (<0.5µm) spherulitic particles of what may be vaterite or ACC bridging between the agglomerates
(c) Amorphous structures of what may be transitional crystal or ACC alongside very crystalline material, more frequently seen in the high [NH_4Cl] runs
(d) Amorphous crystal masses covered in blotchy specks, typical of runs with short carbonation times (<10 minutes) suggesting undeveloped crystals and incomplete phase transformations
(e) Very large agglomerates (>80µm)
(f) Nano-scale pitting and crevices on flat crystal faces
(g) Squared-off, poorly defined, incomplete edges and corners on some rhombohedral crystals
(h) Layered growth patterns

From these observations, the following conclusions are drawn:

- Under the conditions of the experiments, very short carbonation times (<10 minutes) are not sufficient to allow the necessary phase transformations to take place, resulting in the production of vaterite, irregular and incomplete crystal morphologies.
- Amorphous PCC and/or vaterite is produced as a precursor, which then transforms into the stable calcite phase. Chain-like structures of this material bridging between crystals may be how agglomeration takes place.
- Pitting, crevices and poorly defined crystal edges seem to confirm that the PCC is redissolving at low final pH levels (<7.5) and that stopping at a higher pH (~8) should be considered.

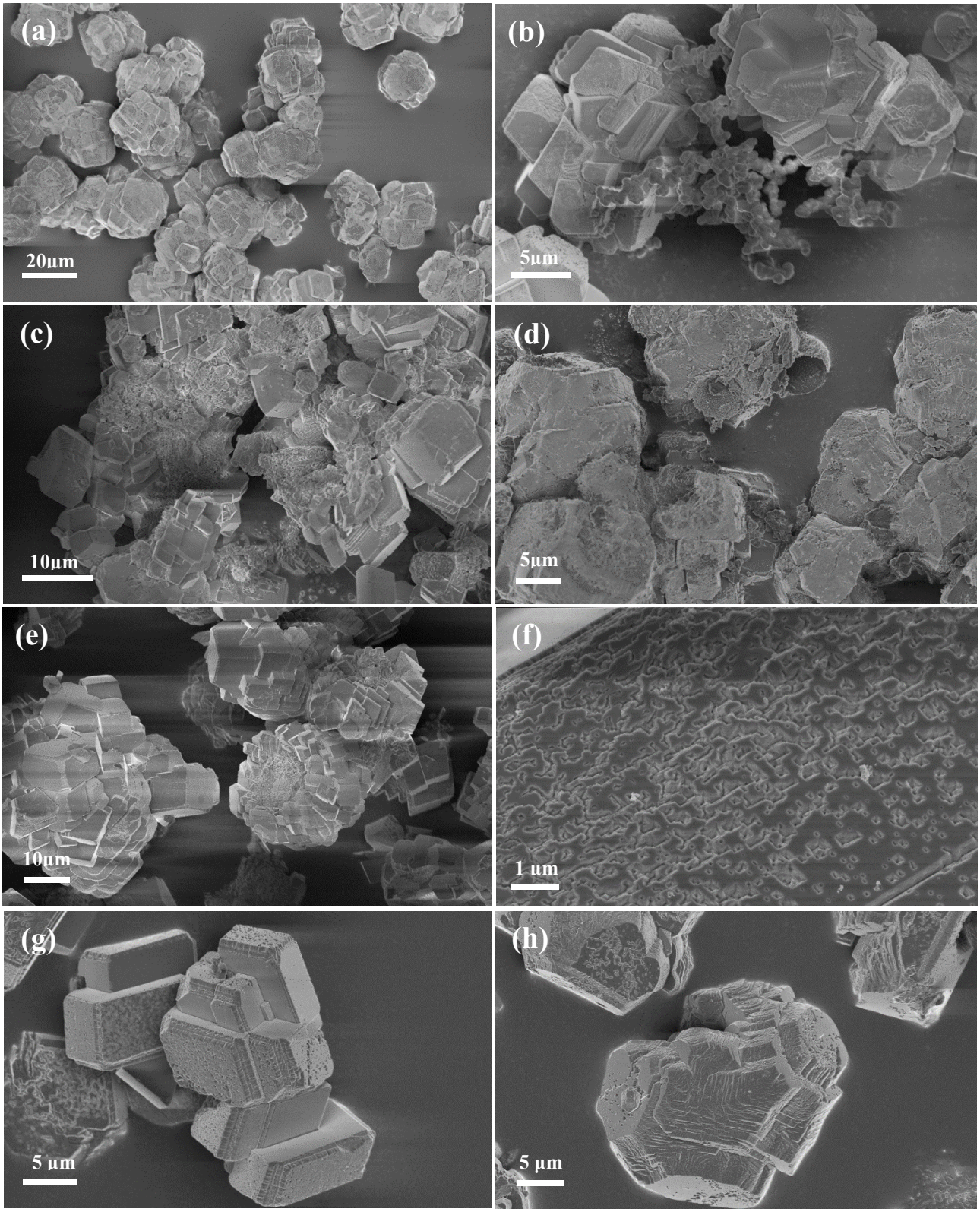

Figure 7.19 – Selected SEM micrographs of PCC produced in the factorial experiments
(a) Typical large PCC agglomerates, Run 1, 500x
(b) Chainlike ACC/vaterite between agglomerates, Run 1, 3300x
(c) Irregular, amorphous structures between agglomerates, Run 3, 1600x
(d) Amorphous unformed crystals, Run 6, 2000x
(e) Very large agglomerates, some in spherical structures, Run 8, 1000x
(f) Pitting on flat surfaces, Run 10, 10000x
(g) Pitting at corners and edges, Run 11, 2000x
(h) Layered growth patterns, Run 13, 2000x

Considering the stoichiometry of the factorial runs, the high and low calcium concentrations used for all tests were relatively low. While the concentration of carbonate was not known, the solubility of CO_2 in the solution at the temperatures and NH_4Cl concentrations was in the range of 0.032-0.045 mol/L for all tests. Once converted to HCO_3^- and CO_3^-, this is very close to the stoichiometric requirement.

7.1.8 Results for Interactions

As mentioned in 7.1.6, due to the saturated experiment design it was necessary to exclude 2-way interactions from the ANOVA calculations to be able to give statistical certainty to the results for main effects, thus no statistical information was gained from the ANOVA calculations on these interactions. However, alternative methods for identifying and separating significant interactions from main effects from the experimental data are available. One such method is by examining the calculated effects of each main factor and 2-way interaction on the response variable and ranking these in order of magnitude on a Pareto chart. A significant advantage of these charts is that the magnitude of the effect due to each factor and interaction can be clearly seen. In saturated designs, Lenth's method [141] is often used to assess which effects are statistically significant based on comparing the calculated effects. This has been done for each of the response variables and the Pareto charts have been included in Appendix D. This analysis yielded the following factors and interactions as significant.

Table 7.5 - Results for significant main factors and interactions based on Pareto charts of calculated effects

Variable	Main Factors	2-way Interactions
d_{50}	-	-
d_{50}^{US}	-	-
d_{90}	-	-
d_{90}^{US}	A	-
t_{ind}	A,C	-
t_{carb}	C,D,E	AB,CD,DE
Agg_{d90}	C	AE,CD
ΔT_{max}	C	AC
η_{Ca}	C	-
η_{CO_2}	C,D,E	-

The results for the main effects are largely in agreement with the results from the earlier ANOVA analysis for all variables apart from the PSD-parameters d_{50} and d_{90} (before and after US) with a statistically significant effect of temperature and $[Ca^{2+}]$ not seen, except for temperature with d_{90} (with US). This is most likely because the method of Lenth results in a more conservative effective significance level than was used in the ANOVA calculations. Table 7.5 shows that several statistically significant interactions were identified, particularly in the case of carbonation time. These are probably due to the gas-liquid mass transfer of CO_2 into solution which, as shown in the CO_2 flux equations in Chapter 6.3 are usually non-linear. Taking the CD interaction on carbonation time for example, what this interaction analysis means is that the effect of CO_2 flow (D) on carbonation time depends on the level of the NH_4Cl concentration (C).

7.2 Additional Laboratory-Scale Tests

During the factorial experiments several interesting phenomena were noticed and considered worthy of further investigation with separate follow-up tests, namely low-temperature carbonation, the effect of adding NaOH to the high [NH_4Cl] runs, as well as the effect of final pH and carbonation time on calcium conversion. These results of these tests are described in the following section.

7.2.1 Low-temperature Carbonation

When the factorial experiment was conceived, the intention was to make the low level for initial temperature 5°C. When this was attempted the first time with factorial run 5 however, within 14 minutes the pH had already dropped below 7 and no PCC was formed even after 45 mins of continuous carbonation. The recorded pH during this test is shown in Figure 7.20 below which exhibits again two equivalence points that in this test occurred at pH levels of approximately 7 and 9.2 (incidentally, this was a low [NH_4Cl] run). The initial temperature at the start of the test was actually 4.1°C, not 5°C. After 45 minutes of carbonation, the solution temperature had increased to 7.5°C and the pH had dropped to 6.30. At this point, still with no PCC formed, the reactor was slowly heated using the water bath to try to precipitate PCC in the belief that the kinetics of precipitation had been slowed so much by the low temperature that nothing would precipitate. After a further 30 minutes the temperature had increased to 16°C and pH remained at 6.23 with still no PCC formed. At this point agitation was increased. It was not until after a further 40 minutes of carbonation that pH began to drop significantly again. After 2 hours of total carbonation time the test was stopped at a temperature of 33°C and pH of 6.1 with still no PCC produced.

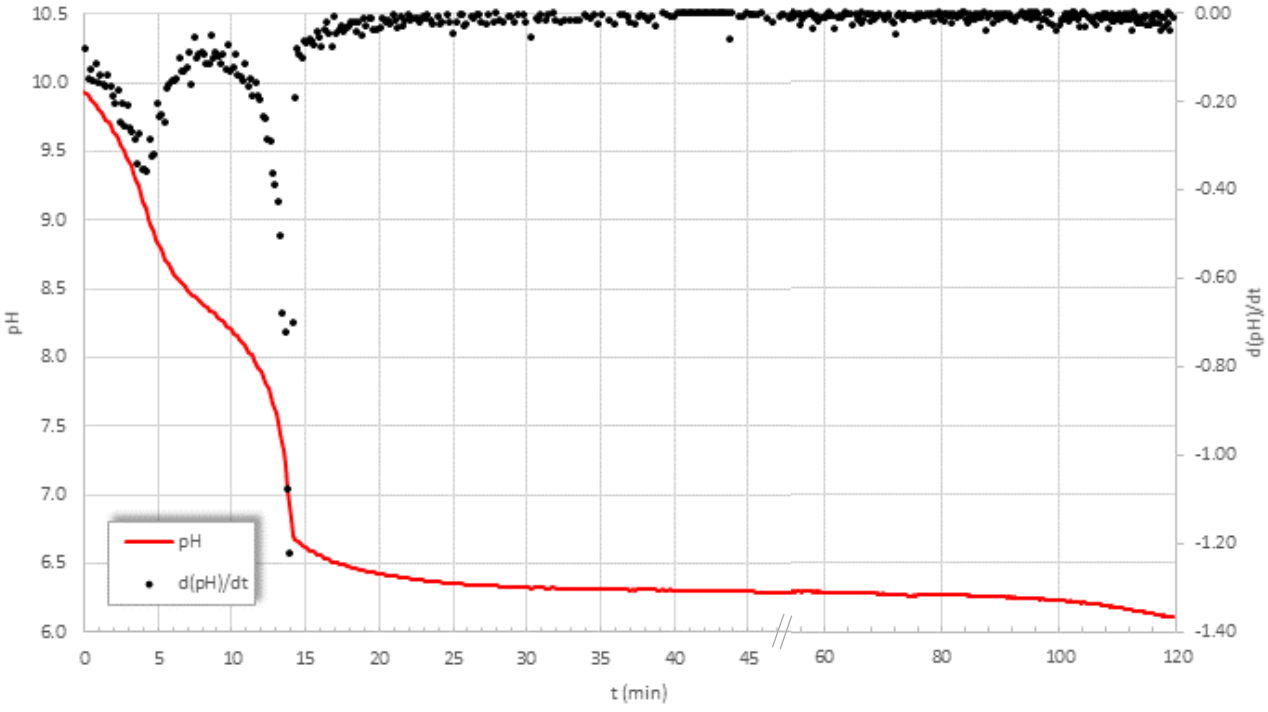

Figure 7.20 – Recorded pH during low-temperature carbonation test

It was hypothesised that the reaction kinetics of the formation of PCC had been slowed by the low temperature to such an extent that the pH had fallen into the acidic region of $CaCO_3$ instability before precipitation of PCC could take place, resulting in a solution containing a mixture of HCO_3^- and H_2CO_3.

To test this theory a few drops of 50% NaOH were added to a 50mL sample of the low-temperature carbonated liquid to supply OH^- ions and increase the pH. This resulted in instantaneous precipitation of PCC. As the initial Ca-rich solution after extraction also has a high pH it was thought that this could also be used to precipitate PCC. To test this theory, a 250mL sample of the solution carbonated at low-temperature was mixed with 250mL of fresh Ca-rich solution at room temperature in a volumetric flask with no agitation other than swirling. This also resulted in instantaneous precipitation of PCC. The resulting slurry was then left overnight, filtered and washed the following morning with 0.25µm filter paper. SEM micrographs of the solids collected are shown below in Figure 7.21.

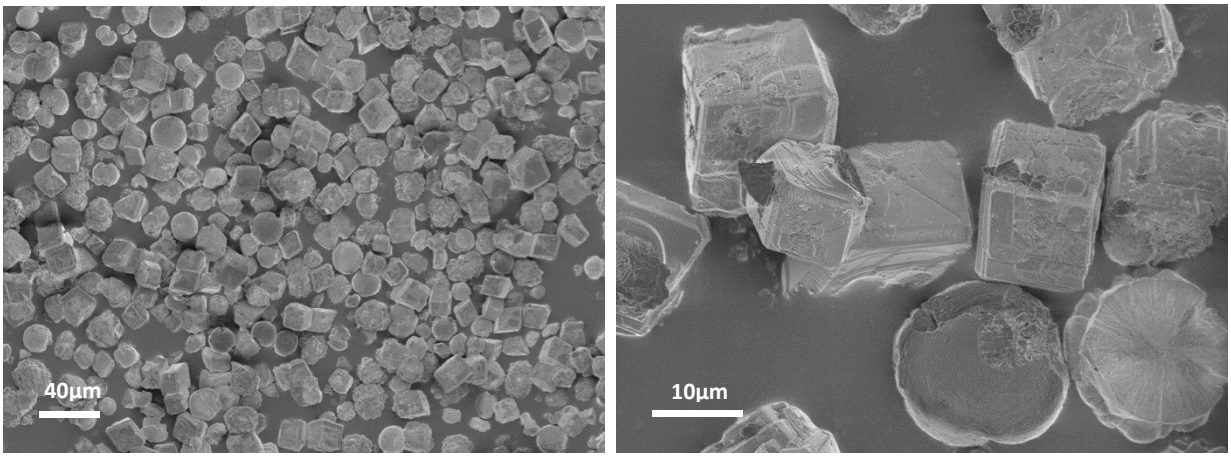

Figure 7.21 - SEM micrograph of PCC produced by mixing equal proportions of Ca-rich solution carbonated at low temperature and fresh Ca-solution (left: 255x, right: 1500x)

Although there was unfortunately insufficient solid sample to be analysed for PSD, it is clear from the SEM micrographs that the PSD of the particles is very narrow and quite fine. Furthermore, the particles showed no significant agglomeration. The morphology is a mixture of spherical vaterite and nearly perfect rhombohedral calcite.

While not fully developed, this process of low-temperature carbonation followed by mixing with fresh Ca-rich solution could be described as a hybrid between conventional carbonation and inverse carbonation, and it may offer a new method of producing PCC with some significant potential advantages:

- Decoupling of gas-liquid mass-transfer kinetics and precipitation kinetics
- Tighter control of $[Ca^{2+}]/[CO_3^{2-}]$ stoichiometry and minimisation of concentration gradients, hence potentially easier control of morphology
- Very high initial supersaturation leading to nucleation of many fine particles
- Simpler conversion to a continuous process
- Minimisation of agglomeration

7.2.2 Effect of Adding NaOH to High [NH_4Cl] Runs

As mentioned previously, dissolving additional solid NH_4Cl to create the high [NH_4Cl] runs caused the pH of the solution to drop by about 1 pH point, which would affect the carbonation and potentially the morphology. As this would not be consistent through all experiments, a small amount of concentrated 50% NaOH (~50 mL) was also added to these runs to bring the pH back up to the level before the NH_4Cl was added. To see the impact of this decision, an additional high [NH_4Cl] run identical to factorial Run 16 was performed but without the addition of NaOH for pH correction. Figure 7.22 shows the solution pH and temperature plotted for both cases.

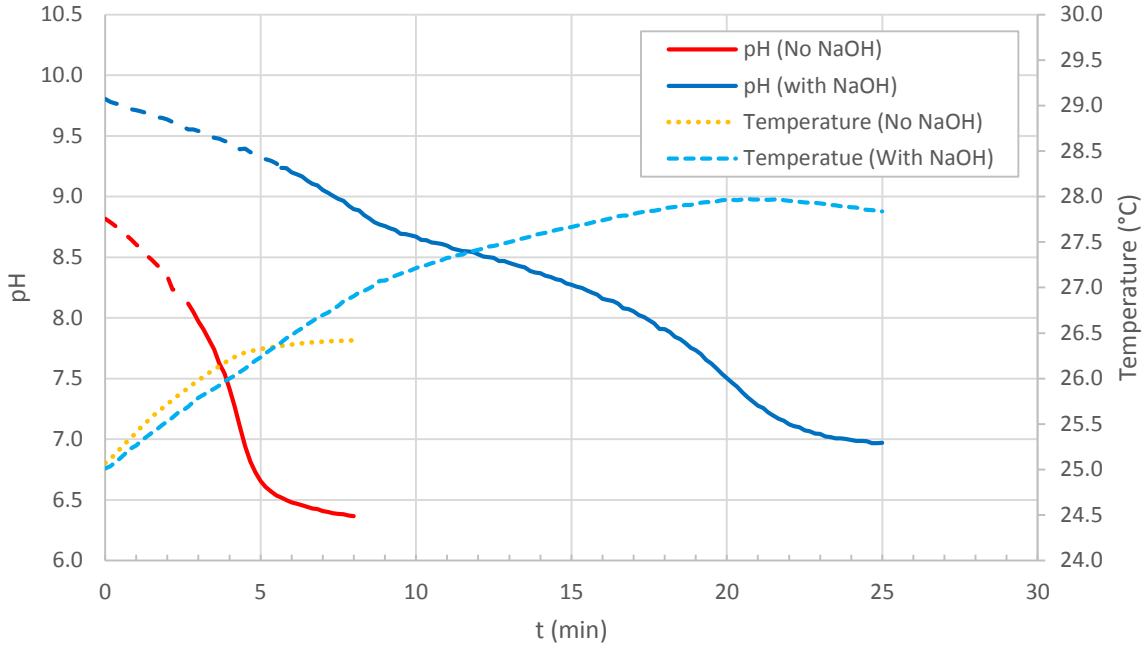

Figure 7.22 – Dynamic pH and temperature plot for factorial Run 16 with and without NaOH addition, [NH_4Cl] = 0.5 M

Aside from increasing the initial pH as expected, the addition of NaOH increased carbonation time. It also results in a higher solution temperature rise. Comparing the slopes of the pH trends shows that the carbonation reactions seem to proceed at a slower rate with the addition of NaOH which results in the longer carbonation time. One explanation may be that the HCO_3^- and CO_3^{2-} became associated with the sodium in solution (approx. 0.24 M) and were less available for the PCC-forming reactions. Another is that the higher ionic strength slowed the diffusion of ions through the liquid film and reduced the rate of reaction. The calculated calcium conversion was ~99% for the run with NaOH added, while for the solution without NaOH added the calcium conversion was only 65.7% Thus the higher temperature rise in the run with NaOH may be due to the higher degree of calcium conversion achieved, or potentially due to another exothermic reaction such as the precipitation of as $NaHCO_3$. SEM micrographs of the PCC from both runs are shown in Figure 7.23.

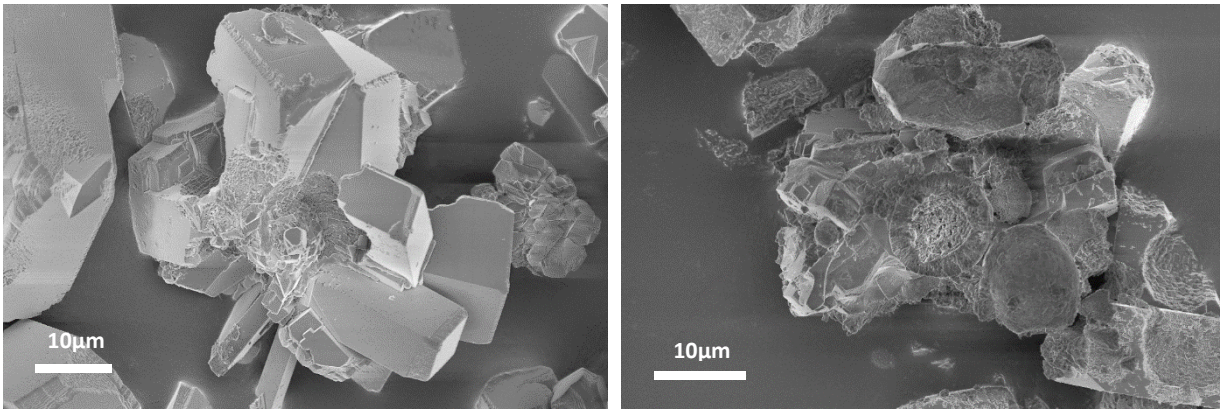

Figure 7.23 - SEM micrograph of Run 16 PCC (high [NH_4CL]) with (left) and without (right) NaOH addition

The PCC produced from the run without NaOH has clearly not had sufficient time to undergo the necessary phase transformations, with significant vaterite and amorphous material still present. This is most likely due to the shorter carbonation time as a result of the lower starting pH. Thus whether NaOH were added or not, neither method would have been entirely adequate for representing solely the effect of NH_4Cl on carbonation. Of the two however, adding NaOH is slightly more realistic as the

starting pH is more accurate but, as an experimental factor, the [NH_4Cl] would be better interpreted as the effect of total ionic strength (Ca^{2+}, Cl^-, NH_4^+, Na^+ etc.). XRD analysis was planned for samples of both tests to determine if sodium also precipitated and was responsible for the higher temperature rise, but results were not available at the time of writing.

7.2.3 Effect of Final pH and Carbonation Time

In an attempt to assess the effect of final pH and carbonation time on the PCC produced, and to try to confirm whether PCC was re-dissolving at lower pH levels, three separate carbonation tests were performed with some high [Ca^{2+}] solution remaining from the factorial experiments with carbonation stopped at three different pH levels: 7.5, 8, and 8.5. The same conditions were used for each test (T = 15°C, [Ca^{2+}] = 0.050 M, [NH_4Cl] = 0.1 M, CO_2 = 0.4 L/min, agitation = 555 rpm) and the resulting solutions were filtered with 0.25µm filter paper. Table 7.6 below shows the results for each run and Figure 7.24 shows the recorded temperature and pH during carbonation. The initial pH for each test was 10.1.

Table 7.6 – Results for replicate carbonation tests terminating at different pH levels

Run	Final pH	t_{ind} (min)	d_{90} (µm)	d_{90}^{US} (µm)	t_{car} (min)	Agg_{d90} (%)	ΔT_{max} (°C)	η_{Ca} (%)
pH Test 1	7.5	7.3	173	117	18.9	48%	1.6	61
pH Test 2	8	5.4	181	80	12.1	126%	1.0	62
pH Test 3	8.5	6.7	246	164	10.7	50%	0.8	72

The analysis for calcium conversion seems to show that allowing the pH of the solution to go below 8.5 causes the PCC to start redissolving as the calcium conversion dropped from 72% down to 62% after this level. This is higher than the value estimated from the video recordings of about 8. Aside from this, several other interesting phenomena where observed during these tests which may have implications for the pilot plant development and commercial scale-up.

Firstly, the tests themselves were not easily reproducible. As the same conditions were used in each test one would expect the pH and temperature plots in Figure 7.24 to closely resemble each other, however they were quite different. This could have been due to the slightly different starting temperatures or slightly different gas flows which are hard to set precisely using a rotameter.

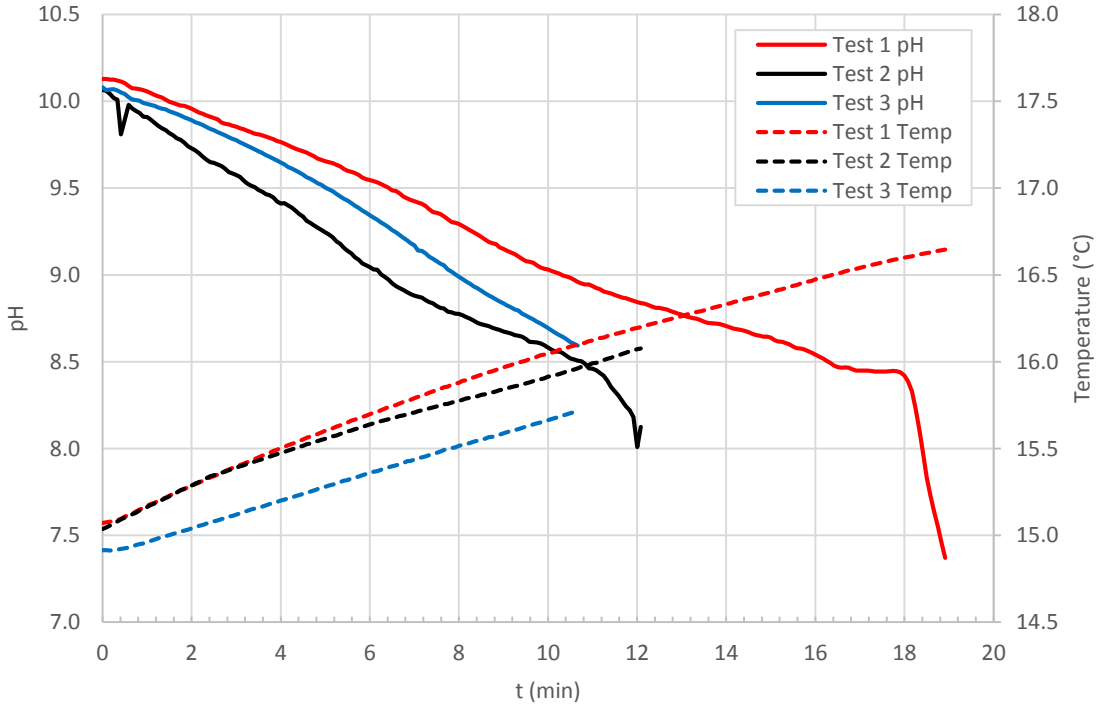

Figure 7.24 - Dynamic pH and temperature plot for pH Test 1,2 and 3

Secondly, it was quite difficult to terminate carbonation at a particular pH. When CO_2 was stopped during the tests, the pH continued to decrease due to (what is believed to be) unreacted dissolved CO_2 built up in solution continuing to react with OH^- and H_2O to form HCO_3^-, CO_3^{2-} and $CaCO_3$. This would only be the case if the rate of consumption of CO_2 via the liquid phase reactions (6.21) and (6.23) and/or subsequent reactions was slower than the rate at which CO_2 could be absorbed into solution from the gas phase. Under these conditions of excess CO_2, it would not be advisable to control carbonation on a commercial scale using pH measurements alone, unless this additional built-up CO_2 was taken into account and carbonation stopped at a higher pH than actually desired.

Thirdly, SEM micrographs taken from test samples showed that none of them yielded well-developed crystalline phases, instead all tests contained a large amount of ACC and vaterite with the phase transformation to calcite still underway. This is best exemplified by Figure 7.25 below which gives evidence for the solution-mediated transformation pathway for vaterite to calcite with what appears to be spherical vaterite particles seemingly dissolving and recrystallising around a newly forming rhombohedral calcite particle.

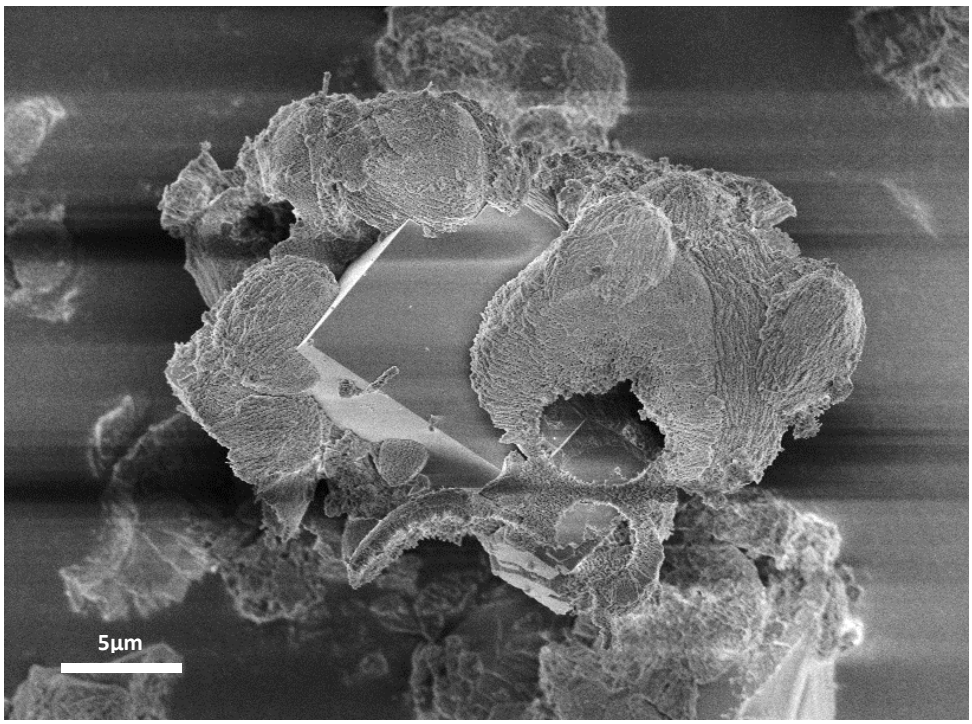

Figure 7.25 - SEM micrograph from pH Test 3 showing solution-mediated transformation of vaterite into calcite, 2000x

An implication of this is that if the Slag2PCC process is to be modelled dynamically in future work, in addition to the precipitation kinetics and growth of calcite, it may also be necessary to take into account the precipitation and dissolution kinetics of ACC and vaterite as well.

7.3 Pilot-scale Experimental Work

During commissioning of the pilot-scale Slag2PCC plant several problems were encountered which considerably delayed the experimental work. The main challenges were poor filtration system performance, corrosion problems in the pipework, poor agitation performance in the extraction reactor, and discolouration of the PCC production. After considerable troubleshooting, short- and long-term solutions were put in place so that experimental work could begin, but the corrective actions took quite some time to implement. For example, the original steel slag was too coarse (<1mm) to be suspended completely in the reactor with the existing agitator and so it was sieved to a finer particle size (<250 µm). Discolouration of the PCC was found to be due to corrosion of the gas spargers in the carbonation reactor as the welding materials used by the supplier were not compatible with the corrosive NH_4Cl solvent. The solution for this was to replace the spargers with simplified temporary spargers, and to coat the bottom of the carbonation reactors and the sparger with a corrosion resistant Teflon coating.

As a result of these delays which took months to address, only a limited number of tests could be performed in the remaining time available for the thesis. Thus, rather than a detailed experimental plan, it was decided that the focus of the pilot-scale test work would be to try to directly produce two of the most common commercial grades of PCC: scalenohedral calcite and aragonite, whilst simultaneously testing the limitations of the pilot plant equipment.

7.3.1 Equipment Setup

Figure 7.26 on the next page shows the setup of the Slag2PCC pilot plant which has three 200L reactors: an extraction reactor (ER) and two carbonation reactors (CR). In the ER, calcium is extracted from steel slag, after which this Ca-rich solution is filtered through one of the extraction filters (1µm). Not shown in the diagram is a secondary filtration stage (two further 1µm and one 0.45 µm filter in series) after the first extraction filter that had to be added to the system during commissioning due to poor filtration performance. After filtration, the Ca-rich solution can be stored in Tank 1 or carbonated directly in Carbonation Reactor 1 (CR1) or 2 (CR2). The original design intent is for most of the Ca-rich solution to be carbonated in CR1, with a small amount of unreacted Ca-rich solution kept aside in CR2 using a flow splitting valve (V4). This is then mixed with the carbonated liquid from CR1 to precipitate any remaining dissolved HCO_3^- and prevent it from precipitating PCC in the ER when the solvent is recycled. After carbonation is complete, the liquid from CR1 (or CR2) is filtered to collect the PCC using an identical filtration system as the extraction filters (also with a secondary filtration stage) and the solvent stored in one of the solvent tanks (ST1 or ST2) to be reused again.

Each reactor (ER, CR1 and CR2) is equipped with temperature and pH indication as well as a three-level 2-bladed variable speed drive (VSD) agitator with a maximum speed of 170 rpm. The two carbonation reactors have gas spargers at their base with hole diameter 1mm mounted below the agitator. The pilot plant also includes two plate and frame heat exchangers (HX) which can be used to heat or cool the solvent going into the ER, or to heat or cool the Ca-rich solution to be carbonated. The HXs can be supplied with hot or cold tap water, whose maximum and minimum temperature depends on the season. In summer the maximum temperature is 60°C but in winter this increases to 80°C. The carbonating gas flow into CR1 or CR2 is set with a rotameter.

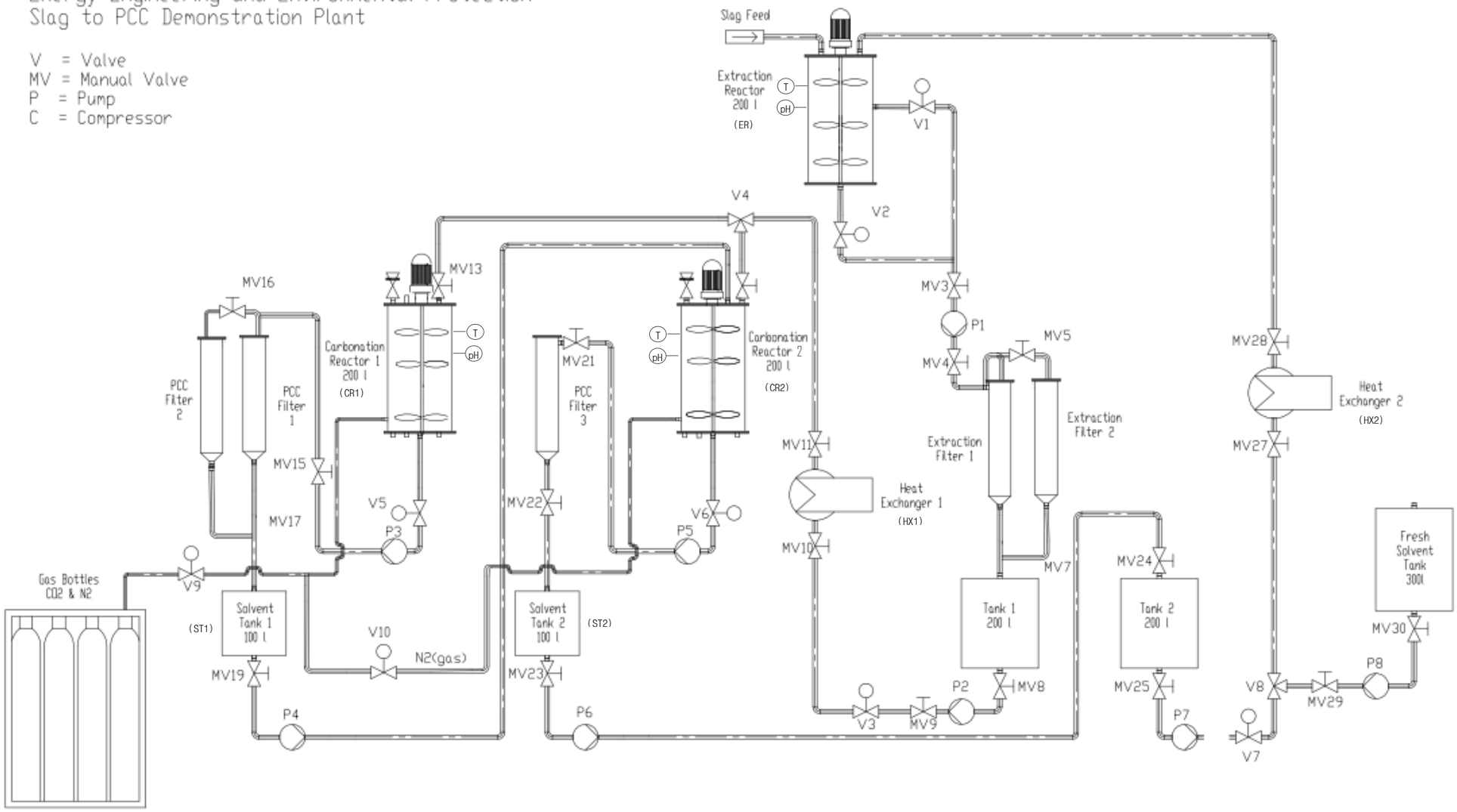

Figure 7.26 – Equipment Diagram of the Slag2PCC Pilot Plant

7.3.2 Pilot Plant Test Conditions

Due to time constraints only three tests could be completed with the pilot plant which were much more time consuming than the laboratory tests. The aim of the first test was to try to produce scalenohedral PCC by attempting to replicate the experimental conditions suggested by Hannu-Petteri Matilla (HPM) from Åbo Academy who successfully produced scalenohedral PCC at the laboratory scale during his PhD studies. The second test was an attempt to produce scalenohedral calcite based on conditions given in US patent 5,695,733 filed by Kroc and Fairchild [142] and in US patent 5,232,678A filed by Bleakley & Jones [143], both of which give quite detailed information on the typical conditions required to make scalenohedral PCC from conventional $Ca(OH)_2$ suspensions. These scalenohedral 'recipes' have given in Appendix E. The reported conditions were similar to those used by Jonna Kuusisto from Aalto University's Department of Forrest Products Technology for producing scalenohedral PCC, adding further confidence [144]. Although these conditions were for producing scalenohedral PCC by carbonation of $Ca(OH)_2$ suspensions, the Ca-rich solution in the Slag2PCC process contains both dissolved Ca^{2+} and OH^- and so using the conditions for $Ca(OH)_2$ carbonation seem a likely good starting point. The third test was an attempt to produce aragonite simply by increasing precipitation temperature with other parameters held the same as in the scalenohedral test.

The experimental conditions used for the pilot plant tests are given in Table 7.7. Each test consisted of an extraction and a carbonation step. The conditions for the HPM test were taken from his data [138].

Table 7.7 - Experimental conditions for the pilot plant runs

	Extraction				Carbonation					
Test	**Solvent (L)**	**SLR (g/L)**	**Slag (kg)**	**[NH_4Cl] (M)**	**Solution (L)**	**Starting T (°C)**	**Agitation (rpm)**	**CO_2 Flow (L/min)**	**CO_2CR (min^{-1}) Est.**	**Act.**
HPM Test	150	100	15	1.0	126	20	55	3[a]	-	0.0032
Scal-Test	150	50	7.5	1.0	120	50	170	14[b]	0.028	0.024
Arag-Test	150	50	7.5[d]	1.0	114	58	170	13[c]	0.028	0.023

a) CO_2 flow scaled up from laboratory flow using GLR= 0.018 L CO_2/L.min
b) CO_2 flow set based on estimated [Ca^{2+}] of 0.18M and setting CO_2CR in the typical range employed in Kroc and Fairchild [142] *(0.028 min^{-1})*
c) CO_2 flow set based on estimated [Ca^{2+}] of 0.18M and setting CO_2CR in the typical range employed in Kroc and Fairchild [142] *(0.028 min^{-1})*
d) Slag added stage-wise in three 2.5 kg increments, waiting 5 minutes after each addition

The intention in all three tests was to have a high [Ca^{2+}]/[CO_3^{2-}] ratio as from the literature this seemed to be a requirement for producing scalenohedral calcite and probably aragonite as well. In traditional commercial PCC carbonation processes a very high [Ca^{2+}] is typically used (1-3 M) by preparing a 5-25 wt% solution of $Ca(OH)_2$ [142]. Thus, maximising [Ca^{2+}] from the extraction stage of the Slag2PCC process to mimic the high [Ca^{2+}] was considered key. However, given that slag is only 45% CaO and the range of extraction conditions studied thus far, achieving a [Ca^{2+}] in the Ca-rich solution higher than 1 M is challenging. In particular, it was unclear from previous test work whether a SLR of 50 or 100 g/L would lead to a higher [Ca^{2+}] in solution as from Figure 5.4, a significant drop in extraction efficiency was observed between 50 g/L and 100 g/L using a 1M NH_4Cl solution. Doubling the SLR should result in a higher [Ca^{2+}] due to the greater supply of calcium, providing the drop in extraction efficiency is not proportional. Given the uncertainty surrounding the high SLR data in Figure 5.4, a SLR of 50 g/L was used for the second two tests.

The CO_2 flow for the HPM test was set based on a GLR of 0.018 L CO_2/L.min that was used by H-P Matilla in his test. The CO_2 flow for the scalenohedral test was set based on the CO_2 flows, reaction volumes and calcium concentrations used in the patent by Kroc and Fairchild [142] to produce scalenohedral calcite particles. From analysis of the work of Kroc & Fairchild it was found that for each of example tests producing scalenohedral PCC given in their patent (see Appendix E), the moles of CO_2

added per mole of calcium per minute varied between 0.01 and 0.05 with an average of ~0.028. This level was supported by the patent of Bleakley & Jones [143] which recommended a CO_2 flow of 0.02 to 0.10 moles per mol $Ca(OH)_2$ per minute in order to produce scalenohedral PCC. This quantity – the moles of CO_2 added per mole of calcium per minute, is hereafter referred to as the *CO_2 to calcium ratio* (CO_2CR), defined in equation (7.5) as

$$CO_2CR = \frac{Q_{CO_2}}{c_{Ca^{2+}}\,\hat{v}V} \tag{7.5}$$

where Q_{CO_2} is the flow rate of CO_2 gas (L/min), $\hat{v}_{CO_2}$ is the molar volume of ideal gas at the calibration temperature and pressure (24.05 L/mol at 20°C, 1 atm), $c_{Ca^{2+}}$ is the concentration of calcium (M) and V is the volume of the Ca-rich solution being carbonated (L). The CO_2CR has units of min^{-1}. From a practical scale-up point of view, it is conceptually a more insightful ratio than the GLR described earlier as it incorporates the calcium content of the solution and should better represent the stoichiometry between $[Ca^{2+}]/[CO_3^{2-}]$ at least at the start of the carbonation. For the scalenohedral test, the CO_2 flow was based on having a CO_2CR of approximately 0.028. The calcium concentration was not known at the time of the test but it was estimated as 0.18 M using the equation below assuming x_{CaO} = 45% and estimated calcium extraction efficiency, η_{Ca} of 43%, based on previous data given in Chapter 5.

$$c_{Ca^{2+}} = \frac{\eta_{Ca} x_{CaO} SLR}{M_{CaO}} \tag{7.6}$$

Kroc & Fairchild reported using 'vigorous' agitation, whilst J. Kuusisto reported using 800 rpm. This level of agitation was not possible to achieve in the pilot plant as the maximum speed of the agitator drive was 170rpm, so 170 rpm was used instead. The same agitation speed and CO_2CR ratio were also used for the aragonite test.

The HPM replicate test was conducted at room temperature, essentially the same as in the original test (20°C). In the scalenohedral test, the initial temperature of the Ca-rich solution was set at 50°C based on the recommendation of J. Kuusisto , which was close to the 45°C used by Kroc & Fairchild and within the range of 40-65°C recommended by Bleakley & Jones. The solution was heated by recirculating it between CR1, Tank 1, and Heat Exchanger 1 (HX1) through temporary pipework not shown in the schematic. Hot tap water was used on the hot side of HX1. For the aragonite test, the tap water was not hot enough to increase the solution temperature beyond 52°C so, a temporary boiler was used to heat up tap water to 95°C which was then connected to the hot side of HX1 via temporary piping. The target temperate of the Ca-rich solution had been 80°C as identified as a typical aragonite-yielding temperature from the literature review however, due to the limited size of the boiler and large amount of heat loss between the boiler and the reactor and in the solvent tanks, the temperature of the Ca-rich solution could not be increased any higher than 58°C and so this temperature was used for the aragonite test.

7.3.3 Experimental Procedure

A fresh batch of 1M NH_4Cl solvent was prepared for each test by dissolving 8 kg of solid NH_4Cl in 150L of water and agitating thoroughly at room temperature (~20°C). Being strictly accurate this means that the solvent was actually 1 molal (1 mol NH_4Cl/kg H_2O or 0.962 M) and not 1 molar, but in the large volumes dealt with the difference is small, and because qualitative results (i.e. PCC morphology) were of primary concern rather than quantitative results, a nominal concentration of 1M was considered sufficient. In the first two tests the slag was added all at once but in the aragonite test, the slag was added stage-wise in three 2.5 kg increments, waiting 5 minutes after each addition to see if this would improve extraction efficiency.

For each test, 150L of solvent was pumped from the Fresh Solvent Tank (FST) into the ER. The required amount of slag (ground to <250µm) was weighed, then added at the top of the reactor with agitation at 170rpm. Extractions were run for one hour. After extraction was complete, the Ca-rich solution was filtered and pumped to CR1 with CR2 isolated so that all the available solution went to CR1. The design of the filtration system, tanks, and piping meant that some 20-30L of the Ca-rich solution remains in the dead volume of the system and could not be easily recovered for carbonation, which is why the solvent and Ca-rich solution volumes in Table 7.7 differ. The agitation rate was set by modifying the setting on the agitator drive frequency converter. The CO_2 flow was set using a CO_2-calibrated rotameter and carbonation time begun when the flow of CO_2 started. Pure CO_2 was used in all tests. The pH and temperature of the carbonating solution were logged automatically at 5 second intervals.

Unlike in the factorial tests, the pilot plant carbonation tests were stopped at specific pH levels. In the HPM replicate test, carbonation was stopped once pH reached approximately 7, close to the final pH in his original test. The scalenohedral test was stopped at pH 7.5, the level used in the patent. The aragonite test was stopped at pH 7 as, due to the lower starting pH, it was thought that stopping at pH 7.5 may not provide sufficient reaction time.

Samples of the PCC produced in each test were taken for PSD analysis and SEM imaging. The PCC was washed with deionised water and filtered using 0.25µm paper. Samples were also taken of the Ca-rich solutions from each extraction as well as the final carbonated solution for calcium concentration analysis to determine both calcium extraction efficiency and calcium conversion.

7.3.4 Results for Pilot-scale Experiments

The table below presents the results for the three pilot plant tests. The calcium extraction efficiencies calculated from the analysed calcium concentrations were higher than expected based on the work by Said et al. [5]. From Figure 5.4 the expected extraction efficiency from slag using 1M NH_4Cl and 100 g/L SLR was approximately 6%, which would give calcium concentration of approximately 0.06 M, yet the $[Ca^{2+}]$ in the Ca-rich solution was approximately 0.3 M, from which the calculated extraction efficiency was 38%. For the scalenohedral and aragonite tests the calcium concentration after extraction was approximately 0.2 M for both tests, with calculated extraction efficiencies both in the order of 50%.

Table 7.8 – Results for the pilot-scale extraction and carbonation tests

	Extraction			Carbonation								
Test	**Final pH**	**$[Ca^{2+}]$ (M)**	**η_{ext} (%)[a]**	**Initial pH**	**Final pH**	**ΔT_{max} (°C)**	**t_{car} (min)**	**η_{Ca} (%)**	**η_{CO_2} (%)**	**d_{50}/d_{50}^{US} (µm)**	**d_{90}/d_{90}^{US} (µm)**	**Agg_{d90} (%)**
HPM Test	9.7	0.308	38	9.7	7.2	4.4	348	94	84	-	-	-
Scal-Test	9.3	0.204	51	8.7	7.5	1.6	35	72	88	40/37	74/68	9
Arag-Test	9.3	0.207	52	8.3	7	2.8	35	82	102	24/23	80/69	15

Figure 7.27 - Figure 7.29 on the following page show the recorded pH and temperature during each carbonation test. The pH readings recorded at the start of each carbonation showed that the higher solution temperature reduced the starting pH, to be expected from the temperature dependence of the water dissociation equilibrium (6.36). The particles produced in the scalenohedral and aragonite test were not as large as the particles in the factorial experiment and had a lower calculated Agg_{d90}. The reduction in particle size may be due to the slower rate of CO_2 addition in the pilot tests compared with the laboratory factorial tests, or the shorter delay between the test and the PSD analysis which was only 1-2 days for the pilot tests.

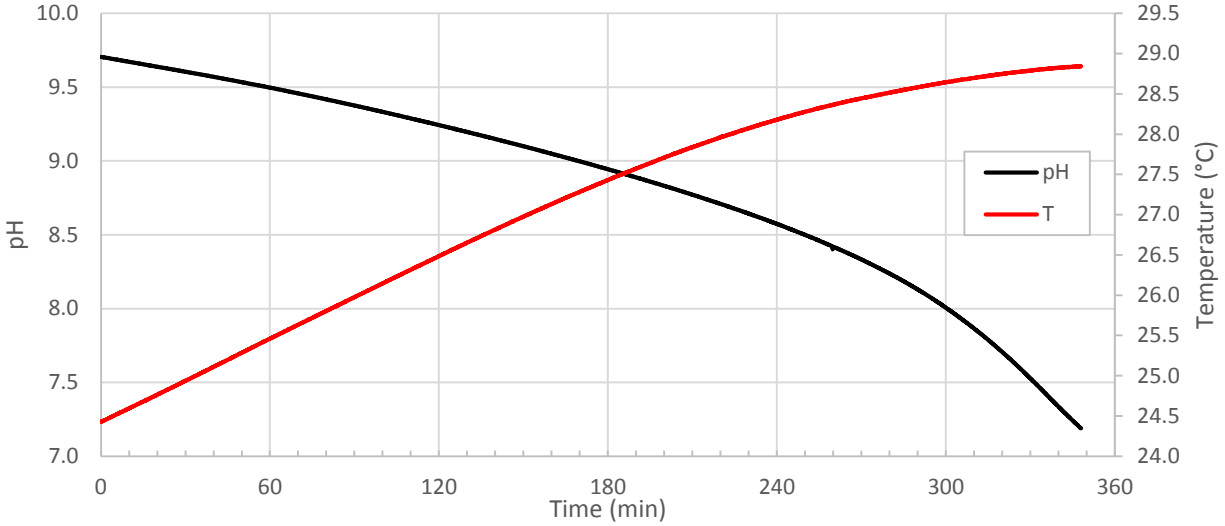

Figure 7.27 - Recorded pH and temperature during the HPM replicate pilot plant test

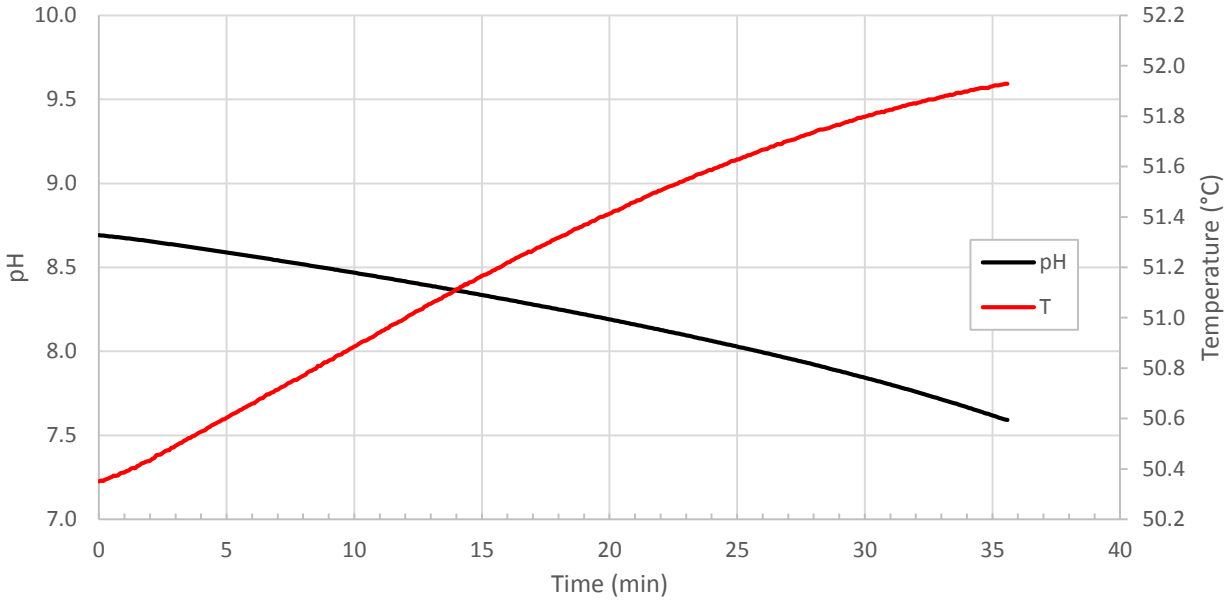

Figure 7.28 - Recorded pH and temperature during the scalenohedral pilot plant test

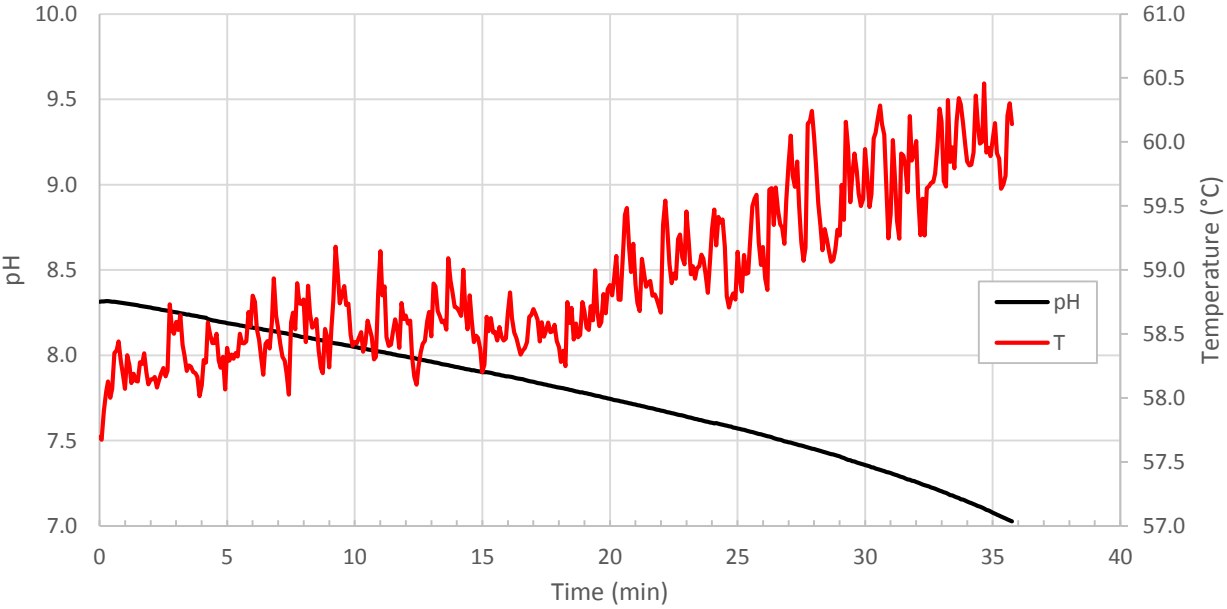

Figure 7.29 - Recorded pH and temperature during the aragonite pilot plant test

The pH trends show that by stopping at higher pH, the region of rapid pH change around the equivalence point seen in the factorial tests was avoided. Interestingly, despite the higher final pH the calculated carbonation efficiencies of the pilot plant tests were of similar levels to those in factorial tests (60-80% excluding the high [NH_4Cl] runs to which NaOH had also been added), apart from the HPM test which had a higher efficiency of 94%. Also, no equivalence point was seen at pH 8.9 as had been seen in some of the factorial tests, despite the even higher concentration of NH_4Cl.

Figure 7.30 on the next page shows SEM micrographs taken of PCC samples from each of the pilot plant tests. Due to the very long duration of the HPM test, a few additional samples were taken during the course of carbonation to look at how the morphology changed over time. When these samples were taken from the reactor, the solution was quite transparent and contained very few solids. After some minutes, the sample began to turn cloudy indicating PCC was precipitating. A sample taken during the HPM test after 270 minutes of carbonation (pH 8.3) indicated that the PCC precipitating was spherical vaterite of approximately 10 µm (a). At the end of carbonation, a mixture of rhombohedral calcite and cotton wool ball-like structures of presumably vaterite were formed (b). The attempt to make scalenohedral calcite according to Kroc & Fairchild, rather than producing scalenohedral PCC, instead yielded large agglomerates of a variety of crystals morphologies including spherical and disclike vaterite, rhombohedral calcite, as well as aragonite (c-d). The aragonite test was more successful, yielding essentially 100% aragonite needles of various sizes, ranging from 2-50 µm in length and maximum width of around 3 µm (e-f).

While the test at 58°C in the pilot plant successfully produced aragonite, neither the test intended to replicate HPM's conditions nor the test at 50°C using the conditions of Kroc & Fairchild produced the scalenohedral PCC morphology. Given that the latter had been described in two patents, were supported by J. Kuusisto, and did not require such long carbonation time, this was considered a more promising route than that of HPM and worth pursuing further. The only differences between the conditions reported by Kroc & Fairchild and those used in the pilot plant test were the slower agitation speed (170 vs ~800rpm), lower [Ca^{2+}] (0.2 M vs >1 M), lower pH (8.7 vs > 11), slightly higher temperature (50°C vs 45°C), and the presence of the 1M NH_4Cl solvent. From Figure 7.30 (a-c), the wide range of morphologies produced suggested that there may not have been adequate mixing in the reactor as this would lead to temperature and concentration gradients, affecting precipitation conditions and hence morphology. Thus, it was decided to do the same experiment in the laboratory where the 800 rpm agitation speed used by J. Kuusisto could be achieved, using some 0.3 M Ca-rich solution remaining from the HPM test. The CO_2 flow was set at approximately 0.4 L/min, giving a CO_2CR of 0.014 min^{-1}, still in the region which should produce scalenohedral particles according to Kroc & Fairchild. The temperature was set at 45°C. As it had not been possible to reach 80°C in the pilot plant, one additional laboratory test was done with the same 0.3 M Ca-rich solution and identical conditions (800 rpm, 0.4 L/min CO_2) except the initial temperature was set to 80°C which was possible with the heated water bath. Carbonation was stopped at pH 8 for the 45°C test and at pH 7.6 for the 80°C test.

Table 7.9 - Results for follow-up laboratory tests at 45°C and 80°C

Test	Initial pH	Final pH	ΔT_{max} (°C)	t_{car} (min)	η_{Ca}(%)	η_{CO_2}(%)	d_{50}/d_{50}^{US} (µm)	d_{90}/d_{90}^{US} (µm)	Agg_{d90} (%)
45°C Lab Test	9.1	8.0	0.83	43	71	122	22/21	41/37	12
80°C Lab Test	8.3	7.6	-	45	46	76	30/28	62/58	6

The carbonation time for both tests was 45 minutes as shown in Table 7.9 above. The calcium conversions were 71% for the 45°C test and 46% for the 80°C test. The particles produced in these follow-up laboratory tests were also smaller than in the pilot-scale tests, perhaps due to the higher

agitation. SEM micrographs of the PCC produced in the follow-up lab tests are shown in Figure 7.31. The test at 45°C (a-b) produced clustered agglomerates of around 20µm in size, comprised of disc-shaped vaterite primary particles varying from 2-10 µm in diameter. Less variety in morphology was observed suggesting that better mixing had reduced concentration gradients. The test at 80°C produced essentially pure aragonite crystals with lengths of 5-30 µm and widths from 0.5-1.5 µm, giving typical aspects ratios of 10-15. Many of the larger crystals were broken and it was difficult to know the exact size of the original needles. The aragonite also showed some degree of agglomeration.

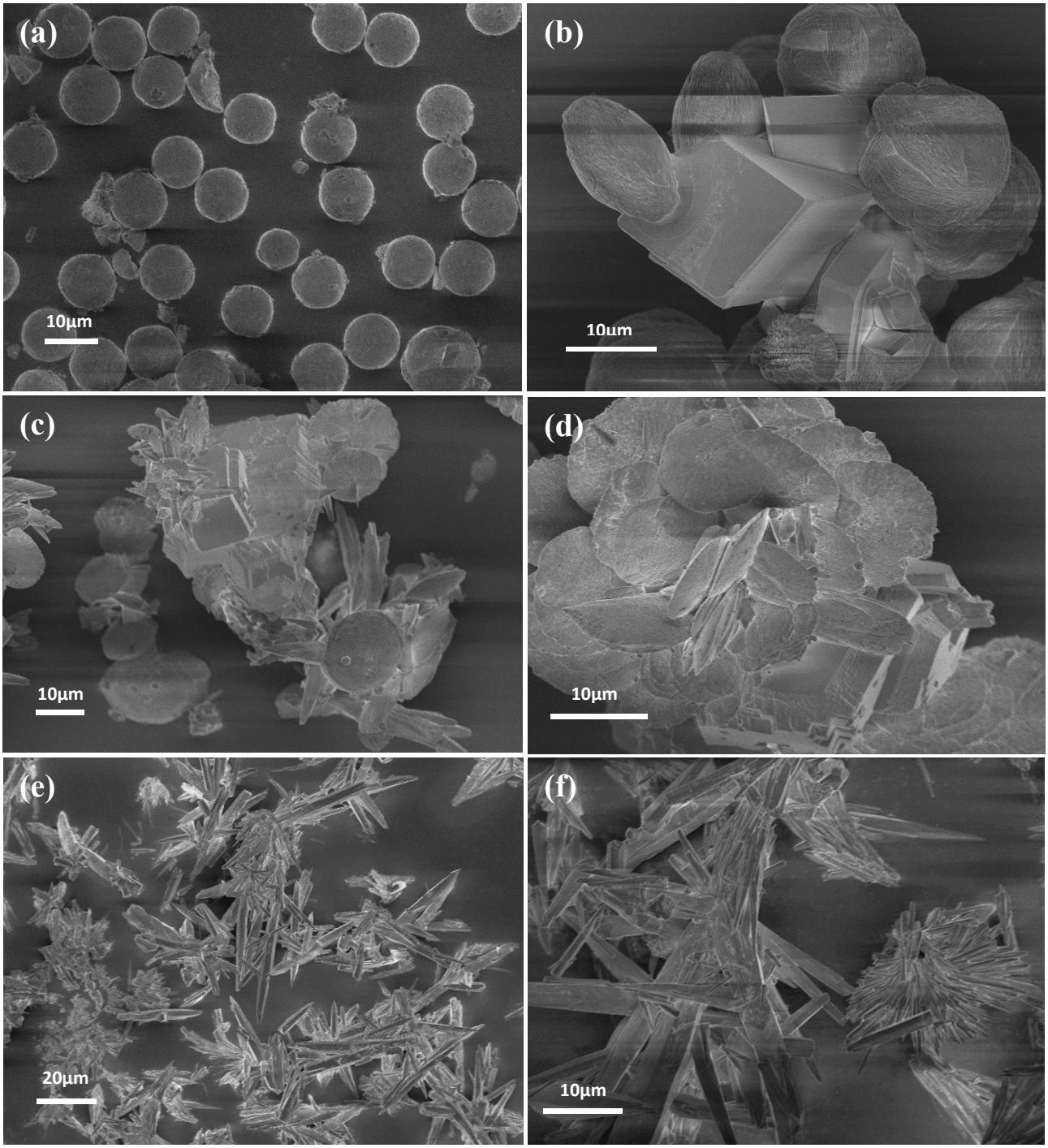

Figure 7.30 – SEM micrographs from pilot plant tests
a) HPM test sample taken after 270 min, pH 8.3, 1000x
b) HPM tests after carbonation stopped, pH 7.1, 1750x
c) Scalenohedral test, 1000x
d) Scalenohedral test, 1500x
e) Aragonite test, 500x
f) Aragonite test, 2000x

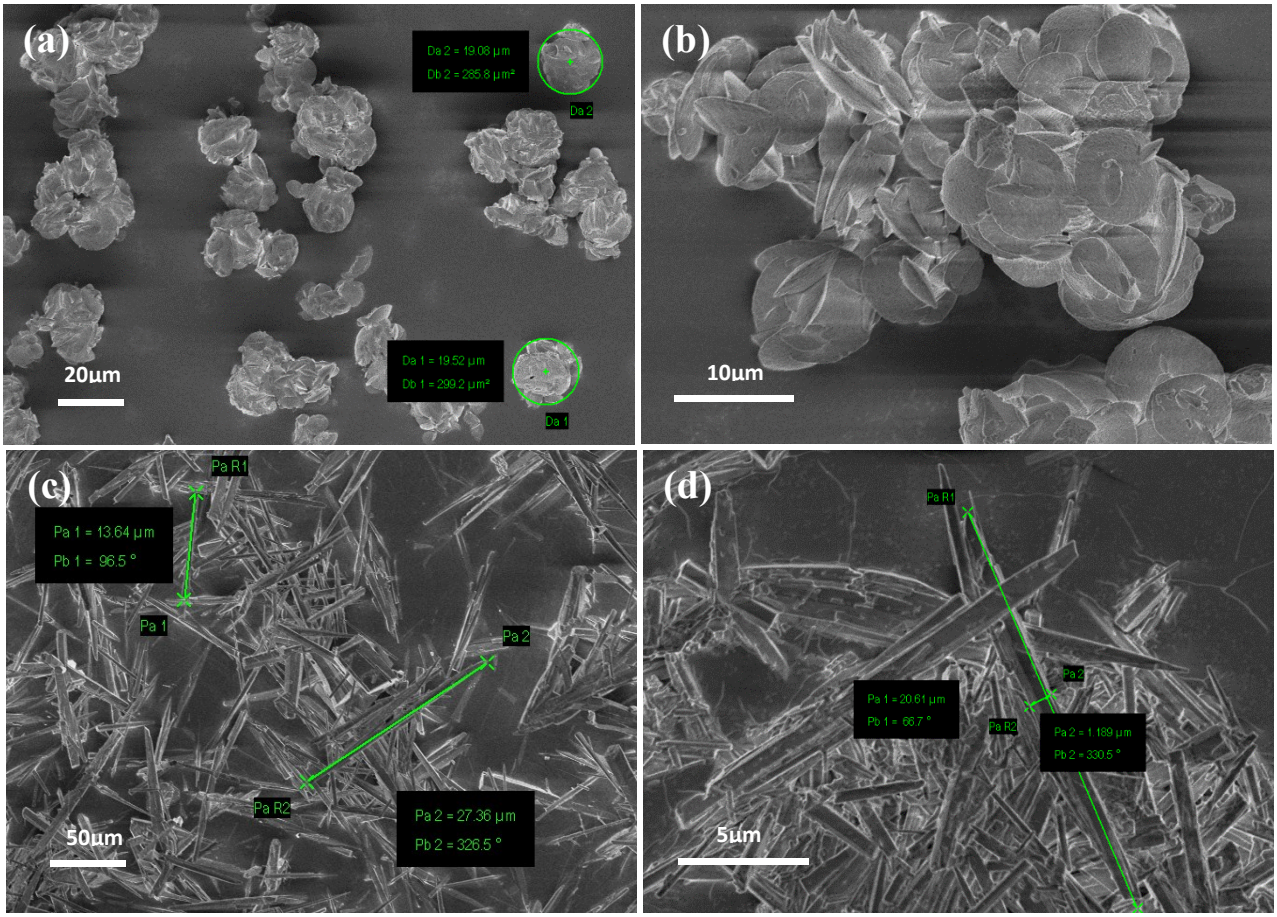

Figure 7.31 – SEM micrographs of laboratory-scale attempts to produce scalenohedral and aragonite PCC
a) 45°C lab test, 500x
b) 45°C lab test, 2000x
c) 80°C lab test, 940x
d) 80°C lab test, 3200x

In addition to the PSD analysis, BET surface area and ζ-potential analysis was also performed on the pilot scale and follow up laboratory run samples. In the case of ζ-potential, selected samples from earlier tests were also analysed for comparative purposes. The results of the analysis are shown in Table 7.10.

Table 7.10 - Results for ζ-potential and BET specific surface area analysis

Test	pH	ζ-potential (mV)	SSA (m^2/g)
Factorial Run 5	9.7	-6.3	-
Factorial Run 12	9.4	-7.1	-
Factorial Run 16	9.2	-8.5	-
Factorial Run 16 (No NaOH)	9.7	-8.0	-
pH Test 1	9.8	-10.3	-
pH Test 2	9.8	-10.8	-
pH Test 3	9.7	-11.2	-
Scal-Test (50°C pilot test)	9.6	4.2	0.64
Arag-Test (58°C pilot test)	9.3	-5.9	0.76
45°C Lab Test	9.6	10.4	1.3
80°C Lab Test	8.9	13.6	1.5

All PCC samples reported negative ζ-potential results, except for the 50°C pilot test and the two follow-up lab tests at 45°C and 80°C which yielded positive results ζ-potentials. These three tests were all conducted with a higher [Ca^{2+}] (>0.2M) and this is in agreement with the theory that an excess of calcium during carbonation results in PCC with a positive ζ-potential. Although the surface charge was positive in these tests, it was only just approaching the range reported for commercial PCC suggesting the intention of excess calcium had been achieved, but the excess was lower than used in industry. The 58°C pilot test was conducted at the same [Ca^{2+}] as the 50°C pilot test thus one would expect this also to have exhibited a slight positive surface charge as was seen with the 80°C lab test, but it did not. Comparing the ζ-potential for factorial runs 12 and 16 also seems to suggest that NH_4Cl has minimal effect on surface charge as increasing from 0.1 to 0.5 M NH_4Cl made no appreciable difference in ζ-potential. This is only one sample comparison however and no firm conclusion can be drawn from it. The SSA of all samples was below the range seen in the commercial PCC products listed in Table 3.5, most probably due to the much larger particle size.

7.3.5 Discussion

The results for calcium extraction efficiency showed that using the higher SLR of 100 g/L resulted in a higher [Ca^{2+}] in the extraction solution than when 50 g/L was used, despite the lower extraction efficiency. While the extraction efficiency at 100 g/L was lower than at 50 g/L (38% vs 51%), it was not as low as expected from the earlier work (6%) shown in Figure 5.4. Thus the original test may have been in error, or, another factor was at play. Assuming that the stoichiometry of the dissolution reactions (4.2)-(4.4) holds and two moles of NH_4Cl solvent are required to dissolve one mole of calcium from the slag, an equation for the minimum theoretical [NH_4Cl] required to dissolve all the calcium can be derived which depends only on the calcium content of the slag, x_{CaO}, typically 45% [5], the SLR used in the extraction (g/L) and the molecular weight of CaO. This is shown in equation (7.7) below

$$[NH_4Cl]_{min} = \frac{2x_{CaO}(SLR)}{M_{CaO}} \tag{7.7}$$

If the slag composition is reported as elemental calcium rather than CaO, or as a mixture of silicates, the mass fraction and molecular weight should be adjusted accordingly. From this equation, the minimum solvent concentration required for 100% extraction efficiency was calculated for various SLRs assuming 45% CaO in the slag, as shown in Table 7.11 below.

Table 7.11 - Minimum NH4Cl solvent concentration as a function of SLR (45% CaO in slag)

SLR (g/L)	$[NH_4Cl]_{min}$ (M)
5	0.08
10	0.16
20	0.32
50	0.80
100	1.60

Thus for a SLR of 100 g/L, an NH_4Cl solvent concentration of 1.6M should in theory be required to dissolve all the calcium. In the experimental work on which Figure 5.4 was based a 1M NH_4Cl solution was used for all tests and so this may explain the sharp decrease in extraction efficiency observed if insufficient NH_4Cl was available. Of course, having the minimum NH_4Cl concentration does not mean that 100% extraction efficiency is guaranteed and mass transfer limitations will likely prevent this from being achieved. The calcium in the slag may also be in a less available form bound with silicates which would further hinder timely dissolution. Additionally, the equation is only a rough guide and will

probably lead to an overestimation of the NH_4Cl required as, from Figure 5.1, water alone is able to dissolve some calcium, particularly free CaO, from the slag. If the amount of NH_4Cl required is overestimated and it is in strong excess, this will reduce the maximum pH achieved by the extraction reaction and hence the pH used for carbonation.

When the calcium analysis for the pilot plant tests was attempted by complexometric titration, the end point of the titration was difficult to determine as the indicator colour change was not rapid. In the pilot experiments the [NH_4Cl] in solution was much higher than in the factorial experiments and this was thought to be the cause of the problem given that NH_3 is known to interfere in the titration. Thus, a method of removing the NH_3 as $NH_{3(g)}$ by alkalisation and evaporation before the titration was developed. This approach seemed quite successful and was employed for all the pilot plant runs at 1M NH_4Cl as well as the follow-up laboratory work. The procedure for NH_3 removal has also been detailed in Appendix A.

Comparing the extraction efficiencies of the scalenohedral and aragonite test shows that adding the slag stage-wise led to no significant improvement in extraction efficiency. Also, the results show that the final pH during extraction is a better indicator of the final [Ca^{2+}] in solution, not extraction efficiency. This is because it's the amount of calcium extracted which determines the OH^- generated and consequently the pH.

The cause of the very erratic temperature measurements in the aragonite tests but may be due to signal noise or the thermocouple in the carbonation reactor being continually submerged and unsubmerged in liquid as a result of the lower liquid level in the tank. The thermocouple on this reactor is 55 cm above the reactor floor and would be very close to the liquid surface when a solution volume of only 114 L was used. Vortices caused by agitation may also affect the reading.

In 1M solutions of (pure) NH_4Cl, $CaCO_3$ has a solubility of approximately 0.0064, 0.0086 and 0.0091 M at 20°C, 50°C and 58°C respectively. From this, the maximum calcium conversion for the HPM test, scalenohedral test and aragonite test can be estimated at about 98%, 96% and 96% respectively, ignoring the effect of other ions (Cl^-, OH^-) on the solubility of $CaCO_3$. It had been observed in the factorial experiments that the PCC began to redissolve below a pH of about 8, thus it is surprising that only the HPM replicate test approached the theoretical maximum calcium conversion even though other tests were stopped at higher pH levels. This may have been because insufficient CO_2 had been added to convert all the Ca^{2+} to $CaCO_3$, even though the pH had dropped to levels at which PCC would start dissolving. As the CO_2CR has units of min^{-1}, its reciprocal ($1/CO_2CR$) will give the amount of time theoretically required to add the stoichiometric amount of CO_2 required to convert all Ca^{2+} present in solution to $CaCO_3$, assuming 100% CO_2 conversion. Thus by further dividing $1/CO_2CR$ by the CO_2 conversion should account for this additional factor and be a good predictor of carbonation time. This is evidenced by Figure 7.32 on the next page which shows the quantity $1/(CO_2CR.\eta_{CO_2})$ plotted against carbonation time for the pilot scale tests as well as the laboratory tests for comparison. In the case of the laboratory factorial experiments, there is very good agreement between the carbonation time and the predicted value from $1/(CO_2CR.\eta_{CO_2})$ with a correlation coefficient of 99.3%. Interestingly, the prediction is even better for the high 0.5M [NH_4Cl] runs, the measured and calculated values being within +/- 1 min from each other. For the pilot-scale and follow-up laboratory tests however, the predicted carbonation times do not match well with the actual carbonation time. This may due to several reasons. Firstly, the calculated CO_2 conversion in the 45°C lab test and 58°C pilot test was over 100%. Assuming CO_2 did not enter the solution by other means, this points to an error in either the calcium analysis or the CO_2 flow measurement. The calcium analysis procedure was modified for the pilot scale and follow-up laboratory tests to try to remove NH_3 from solution (as discussed in Appendix A), and this seems more likely to be the cause as even though a different rotameter was used for the

pilot tests, the same CO_2 rotameter and calibration was used for all laboratory scale tests. Secondly, Figure 7.32 would seem to suggest that insufficient CO_2 had been added to precipitate all the calcium as PCC. As the pilot plant and follow up tests were stopped at arbitrary pH levels, it may be that carbonation had been stopped prematurely and simply not enough CO_2 had been added.

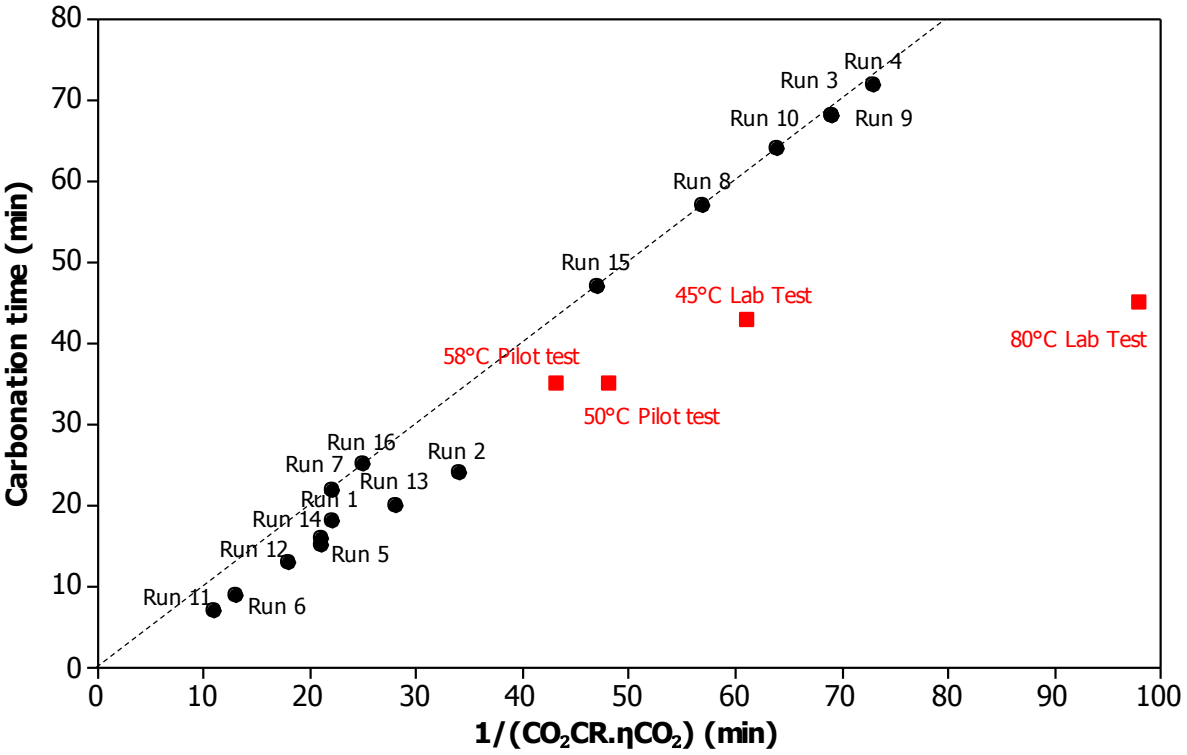

Figure 7.32 - Plot of $1/(CO_2CR.\eta CO_2)$ vs recorded carbonation time

After each pilot-scale carbonation inspection of the reactor showed that significant PCC remained in the bottom of the reactor after it had been drained. Agitation was always left on when the reactor was drained, suggesting that the level of mixing was not sufficient to suspend all the PCC particles and many were settling to the bottom.

The aragonite produced from the 58°C pilot plant test and the 80°C laboratory scale tests was quite similar, the only noticeable difference being that the PCC produced in the 80°C laboratory scale test appeared to have a higher aspect ratio than the lower temperature pilot plant test based on qualitative examination of the SEM micrographs. The SSA of the aragonite product in both tests was much lower than that of commercial aragonite products such as Opacarb, most likely due to the larger particle size.

Not one of the three tests intended to produce scalenohedral PCC in either the pilot plant or laboratory was successful. The conditions during the 45°C lab test were the closest to those given in the patents by Kroc & Fairchild [142] and Bleakley & Jones [143] and were most likely to produce scalenohedral PCC; namely vigorous agitation, 45°C temperature and CO_2CR in the range of 0.01-0.05 min^{-1}. However, there were some differences which could explain why the scalenohedral morphology was not produced.

Firstly, the pH of the solution was much lower than would be the case in $Ca(OH)_2$ slurry carbonation which, for saturated solutions of $Ca(OH)_2$, is 12.4, 11.8 and 11.5 at 25°C, 45°C and 60°C respectively [145]. Secondly, NH_4Cl has been reported in the literature to affect the morphology of PCC. As the major product from the 45°C lab test and scalenohedral pilot test was vaterite, it could be that the phase transformation had simply not fully, perhaps due to a stabilising effect of NH_4Cl on vaterite at

high [Ca^{2+}] concentration, and if the solution had been left to mature for a longer period after carbonation had stopped, or the crystals filtered and left in water, the transition to calcite may have taken place and produced the scalenohedral form. This is partly supported by Evans [146], who found that more vaterite is found in PCC precipitation as the ionic concentration increases in the solutions especially when NH^{4+} is present. Jung et al. [123] also report quite different impacts on morphology when NH_4Cl is present, depending on whether Ca^{2+} or CO_3^{2-} is in excess. Thirdly, there is the question of calcium concentration. The minimum reported $Ca(OH)_2$ slurry concentration used to produce scalenohedral PCC by Bleakley & Jones was 0.7 M or a 5% solution of $Ca(OH)_2$ in water, however in the 45°C lab test the [Ca^{2+}] was only 0.3 M. This would seem to suggest that higher concentrations of calcium may be required to produce scalenohedral PCC. However, $Ca(OH)_2$ is only slightly soluble in water as shown in Figure 7.33. At a temperature of 45°C, reportedly the optimum for producing scalenohedral, the maximum possible [Ca^{2+}] in a saturated $Ca(OH)_2$ suspension is only 0.018 M. Comparing this with the calcium concentrations measured in the experimental work (e.g. 0.050 M in the factorial, 0.1-0.3 M in the pilot plant tests) shows that in fact higher concentrations of dissolved Ca^{2+} are encountered in the Slag2PCC process than would be seen in conventional carbonation of $Ca(OH)_2$ suspensions. This may be another reason for the difficulty in producing scalenohedral PCC.

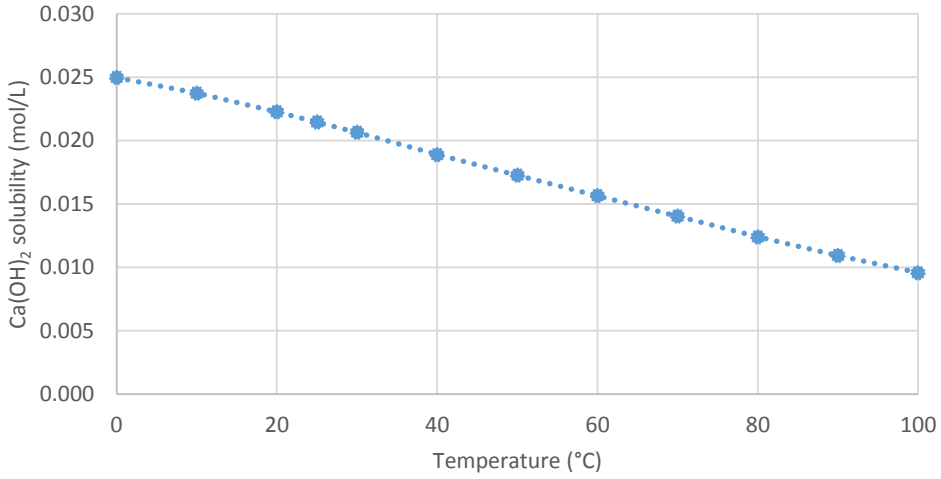

Figure 7.33 - Solubility of $Ca(OH)_2$ in water [145]

Taking the concentration of calcium in a 45°C saturated solution of $Ca(OH)_2$ as 0.018 M and recalculating the CO_2CR values recommended by Kroc & Fairchild and Bleakley & Jones based only on the calcium in solution (not including calcium as solid $Ca(OH)_2$) gives values in the range of 1.5 – 5.2 showing that not only is the calcium concentration lower in limewater carbonation but that the molar rate of CO_2 addition per mole of calcium in solution (i.e. CO_2CR) reported by Kroc & Fairchild and Bleakley & Jones for scalenohedral PCC formation is actually much higher than it seems at first glance. Assuming that the [Ca^{2+}]/[CO_3^{2-}] ratio is the major factor determining PCC morphology as reported by the literature (providing temperature is in the correct range), and that this ratio is determined mainly by the rate of CO_2 addition, the concentration of $Ca(OH)_2$ slurry should not affect the morphology of PCC as the solution is saturated and the concentration of dissolved Ca^{2+} does not vary with increasing solid content. Exactly why Bleakley & Jones recommend $Ca(OH)_2$ concentrations of 0.7M to 4M (5-30 wt%), preferably diluted to 15% for production of scalenohedral PCC is thus not clear.

Given that the attempts to produce scalenohedral PCC via the Slag2PCC process in this work have been based on data for conventional limewater carbonation, it is worth examining this process in somewhat more detail to better understand the differences between it and the Slag2PCC process. As was just shown, although high solid concentrations of $Ca(OH)_2$ are used in conventional lime slurry carbonation,

the actual concentration of calcium in solution is limited due to the poor solubility of $Ca(OH)_2$ and the majority remains as a solid. Over the course of carbonation CO_3^{2-} is produced by the reactions of OH^- with CO_2 and HCO_3^-. This CO_3^- then reacts with dissolved Ca^{2+} to precipitate $CaCO_3$. The removal of Ca^{2+} from solution allows further $Ca(OH)_2$ to dissolve until eventually all the solid $Ca(OH)_2$ has been converted to $CaCO_3$. The reaction between Ca^{2+} and CO_3^{2-} is almost instantaneous and the dissolution of solid $Ca(OH)_2$ is generally considered limiting [147]. Thus, the concentration of Ca^{2+} should remain essentially constant throughout carbonation, at a value which makes the reaction rate between Ca^{2+} and CO_3^{2-} equal to the dissolution rate of Ca(OH)2. If the CO_2 flow is also constant, this would mean that the supersaturation with respect to $CaCO_3$ given by equation (6.16) should also be essentially constant throughout most of the carbonation reaction. In the Slag2PCC process however, all the available Ca^{2+} is already in solution and is free to react with CO_3^{2-} as it forms. As the Ca^{2+} reacts its concentration will drop, which means that supersaturation with respect to $CaCO_3$ will also drop over time. This is another critical difference between the Slag2PCC process and conventional carbonation which may explain the difficulties in forming the scalenohedral morphology.

Despite the difficulties in making scalenohedral PCC in this work, production of scalenohedral PCC from the Slag2PCC process should be feasible as not only has HPM demonstrated the production of scalenohedral PCC, but Sun et al. [117] also report producing scalenohedral PCC in the size range 1-2 µm using a 2 M NH_4Cl solution, 0.37 M calcium concentration, carbonation temperature between 20-40°C, starting pH of 9, one hour carbonation time and 400 rpm agitation. However, rather than bubbling CO_2 through at atmospheric pressure they operated at 10 bar CO_2 pressure. This is encouraging as it shows that it must be possible to produce scalenohedral PCC with relatively high calcium concentrations even in the presence of high concentrations of NH_4Cl. However, future work on producing scalenohedral PCC could focus on either a low-concentration pathway (based on saturated $Ca(OH)_2$) or a high-concentration pathway (maximising $[Ca^{2+}]$). The latter is potentially more promising as it would allow for smaller reactors and lower system capital costs.

7.4 Experimental Learning and Challenges for Scale-up

This section highlights some learnings and challenges identified from the laboratory and pilot-scale tests which will need consideration when the Slag2PCC process is brought to a larger scale and commercialised.

7.4.1 Agitator Design

During commissioning of the pilot plant it was found that the outlet of the extraction reactor would continuously block with solid material preventing normal drainage. This was because the coarse slag solids were settling to the bottom of the reactor, even with agitation at the maximum setting of 170 rpm. Not only did the settled slag cause blockages, but it would also reduce the calcium extraction efficiency as the mass transfer from solid to liquid would be significantly impaired. To try to alleviate the problem, subsequent slag was sieved through a 250 µm sieve before being added to the reactor. This reduced the frequency of blockages, but grinding the slag particles to 250 µm requires more energy than grinding to 1mm and this should be taken into account in the overall process.

The extraction and carbonation reactors are equipped with identical 2-blade 45° pitched-blade impellers staged at three locations along the agitator shaft. This type of impeller is often referred to as a mixed-flow impeller as it induces flow in both radial and axial directions. In the extraction reactor, the mixing objective is complete solids suspension and some degree of radial mixing to ensure the slag does not settle out and that concentration gradients do not develop in the reactor. In solids suspension applications such as this, predominantly axial flow impellers with high pumping efficiencies are generally recommended [148]. These impellers generate a flow pattern which sweeps the tank bottom and suspends the solids. The figure below depicts a typical agitated vessel with the main dimensions highlighted. In the Slag2PCC pilot plant extraction and carbonation reactors, Z=1 m, T=0.5 m and D=0.3. No baffles are installed and the reactor bottom is flat.

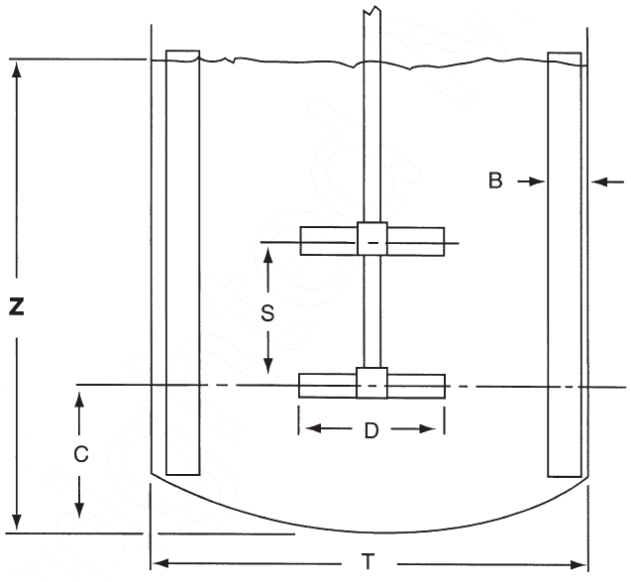

Z – Height from bottom to liquid surface
T – Vessel width
B – Baffle width
S – Impeller spacing
C – Impeller bottom clearance
D – Impeller diameter

Figure 7.34 - Standard agitated vessel configuration [148]

A commonly-reported effective mixing configuration for solids consists of a tank with a dished or ellipsoidal bottom, a down-pumping axial flow impeller, four wall baffles having width equal to T/12, a baffle wall clearance of about 1.5% T, and an impeller bottom clearance equal to T/4 [148]. A large-diameter pitched blade turbine is poor at solid suspension because of the resulting flow patterns and

when the ratio D/T is greater than about 0.55, pitched blade turbines becomes radial flow impellers [148] [149]. The agitator D/T ratio in the pilot plant is 0.6, suggesting that radial rather than axial flow is predominant which may account for the poor solids suspension encountered. When the power number of the impellers is taken into account, high efficiency axial flow impellers (such as the Lightnin A-310 or Chemineer HE-3, see Figure 7.35) are able to achieve a just-suspended state at a lower rotational speed than can a pitched blade or disc turbine and the resulting axial flow developed by high efficiency impellers is higher at the vessel base than for radial flow impellers. They are also more effective at higher clearances from the vessel base (i.e. larger values of C/T). Full-solids suspension is also more easily achieved in dish-bottomed vessels than in flat-bottomed ones and is impractical to achieve with conical bottoms [149].

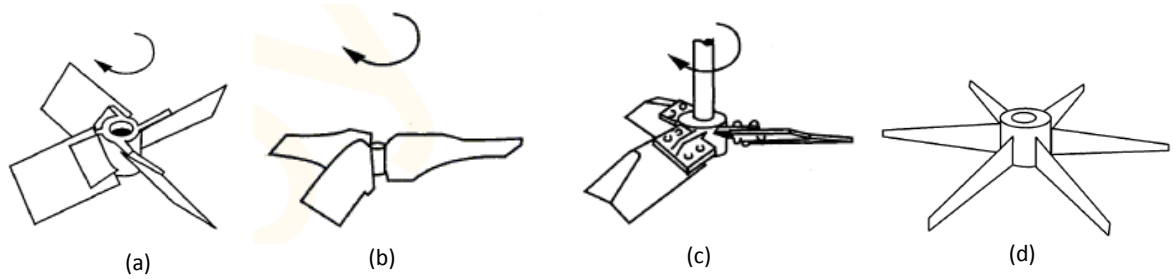

Figure 7.35 - Common impeller blade designs: (a) pitched (b) Lightnin-A310 (c) Chemineer HE3 (d) Chemshear [148]

In the carbonation reactor, the mixing objectives are more complex. In addition to full suspension of the produced PCC crystals and prevention of concentration gradients, break-up and dispersion of CO_2 gas bubbles throughout the solution is also desired. This latter objective is best served with a high-shear impeller such as the Chemshear. These dispersing impellers are low pumping and therefore are often used with axial flow impellers to provide both high-shear and homogeneous distribution [148].

Another potential method of agitation is ultrasonic mixing. This is currently under investigation for the extraction of calcium from steel slag and preliminary results are promising with extraction efficiencies of between 38-96% achieved with ultrasonic mixing, compared with 18-38% for mechanical agitation, depending on the particle size [150]. However, even if ultrasonic mixing proves successful some mechanical axial mixing is still likely to be required in a commercial context as the local mixing achieved with ultrasound will probably be insufficient to maintain particles in suspension.

7.4.2 Baffles

Baffles are highly recommended for solids suspension applications when the solids are heavier than the liquid, as is the case with PCC. They help convert the swirling motion into axial fluid motion that helps to lift, mix and suspend the solids [149]. They would also help to prevent vortices forming at the agitator. For these reasons, the installation of baffles into the pilot plant reactors should be considered.

7.4.3 Ammonia Release

During the commissioning stage of the pilot plant equipment it was noticed that a considerable amount of NH_3 gas was being given off by the solvent solution during and after the calcium extraction stage. If not recaptured, this loss of NH_3 will gradually weaken the strength of the solvent and reduce the calcium extraction efficiency.

Mannisto [69] tried to quantify the loss of NH_3 experimentally during carbonation tests using 500 mL of 2 M NH_4NO_3 and NH_4Cl solvents, with a fixed gas flow of 2 L/min and different CO_2 concentrations. Bubbling CO_2/N_2 gas through the carbonation solution effectively acts a stripping operation, and so NH_3 losses may be high. He found that for CO_2 concentrations from 25-100% the loss of NH_3 in each case was below 1 wt%, and that in fact the loss of water from the solution as vapour was 2-3 times higher. No studies have been done to quantify the loss of NH_3 during extraction, but it is likely to be lower than from carbonation as there is no gas-liquid mixing and hence there will be no stripping effect.

7.4.4 Copper Compatibility

During test work with the pilot plant it was noticed that the Ca-rich solution leaving the ER and filters would at times take on a deep blue colour, which was particularly strong when residual extraction solution was left in the system for several hours or days. After some investigation it was theorised that the deep blue colour was due to the complex ion $[Cu(NH_3)_4(H_2O)_2]^{2+}$, formed from the reaction between NH_3 and copper ions resulting from chemical attack of brass components in the system. In aqueous solutions copper ions are actually present hexaaquacopper(II) $[Cu(H_2O)_6]^{2+}$ ions, which will react with NH_3 to produce the complex $[Cu(NH_3)_4(H_2O)_2]^{2+}$. This was confirmed by addition of acid to the deep blue solution, which converted the copper-ammonium complex back to the characteristic pale blue hexaaquacopper (II) ion. Final proof came from the addition of NaOH to the pale blue solution which precipitated insoluble light blue copper(II) hydroxide dihydrate. This also explained the presence of a light blue scale observed around the extraction filters. From these findings it was concluded that no copper-containing materials should be used in the Slag2PCC system due to the incompatibility of copper with the NH_4Cl solvent and the brass components (mainly drain valves and threaded connections in the extraction filters).

7.4.5 PCC Discolouration

During initial commissioning of the pilot plant it was noticed that the PCC produced from the carbonation reactor would have a yellow or brownish colour. Inspection of the reactor identified that the welding material used in the sparger had corroded, causing iron and rust to discolour the PCC. This problem was resolved by replacing the sparger and coating the sparger and base of the reactor with a fluoropolymer resin. However, previous work highlighted that PCC can be discoloured even in the laboratory where rust could not be the cause.

Mannisto [69] found that the PCC produced from steel slag using NH_4Cl and NH_4NO_3 would sometimes be discoloured yellow, which he suggested was due to precipitation of impurity compounds (e.g. $Fe_2O_3.H_2O$, $PbCrO_4$) formed from dissolved metals in the slag such as iron, chromium and nickel. Washing the PCC with distilled water improved the colour in most cases, but not in all. A yellow discolouration was also seen during this work in the samples from factorial Runs 12, 13 and 14 in particular. This discolouration was not so obvious at the time of carbonation, but was eminently clear 1-2 weeks later when the samples were analysed for PSD. Given all samples were washed equally well and all should have contained the same level of metal impurities from the slag (same Ca-rich solution), it is not clear why these three samples in particular should show signs of yellowing. These three runs were also low [NH_4Cl] runs, suggesting that NH_4Cl is not the cause of yellowing. If this were the case then one would expect the high-[NH_4Cl] runs to show the same if not higher degree of yellowing. No yellowing of the product was seen in the pilot-scale tests or follow-up laboratory tests. However, K. Salminen and M. Pusa, while trying to develop a method for determining dissolved carbonate concentration, reported that the solution turned a yellow colour when HCl was added. Given the history of problems related to discoloured product, this warranted further investigation.

A small amount of HCl (1M) was added to samples of un-carbonated low-Ca solution from the factorial experiments, carbonated solution from factorial run 12, freshly prepared 1M NH_4Cl solvent and spent 1M NH_4Cl solvent from the 58°C aragonite pilot plant test. Both the un-carbonated low-Ca solution and the carbonated solution from factorial run 12 turned yellow and stayed yellow after vigorous mixing. In the case of the un-carbonated low-Ca solution, it turned yellow even though the pH only dropped from 9.8 to 9 indicating that the species imparting the yellow colour was stable at alkaline as well as acid pH. No change was observed in the other two solutions. Nitric acid (HNO_3) was subsequently added to fresh samples of the same solutions. Again, only the first two turned yellow. This indicated that it was not the HCl which was causing the change, but rather the H^+ ion or its oxidative effect. From these simple tests it seems that NH_4Cl itself is not responsible for the yellow colour when acid is added, and the cause is more likely to be related to the compounds dissolved from the slag (i.e. Ca, Fe, Si and other trace elements). However, if this were the case then adding acid to the spent solvent should also have turned it yellow as the impurities would still be in solution. Thus the issue of PCC discolouration remains an open question.

7.4.6 Impurity Accumulation

While not demonstrated in this work, recycling the solvent solution will, over time, result in the accumulation of other elements also dissolved from the slag including Fe, Si and Mg. Furthermore as NH_3 gas is lost from the solution and replaced presumably with makeup NH_4Cl solvent, the concentration of Cl^- will also continue to rise. The factorial experiments showed that increasing the ionic content of the carbonation solution will slow the kinetics of the carbonation process, and the same may be true for extraction. As the concentration of impurities rises this is likely to reduce the purity of the PCC produced as more impurities become trapped in the crystal. Both of these impacts would negatively impact the Slag2PCC process, thus a method of removing impurities from solution, such as purging, is required.

7.4.7 Scale Formation

Tests in the laboratory and at the pilot plant have highlighted that considerable $CaCO_3$ scale forms on the reactor vessel walls as well as the pH probe and thermocouple during carbonation. The scale can be quite hard to remove, especially if allowed to dry. While this is easily dealt with in the laboratory by manual scrubbing and an occasional acid wash, it would become challenging for a larger plant where manual descaling would be time consuming and contribute to significant equipment downtime. The $CaCO_3$ scale will slowly degrade the performance of the instrumentation and lead to measurement lag with temperature and cause incorrect readings on the pH meter. If not removed, any scale will continue to grow as it acts as a nucleation site for PCC precipitation in subsequent carbonation reactions. One solution on a commercial scale would be to operate two reactors; one online and one standby so that the standby reactor could be acid-washed while the other was operating. This would increase chemical costs and thus other options should be investigated. For example, Parsons et al. [151] & Dalas et al. [152] report that application of a magnetic field can reduce $CaCO_3$ scale formation by up to 50%. pH was also found to play a role with scale rates exhibiting a maximum in the pH range 8-8.5. The application of an ultrasonic field has also been shown to retard PCC growth by up to 76% [153]. Ultrasonics have also been used to modify the PCC morphology and reduce particle size [154]. The ζ-potential of the PCC during precipitation is also likely to effect is propensity to scale thus any factors which effect ζ-potential ($[Ca^{2+}]$, pH, $[NH_4Cl]$ etc.) could also be considered as potential ways of reducing scaling rates.

8 Economics of the Slag2PCC Process

It is crucial for the development and eventual commercialisation of the Slag2PCC process that it be not only technically viable, but also economically viable. Work until now has focussed primarily on the technical aspects of the Slag2PCC process. The purpose of this chapter is to investigate the economic viability of the Slag2PCC process, albeit at a somewhat crude level, by estimating the cost of producing PCC commercially via the Slag2PCC process extrapolated from batch operation of the pilot plant. This is done by considering the major material and energy inputs, data from the pilot plant, relevant literature, as well as some key assumptions. In addition to the economics, some rough CO_2 impact calculations are also made so that the cost of CO_2 sequestration via the Slag2PCC process can be estimated.

8.1 Base Case & Assumptions

The Slag2PCC process is assumed to take place under the following extraction and carbonation conditions based essentially on the 50°C pilot plant test (Scal-Test) data, assuming the process conditions required to produce the scalenohedral morphology, while still not known exactly, are minor.

- Solution volume = 150L
- SLR = 50 g/L
- $[NH_4Cl]$ = 1M
- Extraction efficiency = 50%
- Carbonation temperature = 45°C
- CO_2CR = 0.025 min^{-1}
- Carbonation time = $1/CO_2CR$ = 40 mins
- Extraction time = 40 mins
- Agitation
    - Constant agitation at 170 rpm (both reactors)
    - Agitator power draw = 370W (as installed)
- Pumping
    - Three pumping stages: Solvent to extraction reactor, Ca-rich solution to carbonation reactor, Spent solvent to storage
    - Pump capacity = 18 L/min
    - Pumping time = 150/18 = ~8.3 mins
    - Pump power draw = 250W (as installed)

Under these conditions, the carbonation run is expected to produce 2.86 kg PCC from 7.5 kg slag and capture 1.26 kg CO_2. In addition to the carbonation and extraction conditions, the following assumptions have been made regarding the other unstudied aspects of the Slag2PCC process and extrapolation to commercial scale.

- Steel converter slag is used as a feedstock with 45% effective CaO content
- The Slag2PCC plant is located in Finland either at the steel mill where the slag is produced, or, at the site of a PCC consumer 200 km away. If the plant is located at the steel mill, the PCC is transported as a 70% slurry in water to the PCC customer. If the plant is located at the PCC consumer, slag is transported (dry) from the steel mill. Both options are considered. There is

also the option that the PCC is manufactured by a third party at a third location which would then require transport of both slag and PCC, however this is not considered.

- Transport of slag or PCC is by full road trailer with 40t payload, travelling on major highways. Trailers are dispatched full and return empty. Trailers use diesel fuel with calorific value of 36 MJ/L. When fully loaded, the trailers have a fuel economy of 0.5 L/km (18 MJ/km) and emit 1.26 $kgCO_2e$/km. When empty, the trailers have a fuel economy of 0.33 L/km (12 MJ/km) and emit 0.821 $kgCO_2e$/km [155]. The price of diesel is 1.5 €/L (2014) [156].
- If the Slag2PCC plant is owned by the steel producer, the slag is available at no cost. If the Slag2PCC plant is owned by the PCC consumer, the price of slag is assumed to be 8 €/t [68]
- Electricity is assumed to be purchased from the Finnish national grid at 0.0679 €/kWh with CO_2 emission intensity of 0.199 $kgCO_2e$/kWh [157] [158]
- 100% of the Ca-rich solution is recovered from the slag extraction and filtration processes for carbonation.
- Calcium conversion is assumed to be 95%
- Flue gas is added in such a way (slowly or with recovery step) that CO_2 conversion is 100%.
- Slag is ground from a size of 100mm to 250µm, with power requirement estimated using Bond's equation and work index (30.4 kWh/t) as 18.3 kWh/t slag [115].
- Flue gases are cleaned and compressed to 1.2 bar (abs) with composition 30% CO_2, 70% N_2. The power requirement for flue gas compression is estimated at 0.025 kWh/kg PCC [70].
- The spent slag and product PCC are washed and filtered for quality and environmental reasons in additional processes not included in the pilot plant. The power requirement for the filtration is estimated as 0.0213 kWh/kg PCC [70].
- Heating for the carbonation solution is provided by combustion of either bituminous coal or natural gas combustion from an assumed average water supply temperature of 10°C. Of this heat, 70% is assumed to be recoverable (not lost) from one carbonation to the next extraction step with the remaining 30% lost through pipework, the reactor, slag washing and filtration steps. The heat capacity of the solution is taken as that of a 1M NH_4Cl solution for which the heat capacity is ~95% that of pure water at the same temperature [159]. The costs of coal and natural gas are taken as 27 €/MWh and 45 €/MWh respectively [160]. CO_2 intensities for combustion of coal and natural gas are calculated as 103 and 64 g CO_2e/MJ respectively based on a specific carbon content of 0.75 g C/g fuel for both fuels. Heat provided by the carbonation reaction (which would partly offset the losses) is not considered
- Data on CO_2 emissions associated with the manufacture of NH_4Cl could not be found and so this has not been considered.
- Due to losses from solution and purging to remove impurities, the NH_4Cl solvent is lost at a rate of 3% of the total amount in solution and consequently must be replaced at this level at a cost of 110 €/t solid NH_4Cl [161]. The energy for recovering the NH_4Cl from solution (e.g. membranes, ion exchange, evaporation etc.) is not considered.
- The process is assumed to have developed to such a level that water use is well integrated and recovery is quite high (recycling wash water etc.) and that water is only required to replace the water lost from the process in the PCC product slurry (0.3 t H_2O/t PCC) and a small water purge equal to 10% of the carbonation liquid volume. The heat and power requirements for treating the water are not considered. Industrial fresh water costs are estimated at 0.1 €/kL.
- Costs associated with the final disposal (landfilling) of spent slag are not considered as no data could be found. This means savings from reducing the amount of slag landfilled will not be taken into account.
- Potential revenues from CO_2 credits or other carbon trading mechanisms are not considered

8.2 Cost of PCC Production

Table 8.1 below shows the estimated PCC production cost from the Slag2PCC process if the plant is constructed at a steel mill or at a PCC consumer located 200 km away. It can be seen that the overall PCC production cost is estimated at 65.2 and 93.6 €/t if the plant is located at the steel mill or the PCC consumer respectively. Production costs are approximately 40% higher if the Slag2PCC plant is built by the PCC consumer at their own site as they must pay the steelmaker for the slag as well as for transportation of the slag to their own site. Transport costs are more than 80% higher when the plant is located at the PCC consumer simply due to the much larger quantity of slag which must be transported compared to the mass of PCC product even when transported as a slurry. Given that the price of a typical scalenohedral filler PCC from a satellite plant is probably in the range of 100-120 €/t, the PCC consumer is unlikely to go to the trouble of building a Slag2PCC plant if the price difference is small compared with proven technologies. Many costs have also been left out of this analysis, and it is likely the true production cost of PCC via the Slag2PCC process would be higher. On this basis alone, not even considering what the PCC consumer would do with the spent slag, locating the Slag2PCC plant at the steel mill and on-selling the PCC would make the process much more favourable and financially competitive. Further discussion will therefore be limited to this case only.

Table 8.1 - Estimated PCC production cost based on extrapolated pilot plant data

	Steel Mill		PCC Consumer	
Cost Breakdown	Qty/t PCC	€/t PCC	Qty/t PCC	€/t PCC
Converter slag (t)	2.62	0.0	2.6	21.0
Slag transport (Road)		0.0		16.3
PCC transport (Road)		8.9		0.0
NH_4Cl solvent (t)	0.084	9.3	0.084	9.3
Electricity (kWh)	281.4	19.1	281.4	19.1
Slag grinding	47.9	3.3	47.9	3.3
Agitation	150.9	10.2	150.9	10.2
Pumping	36.4	2.5	36.4	2.5
Flue gas compression	25.0	1.7	25.0	1.7
Slag and PCC filtration	21.3	1.4	21.3	1.4
Process heat (natural gas) (kWh)	607.8	27.3	607.8	27.3
Process water (t)	5.5	0.6	5.5	0.6
PCC Production Cost (€/t PCC)	**65.2**		**93.6**	

Electricity consumption is estimated at 281 kWh/t PCC and electricity costs amount to 30% of the total PCC product cost, of which agitation (53%) and slag grinding (17%) form the main part. The Slag2PCC process is at a slight disadvantage to conventional lime carbonation in terms of agitation as the latter is normally done in a single step in a single agitated vessel, whereas two agitated steps are required in the Slag2PCC process. The agitation power consumption estimated here based on the pilot plant is quite high and due to efficiencies gained in scale-up is likely to be lower in practice. Pumping energy is only a minor contribution to the total cost however this cost is very site specific and will depend on the configuration of the plant, elevation difference, and pump selection in practice. Flue gas compression and filtration surprisingly contribute only a small amount to the total PCC production cost based on the estimates available.

Heating contributes a significant amount to the cost of the PCC production (41%), even when 70% of the heat is assumed to be recoverable. While it is true that the carbonation reaction will generate some heat, this is unlikely to be enough to offset the losses in the system especially as the heat generation and corresponding temperature rise during carbonation will only be significant if concentrated solutions are used (high [Ca^{2+}], high pH, high [NH_4Cl]). The results in Table 8.1 are based on natural gas as a fuel. If however natural gas is unavailable and bituminous coal is used to provide the heat (which should already be available on site at a steel mill to supply the coking plant), heating costs reduce by 40% to 16.4 €/t and the PCC production cost reduces to 54.2 €/t. The process heating calculations have assumed that additional fuel must be burnt at the site to provide heat for the Slag2PCC process, however low-quality waste process heat may be available at the steel plant which would significantly reduce cost.

Sensitivity analysis was also performed as part of the economic calculations to see the impact of major variables on the cost of production. As these a differential in nature, they are less sensitive to errors in the absolute values of the model assumptions. From the base case values, changes were made (up and down) to determine the average change in PCC production cost in the vicinity of the base case values. The results are shown in Table 8.2 below.

Table 8.2 - Effect of Slag2PCC process parameters on the production cost of PCC

Parameter	Base	Change	Cost impact (€/t PCC)
Slag cost (€/t)	0	+1 €/t	2.6
Slag CaO content (%)	45%	+1%	-1.1
Slag transport distance (km)	0	+100km	8.2
PCC transport distance (km)	200	+100km	4.5
SLR (g/L)[a]	50	+10g/L	-2.8
NH_4Cl replacement rate (%)	3%	+1%	2.9
Extraction efficiency (%)	50%	+1%	-1.1
Calcium Conversion (%)	95%	+1%	-0.5
Extraction/carbonation time (min)	35	+10 min	1.5
Carbonation temperature (°C)	45	+5 °C	3.9
Heat recovery (%)	70%	+1%	-0.6

[a]Extraction efficiency adjusted to 38% at 100 g/L as observed in pilot plant tests

For some parameters, such as calcium conversion and extraction efficiency, the cost impact was non-linear and a 'diminishing return' impact was seen. From a base level of 50% extraction efficiency for example, increasing extraction efficiency by 1% reduces the cost of PCC by 1.1 €/t. However if the base level were 80%, as might be possible with ultrasonic mixing, increasing extraction efficiency by 1% would only reduce the cost of PCC production by 0.4 €/t. This is why improving extraction efficiency by 1% makes a larger impact to the cost of PCC than improving calcium conversion by the same percentage. For other factors such as the transport distances, slag cost and solvent concentration, the cost impacts are constant if all other factors remain constant.

In the case of SLR, the calculations were slightly modified to take into account the known drop in extraction efficiency observed when a higher SLR was used. Several other important variables (solvent concentration, slag particle size, agitation rate and CO_2CR etc.) were not considered in the sensitivity analysis. This is because these variables are highly non-linear and the dependence of other variables (e.g. extraction efficiency, carbonation time) on these primary variables due to more complex phenomena such as mass transfer characteristics are not fully known and could not be expressed mathematically in the simple model used. Without including their impacts on all factors, the cost

impacts may not be representative as the positive impact of a known factor may actually be offset by the negative impact of an unknown one. Thus establishing and describing these relationships so that they can be included in a more comprehensive model remains an area of work to be completed.

In developing the Slag2PCC process therefore, attention should focus on those aspects which can lead to clear cost reductions such as: being able to perform carbonation at higher SLR, lower temperature and minimum carbonation time whilst meeting PCC quality constraints, minimising NH_4Cl losses, maximising extraction efficiency and heat recovery.

Assuming that PCC could be produced at a cost of 65.2 €/t sold at a price of 120 €/t, the potential profit to the steel mill would be approximately 55 €/t PCC sold. As an example, Ruukki's Raahe works produced approximately 226,000 tpy of steel converter slag in 2007 [162]. If all this slag was used as feed material for an on-site Slag2PCC plant, with the assumptions made in this analysis approximately 86,000 tpy of PCC could be produced and sold for a total profit to Ruukki of €4.7M/y. Thus if the Slag2PCC plant could be designed, constructed and installed at a capital cost of €24M or less it the simple payback time for the plant (undiscounted) would be five years.

8.3 Cost of CO_2 Capture

Turning now to the CO_2 impacts of the Slag2PCC process, Table 8.3 below shows the calculated CO_2 emissions from the Slag2PCC process located at a steel mill per tonne of PCC produced. Accounting for the CO_2 emissions associated with generating heat and electricity for the production of the PCC, transport of the PCC to the customer, and the CO_2 locked up from the flue gases, the process delivers a net reduction in CO_2 emissions of 229 kg CO_2e/t PCC produced.

Table 8.3 - Estimated CO_2 emissions of the Slag2PCC process

Source	CO_2 impact (kg CO_2e/t PCC)
Transport	14.9
Electricity	56.0
Process heat	139.8
Total	**210.7**
- CO_2 captured as PCC	-439.7
Net CO_2 Emissions	**-229**

Nearly two-thirds of the CO_2 emissions from the production of PCC are due to natural gas combustion for process heat. Although coal was shown to reduce the cost of PCC production, recalculating the CO_2 emissions using coal as the fuel source instead of natural gas increases the CO_2 emissions from process heat by 60% to 225 kg CO_2/t PCC and results in Net CO_2 emissions of -144 kg CO_2/t PCC, reducing the CO_2 benefits of the Slag2PCC process by 38%. Given the uncertainty in the calculations, the omission of the solvent recovery process, and the quite generous assumption of 70% heat recovery, using coal in lieu of natural gas for heating would risk negating much of the CO_2 benefit of the Slag2PCC process.

The calculated value of -229 kg CO_2e/t PCC is similar to the value of -324 kg CO_2e/t PCC determined by Matilla et al. [70] for the Slag2PCC process using a 0.01M NH_4Cl solvent solution. For a 0.65M NH_4Cl process however they calculated the CO_2 emissions to be +3290 kg CO_2e/t PCC, or nearly three times more polluting than conventional PCC production from limestone which emits approximately 1040 kg CO_2/t PCC produced [70]. Thus, replacing one tonne of conventional PCC (1040 kg CO_2/t PCC) with 1 tonne of Slag2PCC would reduce CO_2 emissions by -1.27 t CO_2/t PCC.

The reason for the much high emissions from the 0.65M NH_4Cl process is that Mattila et al. assumed that the slag and PCC wash water would need to be evaporated to recover the NH_4Cl solvent using

steam produced by the combustion of fossil fuels; a step which, in the case of the 0.01M NH_4Cl process, would not be required as the loss of solvent from washing would be small. However, there are other less energy intensive processes such as ion exchange and membrane separation would could also be used to recover the solvent. Although these have not been considered in this analysis it shows that evaporation for solvent recovery is counterproductive to the Slag2PCC process aim of reducing CO_2 emissions, and highlights that the slag and PCC post-treatment and solvent recovery processes need further investigation and improvement.

At the Raahe plant example, using all the available steel converter slag would capture 38,000 t CO_2/a, or nearly 1% of its total annual CO_2 emissions of 4.5 Mtpy [162]. While this is only a small fraction of the total CO_2 emissions from the plant, the revenue provided by the sale of the PCC could be used to finance other more ambitious but costly CO_2 emission reduction measures.

Assuming for the moment that the Slag2PCC process could indeed capture 229 kg CO_2e/t PCC at a cost of 65.2 €/t PCC, the effective cost of CO_2 capture is calculated as 284 €/t CO_2. This is quite high compared to other post-combustion carbon capture and storage (CCS) or CO_2 mitigation methods reported in the literature such as MEA scrubbing with geological storage having typical CO_2 avoidance costs in the range of 45-100 €/t [163]. However, taking into account that the PCC can be sold for 120 €/t, the cost of CO_2 capture becomes -239 €/t i.e. capturing the CO_2 delivers a positive cash flow. This is a strong advantage of the Slag2PCC process over other forms of CCS and, to the knowledge of the author, is the only method of CCS which is potentially profitable without CO_2 trading and other support mechanisms. Furthermore, even if the cost of PCC production increased or the sale price of PCC decreased to the point where the Slag2PCC plant was operating at break-even or a mild loss, as long as the loss per tonne of CO_2 captured was below the cost of alternative CCS methods (e.g. 45 €/t CO_2) the Slag2PCC would still offer the cheapest method of reducing CO_2 emissions from the plant.

9 Business Potential of the Slag2PCC Process

With some basic economic analysis of the Slag2PCC process laid out the previous section, this chapter briefly examines the business potential of the process by looking at the availability of suitable slag feedstocks, as well as PCC production and consumption on a global and regional level. Without an adequate supply of suitable slag and potential market for the PCC, commercialisation of the Slag2PCC process will prove difficult.

9.1 The Market for PCC

In 2008, global PCC production capacity was estimated at around 14 Mtpy [164]. Of this capacity, around 40% was produced by satellite PCC plants with the remainder produced by merchant plants. Figure 9.1 shows the estimated world consumption of PCC by region and industry in 2007. The paper industry was the largest consumer of PCC (5.5 Mtpy, 40%) followed by the plastics (3.6 Mtpy, 27%) and paint (1.6 Mtpy, 12%) industries [164]. Consumption is highest in Asia (8 Mtpy, 60%) with China responsible for 75% of demand there, followed by North America and Europe both comprising around 17% each of the global PCC market. While this data is somewhat old, total PCC capacity grew to 17Mtpy by 2011 and the industrial consumption share are unlikely to have changed significantly since [165].

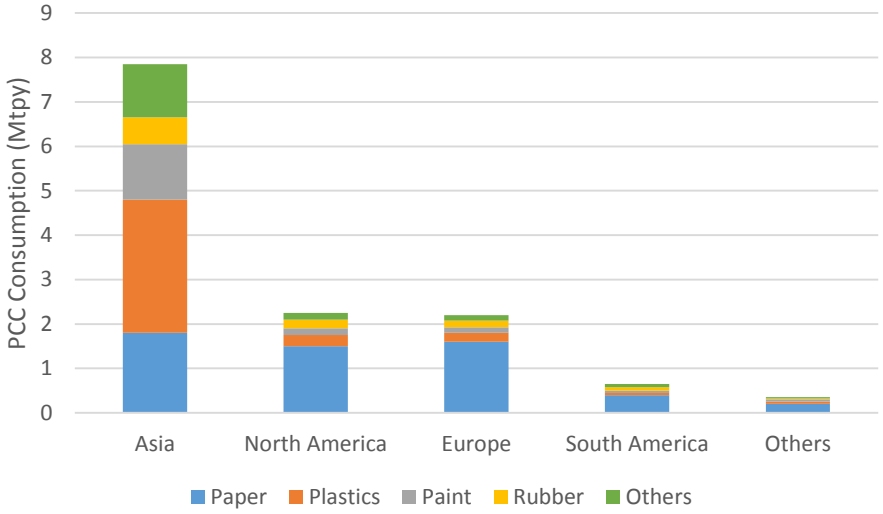

Figure 9.1 - World consumption of PCC by region and industry in 2007 [164]

Over the last decade the global market for PCC has shown consistent growth of between 1-3% and is expected to continue to grow due to strong growth in the plastic (6%) and rubber (4%) industries in China, as well as the trend for increasing mineral filler use in the paper industry [164]. No more recent figures on global PCC capacity could be found, but assuming a growth rate of 1.5% the market could be expected to have risen to between 15-16 Mtpy PCC by 2014. The $CaCO_3$ industry is characterised by a few multinational producers and thousands of often very small producers. Twelve companies control half of global GCC and PCC capacity. The three leading producers (Omya, Imerys & MTI) hold over 40% of GCC capacity and 35% of PCC capacity [165].

In Finland, the main producers of GCC and PCC are Suomen Karbonaatti, Omya, MTI, and Schaefer Kalk [165]. Production of PCC was approximately 480,000 tpy in 2006 up from 370,000 tpy in 1999, giving an average growth rate of 3.8% per year [164]. By 2008 this had risen to 550,000 Mtpy produced by three companies operating six PCC plants as shown in Table 9.1.

Table 9.1 - Known PCC-producing plants in Finland [164]

Company	Plant	Type	PCC produced	Capacity in 2008 (tpy PCC)
MTI	Äänekoski	Satellite	Opacarb® Coating (100,000t) Filler (35,000t)	135,000
	Anjalankoski	Satellite	AT® acid-tolerant PCC + other	40,000
	Tervakoski	Satellite	n/a	30,000
Omya	Imatra	Satellite	n/a	60,000
	Kemi	Satellite	n/a	130,000
Schaefer Kalk	Kuusankoski	Satellite	n/a	155,000
		Total		**550,000**

Table 9.1 demonstrates that if Ruuki's Raahe works went ahead with a Slag2PCC plant and used all their steel converter slag to produce 86,000 tpy PCC (as discussed in Chapter 8), its output would be comparable with a mid-sized satellite PCC plant and be a significant competitor in the Finnish PCC industry. This data also shows that there would only be market capacity for 6-7 such PCC plants in Finland based on 2008 figures. The recent slowdown in the pulp and paper industry in Finland has likely reduced the requirement for PCC, however more recent data were not available to confirm this.

9.2 Demand for PCC in the Pulp and Paper Industry

As the major global consumer of PCC, it is prudent to look at this industry in a bit more detail. Mineral use in the global pulp and paper industry is widespread, with approximately 31.7 Mtpy consumed in 2010 as seen in Figure 9.2. $CaCO_3$ represents over 70% of this market, with GCC and PCC constituting 16.5 Mtpy (52%) and 6.6 Mtpy (21%) respectively.

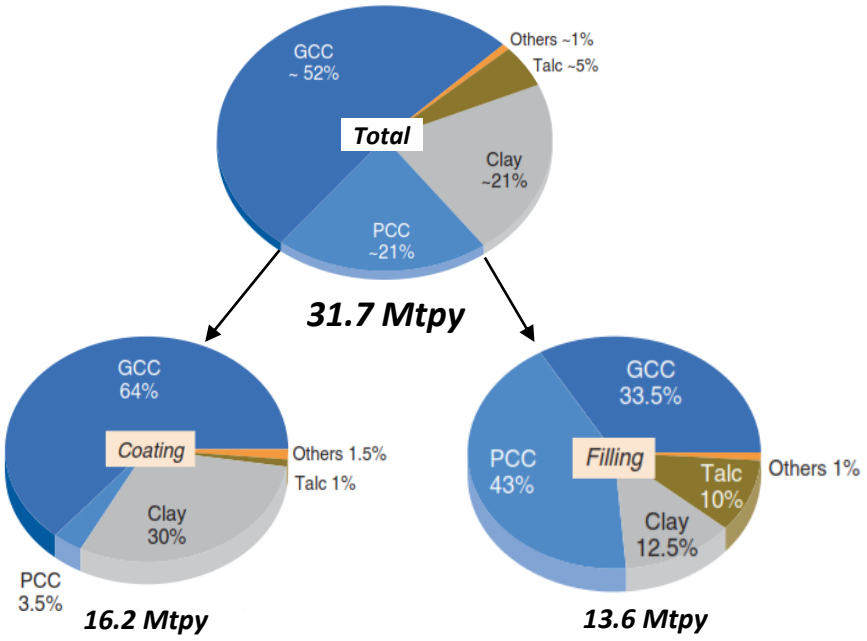

Figure 9.2 - Global mineral consumption in paper and board in 2010 [30]

PCC has become the most widely used filler in the paper and board industry, having approximately 43% of the market [30]. Its use as a coating is less common where GCC has a much greater share mainly for cost reasons. As a general trend however, mined minerals like GCC are being substituted by PCC due to its higher quality [35].

In Finland four pulp and paper and two paper plants are capturing and directing a part of their fuel combustion based CO_2 emissions to PCC plants nearby [3]. Prior to 2006, the American J.M. Huber Corporation had been a major player in the Finnish PCC market. In 2006, Omya purchased Huber's global PCC business including its three Finnish satellite PCC plants located at Imatra, Kemi and Kuusankoski. This was raised as a potential market concentration and a threat to competition by the Finnish Competition Authority and a legal challenge against the purchase was made to the European Commission (EC) [48]. As a result of their investigations the EC found that the purchase of the Kuusankoski plant in particular would effectively give Omya a monopoly in the PCC coating market in southern Finland as Huber had been supplying a coating PCC from this plant for local paper mills which could be used in conjunction with PCC. With the purchase of the other two Huber PCC plants there would be no local producer of PCC for these customers and the location of other potential suppliers (MTI) in northern Finland was so distant that the transport of coating PCC from this distance was not economic. With Omya already controlling most GCC in northern Europe, they would be in an even more powerful position. As a result, Omya was obliged to divest the Kuusankoski plant from the purchase. Huber was also obliged to divest its technology for producing its coating PCC to the purchaser of the plant. The plant was subsequently purchased by Schaefer Kalk [48] [164]. This shows that there may be a potentially favourable market in southern Finland for producing PCC for coating applications from the Slag2PCC process as there are only two major competitors.

The market for PCC in other industries in Finland such as plastics and pharmaceuticals was investigated but no information on PCC consumption could be found.

9.3 Steel Slag Availability

More than 400 million tonnes of iron and steel slag is produced around the world each year [9]. Previously landfilled as useless by-products, slags are now recognised as marketable products and the worldwide average recovery rate for slag varies from over 80% for steelmaking slag to nearly 100% for ironmaking slag. In Europe, 90-100% of BF slag is used in the production of cement and concrete. When it comes to steelmaking slag, 76% is used for building purposes or as a filler while around 13% must be dumped due to its fine grained properties or environmentally related leaching behaviour [7].

Working on the basis of 1400Mtpy global steel production of which approximately 70% is produced via the integrated steel process and 30% by the EAF process [9], the respective slag production data given in Figure 2.2 for these processes can be used to estimate the annual production of BF slag, BOF slag and EAF slag as approximately 270, 123 and 70 Mtpy respectively. Given that good markets already exist for BF slag and a significant proportion of steelmaking slag, the optimum slag to target as feedstock for the Slag2PCC process would be the part of steelmaking slag (~13%) which is currently landfilled. If only this landfilled 13% of the BOF slag is used, this leads to a figure of about 16 Mtpy BOF slag which would be ideal for treatment with the Slag2PCC process. Assuming 13% of EAF slag could also be used this amount increases to around 25 Mtpy. If all the calcium in this steel slag could be recovered with the Slag2PCC process, approximately 19 Mtpy of PCC could be produced, simultaneously sequestering nearly 8.4 Mtpy of CO_2. While the Slag2PCC process could also use other slags as feedstock, if this reduces the utilisation of slag in cementmaking leading to an increase in raw limestone consumption in another industry, the CO_2 benefits of the Slag2PCC process would be eroded.

Thus, considering only the use of currently landfilled steel slags with capacity to produce 19 Mtpy PCC, there is enough suitable slag available worldwide to meet the entire demand of the estimated current global PCC market of 16 Mtpy.

10 Conclusions

This thesis has investigated the production of PCC from steel slag based on literature, equilibrium modelling and experimental approaches. While the focus of the experimental work was on the carbonation side of the Slag2PCC process and how precipitation variables affect the PCC quality and carbonation process, attention was also given to the economic and business aspects of the Slag2PCC process which will play a crucial role in the eventual commercialisation of the technology.

The feasibility of PCC production from steelmaking slag has been successfully demonstrated at the pilot scale. Although the quality of the PCC produced from the Slag2PCC process is not yet of commercial standard, this work has identified several important factors affecting the quality of PCC from the literature which have been verified with laboratory tests. Other phenomena observed during the experimental work have highlighted potential new promising research areas.

Based on this work, a number of conclusions can be made regarding both the technical and business aspects of the Slag2PCC process.

From a ***technical*** perspective,

- All five of the studied variables: initial temperature, calcium concentration, NH_4Cl solvent concentration, CO_2 flow and agitation speed have important effects on the carbonation process and the quality of the PCC produced.

- PCC particle size can be reduced by lower carbonation temperatures, lower calcium concentration, lower NH_4Cl concentration, lower CO_2 flow and higher agitation speed.

- All tests in both the laboratory and pilot plant produced particles that were too large to be used as commercial filler or coating PCC. These tests all displayed various degrees of particle agglomeration. High flows and concentrations of CO_2, as well as NH_4Cl are considered to be key factors increasing agglomeration behaviour based on findings from the experimental work and the literature.

- None of the PCC produced in either the laboratory or Slag2PCC plant produced PCC of sufficiently high SSA to be used as a filler or coating, most likely a consequence of the large particle size described above.

- The initial temperature, calcium concentration, NH_4Cl solvent concentration and calcium to carbonate ratio seem to be the most significant factors determining the crystal morphology in the Slag2PCC process. Exactly how the NH_4Cl solvent, more specifically NH_4^+, affects morphology has not been demonstrated experimentally in this work, but it has been shown in the literature to favour the rhombohedral form of calcite, as well as increase the formation of vaterite. While not studied here, pH is also likely to have an effect on morphology based on reports from the literature.

- The kinetics of the carbonation reaction are affected by ionic strength, temperature, CO_2 flow, and agitation speed. Increasing CO_2 and agitation speed increase the rate of carbonation due to the improved gas-liquid mass transfer. Temperature has a stronger effect during the nucleation process at the start of carbonation with lower temperatures increasing induction time (reducing nucleation rate). Higher ionic strength slows the rate of carbonation.

- Rhombohedral calcite has been produced using the Slag2PCC process at the laboratory scale in the temperature range 15-25°C, low-moderate agitation, low calcium concentration (0.04-0.05 M), quasi-stoichiometric $[Ca]_T/[CO_3]_T$ and with NH_4Cl in the range of 0.1-0.5 M.

- Aragonite can be produced from the Slag2PCC process at both laboratory and pilot scale with temperatures of 58°C and above, at moderate $[Ca^{2+}]$ (>0.2M), moderate-strong agitation, under conditions of excess calcium (CO_2CR of 0.01-0.028 min^{-1}) in the presence of 1M NH_4Cl.

- Attempts to produce scalenohedral calcite have not been successful on either the laboratory or the pilot scale, even under agitation, temperature and CO_2 flows reported to produce scalenohedral PCC in conventional carbonation. Instead, disclike vaterite was formed. Whether this would have transformed to calcite if left in solution longer, or whether the high $[Ca^{2+}]$ or $[NH_4Cl]$ stabilised the vaterite is unknown. However, scalenohedral PCC is known to have been produced from solutions containing high calcium and NH_4Cl concentrations thus it must be possible.

- Unlike in conventional carbonation of high solids $Ca(OH)_2$ slurries where the liquid supersaturation should remain essentially constant throughout most of the process, supersaturation will gradually decrease in Slag2PCC carbonation due to the consumption of Ca^{2+} which is not replaced by dissolving solids. The impact of this on PCC morphology and growth should be further studied.

- The calcium concentration can be maximised during the extraction step by optimising SLR. Assuming sufficient solvent is available, a higher SLR during extraction will give a higher final calcium concentration for carbonation, providing this increase in SLR does not result in a commensurate drop in extraction efficiency.

- The concentration of NH_4Cl solvent is a critical parameter in the Slag2PCC process as it impacts the process in many ways:
    - Higher concentrations increase the solubility of PCC
    - Higher concentrations reduce the solubility of CO_2
    - Excess unreacted NH_4Cl from extraction reduces the pH of the carbonation solution
    - Higher concentrations slow down carbonation kinetics
    - The ammonia may bind with excess calcium to form complexes ($CaNH_3^{2+}$, $Ca(NH_3)_2^{3+}$) or react with HCO_3^- to form carbamate, whose effects on the carbonation process are still not understood
    - NH_4^+ affects PCC morphology and agglomeration behaviour
    - Higher concentrations lead to higher NH_3 losses
    - PCC agglomerate strength may be increased

- Carbonation should be stopped in the pH range of 7-8 to maximise calcium conversion and prevent dissolution of PCC. The exact optimum will depend on the carbonation specific temperature, solvent and calcium concentrations used and requires further modelling and test work to define exactly. The inverse of CO_2CR can provide a rough estimate of the time required to add the stoichiometric requirement of CO_2 (taking into account expected CO_2 conversion) as stopping carbonation at an arbitrarily high pH may mean that insufficient CO_2 will be added.

- Stopping the carbonation reaction at a specific pH may prove challenging when CO_2 is in excess as dispersed and built-up dissolved CO_2 will continue to react and reduce the solution pH even after gas flow has ceased. In these cases the best option may be to stop gas flow at a higher pH (based on experience) and continue agitation until dissolved CO_2 is consumed and equilibrium reached at the final target pH value.

- Activity coefficients should be taken into account in any future modelling work as at the very least, including the effect of activity appears to result in a reduced pH stability window for $CaCO_3$ with PCC dissolving at a higher pH than would be expected.

- A detailed equilibrium model of the Slag2PCC process should be developed incorporating non-ideal solution thermodynamics and activity coefficient estimation. It should also include carbamic species as well as calcium-ammonia complexes. The activity coefficient calculations should then be combined with mass transfer, reaction kinetics and population balance modelling to develop a rigorous dynamic model of the Slag2PCC process. This could be used to better understand the process, study dynamic species concentrations, supersaturation, and would be crucial for the chemical engineering design of a full-scale demonstration PCC plant.

- Removing residual HCO_3^- ions in the solution after carbonation by mixing with some fresh Ca-rich solution left aside in the second reactor will most likely produce PCC with different quality parameters than then main PCC product. The effect of this on overall product quality will need to be considered if the two are combined.

- Carbonation at low-temperature (<5°C) followed by mixing with fresh Ca-rich solution may be a promising new area of research as a method of producing PCC with significant potential advantages.

- The PCC industry seems to use the sedimentation method (sedigraph) for analysing PSD, rather than laser diffraction. This is evident from the PCC product brochures acquired and from discussions with Prof. Thaddeus Maloney. This method reportedly gives particle sizes about half that of laser diffraction and this needs to be kept in mind when comparing Malvern PSD results with quoted literature and commercial product PSD data which is often produced using a sedigraph.

- The CO_2 emissions from the Slag2PCC process are estimated as -229 kg CO_2/t PCC, thus the Slag2PCC process sequesters more CO_2 than it produces. Replacing one tonne of conventional PCC (1040 kg CO_2/t PCC) with one tonne of Slag2PCC would therefore reduce net CO_2 emissions by 1.27 t CO_2/t PCC.

From the ***business*** perspective of the Slag2PCC process,

- There is a significant market for PCC globally (~16Mtpy) and within Finland (~550,000 tpy) and thus significant potential for the Slag2PCC process.

- The focus of the Slag2PCC process should primarily be those slag wastes which are currently stored or landfilled and which cannot be used to reduce CO_2 emissions in another industry. The worldwide supply of these slags (approximately 13% BOF slag and EAF slag) has been

estimated as 25 Mtpy which, if all the calcium could be recovered, could be used to produce 19 Mtpy PCC and sequester 8.4Mtpy CO_2.

- The cost of producing PCC using the Slag2PCC process has been estimated from the pilot plant data at 65 €/t PCC when the Slag2PCC plant is located at a steel mill and PCC is transported to a consumer 200km away. The major costs are heating (42%) and electricity (29%), followed by the solvent (14%) and PCC transport (14%). The cost of producing PCC can be minimised by maximising calcium extraction efficiency, running at higher SLR, being able to use coarser slag, minimising carbonation and extraction times, minimising solvent losses and minimising carbonation temperature.

- The economics of the Slag2PCC process are heavily dependent on the location of the slag producer and the PCC consumer. If slag is transported to the PCC consumer and produced at a Slag2PCC plant on-site, slag purchase and transport costs are significant but PCC transport costs are negligible. On the other hand if the Slag2PCC plant is located at the steel mill then slag transport costs are negligible but PCC transport costs are significant. From a cost point of view it is more favourable that the Slag2PCC be owned by and built at the steel plant as this reduces the cost of PCC production by approximately 40%.

- The decision on what PCC product quality to be targeted by the Slag2PCC process should be made considering the limitations (technical and economic) of the Slag2PCC process as well as the local PCC-consuming industries. Given that the estimated PCC cost (with many factors excluded) is approaching the price range of bulk filler PCC from satellite plants, it may be more favourable to target a higher value PCC grade from the Slag2PCC process, such as paper coating PCC, nano-sized PCC or products for the pharmaceutical or plastics industry.

- The cost of CO_2 capture using the Slag2PCC process is estimated as 284 €/t CO_2. However, if the PCC can be sold at 120 €/t PCC the cost of CO_2 capture becomes -239 €/t CO_2 i.e. the capture of carbon is profitable.

- The pulp and paper industry may not be the most favourable market for PCC from this process due to the strong cost competitiveness of satellite PCC plants which often lock pulp and paper mills into long-term contracts to buy their PCC.

11 Recommendations

Based on the findings of the literature review, modelling and experimental work undertaken as part of this thesis, a number of recommendations have been made. These pertain specifically to future research work that should be undertaken, the pilot plant design, as well as the development of the Slag2PCC process in general.

The recommendations for ***future research work*** are:

- Tests should be performed to investigate the effect of PCC sample preparation (washing with DI water, filtration, analysis delay) and analysis method (laser diffraction, sedigraph) on the results for PSD as this is a critical quality parameter and there should be confidence in future experimental work that the analysis for PSD is compatible with commercially-used analysis

- A study should be undertaken to confirm the accuracy and validity of the complexometric titration method for Ca^{2+} analysis, especially in the presence of NH_4Cl, by comparing [Ca^{2+}] results from a standard set of samples of known [Ca^{2+}] (determined via a more accurate method such as ICP-AES or atomic absorption spectrometry (AAS)) at various [Ca^{2+}] and [NH_4Cl] levels. Both complexometric procedures outlined in Appendix A (with and without NH_3 removal) should be tested to see which gives the most accurate results. This procedure could then be standardised and used confidently as a low-cost method of in-house calcium analysis for the development of the Slag2PCC process.

- Conductivity measurement should be included and tested in further carbonation experiments to determine if it can be used to infer the completion of carbonation even in the presence of a high NH_4Cl solvent concentration.

- In the search to produce scalenohedral PCC from the Slag2PCC process, the following carbonation experiments should be performed in the laboratory as a first step,
    a) A conventional $Ca(OH)_2$ slurry carbonation according to conditions given by Kroc & Fairchild [142] to confirm basic production of scalenohedral PCC according to the standard method
    b) Experiment (a) above repeated but with the addition of 0.01, 0.1, 0.5 and 1M NH_4Cl to observe how the PCC morphology is affected
    c) The 45°C laboratory test to produce scalenohedral PCC should be repeated with [Ca^{2+}]=0.3, however, several PCC samples should be taken and left in the mother solution for 1h, 6h, 24h before being filtered, while a second set should be filtered straight away and left in DI water for 1hr, 6h, and 24h. This would be to identify if the transition to calcite is effected by [Ca^{2+}] and [NH_4^+] rich environment.
    d) The 45°C laboratory test should be repeated but with a target calcium concentration of 1M, giving total calcium equivalent to a 7.6 wt% solution of $Ca(OH)_2$ to identify if the higher concentration produces scalenohedral PCC
    e) The 45°C laboratory test should be repeated but with a target calcium concentration of 0.02M, giving total calcium equivalent to a saturated solution of $Ca(OH)_2$ to identify if the lower concentration produces scalenohedral PCC

- The low-temperature (<5°C) carbonation route outlined in section 7.2.1 should be further investigated as it may lead to a new method of combined inverse carbonation offering a way to produce small particles with a very narrow PSD and simpler control of morphology. No examples in the literature could be found of such a process and it may be patentable.

- Tests should be done to confirm how CO_2 concentration impacts on particle agglomeration behaviour by performing carbonations with various N_2-diluted concentrations of CO_2 (e.g. 100%, 50%, 20%, 10%) and measuring PSD. Similar tests should also be done for NH_4Cl.

- Calcium extraction tests should be performed at varying SLRs, but using extraction solutions with [NH_4Cl] at the minimum calculated level (equation (7.7)) to ensure that insufficient solvent does not affect the results and confirm whether the 2:1 ratio is necessary.

- Ultrasonic agitation should be further investigated for the extraction of calcium from steel slag as a method of greatly improving calcium extraction efficiency, increasing the maximum calcium concentration achievable, and greatly improving the overall economics of the Slag2PCC process.

- Tests should be done with a dispersant such as sodium or ammonium metaphosphate (preferably ammonium to prevent adding Na^+ into the system) to see if this is a viable option for preventing agglomeration in the Slag2PCC process in the presence of NH_4Cl.

- Studies should be undertaken into the other PCC-consuming industries, starting with Finland, to determine which types of PCC and quality requirements are needed by these industries as they may be easier markets to enter.

- Linear crystal growth and nucleation rate experiments should be performed for the Slag2PCC process using either batch or continuous experiments under several NH_4Cl concentrations and temperatures so that the effects of these parameters can also be studied.

- Tests should be completed in the pilot plant to see how the extraction and carbonation processes are affected as the solvent is recycled. Samples could be taken of the liquid to monitor how impurity concentrations build and NH_4^+ concentration falls.

- Tests should be done in the pilot plant using FTIR measurements during carbonation to determine the rates of CO_2 absorption and NH_3 loss at various gas flows, compositions and agitation speeds.

The following recommendations are made for the ***pilot plant design:***

- Dished bottoms should be installed on the ER and CR to improve mixing, solid suspension, and recovery of slag and PCC from the bottom of the reactor

- Baffles should be installed on all reactors to improve mixing and minimise vortex formation.

- In the ER, primarily axial-flow impellers should be installed to ensure the slag is completely suspended in solution and does not settle out in order to maximise extraction efficiency

- In the CR, an up-pumping axial-flow impeller should be used at the reactor bottom along with a down-pumping axial impeller at the top. This would help to increase the residence time of the gas bubbles and lead to better CO_2 capture efficiency whilst ensuring full suspension of the PCC produced.

- The agitator motors for both reactors should be upgraded to allow higher mixing speeds and improve solids suspension, particularly in the ER if the above improvements are not sufficient.

- If laboratory-scale experimental work shows that conductivity measurement provides useful information on the carbonation reaction, even in the presence of the strong NH_4Cl solvent, a conductivity probe should be installed at least on the primary CR so that the benefits of conductivity measurement can be trialled at the pilot scale.

- The filtration system should be modified so that all Ca-rich or carbonated solution can be recovered easily under either batch or continuous operation, i.e. without significant vessel void volumes.

- A new line should be considered between PCC Filter 1 and Tank 1 so that Ca-rich solution can be more easily recirculated through HX1 when the Ca-rich solution is heated. Alternatively, extraction could be performed at a higher temperature so that the solution is already warm when it enters the CR. This would have the added benefit of improving the filtration rate of the slag after extraction due to the lower viscosity. Alternatively, including an internal resistive heating element for CR1 rather than using HX1 should be considered if heating is desired. This would deliver heat more effectively to the solution, minimise heat losses through pipework, allow high-temperature tests to be conducted year-round and be a potentially cheaper option than buying a standalone electrical boiler and insulating the interconnecting pipework. A good position for the element would be below the level of the agitator for safety, as well as heat transfer reasons.

And finally, recommendations for the **development** of the Slag2PCC process:

- The use of alternative technologies to evaporation for recovering the NH_4Cl solvent should be seriously considered, including membrane separation and ion exchange, as evaporation of wash water will seriously erode or even negate the economic and environmental benefits of the Slag2PCC process.

- Consider using the magnetic properties of steel slag as a way to separate PCC from residual slag particles, particularly if precipitation of PCC in the extraction reactor becomes a problem.

- The extraction reaction should be conducted in a closed environment not open to the atmosphere. This will minimise NH_3 losses from solution at high pH by providing an NH_3 partial pressure in the gas phase. This would need to be done carefully as the air displaced from the reactor during the addition of slag can cause air backflow problems in the slag feeding system if there is no way for it to escape.

- If pure CO_2 is used for carbonation, this could also be conducted in a closed, pressurised environment to increase the solubility of CO_2 and prevent stripping of NH_3 from solution by the flow of excess CO_2. A sustained rise in vessel pressure could be used to indicate when the

CO_2 addition rate is higher than the rate at which it could be absorbed into solution and flow should be reduced. If flue gases are used for carbonation then a CO_2 flow meter on the CR outlet could be used to monitor and regulate the flow of carbonating gas. This would maximise CO_2 conversion efficiency and minimise flue gas compression costs because every litre of CO_2 leaving the carbonation reactor not converted to PCC represents ~5L of unnecessarily compressed inert gas

- Rather than trying to mimic existing processes and produce standard PCC grades from the Slag2PCC process, it may be better to look at the unique conditions of the Slag2PCC process itself and take advantage of the types of crystals it can produce to see if a new kind of PCC can be developed with particular advantages for industry. The NH_4Cl solvent for example, appears to result in very strong crystal agglomerates. This may be a beneficial property in the paper industry, as some literature has reported. Alternatively, it was reported that microcrystals (<100nm) can be produced in solutions containing NH_4^+ when CO_3^{2-} is in excess, thus this may be another option.

12 References

[1] World Steel Association, March 2013. [Online]. Available: http://www.worldsteel.org/dms/internetDocumentList/bookshop/Steel-s-Contribution-to-a-Low-Carbon-Future-/document/Steel%27s%20Contribution%20to%20a%20Low%20Carbon%20Future%20.pdf. [Accessed 1 Feb 2014].

[2] Geological Survey of Finland, "Metals and minerals production 2011-2013," Geological Survey of Finland, 24 April 2014. [Online]. Available: http://en.gtk.fi/informationservices/mineralproduction/finmipr1115.html. [Accessed 19 May 2014].

[3] Statistics Finland, "Greenhouse Gas Emissions in Finland 1990-2011: Draft National Inventory Report under the UNFCCC and the Kyoto Protocol," 2013. [Online]. Available: http://www.stat.fi/tup/khkinv/fin_nir_2011_2013_01_15.pdf. [Accessed 15 Jan 2014].

[4] H. P. Matilla and R. Zevenhoven, "Production of precipitated calcium carbonate from steel converter slag and other calcium-containing industrial wastes and residues," *in Advances in Inorganic Chemistry Volume 66, Chapter 6,* 2013.

[5] A. Said, H. P. Mattila, M. Järvinen and R. Zevenhoven, "Production of precipitated calcium carbonate (PCC) from steelmaking slag for fixation of CO_2," *Applied Energy,* vol. 112, p. 765—771, 2013.

[6] Statistics Finland, "Industrial statistics, 2012," Statistics Finland, 2014 April 15. [Online]. Available: http://www.stat.fi/tup/suoluk/suoluk_teollisuus_en.html. [Accessed 14 May 2014].

[7] European Slag Association & European Steel Association , "Position Paper on the Status of Ferrous Slag," April 2012. [Online]. Available: http://www.euroslag.com/fileadmin/_media/images/Status_of_slag/Position_Paper_April_2012.pdf . [Accessed 16 June 2014].

[8] S. Eloneva, S. Teir, J. Salminen, C. J. Fogelhom and R. Zevenhoven, "Steel Converter Slag as a Raw Material for Precipitation of Pure Calcium Carbonate," *Industrial & Engineering Chemistry Research,* vol. 47, no. 18, pp. 7104-7111, 2008.

[9] World Steel Association, "Fact sheet - Steel Industry Byproducts," February 2010. [Online]. Available: https://www.worldsteel.org/dms/internetDocumentList/fact-sheets/Fact-sheet_By-products/document/Fact%20sheet_By-products.pdf. [Accessed 26 July 2014].

[10] Nippon Slag Association, 2003. [Online]. Available: http://www.slg.jp/e/slag/character.html. [Accessed 4 Feb 2014].

[11] D. W. Lewis, "Properties and uses of iron and steel slags," in *Symposium on Slag, National Institute for Transport and Road Research South Africa*, 1982.

[12] S. Teir, “Fixation of carbon dioxide by producing calcium carbonate from minerals and steelmaking slags,” PhD Thesis, Aalto University, Espoo, 2008.

[13] S. Teir, S. Eloneva, C. J. Fogelholm and R. Zevenhoven, “Dissolution of steelmaking slags in acetic acid for precipitated calcium carbonate production,” *Energy,* vol. 32, pp. 528-539, 2007.

[14] M. M. Reddy and G. H. Nancollas, “The Crystallization of Calcium Carbonate I: Isotopic Exchange and Kinetics,” *Journal of Colloid and Interface Science,* vol. 36, no. 2, pp. 166-172, 1971.

[15] Y. S. Han, G. Hadiko, M. Fuji and M. Takahashi, “Effect of flow rate and CO_2 content on the phase and morphology of $CaCO_3$ prepared by bubbling method,” *Journal of Crystal Growth,* vol. 276, pp. 541-548, 2005.

[16] E. Lehtinen, Ed., *Papermaking Science and Technology,* vol. 11: Pigment Coating and Surface Sizing of Paper, Helsinki: Fapet Oy, 2000, pp. 54,61,141-149.

[17] M. J. O'Neil, Ed., “Lime and limestone,” *in The Merck Index,* 13th ed., London, Wiley, 2001.

[18] D. Chakraborty, V. K. Agarwal, S. K. Bhatia and J. Bellare, “Steady-state Transitions and Polymorph Transformations in Continuous Precipitation of Calcium Carbonate,” *Industrial & Engineering Chemistry Research,* vol. 33, no. 9, pp. 2187-2197, 1994.

[19] M. Ukrainczyk, J. Kontrec and D. Kralj, “Precipitation of different calcite crystal morphologies in the presence of sodium stearate,” *Journal of Colloid and Interface Science,* vol. 329, pp. 89-96, 2009.

[20] H. Nebel, M. Neumann, C. Mayer and M. Epple, “On the structure of amophous calcium carbonate - A detailed study by solid-state NMR spectroscopy,” *Inorganic Chemistry,* vol. 47, no. 17, pp. 7874-7879, 2008.

[21] IMA Europe, “Calcium carbonate,” IMA Europe, [Online]. Available: http://www.ima-europe.eu/about-industrial-minerals/industrial-minerals-ima-europe/calcium-carbonate. [Accessed 14 Feb 2014].

[22] The European Calcium Carbonate Association, “Mineral Applications,” [Online]. Available: http://www.cca-europe.eu/mineral-applications.html. [Accessed 7 Feb 2014].

[23] P. Stratton, “An overview of the North American calcium carbonate market,” October 2012. [Online]. Available: http://www.roskill.com/news/download-roskills-paper-on-the-north-american-calcium-carbonate-market. [Accessed 11 March 2014].

[24] S. Eloneva, “Reduction of CO_2 emissions by mineral carbonation: steelmaking slags as raw material with a pure calcium carbonate end product,” PhD Thesis, Aalto University, Helsinki, 2010.

[25] T. Maloney, *Meeting between T. Maloney, A. Said and W. Zappa,* Helsinki, 5 June 2014.

[26] C. Nover, *Private email communication (Schaefer Kalk),* Helsinki, February 10 2014.

[27] Specialty Minerals Inc., "Albacar® Precipitated Calcium Carbonate (PCC) Family," 2012. [Online]. Available: http://www.specialtyminerals.com/paper/products-and-applications-for-paper/paper-applications/albacar-pcc-family/. [Accessed 28 Jan 2014].

[28] W. M. Jung, S. H. Kang, W. S. Kim and C. K. Choi, "Particle morphology of calcium carbonate precipitated by gas-liquid reaction in a Couette-Taylor reactor," *Chemical Engineering Science,* vol. 55, pp. 733-747, 2000.

[29] J. Chen and L. Xiang, "Controllable synthesis of calcium carbonate polymorphs at different temperatures," *Powder Technology,* vol. 189, pp. 64-69, 2009.

[30] H. Holik, Ed., *Handbook of Paper and Board,* 2nd ed., vol. 1, Weinheim: Wiley-VCH Verlag GmbH & Co. KGaA, 2013, p. 110.

[31] J. A. Oates, *Lime and Limestone: Chemistry and Technology, Production and Uses,* Weinheim: Wiley-VCH, 1998, p. 353.

[32] J. A. Kosin and C. R. Andrews, "Process for producing calcium carbonate and products thereof". United States Patent 4888160, 19 December 1989.

[33] Specialty Minerals Inc., "Specialty Minerals Precipitated Calcium Carbonate (PCC) Satellite Plants," 2012. [Online]. Available: http://www.specialtyminerals.com/paper/paper-pcc-production-facilities/paper-pcc-satellite-plants/. [Accessed 5 Feb 2014].

[34] P. A. Ciullo, *Industrial minerals and their uses: a handbook and formulary,* New Jersey: Noyes, 1997, pp. 161-195.

[35] R. Alén, Ed., *Papermaking Science and Technology, Book 4: Papermaking Chemistry,* 2nd ed., Helsinki: Paperi ja Puu Oy, 2007, p. 75.

[36] M. Skrzypczak, M. Maurer and T. Schmölzer, "Process for the production of precipitated calcium carbonate, precipitated calcium carbonate and uses thereof". European Union Patent 2537900, 27 December 2012.

[37] R. W. Hagemeyer, "Pigment Coating," *in Pulp and Paper: Chemistry and Chemical Technology,* 3rd ed., vol. IV, J. P. Casey, Ed., New York, John Wiley & Sons, Inc., 1983, pp. 2013-2189.

[38] European Commission, "Integrated Pollution Prevention and Control: Reference Document on Best Available Techniques for the Manufacture of Large Volume Inorganic Chemicals - Solids and Others Industry," August 2007. [Online]. Available: http://eippcb.jrc.ec.europa.eu/reference/lvic-aaf.html. [Accessed 5 April 2014].

[39] Specialty Minerals Inc., "Specialty Minerals Precipitated Calcium Carbonates in Sealants and Adhesives," 2012. [Online]. Available: http://www.specialtyminerals.com/specialty-applications/specialty-markets-for-minerals/adhesives-and-sealants/pccs-for-sealants/.

[40] Specialty Minerals Inc., “Specialty Minerals Products for Plastics,” 2012. [Online]. Available: http://www.specialtyminerals.com/specialty-applications/specialty-markets-for-minerals/plastics/.

[41] Y. Sheng, B. Zhou, J. Zhao, N. Tao, K. Yu, Y. Tian and Z. Wang, “Influence of octadecyl dihydrogen phosphate on the formation of active super-fine calcium carbonate,” *Journal of Colloid and Interface SCience,* vol. 272, pp. 326-329, 2004.

[42] Specialty Minerals Inc., “Personal Care Products,” 2012. [Online]. Available: http://www.specialtyminerals.com/specialty-applications/specialty-markets-for-minerals/personal-care-and-cosmetics/.

[43] Specialty Minerals Inc., “Specialty Minerals Precipitated Calcium Carbonates In Pharmaceuticals,” 2012. [Online]. Available: http://www.specialtyminerals.com/specialty-applications/specialty-markets-for-minerals/pharmaceuticals/.

[44] G. A. Smook, *Handbook for Pulp & Paper Technologists,* 3rd ed., Vancouver: Angus Wilde Publications Inc., 2002, p. 223.

[45] P. Svending, C. Nutbeem and I. Elliott, “Mineral filler solutions for cost and quality enhancement in graphic papers,” 2010. [Online]. Available: http://www.imerys-paper.com/pdf/mineral_filler_solutions_for_cost_and_quality_enhancement_in_graphic_papers.pdf. [Accessed 28 Jan 2014].

[46] J. M. Rodriguez, K. Snowden and K.-T. Wu, “Acid tolerant calcium carbonate composition and uses therefor”. Europe Patent EP0886626A1, 30 December 1998.

[47] K. Koivunen and H. Paulapuro, “Papermaking potential of novel structure PCC fillers with enhanced refractive index,” *TAPPI Journal,* no. January, pp. 4-12, 2010.

[48] European Commission, “Omya/Huber PCC,” 19 July 2006. [Online]. Available: http://ec.europa.eu/competition/mergers/cases/decisions/m3796_20060719_20600_en.pdf. [Accessed 2 August 2014].

[49] Specialty Minerals Inc., “Specialty Minerals Precipitated Calcium Carbonate (PCC) Products for Paper,” 2012. [Online]. Available: http://www.specialtyminerals.com/paper/products-and-applications-for-paper/. [Accessed 28 Jan 2014].

[50] H. P. Mattila, I. Grigaliūnaitė and R. Zevenhoven, “Chemical kinetics modeling and process parameter sensitivity for precipitated calcium carbonate production from steelmaking slags,” *Chemical Engineering Journal,* vol. 192, pp. 77-89, 2012.

[51] M. Ukrainczyk, J. Kontrec, V. Babić-Ivančić, L. Brečević and D. Kralj, “Experimental design approach to calcium carbonate precipitation in a semicontinuous process,” *Powder Technology,* vol. 171, no. 3, pp. 192-199, 2007.

[52] Specialty Minerals Inc., “Precipitated Calcium Carbonate (PCC) Chemical & Physical Properties,” SMI, 2012. [Online]. Available: http://www.specialtyminerals.com/paper/pcc-pigments/features-of-pcc/pcc-morphology-comparison/. [Accessed 29 March 2014].

[53] Specialty Minerals Inc., “Functions of Precipitated Calcium Carbonate (PCC) Fillers,” 2012. [Online]. Available: http://www.specialtyminerals.com/paper/pcc-pigments/functions-of-pcc. [Accessed 27 January 2014].

[54] R. Brown, in *PIRA International Conference on the Use of Minerals in Papermaking*, Manchester, 1997.

[55] Y. Nanri, H. Konno, H. Goto and K. Takahashi, “A new process to produce high-quality PCC by the causticizing process in a kraft pulp mill,” *TAPPI Journal,* pp. 19-24, May 2008.

[56] M. Hubbe, “Mini-Encyclopedia of Papermaking Wet-End Chemistry - Precipitated Calcium Carbonate (PCC),” n.d.. [Online]. Available: http://www4.ncsu.edu/~hubbe/PCC.htm. [Accessed 30 Mar 2014].

[57] Specialty Minerals Inc., “Precipitated Calcium Carbonate (PCC) Pigments,” 2012. [Online]. Available: http://www.specialtyminerals.com/paper/pcc-pigments/. [Accessed 28 Jan 2014].

[58] Specialty Minerals Inc., “Albafil® Precipitated Calcium Carbonate (PCC) Family,” 2012. [Online]. Available: http://www.specialtyminerals.com/paper/products-and-applications-for-paper/paper-applications/albafil-pcc-family/. [Accessed 28 Jan 2014].

[59] Speciality Minerals Inc., “Megafil® Precipitated Calcium Carbonate (PCC) Family,” 2012. [Online]. Available: http://www.specialtyminerals.com/paper/products-and-applications-for-paper/paper-applications/megafil-pcc-family/. [Accessed 28 Jan 2014].

[60] Specialty Minerals Inc., “Albaglos® Precipitated Calcium Carbonate (PCC) Family,” 2012. [Online]. Available: http://www.specialtyminerals.com/paper/products-and-applications-for-paper/paper-applications/albaglos-pcc-family/. [Accessed 28 Jan 2014].

[61] Specialty Minerals Inc., 2012. [Online]. Available: http://www.specialtyminerals.com/paper/products-and-applications-for-paper/paper-applications/opacarb-pcc-family/. [Accessed 28 Jan 2014].

[62] Specialty Minerals Inc., “SMI Products - MSDS and Technical Data Sheets,” 2012. [Online]. Available: http://www.mineralstech.com/corporate-responsibility/environmental-health-and-safety-ehs/material-safety-data-sheets/smi-products-msds-and-technical-data-sheets/. [Accessed 5 Feb 2014].

[63] R. Rohe, *Private email communication (Omya),* Helsinki, February 5 2014.

[64] W. Seifritz, “CO_2 disposal by means of silicates,” *Nature,* vol. 345, p. 486, June 1990.

[65] W. J. Huijgen, G. J. Witkamp and R. N. Comans, “Mineral CO_2 Sequestration by Steel Slag Carbonation,” *Environmental Sciance & Technology,* vol. 39, no. 24, pp. 9676-9682, 2005.

[66] K. S. Lackner, C. H. Wendt, D. P. Butt, E. L. Joyce and D. H. Sharp, “Carbon dioxide disposal in carbonate minerals,” *Energy,* vol. 20, no. 11, pp. 1153-1170, 1995.

[67] J. Sipilä, S. Teir and R. Zevenhoven, “Carbon dioxide sequestration by mineral carbonation: Literature review update 2005-2007,” Turku, 2008.

[68] N. Pardo, J. A. Moya and K. Vatopoulos, “Prospective Scenarios on Energy Efficiency and CO2 Emissions in the EU Iron & Steel Industry,” 2012.

[69] P. Mannisto, “Carbon dioxide capture from flue gases based on calcium-rich ammonium salt solutions: Escape of ammonia vapour and quality of calcium carbonate precipitate,” Espoo, 2010.

[70] H. P. Mattila, H. Hudd and R. Zevenhoven, “Cradle-to-gate life cycle assessment of precipitated calcium carbonate,” *Journal of Cleaner Production,* vol. Article in press, 2014.

[71] H. P. Mattila, “Steelmaking slag utilization for production of calcium carbonate ($CaCO_3$),” PhD Thesis, Åbo Akademi University, Turku, Finland, 2014.

[72] M. Kakizawa, A. Yamasaki and Y. Yanagisawa, “A new CO_2 disposal process via artificial weathering of calcium silicate accelerated by acetic acid,” *Energy,* vol. 26, no. 4, pp. 341-354, 2001.

[73] A. Said, H.-P. Mattila, C.-J. Fogelholm and R. Zevenhoven, “Effect of steelmaking slag properties to the extraction of calcium by using ammonium salts,” in *International Conference on Applied Energy*, Suzhou, China, 2012.

[74] P. Chen, C. Y. Tai and K. C. Lee, “Morphology and growth rate of calcium carbonate crystals in a gas-liquid-solid reactive crystallizer,” *Chemical Engineering Science,* vol. 52, no. 21-22, pp. 4171-4177, 1997.

[75] J. A. Dirksen and T. A. Ring, “Fundamentals of crystallization: Kinetic effects on particle size distributions and morphlogy,” *Chemical Enginering Science,* vol. 46, no. 10, pp. 2389-2427, 1991.

[76] J. W. Mullin, *Crystallization,* 4th ed., London: Butterworth-Heinemann, 2001, pp. 214,217.

[77] D. R. Lide, Ed., *CRC Handbook of Chemistry and Physics,* 85th ed., Boca Raton: CRC Press, 2005.

[78] A. Seidell, *Solubilities of Inorganic and Organic Substances: A compilation of quantitative solubility data from the periodical literature,* 2nd ed., New York: D. Van Nostrand Company, 1919.

[79] A. Findlay and B. Shen, “CLVI.—The influence of colloids and fine suspensions on the solubility of gases in water. Part II. Solubility of carbon dioxide and of hydrogen,” *Journal of the Chemical Society, Transactions,* vol. 101, pp. 1459-1468, 1912.

[80] B. Rumpf, H. Nicolaisen and G. Maurer, “Solubility of carbon dioxide in aqueous solutions of ammonium chloride at temperatures from 313 K to 433 K and pressures up to 10 MPa,” *Berichte der Bunsengesellschaft für physikalische Chemie,* vol. 98, no. 8, pp. 1077-1081, 1994.

[81] A. Yasunishi and F. Yoshida, “Solubility of carbon dioxide in aqueous electrolyte solutions,” *Journal of Chemical and Engineering Data,* vol. 24, no. 1, pp. 11-14, 1979.

[82] J. Franke and A. Mersmann, “The influence of the operation conditions on the precipitation process,” *Chemical Engineering Science,* vol. 50, no. 11, pp. 1737-1753, 1995.

[83] J. F. Zemaitis, D. M. Clark, M. Rafal and N. C. Scrivner, *Handbook of Aqueous Solution Thermodynamics,* Hoboken: John Wiley & Sons, 1986, pp. 54-59,71-75,94-95.

[84] A. Mersmann, Ed., *Crystallization Technology Handbook,* 2nd ed., Basel: Marcel Dekker Inc., 2001.

[85] A. Sarkar and S. Mahapatra, “Synthesis of All Crystalline Phases of Anhydrous Calcium Carbonate,” *Crystal Growth and Design,* vol. 10, p. 2129–2135, 2010.

[86] N. H. de Leeuw and S. C. Parker, “Surface Structure and Morphology of Calcium Carbonate Polymorphs Calcite, Aragonite, and Vaterite:,” *Journal of Physical Chemistry B,* vol. 102, pp. 2914-2922, 1998.

[87] C. Domingo, E. Loste, J. Gómez-Morales, J. Garciá-Carmona and J. Fraile, “Calcite precipitation by a high-pressure CO_2 carbontion route,” *Journal of Supercritical Fluids,* vol. 36, pp. 202-215, 2006.

[88] J. García-Carmona, J. G. Morales and R. R. Clemente, “Morphological control of precipitated calcite obtained by adjusting the electrical conductivity in the $Ca(OH)_2$–H_2O–CO_2 system,” *Journal of Crystal Growth,* vol. 249, no. 3-4, pp. 561-571, 2003.

[89] J. García Carmona, J. Gómez Morales and R. R. Clemente, “Rhombohedral–scalenohedral calcite transition produced by adjustingthe solution electrical conductivity in the system Ca(OH)–CO_2–H_2O,” *Journal of Colloid and Interface Science,* vol. 261, p. 434–440, 2003.

[90] N. H. de Leeuw and S. C. Parker, “Surface Structure and Morphology of Calcium Carbonate Polymorphs Calcite, Aragonite and Vaterite: an Atomistic Approach,” *Journal of Physical Chemistry B,* vol. 102, no. 16, pp. 2914-2922, 1998.

[91] W. Sekkal and A. Zaoui, “Nanoscale analysis of the morphology and surface stability of calcium carbonate polymorphs,” *Scientific Reports,* vol. 3, no. 1587, 2013.

[92] D. Chakraborty and S. K. Bhatia, “Formation and Aggregation of Polymorphs in Continuous Precipitation. 2. Kinetics of $CaCO_3$ Precipitation,” *Industrial & Engineering Chemistry Research,* vol. 35, no. 6, pp. 1995-2006, 1996.

[93] S. Knez, D. Klinar and J. Golob, “Stabilization of PCC dispersions prepared directly in the mother-liquid after synthesis through the carbonation of (hydrated) lime,” *Chemical Engineering Science,* vol. 61, p. 5867 – 5880, 2006.

[94] D. R. Skuse, S.-R. T. Chen, W. L. Garforth and G. R. Matz, “Dispersing agents and their use”. United States of America Patent 6,315,867 B1, 13 November 2001.

[95] Outotec, “HSC Chemistry 5,” Outotec, [Online]. Available: http://www.outotec.com/en/Products--services/HSC-Chemistry/.

[96] A. De Visscher and J. Vanderdeelen, “Estimation of the Solubility Constant of Calcite, Aragonite, and Vaterite at 25°C Based on Primary Data Using the Pitzer Ion Interaction Approach,” *Monatshefte für Chemie,* vol. 134, p. 769–775, 2003.

[97] C. E. Harvie, N. Moller and J. H. Weare, “The prediction of mineral solubilities in natural waters: The Na-K-Mg-Ca-H-Cl-SO_4-OH-HCO_3-CO_3-CO_2-H_2O system to high ionic strengths at 25°C,” *Geochimica et Cosmochimica Acta,* vol. 48, pp. 723-751, 1984.

[98] F. Mani, M. Peruzzini and P. Stoppioni, “CO_2 absorption by aqueous NH_3 solutions: speciation of ammonium carbamate, bicarbonate and carbonate by a 13C NMR study,” *Green Chemistry,* vol. 8, pp. 995-1000, 2006.

[99] D. Gómez-Díaz, J. M. Navaza and B. Sanjurjo, “Analysis of mass transfer in the precipitation process of calcium carbonate using a gas/liquid reaction,” *Chemical Engineering Journal,* vol. 116, pp. 203-209, 2006.

[100] V. A. Juvekar and M. M. Sharma, “Absorption of CO_2 in a suspension of lime,” *Chemical Engineering Science,* vol. 28, pp. 825-837, 1973.

[101] M. Vučak, J. Perić, A. Žmikić and M. N. Pons, “A study of carbon dioxide absorption into aqueous monoethanolamine solution containing calcium nitrate in the gas-liquid reactive precipitation of calcium carbonate,” *Chemical Engineering Journal,* vol. 87, pp. 171-179, 2002.

[102] L. Xiang, Y. Xiang, Y. Wen and F. Wei, “Formation of $CaCO_3$ nanoparticles in the presence of terpineol,” *Materials Letters,* vol. 58, no. 6, pp. 959-965, 2004.

[103] X. Wang, W. Conway, R. Burns, N. McCann and M. Maeder, “Comprehensive Study of the Hydration and Dehydration Reactions of Carbon Dioxide in Aqueous Solution,” *J. Phys. Chem. A,* vol. 114, p. 1734–1740, 2010.

[104] G. H. Nancollas and M. M. Reddy, “The Crystallization of Calcium Carbonate II: Calcite Growth Mechanism,” *Journal of Colloid and Interface Science,* vol. 37, no. 4, pp. 824-830, 1971.

[105] W. P. Inskeep and P. R. Bloom, “An evaluation of rate equations for calcite precipitation kinetics at pCO_2 less than 0.01 atm and pH greater than 8,” *Geochimica et Cosmochimica Acta,* vol. 49, pp. 2165-2180, 1985.

[106] C. W. Davies and A. L. Jones, “The precipitation of silver chloride from aqueous solutions. Part 2-Kinetics of growth of seed crystals,” *Transactions of the Faraday Society,* vol. 51, pp. 812-817, 1955.

[107] L. N. Plummer, T. M. Wigley and D. L. Parkhurst, “The kinetics of calcite dissolution in CO_2-water systems at 5° to 60°C and 0.0 to 1.0 atm CO_2,” *American Science Journal,* vol. 278, pp. 179-216, 1978.

[108] L. C. Nielsen, J. J. De Yoreo and D. J. DePaolo, “General model for calcite growth kinetics in the presence of impurity ions,” *Geochimica et Cosmochimica Acta,* vol. 115, pp. 100-114, 2013.

[109] J. Garside, A. Mersmann and J. Nyvlt, Eds., *Measurement of Crystal Growth and Nucleation Rates,* 2nd ed., Rugby: Institution of Chemical Engineers (IChemE), 2002, p. 169.

[110] C. Y. Tai, P.-C. Chen and S.-M. Shih, “Size-Dependent Growth and Contact Nucleation of Calcite Crystals,” *AIChE Journal,* vol. 39, no. 9, pp. 1472-1482, 1993.

[111] Y. Kotaki and H. Tsuge, “Reactive crystallization of calcium carbonate in a batch crystallizer,” *Journal of Crystal Growth,* vol. 99, pp. 1092-1097, 1990.

[112] I. Puigdomenech, “Chemical Equilibrium Diagrams: MEDUSA and HYDRA Software v.2,” 2013. [Online]. Available: https://sites.google.com/site/chemdiagr/home.

[113] H. C. Helgeson, D. H. Kirkham and G. C. Flowers, “Theoretical prediction of the thermodynamic behavior of aqueous electrolytes by high pressures and temperatures; IV, Calculation of activity coefficients, osmotic coefficients, and apparent molal and standard and relative partial molal properties,” *American Journal of Science,* vol. 281, no. 10, pp. 1249-1516, 1981.

[114] M. Kitamura, H. Konno, A. Yasuia and H. Masuoka, “Controlling factors and mechanism of reactive crystallization of calcium carbonate polymorphs from calcium hydroxide suspensions,” *Journal of Crystal Groth,* vol. 236, pp. 323-332, 2002.

[115] S. Kodama, T. Nishimoto, N. Yamamoto, K. Yogo and K. Yamada, “Development of a new pH-swing CO2> mineralization process with a recyclable reaction solution,” *Energy,* vol. 33, pp. 776-784, 2008.

[116] B. Feng, A. K. Yong and H. An, “Effect of various factors on the particle size of calcium carbonate formed in a precipitation process,” *Materials Science and Engineering A,* Vols. 445-446, pp. 170-179, 2007.

[117] Y. Sun, M. S. Yao, J. P. Zhang and G. Yang, “Indirect CO_2 mineral sequestraion by steelmaking slag with NH_4Cl as leaching solution,” *Chemical Engineering Journal,* vol. 173, pp. 437-445, 2011.

[118] Z. Hu and Y. Deng, “Synthesis of needle-like aragonite from calcium chloride and sparingly dissoluble magnesium carbonate,” Atlanta, Georgia, 2002.

[119] C. Y. Tai and F.-. B. Chen, "Polymorphism of $CaCO_3$ Precipitated in a Constant-Composition Environment," *AIChE Journal,* vol. 44, no. 8, pp. 1790-1798, 1998.

[120] J. Hostomsky and A. G. Jones, "Calcium carbonate crystallization, agglomeration and form during continuous precipitation from solution," *Journal of Physics D: Applied Physics,* vol. 24, no. 2, pp. 165-170, 1991.

[121] R. Agnihotri, S. K. Mahuli, S. S. Chauk and L. S. Fan, "Influence of surface modifiers on the structure of precipitated calcium carbonate," *Industrial & Engineering Chemistry Research,* vol. 38, pp. 2283-2291, 1999.

[122] S. H. Wei, S. K. Mahuli, R. Agnihotri and L. S. Fan, "High Surface Area Calcium Carbonate: Pore Structural Properties and Sulfation Characteristics," *Industrial & Engineering Chemistry Research,* vol. 36, no. 6, pp. 2141-2148, 1997.

[123] T. Jung, W.-S. Kim and C. K. Choi, "Effect of monovalent salts on morphology of calcium carbonate crystallized in Couette-Taylor reactor," *Crystal Research and Technology,* vol. 40, no. 6, p. 586–592, 2005.

[124] A. M. López-Periago, R. Pacciani, C. García-González, L. F. Vega and C. Domingo, "A breakthrough technique for the preparation of high-yield precipitated calcium carbonate," *Journal of Supercritical Fluids,* vol. 52, pp. 298-305, 2010.

[125] A. G. Jones, J. Hostomsky and Z. Li, "On the effect of liquid mixing rate on primary crystal size during the gas-liquid precipitation of calcium carbonate," *Chemical Engineering Science,* vol. 47, no. 13/14, pp. 3817-3824, 1992.

[126] L. N. Plummer and E. Busenberg, "The solubilities of calcite, aragonite and vaterite in CO2-H2O solutions between 0 and 90°C, and an evaluation of the aqueous model for the system CaCO3-CO2-H2O," *Geochimica et Cosmochimica Acta,* vol. 46, pp. 1011-1040, 1982.

[127] J. H. Bang, Y. N. Jang, W. Kim, K. S. Song, C. W. Jeon, S. C. Chae, S. W. Lee, S. J. Park and M. G. Lee, "Specific surface area and particle size of calcium carbonate precipitated by carbon dioxide microbubbles," *Chemical Engineering Journal,* Vols. 198-199, pp. 254-260, 2012.

[128] M. Vučak, M. N. Pons, J. Perić and H. Vivier, "Effect of precipitation conditions on the morphology of calcium carbonate: quantification of crystal shapes using image analysis," *Power Technology,* vol. 97, pp. 1-5, 1998.

[129] J. Gómez-Morales, J. Torrent-Burgués, A. Lopez-Macipe and R. Rodríguez-Clemente, "Precipitation of calcium carbonate from solutions with varying Ca^{2+}/carbonate ratios," *Journal of Crystal Growth,* vol. 166, pp. 1020-1026, 1996.

[130] A. P. Collier, C. J. Hetherington and M. J. Hounslow, "Alignment mechanisms between particles in crystalline aggregates," *Journal of Crystal Growth,* vol. 208, no. 1-4, pp. 513-519, 2000.

[131] S. Varma, P. C. Chen and G. Unnikrishnan, “Gas-liquid reactive crystallization for the synthesis of CaCO3 nanocrystals,” *Materials Chemistry and Physics,* vol. 126, pp. 232-236, 2011.

[132] B. Cheng, M. Lei, J. Yu and X. Zhao, “Preparation of monodispersed cubic calcium carbonate particles via precipitation reaction,” *Materials Letters,* vol. 58, pp. 1565-1570, 2004.

[133] L. Xiang, Y. Xiang, Z. G. Wang and Y. Jin, “Influence of chemical additives on the formation of super-fine calcium carbonate,” *Powder Technology,* vol. 126, pp. 129-133, 2002.

[134] O. Söhnel and J. W. Mullin, “Precipitation of calcium carbonate,” *Journal of Crystal Growth,* vol. 60, p. 239—250, 1982.

[135] M. Pohl, C. Rainer and G. Primosch, “Process for obtaining precipitated calcium carbonate”. United States Patent 2013/0195748A1, 1 August 2013.

[136] J. Wenk, G. Saunders, M. Maurer and M. Skrzypczak, “Process for preparing scalenohedral precipitated calcium carbonate”. Worlwide Patent 2013142473, 26 September 2013.

[137] D. R. Deutsch and K. J. Wise, “Process for the preparation of discrete particles of calcium carbonate”. United States Patent 6,294,143 B1, 25 September 2001.

[138] H. P. Mattila, *Private email communication,* Helsinki, March 11 2014.

[139] Minitab Inc., “Minitab® 16,” 2010. [Online]. Available: http://www.minitab.com/en-us/products/minitab/.

[140] G. E. Box, J. S. Hunter and W. G. Hunter, *Statistics for Experimenters: Design, Innovation, and Discovery,* 2nd ed., New Jersey: John Wiley & Sons, Inc., 2005, pp. 173-273.

[141] R. V. Lenth, “Quick and Easy Analysis of Unreplicated Factorials,” *Technometrics,* vol. 31, pp. 469-473, 1989.

[142] V. J. Kroc and G. H. Fairchild, “Clustered precipitated calcium carbonate particles”. United States Patent 5,695,733, 9 December 1997.

[143] I. S. Bleakley and T. R. Jones, “Slaking, carbonating and neutralizing using regant”. United States Patent 5232678A, 3 August 1993.

[144] J. Kuusisto, *Private email communication,* Helsinki, June 16 2014.

[145] National Lime Association, “Properties of typical commercial lime products,” n.d.. [Online]. Available: http://www.lime.org/documents/lime_basics/lime-physical-chemical.pdf. [Accessed 21 July 2014].

[146] T. Evans, “Influence of Ionic strength on calcium carbonate ($CaCO_3$) polymorphism,” 2012. [Online]. Available: http://arxiv.org/ftp/arxiv/papers/1209/1209.3333.pdf. [Accessed 2 August 2014].

[147] V. K. Mathur, “High speed manufacturing process for precipitated calcium carbonate employing sequential pressure carbonation”. United States Patent 6,251,356 B1, 26 June 2001.

[148] R. R. Hemrajani and G. B. Tatterson, “Mechanically Stirred Vessels,” *in Handbook of Industrial Mixing,* E. L. Paul, V. A. Atiemo-Obeng and S. M. Kresta, Eds., New Jersey, John Wiley & Sons Inc., pp. 345-390.

[149] V. A. Atiemo-Obeng, W. R. Penney and P. Armenante, “Solid–Liquid Mixing,” *in Handbook of Industrial Mixing,* E. L. Paul, V. A. Atiemo-Obeng and S. M. Kresta, Eds., New Jersey, John Wiley & Sons Inc., 2003, pp. 543-584.

[150] A. Said, “Enhancement of calcium dissolution from steel slag by ultrasound,” *Unpublished work,* 2014.

[151] S. A. Parsons, B. -L. Wang, S. J. Judd and T. Stephenson, “Magnetic treatment of calcium carbonate scale—effect of pH control,” *Water Research,* vol. 31, no. 2, pp. 339-342, 1997.

[152] E. Dalas and P. G. Koutsoukos, “The effect of magnetic fields on calcium carbonate scale formation,” *Journal of Crystal Growth,* vol. 96, no. 4, pp. 802-806, 1989.

[153] E. Dalas, “The effect of ultrasonic field on calcium carbonate scale formation,” *Journal of Crystal Growth,* vol. 222, no. 1-2, pp. 287-292, 2001.

[154] Y. Kojima, K. Yamaguchi and N. Nishimiya, “Effect of amplitude and frequency of ultrasonic irradiation on morphological characteristics control of calcium carbonate,” *Ultrasonics Sonochemistry,* vol. 17, no. 3, pp. 617-620, 2010.

[155] K. Mäkelä, “LIPASTO Traffic Emissions,” VTT Technical Research Centre of Finland, 25 April 2012. [Online]. Available: http://www.lipasto.vtt.fi/yksikkopaastot/tavaraliikennee/tieliikennee/tavara_tiee.htm. [Accessed 28 June 2014].

[156] “fuel-prices-europe.info,” 14 July 2014. [Online]. Available: http://www.fuel-prices-europe.info/. [Accessed 14 July 2014].

[157] International Energy Agency, “CO_2 Emissions from Fuel Combustion - Highlights,” 2012. [Online]. Available: http://www.iea.org/co2highlights/co2highlights.pdf. [Accessed 20 June 2014].

[158] Eurostat, “Electricity prices by type of user, medium size industries, 2013,” European Commission, 14 July 2014. [Online]. Available: http://epp.eurostat.ec.europa.eu/portal/page/portal/energy/data/main_tables. [Accessed 14 July 2014].

[159] A. V. Sharygin and R. H. Wood, “Volumes and heat capacities of aqueous solutions of ammonium chloride from the temperatures 298.15 K to 623 K and pressures to 28 MPa,” *Journal of Chemical Thermodynamics,* vol. 28, pp. 851-872, 1996.

[160] Statistics Finland, “Fuel prices in heat production,” Statistics Finland, 19 June 2014. [Online]. Available: http://www.stat.fi/til/ehi/2014/01/ehi_2014_01_2014-06-19_kuv_003_en.html. [Accessed 3 August 2014].

[161] Alibaba.com, “Ammonium chloride price,” Alibaba, 10 July 2014. [Online]. Available: http://www.alibaba.com/showroom/ammonium-chloride-price.html. [Accessed 10 July 2014].

[162] Ruukki, “Ruukki's Raahe Works Environmental Report 2007,” 2007. [Online]. Available: http://www.ruukki.com/~/media/Files/Corporate responsibility/Ruukki Raahe Works Environmental report 2007.ashx20Raahe%2520Works%2520Environmental%2520report%25202007.ashx&ei=C6DeU4. [Accessed 27 July 2014].

[163] M. Finkenrath, “Cost and Performance of Carbon Dioxide Capture from Power Generation, Working Paper,” International Energy Agency, Paris, 2011.

[164] Roskill, “The economics of precipitated calcium carbonate, 7th edition,” Roskill, London, 2008.

[165] Roskill, “Ground and Precipitated Calcium Carbonate: Global Industry Markets & Outlook,” 2012. [Online]. Available: http://www.roskill.com/reports/industrial-minerals/ground-and-precipitated-calcium-carbonate-1/leaflet>. [Accessed 25 January 2014].

[166] University of Canterbury, “Determination of Calcium Ion Concentration,” [Online]. Available: http://www.outreach.canterbury.ac.nz/chemistry/documents/calcium.pdf. [Accessed 6 March 2014].

[167] D. Harvey, “Analytical Chemistry 2.0,” 2000. [Online]. Available: http://acad.depauw.edu/harvey_web/eText%20Project/AnalyticalChemistry2.0.html. [Accessed 18 May 2014].

[168] X. Wang, W. Conway, D. Fernandes, G. Lawrance, R. Burns, G. Puxty and M. Maeder, “Kinetics of the Reversible Reaction of CO_2(aq) with Ammonia in Aqueous Solution,” *J. Phys. Chem. A,* vol. 115, p. 6405–6412, 201.

[169] R. Pohorecki and W. Moniuk, “Kinetics of reaction between carbon dioxide and hydroxyl ions in aqueous electrolyte solutions,” *Chemical Engineering Science,* vol. 43, no. 7, p. 1677–1684, 1988.

[170] J. G. Speight, *Lange's Handbook of Chemistry,* 16th ed., New York: McGraw-Hill, 2005.

[171] T. J. Edwards, J. Newman and J. M. Prausnitz, “Thermodynamics of aqueous solutions containing volatile weak electrolytes,” *AIChE Journal,* vol. 21, no. 2, pp. 248-259, 1975.

[172] T. J. Edwards, G. Maurer, J. Newman and J. M. Prausnitz, “Vapour-liquid equilibria in multicomponent aqueous solutions of volatile weak electrolytes,” *AIChE Journal,* vol. 24, no. 6, pp. 966-976, 1978.

[173] P. Verbrugge, “Vapour-liquid equilibria of the ammonia-carbon dioxide-water system,” Delft University Press, Delft, 1979.

[174] F. Kurz, B. Rumpf and G. Maurer, “Vapor-liquid-solid equilibria in the system NH_3-CO_2-H_2O from around 310 to 470 K: New experimental data and modeling,” *Fluid Phase Equilibria,* vol. 104, pp. 261-275, 1995.

[175] E. M. Pawlikowski, J. Newman and J. M. Prausnitz, “Phase Equilibria for Aqueous Solutions of Ammonia and Carbon Dioxide,” *Ind. Eng. Chem. Process Des. Dev,* vol. 21, no. 4, pp. 764-770, 1982.

[176] Z. Duan and D. Li, “Coupled phase and aqueous species equilibrium of the H_2O-CO_2-NaCl-$CaCO_3$ system from 0-100°C, 1-1000 bar with NaCl concentrations up to saturation of halite,” *Geochimica et Cosmochimica Acta,* vol. 72, p. 5128–5145, 2008.

[177] K. Thomsen and P. Rasmussen, “Modeling of vapor–liquid–solid equilibrium in gas–aqueous electrolyte systems,” *Chemical Engineering Science,* vol. 54, no. 12, pp. 1787-1802, 1999.

[178] V. Darde, W. J. van Well, E. H. Stenby and K. Thomsen, “Modeling of carbon dioxide absorption by aqueous ammonia solutions using the Extended UNIQUAC model,” *Ind. Eng. Chem. Res.,* vol. 49, no. 24, p. 12663–12674, 2010.

[179] L. N. Plummer, D. L. Parkhurst, G. W. Fleming and S. A. Dunkle, “A computer program incorporating Pitzer's equations for calculation of geochemical reactions in brines,” US Geological Survey, Reston, 1988.

Appendices

Appendix A – Determination of [Ca^{2+}] by Complexometric Titration

In previous work on the Slag2PCC process at Aalto, the concentration of calcium in solution had been analysed by ICP–AES (Inductively Coupled Plasma–Atomic Emission Spectroscopy). While this is a very good method for determining ion concentrations in solution, the analysis is expensive and given the large number of tests required another method for calcium analysis was sought. A search of the literature and subsequent consultation with the Department of Analytical Chemistry at Aalto University highlighted that complexometric titration of the calcium with Ethylenediaminetetraacetic acid (EDTA) using Patton Reeder indicator (PR, also known as HHSNNA) is a common method used for calcium analysis and should be suitable providing no significant amounts other metals were dissolved.

EDTA is a large molecule which forms a complex with metal ions, including Ca^{2+} ions. HHSNNA also forms a complex with Ca^{2+} ions, however the HHSNNA – Ca^{2+} complex is less stable than the EDTA–Ca^{2+} complex. When uncomplexed HHSNNA is a blue colour, but when complexed with Ca^{2+} it is a pink colour. As a result, when the Ca^{2+}– HHSNNA complex is titrated with EDTA the Ca^{2+} ions react to form a stronger complex with the EDTA. The titration endpoint occurs when the solution turns blue, indicating that the Ca^{2+}- HHSNNA complex has been completely replaced by the Ca^{2+}-EDTA complex and the HHSNNA has reverted to its blue colour. A procedure of the standard analysis method is outlined in reference [166] but in essence, a standardised concentration of EDTA (typically 0.1M) is added drop-wise to a known volume (10ml) of Ca-containing solution sample to which a small amount of HHSNNA has been added and pH raised to 12 with concentration NaOH. When the indicator changes from pink to blue, the total volume of EDTA added to cause this change is recorded and the moles of calcium determined on a 1:1 molar basis. The concentration in the original solution is then the number of moles of calcium divided by the sample volume.

Complicating the analysis in the case of the Slag2PCC process is the fact that calcium can form stable complexes with ammonia in solution [167]. This means that the presence of ammonia can cause an understatement of the calcium concentration via complexation with EDTA as fewer Ca^{2+} ions are free to complex with EDTA. This can be accounted for by knowing the fraction of total calcium in solution present as Ca^{2+}, $\alpha_{Ca}{}^{2+}$, at different concentrations of NH_3. This is shown in the table below for NH_3 concentrations up to 1M.

Effect of NH_3 concentration on $\alpha_{Ca}{}^{2+}$ [167]

[NH_3] (M)	$\alpha_{Ca}{}^{2+}$
1	0.550
0.5	0.736
0.1	0.939
0.05	0.969
0.01	0.994
0.005	0.997
0.001	0.999

Thus by dividing the calcium concentration determined directly from the titration by the $\alpha_{Ca}{}^{2+}$ value corresponding to the [NH_4Cl] in the solution from the table above, the concentration can be corrected to account for the calcium bound with NH_3 in solution. This method of correction was used for all solutions prepared for the factorial experiments in which the [NH_4Cl] was at or below 0.5M. However, in the pilot plant and follow-up experimental work, the titration proved quite challenging and it was

difficult to detect a clear colour-change end-point as had been the case with the factorial experiment analysis. It was believed that the higher [NH_4Cl] concentration was the source of the problem and so a method to remove NH_3 from the sample solution before titration was devised with the help of Kalle Salminen and Matti Pusa so that ammonium interference in the analysis could be avoided. This involved:

1) Alkalisation of the Ca-containing sample using concentrated NaOH until pH was above 12 to ensure most of the NH_4^+ was converted to NH_3
2) Gently boiling the sample for 5-10 minutes to release NH_3 as $NH_{3(g)}$
3) Acidification of the sample to pH<3 with HCl to dissolve any $CaCO_3$ precipitated
4) Re-alkalisation of the sample to pH 12 with concentrated NaOH

The sample was then titrated as before. The method proved quite successful and no correction for NH_3 concentration was applied. This method for determining calcium concentration was used for all the pilot plant tests as well as the follow-up laboratory work with [NH_4Cl] above 1M.

Appendix B – Equilibrium and Kinetic Data

Equilibrium constants for the reactions considered in the Ca-NH_3-CO_2-H_2O system in section 6.2 were calculated using HSC Chemistry 5 over the temperature range 0-100°C. These were then fit to non-linear model equations (R^2>99.5%) with the regression parameters given in the table below.

Reaction	A	B	C	D	E
$CO_{2(g)} \rightleftarrows CO_{2(aq)}$	-6789.04	-11.4519	-0.010454	94.4914	-
$NH_{3(g)} \rightleftarrows NH_{3(aq)}$	-157.552	28.1001	-0.049227	-149.006	-
$H_2O_{(g)} \rightleftarrows H_2O_{(aq)}$					
$CO_{2(aq)} + OH^-_{(aq)} \rightleftarrows HCO^-_{3(aq)}$	0	0	5.17974E-05	-0.05801	20.33199
$HCO^-_{3(aq)} + OH^-_{(aq)} \rightleftarrows CO^{2-}_{3(aq)} + H_2O_{(l)}$	0	0	5.89849E-05	-0.05941	16.13491
$CO_{2(aq)} + H_2O_{(aq)} \rightleftarrows H_2CO_{3(aq)}$	0	0	-6.56278E-05	0.039233	-5.85431
$H^+_{(aq)} + HCO^-_{3(aq)} \rightleftarrows H_2CO_{3(aq)}$	0.005975	0.687049	2.74888E-05	-0.02328	9.16333
$H^+_{(aq)} + CO^{2-}_{3(aq)} \rightleftarrows HCO^-_{3(aq)}$	0	0	8.72621E-05	-0.06102	20.7715
$Ca^{2+}_{(aq)} + HCO^-_{3(aq)} \rightleftarrows CaHCO^+_{3(aq)}$	0	0	7.0004E-05	-0.04128	7.138756
$Ca^{2+}_{(aq)} + CO^{2-}_{3(aq)} \rightleftarrows CaCO^0_{3(aq)}$	0	0	9.40715E-05	-0.07163	23.65589
$Ca^{2+}_{(aq)} + OH^-_{(aq)} \rightleftarrows CaOH^+_{(aq)}$	0	0	6.08603E-06	0.008886	-2.01022
$Ca^{2+}_{(aq)} + Cl^-_{(aq)} \rightleftarrows CaCl^+_{(aq)}$	0	0	4.74365E-05	-0.02574	3.605151
$NH_4^+{}_{(aq)} + HCO^-_{3(aq)} \rightleftarrows NH_4HCO_{3(aq)}$	0	0	4.53702E-05	-0.04436	9.661435
$NH_4^+{}_{(aq)} + Cl^-_{(aq)} \rightleftarrows NH_4Cl_{(aq)}$	0	0	6.14546E-05	-0.04522	6.701553
$NH_{3(aq)} + H^+_{(aq)} \rightleftarrows NH_4^+{}_{(aq)}$	0.012312	1.36881	9.81549E-05	-0.092	24.77693
$NH_{3(aq)} + HCO^-_{3(aq)} \rightleftarrows NH_2CO^-_{2(aq)} + H_2O_{(aq)}$	0	0	4.38755E-05	-0.04048	8.651761
$H^+_{(aq)} + OH^-_{(aq)} \rightleftarrows H_2O_{(aq)}$	0	0	0.000148707	-0.12188	37.1176
$Ca^{2+}_{(aq)} + CO^{2-}_{3(aq)} \rightleftarrows CaCO_{3(s),vat}$	0	0	4.83098E-05	-0.01983	9.386731
$Ca^{2+}_{(aq)} + CO^{2-}_{3(aq)} \rightleftarrows CaCO_{3(s),arg}$	0	0	7.64155E-05	-0.03934	13.17253
$Ca^{2+}_{(aq)} + CO^{2-}_{3(aq)} \rightleftarrows CaCO_{3(s),cal}$	0.039455	7.097686	9.13668E-05	-0.05829	-5.2E-05

For the first three single-component vapour-liquid equilibria, the fits are for the Henry's Law constant H_i (atm/kg.mol),

$$H_i = e^{(\frac{A_i}{T} + B_i \ln(T) + C_i T + D_i)}$$

with T the temperature in Kelvins (range 273.15-423.15K).

For the remaining equilibria, the constants are fits for the equilibrium constant, K_i, in the form

$$\log_{10}(K_i) = \frac{A_i}{T} + B_i \log_{10}(T) + C_i T^2 + D_i T + E_i$$

where T is temperature in Kelvin as before (range 273.15-373.15K).

As well as equilibrium data, kinetic data for some of these reactions has been found from the literature [103] [168] and compiled in the table below.

	E_a (kJ/mol)	A	k(25°C)
$CO_{2(aq)} + H_2O_{(aq)} \rightarrow H_2CO_{3(aq)}$	81.2	1.28×10^{11}	0.00076
$H_2CO_{3(aq)} \rightarrow CO_{2(aq)} + H_2O_{(aq)}$	71.66	9.2×10^{13}	25.63
$CO_{2(aq)} + OH^-_{(aq)} \rightarrow HCO^-_{3(aq)}$	64.1	2.1×10^{14}	1235
$HCO^-_{3(aq)} \rightarrow CO_{2(aq)} + OH^-_{(aq)}$	114.2	3.3×10^{16}	0.0003239
$NH_{3(aq)} + CO_{2(aq)} \rightarrow NH_2COOH_{(aq)}$	52.1	2.1×10^{9}	1.564
$NH_2COOH_{(aq)} \rightarrow NH_{3(aq)} + CO_{2(aq)}$	68.2	5.7×10^{13}	64.13

The rate data follow the classical Arrhenius relationship below where E_a is the activation energy (J/mol) and T is temperature (K).

$$k(T) = A\, exp\left(\frac{-E_a}{RT}\right)$$

These kinetic parameters were gathered for pure solutions containing only components in the carbonate system and they are likely to be effected by the ionic strength of the actual solution. For dependence of some of these rate constants on ionic strength, the reader is referred to Pohorecki & Moniuk [169].

Appendix C –Activity coefficient model interaction parameters

As was highlighted earlier the solution chemistry of the Slag2PCC process is likely to be highly non-ideal due to the presence of the NH_4Cl solvent and the number of other ionic species involved. To accurately understand and eventually develop both equilibrium and dynamic models for the process, the activity coefficients of the components in solution will need to be estimated. One of the simplest and most commonly used equations for estimating single-ion activity coefficients is the extended Debye-Hückel equation [83] [170]:

$$log\,\gamma_i = -\frac{Az_i^2\sqrt{I}}{1+Br_i\sqrt{I}}$$

where r_i is the radius of the hydrated ion in solution and I is the solution ionic strength determined from the sum of the concentration, c_i, and squared charge, z_i, of every ion in solution.

$$I = \frac{1}{2}\sum c_i z_i^2$$

The terms A and B are temperature-dependent parameters related to the unit volume of the solvent, with A=0.5115 and b=0.3291 for water at 25°C. The term A is often called the Debye-Hückel constant and is calculated from the equation below [83].

$$A = \frac{1}{2.303}\left(\frac{e}{\sqrt{DkT}}\right)^3\sqrt{\frac{2\pi d_0 N_A}{1000}}$$

B is calculated from,

$$B = \sqrt{\frac{8\pi d_0 N_A e^2}{1000DkT}}$$

In these equations, e is the charge of an electron (1.60206 x 10^{-19} C), D is the dielectric constant (78.3 for water at 25°C), k is the Boltzmann constant (1.38 x 10^{-23} J K^{-1}), N_A is Avogadro's number 6.02 x 10^{23}, and d_0 is the solvent (water) density. However, the extended Debye-Hückel equation is really only valid in solutions up to an ionic strength of about 0.1M. In the case of the Slag2PCC process the presence of the NH_4Cl solvent increases the ionic content of the solution and even on its own, at a concentration of 1M, it has a mean activity coefficient of about 0.6 highlighting quite non ideal behaviour [77]. Thus, the potential effect of the solvent species NH_4^+ and Cl^-, which at a concentration of 1M will likely be even higher than that of dissolved Ca^{2+}, should not be ignored. For more concentrated solutions, an advanced method such as that of Pitzer [97] is required which takes into account interactions between the dissolved ions and the solvent as well as the effects of temperature. According to the Pitzer model, the activity coefficient of species i in a multicomponent solution is expressed as below,

$$ln\,\gamma_i = z_i^2 f^\gamma + 2\sum_{j\neq H_2O} m_j B_{ij} + z_i^2\sum_{j\neq H_2O}\sum_{k\neq H_2O} m_j m_k B'_{jk}$$

with contributing terms defined as follows.

$$f^\gamma = -A_\phi\left[\frac{\sqrt{I}}{1+1.2\sqrt{I}} + \frac{2ln\left(1+1.2\sqrt{I}\right)}{1.2}\right]$$

$$B_{ij} = \beta_0 + \frac{\beta_0}{21}\left[1 - \left(1 + 2\sqrt{I}\right)e^{-2\sqrt{I}}\right]$$
$$B'_{ij} = \frac{\beta_1}{4I^2} + \left[-1 + \left(1 + 2\sqrt{I} + 2I\right)e^{-2\sqrt{I}}\right]$$

The term A_ϕ is the Debye-Hückel constant on a log e basis and is calculated using the same equation for the except that the 2.303 is replaced by a 3. The terms β_0 and β_1 are Pitzer interaction terms which are specific for each ion-pair interaction and must be determined by experiment. While the original Pitzer equations were only for oppositely charge ion-ion interactions, Edwards et al. [171] [172] included terms for ion-ion, ion-molecule and molecule-molecule interactions, believing it provided good results at ionic strengths up to 10 molar. To support future work in developing a thorough thermodynamic model of the Slag2PCC process, a search of the literature was undertaken to find Pitzer interaction parameters for the Ca - CO_2 - NH_4Cl – H_2O system and these have been collated in the table below for the main chemical components in the Ca-NH_3-CO_2-H_2O system collected from the literature. The units of β_{ij}^0 are (mol/kg). Alongside the data is the reference from where it was taken. If a temperature dependence of the interaction parameter was supplied, it is also given here where temperature, T, is in Kelvin. For some components only a single parameter is required, while for others two are recommended. For a more detailed treatment and further data on equilibria and interaction parameters for the CO_2-NH_3-H_2O system the reader is referred to Verbrugge [173], Kurz et al. [174], Powlikowski et al. [175] and Duan et al. [176]. Thomsen & Rasmussen [177] and Darde et al. [178] have also successfully modelled the CO_2-NH_3-H_2O system using the Extended UNIQUAC model for activity coefficients which may yield better results than the Pitzer equations outlined here.

ION-ION Interactions					MOLECULE-ION Interactions				
i	j	β_{ij}^0	β_{ij}^1	Ref	i	j	β_{ij}^0	β_{ij}^1	Ref
$H^+_{(aq)}$	$HCO_3^-{}_{(aq)}$	0.071	$0.018+3.06\beta_{ij}^0$	[83]	**$CO_{2(aq)}$**	$HCO_3^-{}_{(aq)}$	0	-	[97]
	$CO_3^{2-}{}_{(aq)}$	0.086	$0.018+3.06\beta_{ij}^0$	[83]		$CO_3^{2-}{}_{(aq)}$	0	-	[97]
	$NH_2CO_{2(aq)}$	0.198	$0.018+3.06\beta_{ij}^0$	[83]		$NH_2CO_2^-{}_{(aq)}$	0.017	-	[83]
	$OH^-_{(aq)}$	0.208	$0.018+3.06\beta_{ij}^0$	[83]		$OH^-_{(aq)}$	$0.26-1.62\times10^{-3}T$ $+2.89\times10^{-6}T^2$	-	[83]
	$Cl^-_{(aq)}$	0.18029	0.27837			$Cl^-_{(aq)}$	-0.005	-	[97]
						$Ca^{+2}_{(aq)}$	0.183	-	[97]
$NH_4^+{}_{(aq)}$	$HCO_3^-{}_{(aq)}$	-0.0435	$0.018+3.06\beta_{ij}^0$	[83]		$NH_4^+{}_{(aq)}$	$0.037-2.38\times10^{-4}T$ $+3.83\times10^{-7}T^2$	-	[83]
	$CO_3^{2-}{}_{(aq)}$	-0.062	-	[83]		$H^+_{(aq)}$	0.033	-	[83]
	$NH_2CO_2^-{}_{(aq)}$	0.0505	$0.018+3.06\beta_{ij}^0$	[83]					
	$OH^-_{(aq)}$	0.06	$0.018+3.06\beta_{ij}^0$	[83]	**$NH_{3(aq)}$**	$HCO_3^-{}_{(aq)}$	-0.0816	0.4829	[83]
	$Cl^-_{(aq)}$	0.03603	0.29619			$CO_3^{2-}{}_{(aq)}$	0.068	-	[83]
						$NH_2CO_2^-{}_{(aq)}$	-0.03933+25.263/T	-	[174]
$Ca^{+2}_{(aq)}$	$HCO_3^-{}_{(aq)}$	0.4	2.977	[179]		$OH^-_{(aq)}$	$0.227-1.47\times10^{-3}T$ $+2.6\times10^{-6}T^2$	-	[83]
	$CO_3^{2-}{}_{(aq)}$	0.16	2.1	[179]		$Cl^-_{(aq)}$	n/a		
	$NH_2CO_2^-{}_{(aq)}$	n/a	n/a			$Ca^{+2}_{(aq)}$	n/a		
	$OH^-_{(aq)}$	-0.1747	-0.2303	[179]		$NH_4^+{}_{(aq)}$	0.0117	-0.2	[83]
	$Cl^-_{(aq)}$	0.31231	1.64585	[179]		$H^+_{(aq)}$	0.015	-	[83]

MOLECULE - MOLECULE Interactions			
i	j	β_{ij}^0	
$CO_{2(aq)}$	$CO_{2(aq)}$	0.4922+149.2/T	[83]
$NH_{3(aq)}$	$NH_{3(aq)}$	-0.026+12.29/T	[83]
$CO_{2(aq)}$	$NH_{3(aq)}$	Average of self-interactions above	[83]

Appendix D – Factorial Analysis Results

Main Effects

The following is the raw ANOVA analysis of the main effects from Minitab when the 16 lab-scale factorial runs are fit to a general linear model (GLM). Those factors which return a p-value <0.1 (90% confidence interval) for a response variable have been highlighted.

Factor	Type	Levels	Values
Initial Temp. (°C)	fixed	2	15, 25
[Ca2+] (mol/L)	fixed	2	0.040, 0.048
[NH4Cl] (mol/L)	fixed	2	0.1, 0.5
CO2 flow (L/min)	fixed	2	0.4, 1.2
Agitation speed (rpm)	fixed	2	300, 555

ANOVA for **Induction time (min)**, using Adjusted SS for Tests

Source	DF	Seq SS	Adj SS	Adj MS	F	P
Initial Temp. (°C)	**1**	**83.875**	**83.875**	**83.875**	**9.88**	**0.010**
[Ca2+] (mol/L)	1	0.401	0.401	0.401	0.05	0.832
[NH4Cl] (mol/L)	**1**	**191.592**	**191.592**	**191.592**	**22.56**	**0.001**
CO2 flow (L/min)	**1**	**41.067**	**41.067**	**41.067**	**4.84**	**0.053**
Agitation speed (rpm)	1	13.814	13.814	13.814	1.63	0.231
Error	10	84.908	84.908	8.491		
Total	15	415.657				

S = 2.91390 R-Sq = 79.57% R-Sq(adj) = 69.36%

Unusual Observations for Inc. time (min)

Obs	Inc. time (min)	Fit	SE Fit	Residual	St Resid
9	21.0000	14.9125	1.7844	6.0875	2.64 R

R denotes an observation with a large standardized residual.

ANOVA for **Carbonation time (min)**, using Adjusted SS for Tests

Source	DF	Seq SS	Adj SS	Adj MS	F	P
Initial Temp. (°C)	1	16.5	16.5	16.5	0.15	0.709
[Ca2+] (mol/L)	1	40.9	40.9	40.9	0.37	0.559
[NH4Cl] (mol/L)	**1**	**5646.9**	**5646.9**	**5646.9**	**50.55**	**0.000**
CO2 flow (L/min)	**1**	**1516.1**	**1516.1**	**1516.1**	**13.57**	**0.004**
Agitation speed (rpm)	1	307.0	307.0	307.0	2.75	0.128
Error	10	1117.1	1117.1	111.7		
Total	15	8644.5				

S = 10.5693 R-Sq = 87.08% R-Sq(adj) = 80.62%

Unusual Observations for Carb. time (min)

Obs	Carb. time (min)	Fit	SE Fit	Residual	St Resid
7	21.5833	39.3021	6.4723	-17.7188	-2.12 R

R denotes an observation with a large standardized residual.

ANOVA for **d50 (no US)** (µm), using Adjusted SS for Tests

Source	DF	Seq SS	Adj SS	Adj MS	F	P
Initial Temp. (°C)	**1**	**1068.6**	**1068.6**	**1068.6**	**8.52**	**0.015**
[Ca2+] (mol/L)	**1**	**782.9**	**782.9**	**782.9**	**6.25**	**0.031**
[NH4Cl] (mol/L)	1	346.7	346.7	346.7	2.77	0.127
CO2 flow (L/min)	1	86.9	86.9	86.9	0.69	0.425
Agitation speed (rpm)	1	226.7	226.7	226.7	1.81	0.208
Error	10	1253.6	1253.6	125.4		
Total	15	3765.4				

S = 11.1964 R-Sq = 66.71% R-Sq(adj) = 50.06%

Unusual Observations for d50 (no US) (µm)

Obs	d50 (no US) (µm)	Fit	SE Fit	Residual	St Resid	
12	88.5420	67.7817	6.8563	20.7603	2.35	R

R denotes an observation with a large standardized residual.

ANOVA for **d90 (no US)** (µm), using Adjusted SS for Tests

Source	DF	Seq SS	Adj SS	Adj MS	F	P
Initial Temp. (°C)	**1**	**4114.7**	**4114.7**	**4114.7**	**8.67**	**0.015**
[Ca2+] (mol/L)	**1**	**2919.5**	**2919.5**	**2919.5**	**6.15**	**0.033**
[NH4Cl] (mol/L)	1	1288.4	1288.4	1288.4	2.72	0.130
CO2 flow (L/min)	1	585.0	585.0	585.0	1.23	0.293
Agitation speed (rpm)	1	570.9	570.9	570.9	1.20	0.298
Error	10	4744.7	4744.7	474.5		
Total	15	14223.2				

S = 21.7822 R-Sq = 66.64% R-Sq(adj) = 49.96%

Unusual Observations for d90 (no US) (µm)

Obs	d90 (no US) (µm)	Fit	SE Fit	Residual	St Resid	
12	169.266	131.435	13.339	37.831	2.20	R

R denotes an observation with a large standardized residual.

ANOVA for **d50 (with US)** (µm), using Adjusted SS for Tests

Source	DF	Seq SS	Adj SS	Adj MS	F	P
Initial Temp. (°C)	**1**	**753.42**	**753.42**	**753.42**	**10.97**	**0.008**
[Ca2+] (mol/L)	**1**	**395.95**	**395.95**	**395.95**	**5.77**	**0.037**
[NH4Cl] (mol/L)	**1**	**343.99**	**343.99**	**343.99**	**5.01**	**0.049**
CO2 flow (L/min)	1	66.56	66.56	66.56	0.97	0.348
Agitation speed (rpm)	1	156.60	156.60	156.60	2.28	0.162
Error	10	686.50	686.50	68.65		
Total	15	2403.02				

S = 8.28552 R-Sq = 71.43% R-Sq(adj) = 57.15%

Unusual Observations for d50 (with US) (µm)

Obs	d50 (with US) (µm)	Fit	SE Fit	Residual	St Resid	
12	68.9760	52.7257	5.0738	16.2503	2.48	R

R denotes an observation with a large standardized residual.

ANOVA for **d90 (with US)** (µm), using Adjusted SS for Tests

Source	DF	Seq SS	Adj SS	Adj MS	F	P
Initial Temp. (°C)	**1**	**2120.6**	**2120.6**	**2120.6**	**8.97**	**0.013**
[Ca2+] (mol/L)	**1**	**1082.7**	**1082.7**	**1082.7**	**4.58**	**0.058**
[NH4Cl] (mol/L)	**1**	**1139.7**	**1139.7**	**1139.7**	**4.82**	**0.053**
CO2 flow (L/min)	1	129.5	129.5	129.5	0.55	0.476
Agitation speed (rpm)	1	292.2	292.2	292.2	1.24	0.292
Error	10	2363.9	2363.9	236.4		
Total	15	7128.6				

S = 15.3750 R-Sq = 66.84% R-Sq(adj) = 50.26%

Unusual Observations for d90 (with US) (µm)

Obs	d90 (with US) (µm)	Fit	SE Fit	Residual	St Resid
12	121.980	89.858	9.415	32.122	2.64 R

R denotes an observation with a large standardized residual.

ANOVA for **% Agg (d90)**, using Adjusted SS for Tests

Source	DF	Seq SS	Adj SS	Adj MS	F	P
Initial Temp. (°C)	1	1.86	1.86	1.86	0.03	0.870
[Ca2+] (mol/L)	1	117.51	117.51	117.51	1.77	0.212
[NH4Cl] (mol/L)	**1**	**262.75**	**262.75**	**262.75**	**3.97**	**0.074**
CO2 flow (L/min)	1	89.20	89.20	89.20	1.35	0.273
Agitation speed (rpm)	1	0.36	0.36	0.36	0.01	0.942
Error	10	662.45	662.45	66.25		
Total	15	1134.14				

S = 8.13911 R-Sq = 41.59% R-Sq(adj) = 12.38%

Unusual Observations for % Agg (d90)

Obs	% Agg (d90)	Fit	SE Fit	Residual	St Resid
15	53.8854	39.3250	4.9842	14.5604	2.26 R

R denotes an observation with a large standardized residual.

Analysis of Variance for **Ca Conversion** (%), using Adjusted SS for Tests

Source	DF	Seq SS	Adj SS	Adj MS	F	P
Initial Temp. (°C)	1	2.63	2.63	2.63	0.18	0.680
[Ca2+] (mol/L)	1	5.16	5.16	5.16	0.35	0.565
[NH4Cl] (mol/L)	**1**	**2795.16**	**2795.16**	**2795.16**	**191.92**	**0.000**
CO2 flow (L/min)	1	19.45	19.45	19.45	1.34	0.275
Agitation speed (rpm)	1	6.24	6.24	6.24	0.43	0.528
Error	10	145.64	145.64	14.56		
Total	15	2974.28				

S = 3.81633 R-Sq = 95.10% R-Sq(adj) = 92.65%

Unusual Observations for Ca Conversion (%)

Obs	Ca Conversion (%)	Fit	SE Fit	Residual	St Resid
1	82.5263	74.4358	2.3370	8.0906	2.68 R

R denotes an observation with a large standardized residual.

Analysis of Variance for **Growth time (min)**, using Adjusted SS for Tests

Source	DF	Seq SS	Adj SS	Adj MS	F	P
Initial Temp. (°C)	1	145.5	145.5	145.5	1.52	0.246
[Ca2+] (mol/L)	1	34.5	34.5	34.5	0.36	0.562
[NH4Cl] (mol/L)	**1**	**3877.7**	**3877.7**	**3877.7**	**40.39**	**0.000**
CO2 flow (L/min)	**1**	**1122.0**	**1122.0**	**1122.0**	**11.69**	**0.007**
Agitation speed (rpm)	1	159.9	159.9	159.9	1.67	0.226
Error	10	960.0	960.0	96.0		
Total	15	6299.5				

S = 9.79788 R-Sq = 84.76% R-Sq(adj) = 77.14%

Analysis of Variance for **Max T rise** (°C), using Adjusted SS for Tests

Source	DF	Seq SS	Adj SS	Adj MS	F	P
Initial Temp. (°C)	1	0.7656	0.7656	0.7656	2.80	0.125
[Ca2+] (mol/L)	1	0.7056	0.7056	0.7056	2.58	0.139
[NH4Cl] (mol/L)	**1**	**16.4430**	**16.4430**	**16.4430**	**60.10**	**0.000**
CO2 flow (L/min)	1	0.1482	0.1482	0.1482	0.54	0.479
Agitation speed (rpm)	1	0.1225	0.1225	0.1225	0.45	0.519
Error	10	2.7358	2.7358	0.2736		
Total	15	20.9208				

S = 0.523049 R-Sq = 86.92% R-Sq(adj) = 80.38%

Analysis of Variance for **CO2 Conversion** (%), using Adjusted SS for Tests

Source	DF	Seq SS	Adj SS	Adj MS	F	P
Initial Temp. (°C)	1	2.52	2.52	2.52	0.07	0.804
[Ca2+] (mol/L)	**1**	**138.52**	**138.52**	**138.52**	**3.58**	**0.088**
[NH4Cl] (mol/L)	**1**	**1591.39**	**1591.39**	**1591.39**	**41.10**	**0.000**
CO2 flow (L/min)	**1**	**520.25**	**520.25**	**520.25**	**13.44**	**0.004**
Agitation speed (rpm)	**1**	**280.17**	**280.17**	**280.17**	**7.24**	**0.023**
Error	10	387.19	387.19	38.72		
Total	15	2920.03				

S = 6.22250 R-Sq = 86.74% R-Sq(adj) = 80.11%

Pareto charts of calculated effects

The following Pareto charts show the calculated effects for main factors and 2-way interactions on each response variable in the factorial experiment produced using Mintab. The factors and interactions with the strongest calculated effect are more likely to be significant. Normally a set p-value (e.g. 0.1) is used to determine a cut-off point (the red line) which corresponds to a desired statistical significance level to help determine which effects are significant, but because the factorial experiment was saturated this was not possible. In this case, Minitab uses Lenth's method [141] to estimate the cut-off point for determining which factors are significant based on their calculated effects. Naturally this will yield slightly different results to the earlier GLM ANOVA, as the effects of main factors and interactions have been calculated separately in this analysis.

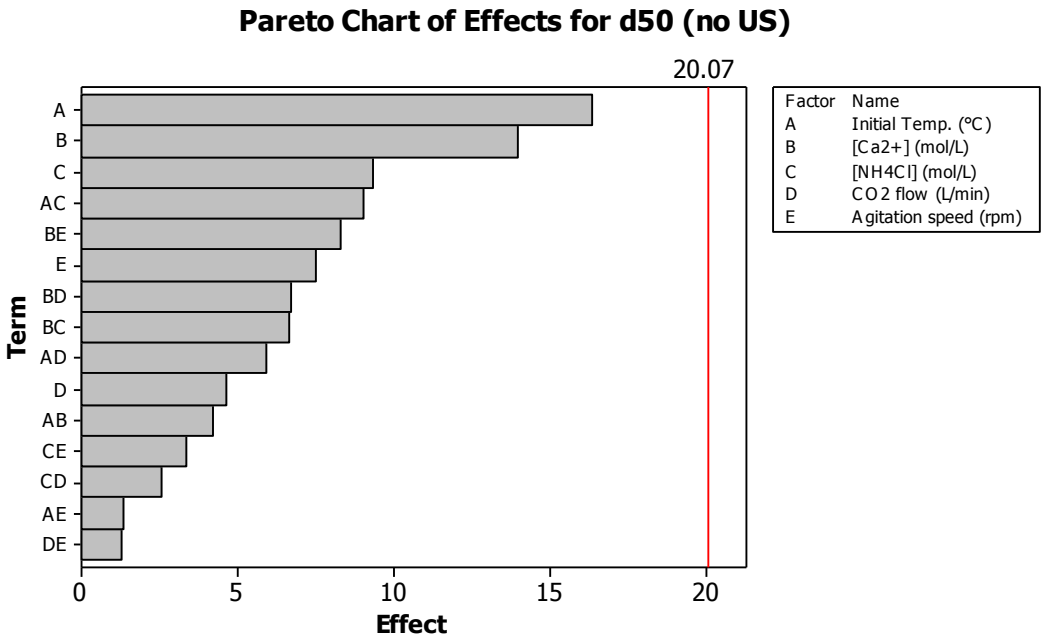

Lenth's PSE = 9.96038

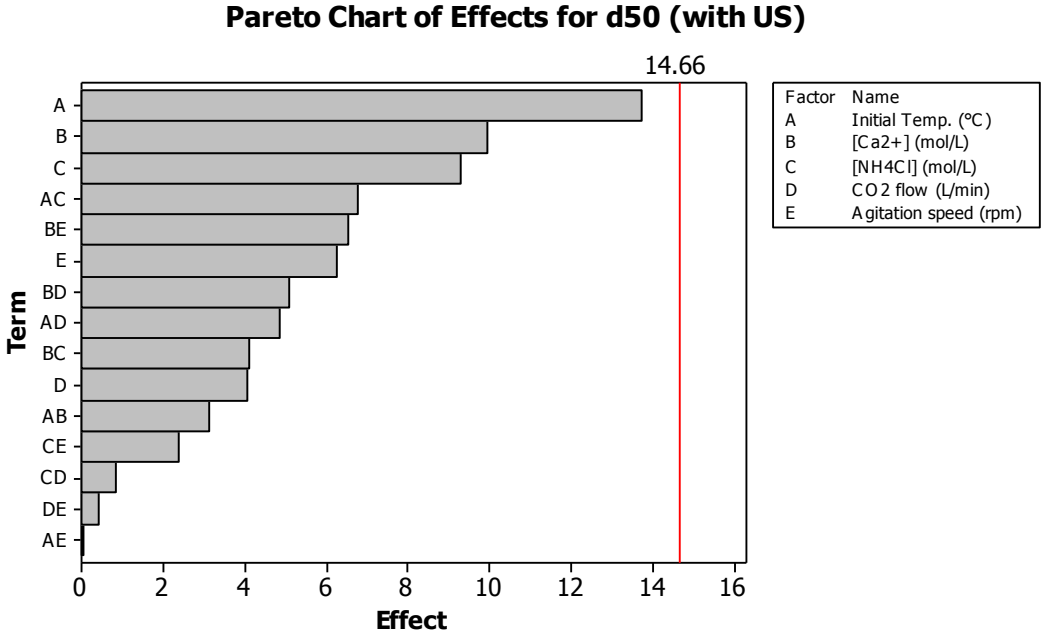

Lenth's PSE = 7.27313

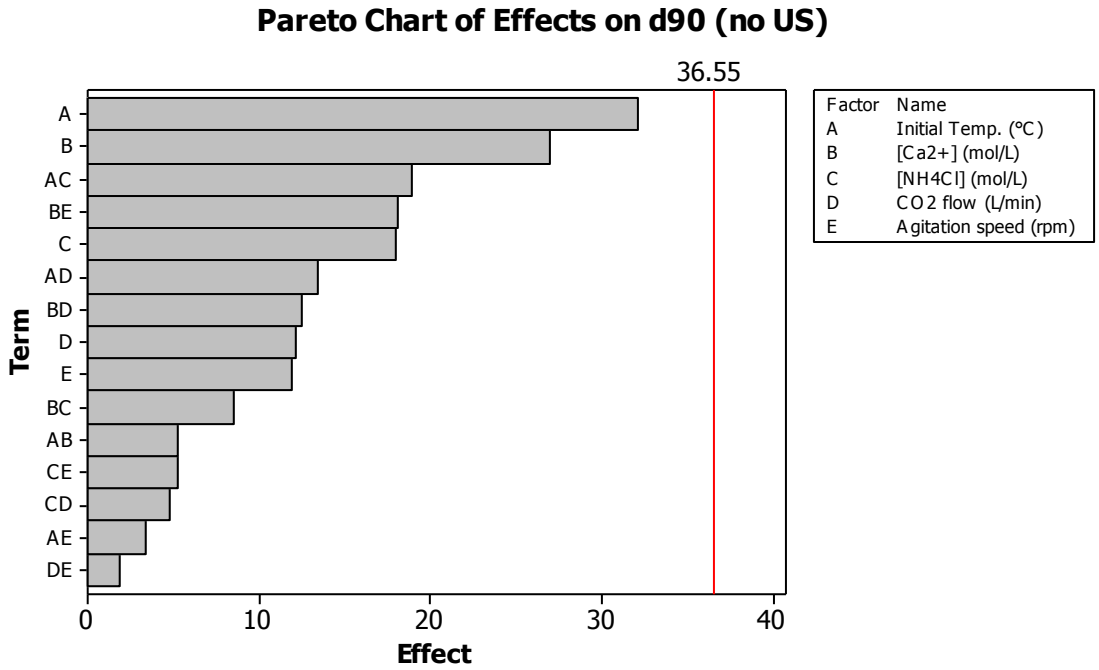

Lenth's PSE = 18.1397

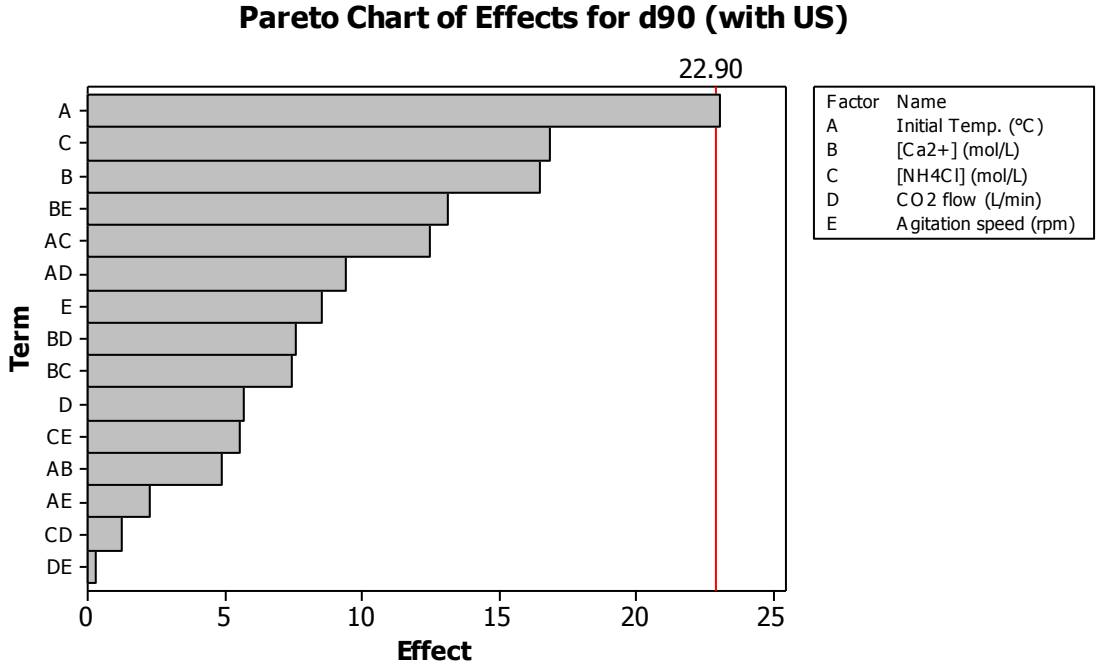

Lenth's PSE = 11.3651

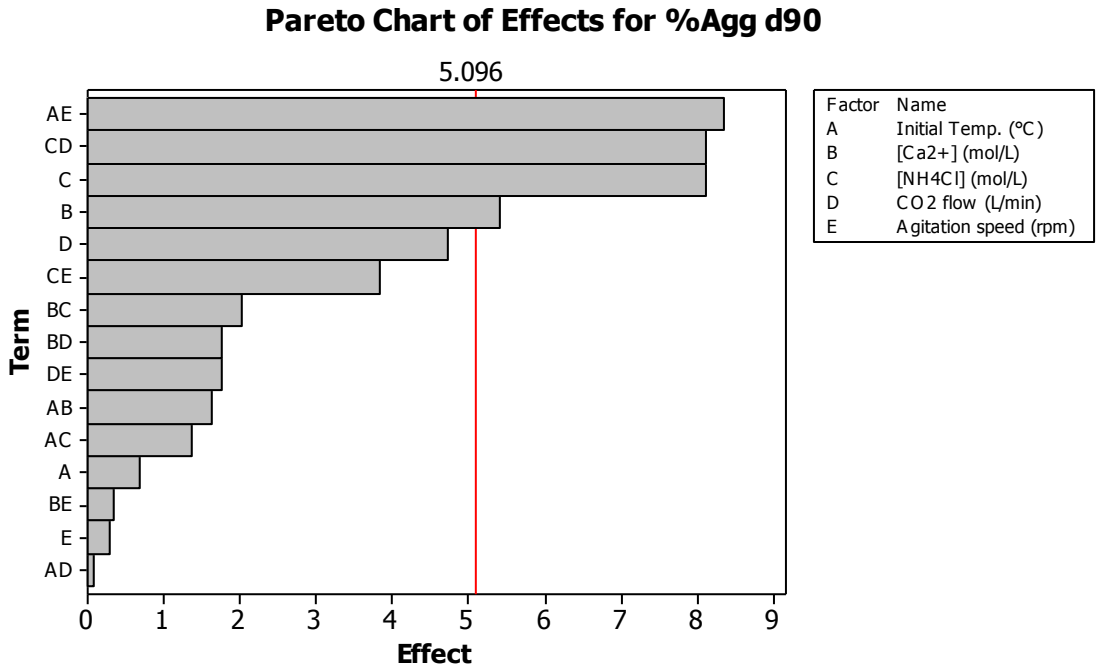

Lenth's PSE = 2.52893

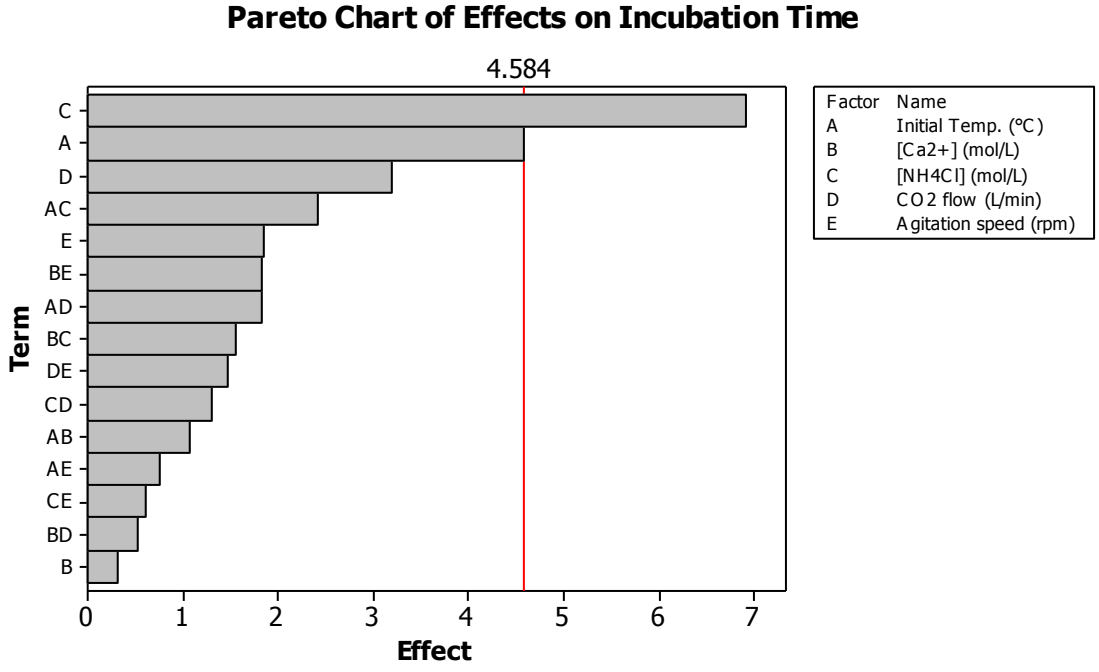

Lenth's PSE = 2.275

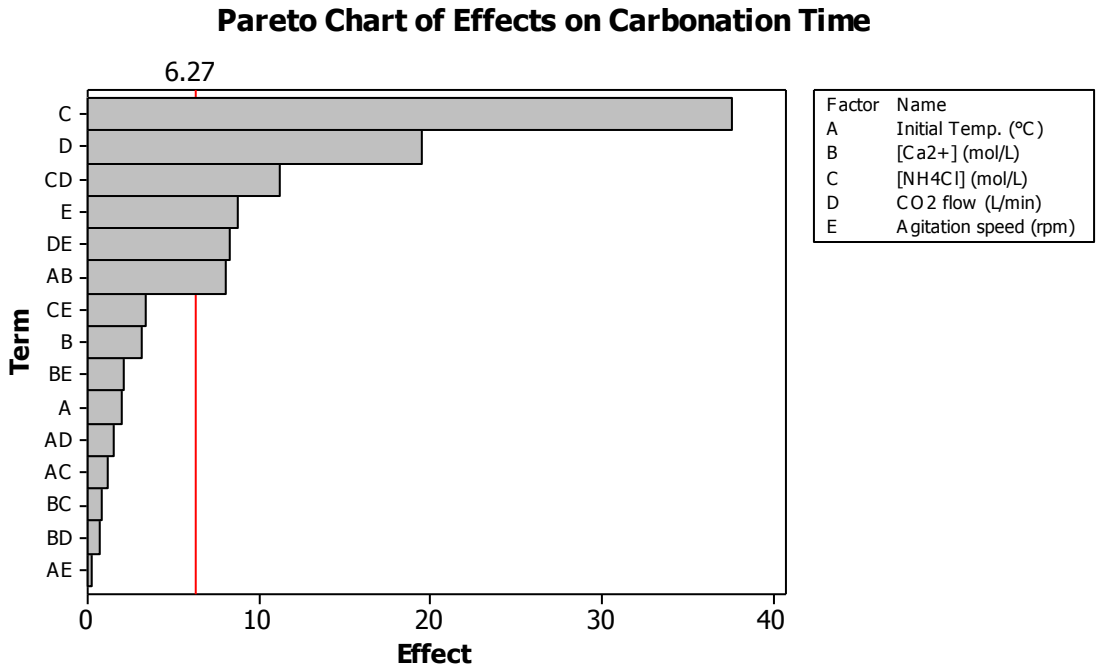

Lenth's PSE = 3.10938

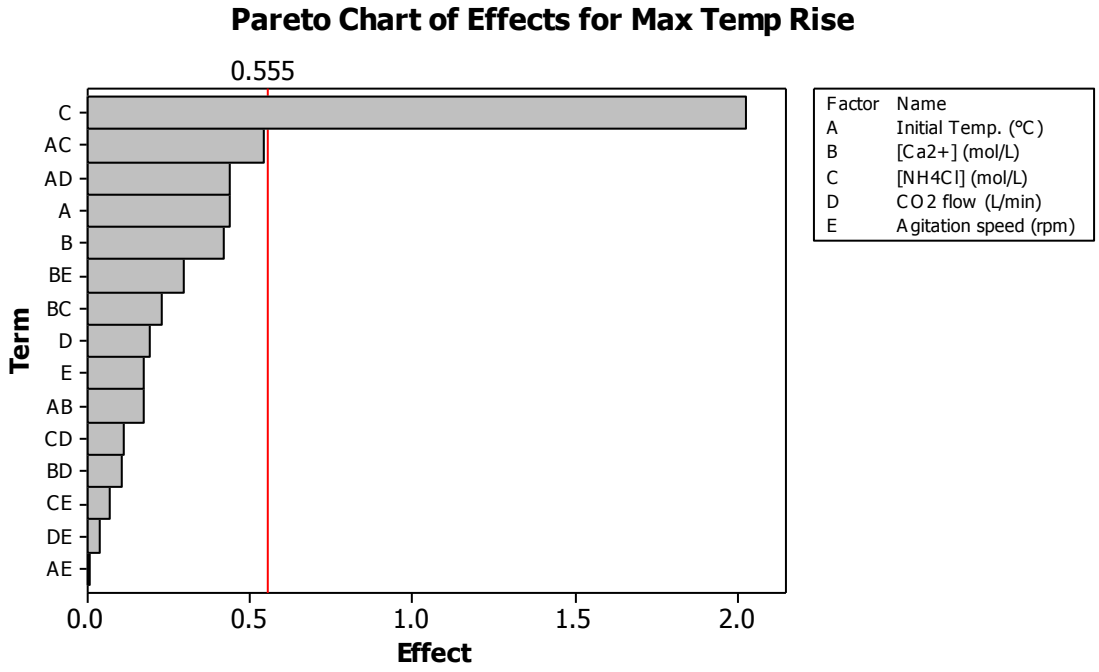

Lenth's PSE = 0.275625

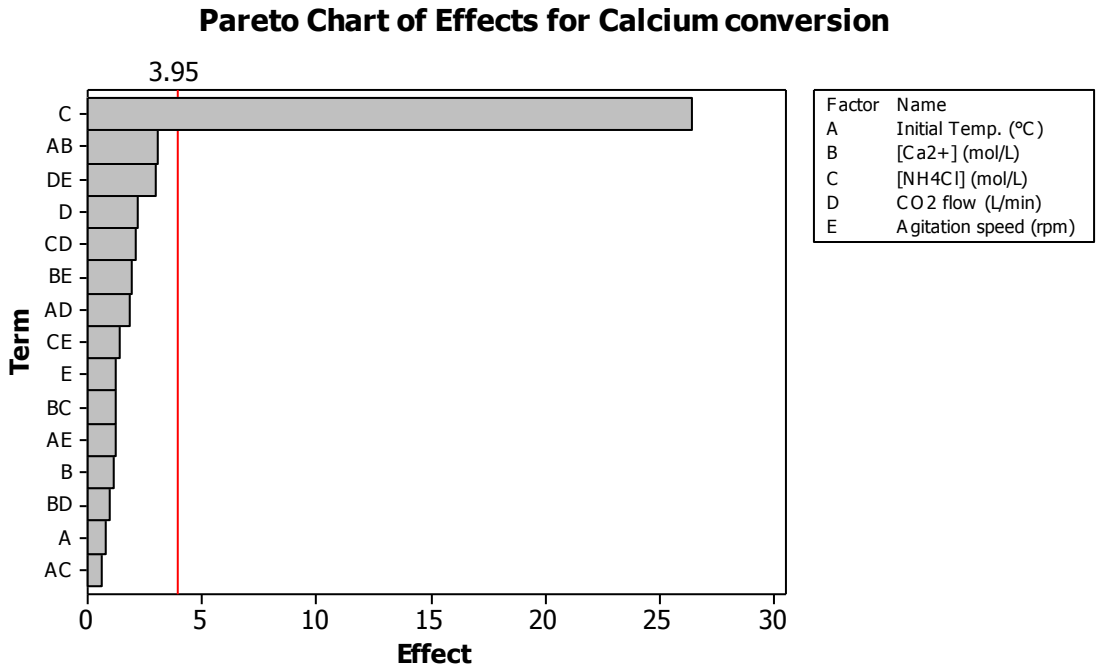

Lenth's PSE = 1.95789

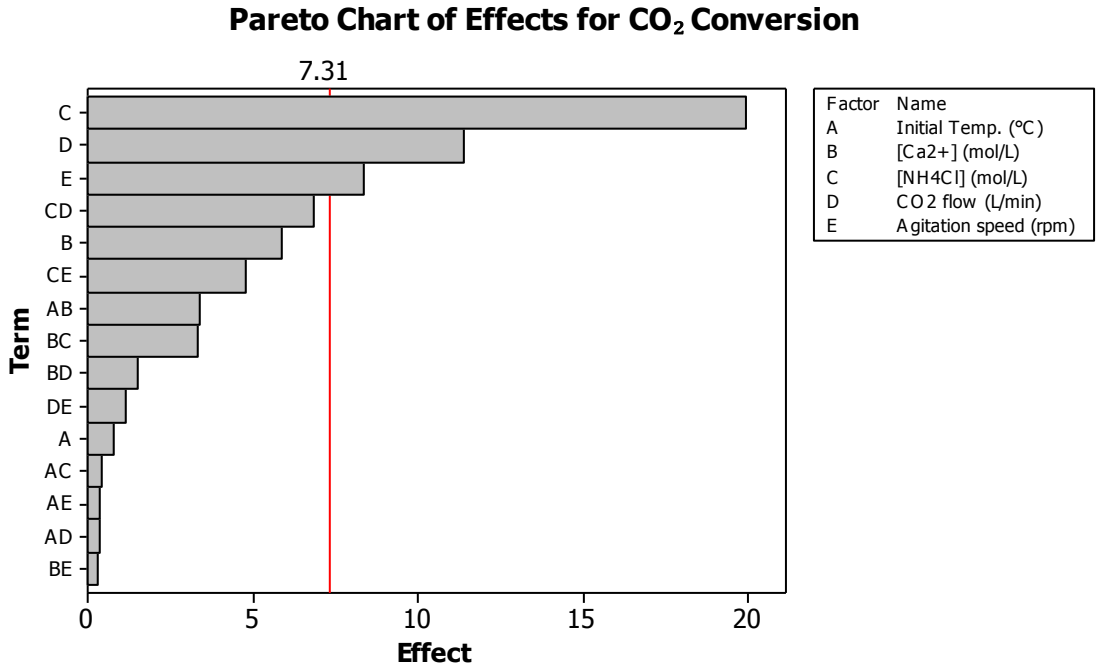

Lenth's PSE = 3.62977

Appendix E – Scalenohedral PCC Recipes from the Patent Literature

A search of the patent literature on typical conditions required to produce scalenohedral PCC from carbonation of a $Ca(OH)_2$ slurry yielded only two patents which gave information at a sufficient level of detail that they could be reproduced. These were:

- US Patent 5,232,678: Precipitated calcium carbonate, filed by Bleakley & Jones [143]
- US Patent 5,695,733: Clustered precipitated calcium carbonate particles, filed by Kroc & Fairchild [142]

According to Bleakley & Jones,

"In order to produce calcium carbonate in the scalenohedral form…quicklime is preferably added to sufficient of the aqueous medium to give, a suspension having a calcium hydroxide concentration of 0.7M to 4M (5-30% w/v)… [In the carbonation step] in order to produce calcium carbonate in the scalenohedral form, the suspension of slaked lime is preferably diluted, if necessary, to a concentration of not more than 15% w/v and maintained at a temperature in the range from 40° to 65° C. The carbonating gas preferably contains from 5% to 50% by volume of carbon dioxide, the remainder being conveniently air or nitrogen. The carbon dioxide-containing gas is preferably admitted into the suspension of slaked lime in the form of fine bubbles. This may be achieved, for example, by admitting the gas under pressure through a perforated plate gas sparger. The rate of admission of the carbon dioxide-containing gas is preferably in the range from 0.02 to 0.10 moles of carbon dioxide per minute per mole of calcium hydroxide. The suspension is preferably agitated substantially continuously throughout the carbonation step, suitably by means of an impeller rotating at a peripheral speed of at least 200 cm.s^{-1} and preferably monitored throughout the carbonation step so that the admission of the carbon dioxide-containing gas may be stopped when the pH has fallen to about 7"

In the patent by Kroc & Fairchild, they describe a method for producing clustered scalenohedral PCC in a two-stage process in which they first make scalenohedral seed particles, followed by a growth stage. They provide the conditions used to make the seed particles in nine different example runs, all of which produced scalenohedral PCC. These conditions are summarised in the table below.

	Starting T (°C)	$Ca(OH)_2$ (wt%)	$Ca(OH)_2$ (M)	Solution (L)	Gas flow (L/min)	CO_2 (%)	Final pH	Carbonation Time (min)	Final T (°C)	d_{50} (µm)	CO_2CR (min^{-1})
Example 1	45	7.6%	*1.026*	1.1	5.6	15%	7.5	32	50	1.33	**0.0305**
Example 2	45	15.1%	*2.038*	0.9	1.7	100%	8	40	76	1.31	**0.0380**
Example 3	42	15.5%	*2.092*	1.1	6.4	10%	-	96	60	1.62	**0.0114**
Example 4	34	15.5%	*2.092*	1.1	8.5	30%	7.7	64	44	1.56	**0.0454**
Example 5	44	13.5%	*1.822*	1.6	7.3	15%	7.5	90	52	1.67	**0.0154**
Example 6	45	11.1%	*1.498*	1.3	6.3	15%	7.5	79	52	1.69	**0.0199**
Example 7	33	15.3%	*2.065*	1.1	6.3	24%	8	120	70	1.16	**0.0273**
Example 8	44	15.0%	*2.025*	0.9	2.1	100%	7.5	33	64	1.99	**0.0472**
Example 9	22	22.0%	*2.970*	1.3	7.4	20%	8	114	46	1.12	**0.0157**

The final column has been added showing the calculated CO_2CR (mol CO_2.mol^{-1}Ca.min^{-1}) based on the other data provided in the patent. This shows that the rate of molar addition of CO_2 to calcium used in this patent agree well with the 0.02-0.1 range given by Bleakley & Jones, seeming to confirm that excess calcium is a requirement for scalenohedral PCC production.